

# **THE MITOCHONDRIAL REDOX REGULATION OF STEROIDOGENESIS**

*Aliesha Leonie Griffin*

A thesis presented to the Faculty of Medicine of the University of  
Birmingham for the degree of Doctor of Philosophy

Centre for Endocrinology, Diabetes and Metabolism  
School of Clinical and Experimental Medicine  
College of Medical and Dental Sciences  
University of Birmingham  
United Kingdom

UNIVERSITY OF  
BIRMINGHAM

**University of Birmingham Research Archive**

**e-theses repository**

This unpublished thesis/dissertation is copyright of the author and/or third parties. The intellectual property rights of the author or third parties in respect of this work are as defined by The Copyright Designs and Patents Act 1988 or as modified by any successor legislation.

Any use made of information contained in this thesis/dissertation must be in accordance with that legislation and must be properly acknowledged. Further distribution or reproduction in any format is prohibited without the permission of the copyright holder.

## ABSTRACT

Mitochondrial steroidogenic cytochrome P450 (CYP) enzymes rely on electron transfer from the redox partner ferredoxin for catalytic activity. Previous *in vitro* data suggests these co-factors are key regulators of CYP enzyme activity. However, this has never been studied *in vivo*. Zebrafish have emerged as model to study human steroidogenesis as they have conserved steroidogenic genes, molecular mechanisms and endocrine tissues. This project aimed to establish zebrafish as an *in vivo* model for endocrine development and its disorders, and to investigate the influence of mitochondrial redox regulation on steroid hormone production. This study involved the identification and characterisation of zebrafish mitochondrial steroidogenic CYP enzymes and their ferredoxin co-factors. Through implementation of recent genomic editing methods including Transcription Activator-Like Effector Nucleases (TALENs) and the Clustered Regulatory Interspaced Short Palindromic Repeat Cas9 nuclease (CRISPR/Cas9) system, and steroid hormone analysis from whole zebrafish extracts by liquid chromatography/tandem mass spectrometry, essential mitochondrial redox components required for zebrafish glucocorticoid production were identified. Overall, this work has helped established zebrafish as a model to study the pathophysiological consequences of steroid hormone disease and provided insights into the mechanism of mitochondrial redox regulation of steroid hormone production.

## ACKNOWLEDGEMENTS

First and foremost I would like to thank my supervisors Nils Krone and Ferenc Muller for giving me the opportunity to carry out this research. I am grateful for their continued guidance and enthusiasm for my project. I would also like to acknowledge the financial, academic and technical support of the University of Birmingham and the Centre for Endocrinology, Diabetes and Metabolism. I am also appreciative to members of the Krone and Muller groups and CEDAM colleagues for sharing your ideas, knowledge and reagents with me. I am most appreciative to Silvia Parajes, Irene Miguel-Escalada and Yavor Hadzhiev; your advice, support and friendship have been invaluable both on an academic and a personal level. I am truly grateful to have met such fantastic people during my time in Birmingham.

To my 147 family, Annika Wilhelm, Claire James and Kate Lowe, I will look back on my time in Birmingham with only the best of memories because of you guys. Thanks for the laughs, the wine and all the cups of tea. I wish you all the best of luck for your future adventures, and cannot wait to catch up with you all somewhere in the world. Finally, I am thankful to my Australian family and friends for providing constant love and reassurance from home. You were supportive of me moving to Birmingham and encouraged me to go after my goals. You believed in me and for this I am truly grateful.

Without all of you, this past three years would not have been possible.

# TABLE OF CONTENTS

<b>1.0</b>	<b>General Introduction .....</b>	<b>2</b>
1.1	Steroid hormones .....	2
1.2	Steroid hormone biosynthesis .....	3
1.3	Classical steroid hormone producing tissues.....	6
1.3.1	The adrenal cortex .....	6
1.4	Regulation of steroid hormones and actions.....	8
1.4.1	Hypothalamus-pituitary-adrenal axis.....	8
1.4.2	Renin-angiotensin-aldosterone system.....	9
1.4.3	Mechanisms of action of steroid hormones.....	10
1.5	Cytochrome P450 enzymes and steroid hormone production.....	11
1.5.1	Mitochondrial steroid hormone synthesis .....	12
1.5.2	CYP11A1: The Cholesterol Side Chain-Cleavage Enzyme .....	12
1.5.3	CYP11B1: The steroid 11 $\beta$ -hydroxylase enzyme .....	13
1.5.4	CYP11B2: Aldosterone synthase .....	14
1.5.5	The mitochondrial redox electron transport chain .....	15
1.5.6	Regulation of the mitochondrial electron transfer chain .....	17
1.6	Deregulation of mitochondrial steroid production causes disease .....	20
1.6.1	CYP11A1 deficiency.....	20
1.6.2	CYP11B1 deficiency and deregulation.....	21
1.6.3	CYP11B2 deficiency and deregulation.....	21
1.6.4	Mitochondrial redox co-factors in disease .....	22
1.7	Zebrafish.....	24
1.7.1	Advantages of zebrafish as a vertebrate model system .....	24
1.7.2	Studying vertebrate gene function in zebrafish .....	25
1.7.3	Translational research and modelling genetic diseases in zebrafish .....	29
1.8	Conservation of steroid hormone pathway in zebrafish .....	30
1.8.1	Glucocorticoid production in zebrafish.....	30
1.9	The regulation of glucocorticoid production in zebrafish .....	33
1.9.1	The zebrafish interrenal .....	33
1.9.2	Hypothalamus-pituitary-interrenal axis.....	33
1.9.3	Development of the hypothalamus-pituitary-interrenal axis .....	34
1.10	The role of mitochondrial CYP genes in zebrafish.....	36
1.10.1	Cholesterol Side Chain-Cleavage Enzyme .....	36
1.10.2	Steroid 11 $\beta$ hydroxylase .....	37
1.10.3	Mitochondrial electron transport chain .....	38

1.11	Rational for work .....	40
1.11.1	Hypothesis and aims.....	40
<b>2.0</b>	<b>General Materials and Methodologies .....</b>	<b>43</b>
2.1	Molecular biology materials and methodologies .....	43
2.1.1	Standard solutions.....	43
2.1.2	Transformation of E. coli by heat shock.....	43
2.1.3	Plasmid DNA preparation.....	44
2.1.4	Reverse transcription.....	45
2.1.5	General expression plasmids .....	45
2.1.6	Quantification of nucleic acids.....	47
2.1.7	DNA sequencing.....	47
2.1.8	Agarose gel electrophoresis .....	48
2.1.9	Enzymatic restriction digests.....	48
2.1.10	Alkaline phosphatase treatment of linearised vectors .....	48
2.1.11	DNA purification.....	49
2.1.12	Agarose gel DNA purification .....	49
2.1.13	T4 DNA ligation .....	50
2.1.14	pGEMT-easy ligation .....	50
2.1.15	Colony Polymerase Chain Reaction .....	50
2.1.16	Reverse Transcriptase Polymerase Chain Reaction (RT-PCR) .....	51
2.1.17	RNA extraction .....	51
2.2	In silico protein analysis .....	53
2.2.1	Multiple sequence alignments.....	53
2.3	Zebrafish husbandry and methodologies .....	53
2.3.1	Zebrafish nomenclature .....	53
2.3.2	Standard solutions.....	54
2.3.3	Zebrafish maintenance .....	54
2.3.4	Breeding strategy to generate knockout zebrafish lines .....	55
2.3.5	Embryo collection.....	57
2.3.6	Dechoriation of zebrafish embryos .....	57
2.3.7	In vitro mRNA synthesis .....	58
2.3.8	In vivo knockdown by antisense morpholino .....	59
2.3.9	Morpholino microinjection of single cell zebrafish embryos .....	59
2.3.10	Fin clipping adult zebrafish .....	60
2.3.11	Genomic DNA extraction.....	60
2.4	Cell biology materials and methodologies .....	61
2.4.1	Standard solutions.....	61
2.4.2	Mammalian cell culture .....	61
2.4.3	Transfection of mammalian cell lines .....	61
2.4.4	In vitro enzyme activity assay.....	62

2.4.5	Protein extraction.....	63
2.4.6	Protein quantification .....	63
2.4.7	SDS Poly Acrylamide Gel Electrophoresis .....	64
2.4.8	Protein transfer using the iBlot Blotting System .....	64
2.4.9	Western Blot .....	64
2.5	Biochemical materials and methods .....	66
2.5.1	Standard Solutions .....	66
2.5.2	Steroid hormone extraction from zebrafish.....	66
2.5.3	Steroid hormone extraction from cell media .....	67
2.5.4	Liquid Chromatography/Tandem mass spectrometry (LC-MS/MS) System Setup .....	68
2.5.5	Statistical analysis of steroid hormone measurements.....	72
<b>3.0</b>	<b>The duplicated mitochondrial ferredoxin Fdx1b regulates glucocorticoid production in zebrafish .....</b>	<b>75</b>
3.1	Introduction .....	75
3.2	Rational for work .....	76
3.3	Methods .....	77
3.3.1	PCR amplification and cloning of zebrafish ferredoxin paralogues.....	77
3.3.2	PCR amplification and cloning of zebrafish mitochondrial redox partners for expression assays .....	78
3.3.3	Alignment and phylogenetic analyses of zebrafish Fdx isozymes .....	79
3.3.4	Characterisation of Fdx1 and Fdx1b expression.....	79
3.3.5	Zebrafish fdx1b knockdown studies.....	80
3.3.6	mRNA rescues of fdx1 and fdx1b morphants .....	81
3.3.7	Phenotypic classification of embryos and larvae.....	82
3.4	Results.....	84
3.4.1	Zebrafish Fdx1 and Fdx1b homology with other vertebrate Ferredoxins.....	84
3.4.2	Spatial and temporal expression of fdx1 and fdx1b .....	86
3.4.3	Defining the role of Fdx1 in early zebrafish development .....	88
3.4.4	Pregnenolone synthesis in Fdx1 morphants .....	90
3.4.5	Identifying the role of Fdx1b during zebrafish development .....	91
3.4.6	The effects of fdx1b deficiency on zebrafish steroidogenesis.....	94
3.4.7	mRNA and steroid rescues of fdx1b deficient embryos .....	97
3.5	Discussion and prospective studies .....	99
3.5.1	Evolutional conservation of ferredoxin electron transport system.....	99
3.5.2	The role of Fdx1 in zebrafish development.....	100
3.5.3	Fdx1b expression is required for steroid hormone synthesis in the adult zebrafish .....	102
3.5.4	Fdx1b is essential for cortisol synthesis through interactions with Cyp11c1 and possibly Cyp11a2.....	103

3.5.5	Stability of zebrafish ferredoxin proteins and mRNA.....	104
3.5.6	Investigating the interaction between zebrafish ferredoxins and CYP enzymes.....	105
<b>4.0</b>	<b>Redefining cytochrome P450 side-chain cleavage activity in zebrafish development</b> .....	<b>108</b>
4.1	Introduction.....	108
4.2	Rational for work.....	109
4.3	Methodology.....	110
4.3.1	PCR amplification of zebrafish <i>cyp11a1</i> and <i>cyp11a2</i> .....	110
4.3.2	Alignment and phylogenetic analysis of Cyp11a sequences.....	110
4.3.3	PCR amplification and cloning of zebrafish P450-scc paralogues.....	111
4.3.4	Characterisation of <i>cyp11a1</i> and <i>cyp11a2</i> expression.....	112
4.3.5	Transient knockdown of <i>cyp11a1</i> and <i>cyp11a2</i> in zebrafish embryos.....	112
4.3.6	Phenotypic characterisation of <i>cyp11a</i> morphants.....	113
4.3.7	Rescue experiments of <i>cyp11a2</i> morphants with pregnenolone.....	114
4.4	Results.....	115
4.4.1	Homology of Cyp11a isozymes with vertebrate orthologues.....	115
4.4.2	Identification of polymorphisms in zebrafish <i>cyp11a1</i> and <i>cyp11a2</i> genes.....	120
4.4.3	Functional in vivo assays of <i>cyp11a1</i> and <i>cyp11a2</i> paralogues.....	122
4.4.4	Spatial and temporal <i>cyp11a</i> expression.....	124
4.4.5	Confirmation of <i>cyp11a1</i> function during early zebrafish development.....	125
4.4.6	Determining the specific roles of <i>cyp11a2</i> during early development.....	129
4.4.7	Steroid profiles of <i>cyp11a2</i> deficient embryos.....	132
4.5	Discussion and prospective studies.....	135
4.5.1	Cyp11a1 has low catalytic activity in vitro.....	135
4.5.2	Maternal expression of <i>cyp11a1</i> is essential for embryogenesis.....	136
4.5.3	Transition of <i>cyp11a1</i> to <i>cyp11a2</i> expression correlates to the initiation of de novo steroidogenesis.....	136
4.5.4	Deficiency in <i>cyp11a2</i> impairs interrenal steroidogenesis.....	137
4.6	Conclusion.....	139
<b>5.0</b>	<b>Genome engineering with transcription activator-like effector nucleases</b> .....	<b>141</b>
5.1	Introduction.....	141
5.1.1	Genomic engineering with TALENs.....	141
5.1.2	Generating targeted DNA breaks using TALENs.....	143
5.1.3	Genome editing with TALENs in zebrafish.....	144
5.1.4	Rational for work.....	145
5.2	Methodology.....	146
5.2.1	GoldenGate TALEN assembly method.....	146
5.2.2	Generation of TALEN RNA for microinjection.....	150
5.2.3	Microinjection of TALEN mRNA.....	150

5.2.4	Genotyping by restriction digest.....	150
5.2.5	Genotyping by high resolution melting curve (HRM) analysis.....	151
5.2.6	Visualisation mediated background adaptation assessment.....	153
5.3	Results.....	154
5.3.1	Strategic design of fdx1b and cyp11a2 TALENs.....	154
5.3.2	Assembly of customised TALEN repeat arrays.....	156
5.3.3	Microinjection and validation of in vivo TALEN activity by PCR digest.....	159
5.3.4	Redesign of fdx1b and cyp11a2 TALENs.....	163
5.3.5	Development of high resolution melting curve analysis for genotyping.....	166
5.3.6	Microinjection and validation of in vivo TALEN activity by HRM.....	167
5.3.7	Identification of heritable mutations.....	169
5.3.8	Outcrossing and establishing lines harbouring indels.....	171
5.3.9	Genotyping and characterisation of generation fdx1b F2 TALEN lines.....	173
5.3.10	Preliminary characterisation of fdx1b null zebrafish embryos.....	175
5.4	Discussion and prospective studies.....	177
5.4.1	Using TALENs as an alternative to traditional morpholino knockdown studies.....	177
5.4.2	Designing and optimisation of TALENs targeting fdx1b and cyp11a2.....	177
5.4.3	Optimisation of high resolution melting curve analysis for genotyping.....	179
5.4.4	Generating zebrafish Fdx1b null alleles.....	180
5.4.5	Preliminary data suggests fdx1b knockouts lack glucocorticoid production.....	180
5.4.6	Establishing cyp11a2 null lines.....	183
5.5	Conclusions.....	183
<b>6.0</b>	<b>Characterising the role of mitochondrial Cyp11c1.....</b>	<b>186</b>
6.1	Introduction.....	186
6.1.1	11 $\beta$ -steroid hydroxylase in zebrafish.....	186
6.1.2	CRISPR/Cas9 genome editing.....	187
6.1.3	Rational for work.....	189
6.2	Methodology.....	190
6.2.1	PCR amplification and cloning of cyp11c1.....	190
6.2.2	Alignment and phylogenetic analysis of zebrafish Cyp11c1.....	190
6.2.3	In silico KOZAC sequence analysis.....	191
6.2.4	Cloning of additional zebrafish cyp11c1 constructs for in vitro studies.....	191
6.2.5	Characterisation of Cyp11c1 spatial and temporal expression.....	192
6.2.6	Generation of cyp11c1 short guide RNA plasmids.....	193
6.2.7	Genotyping by high resolution melting curve (HRM) analysis.....	194
6.2.8	In vitro mRNA synthesis of cyp11c1 guide RNAs.....	195
6.2.9	Generation of Cas9 mRNA.....	196
6.2.10	Microinjection of CRISPR/Cas9 for genome editing.....	196
6.3	Results.....	197

6.3.1	Phylogenetic analysis .....	197
6.3.2	Characterisation of cyp11c1 expression.....	201
6.3.3	Cyp11c1 functional in vitro assays .....	202
6.3.4	Generating cyp11c1 null alleles using CRISPR/Cas9.....	204
6.3.5	Optimisation of androgen detection by LC-MS/MS.....	206
6.4	Discussion and prospective studies .....	207
6.4.1	Zebrafish Cyp11c1 shares homology with human aldosterone synthase .....	207
6.4.2	Functional characterisation of predicated Cyp11c1 proteins .....	208
6.4.3	Spatial and temporal expression of cyp11c1 is consistent with its functional activities .....	210
6.4.4	Generating cyp11c1 null zebrafish line by CRISPR/Cas9.....	210
6.4.5	Development of LC-MS/MS methodology to identify zebrafish androgens .....	212
6.4.6	Summary.....	213
<b>7.0</b>	<b>General discussion and prospective studies.....</b>	<b>216</b>
7.1	Characterising steroidogenic enzymes in zebrafish .....	216
7.2	The study of mitochondria redox reactions <i>in vivo</i> .....	217
7.3	Establishing zebrafish as a model for endocrine disease and development .....	219
7.3.1	Genome engineering in zebrafish .....	219
7.3.2	Development of zebrafish whole system steroid assays.....	221
7.4	The future of zebrafish in endocrine research.....	222
<b>8.0</b>	<b>Appendix.....</b>	<b>224</b>
8.1	Appendix One: Redefining Cytochrome P450 side-chain cleavage activity in zebrafish.....	224
<b>9.0</b>	<b>References.....</b>	<b>235</b>

## LIST OF FIGURES

Figure 1.1 Human steroid biosynthesis pathway.....	5
Figure 1.2 Functional zones of the human adrenal cortex .....	7
Figure 1.3 Regulation of glucocorticoid production by the HPA axis.....	8
Figure 1.4 Regulation of aldosterone production by the RAAS .....	10
Figure 1.5 Catalytic activity of Cholesterol P450 side chain-cleavage enzyme .....	13
Figure 1.6 Catalytic activity of 11 $\beta$ -hydroxylase enzyme .....	14
Figure 1.7 Catalytic activity of aldosterone synthase .....	15
Figure 1.8 The mitochondrial electron transfer system .....	16
Figure 1.9 Modulation of Fdx1 dependent CYP enzymatic reactions <i>in vitro</i> .....	18
Figure 1.10 Mechanism of action by antisense morpholino oligonucleotides.....	26
Figure 1.11 Cellular repair mechanisms of chromosomal breaks .....	29
Figure 1.12 The postulated pathway for glucocorticoid production in zebrafish .....	31
Figure 1.13 Comparison of cortisol production between humans and zebrafish .....	35
Figure 1.14 Androgen production in zebrafish .....	38
Figure 2.1 Breeding strategy to generate homozygous mutant zebrafish lines.....	56
Figure 2.2 LC-MS/MS detection of cortisol in whole zebrafish extracts.....	70
Figure 2.3 LC-MS/MS detection of pregnenolone-oxime in whole zebrafish extracts .....	72
Figure 3.1 Phylogenetic analysis of ferredoxin proteins.....	85
Figure 3.2 Spatial and temporal expression of zebrafish fdx1 and fdx1b transcripts.....	87
Figure 3.3 Morphological phenotype of embryos injected with Fdx1 morpholino at 9 hpf.....	89
Figure 3.4 Pregnenolone concentrations of <i>fdx1</i> morphants and controls at 10 hpf .....	90
Figure 3.5 Morphological characterisation of fdx1b morphants at 120 hpf. ....	92
Figure 3.6 The <i>fdx1b</i> splice morpholino ( <i>fdx1b</i> -Spl <sup>MO</sup> ) effectively disrupts the <i>fdx1b</i> mRNA transcript.....	93

Figure 3.7 Pregnenolone concentrations of Fdx1b morphants and controls during development .....	95
Figure 3.8 Cortisol concentrations of Fdx1b morphants and controls during development.....	96
Figure 3.9 Pregnenolone and cortisol measurements in fdx1b rescued larvae.....	98
Figure 4.1 Evolution of Cyp11a paralogues.....	115
Figure 4.2 ClustalW alignment of Cyp11a paralogs.....	119
Figure 4.3 <i>In vitro</i> activity of zebrafish Cyp11a paralogues .....	123
Figure 4.4 Spatial and temporal expression of zebrafish <i>cyp11a1</i> and <i>cyp11a2</i> genes .....	125
Figure 4.5 Pregnenolone concentrations in <i>cyp11a1</i> deficient embryos at 10 hpf.....	126
Figure 4.6 Morphological phenotype of Cyp11a morphants at 10 hpf .....	128
Figure 4.7 Confirmation of disruption of <i>cyp11a2</i> splicing .....	129
Figure 4.8 Classification of <i>cyp11a2</i> deficient embryos at 120 hpf.....	131
Figure 4.9 Pregnenolone and cortisol concentrations in <i>cyp11a2</i> deficient embryos.....	133
Figure 4.10 Cortisol concentrations of <i>cyp11a2</i> -Spl morphants supplemented with pregnenolone .....	134
Figure 5.1 Transcription Activator-Like Effector Nuclease (TALEN) architecture .....	142
Figure 5.2 TALEN induced genetic disruption by non-homologous end joining.....	143
Figure 5.3 GoldenGate TALEN assembly reaction one.....	147
Figure 5.4 GoldenGate TALEN assembly reaction two .....	149
Figure 5.5 Strategic design of TALENs targeting <i>fdx1b</i> and <i>cyp11a2</i> .....	155
Figure 5.6 Confirmation of correct ligation of reaction one of the GoldenGate TALEN assembly .....	157
Figure 5.7 Confirmation of TALEN assembly from GoldenGate reaction two .....	158
Figure 5.8 Sequencing confirmation of the RVD amino acids for each TALEN.....	159
Figure 5.9 Confirmation of <i>in vivo</i> fdx1b TALEN activity by restriction digest.....	161

Figure 5.10 Screening F1 generation for <i>fdx1b</i> indels.....	162
Figure 5.11 Determining <i>cyp11a2</i> TALEN activity <i>in vivo</i> .....	163
Figure 5.12 Redesign of <i>fdx1b</i> and <i>cyp11a2</i> TALENs.....	165
Figure 5.13 Sequencing confirmation of RVD of second generation TALENs.....	166
Figure 5.14 HRM dissociation curves of TALEN injected embryos.....	169
Figure 5.15 Sequencing confirmation of <i>fdx1b</i> and <i>cyp11a2</i> TALEN induced deletion.....	171
Figure 5.16 Sequencing confirmation of F1 heterozygotes for mutations in <i>fdx1b</i> .....	173
Figure 5.17 Identification of <i>fdx1b</i> null alleles by PCR of F2 generation.....	174
Figure 5.18 Phenotypic characterisation of <i>fdx1b</i> null larvae (line five).....	176
Figure 5.19 Cleavage of pro-opimelanocortin (POMC) protein.....	182
Figure 6.1 CRISPR/Cas9 system for genomic engineering.....	189
Figure 6.2 Hybridisation of oligonucleotides for cloning into DR274.....	194
Figure 6.3 Evolution of Cyp11b-like proteins.....	197
Figure 6.4 ClustalW alignment of Cyp11c1 homologues.....	200
Figure 6.5 Spatial and temporal expression of zebrafish <i>cyp11c1</i> transcripts.....	201
Figure 6.6 Catalytic conversion of 11-deoxycortisol to cortisol by Cyp11c1.....	203
Figure 6.7 HRM analysis of larva injected with <i>cyp11c1</i> targeting guide RNA 2.....	205
Figure 6.8 Chromatogram showing optimise solution of the zebrafish androgens.....	206

## LIST OF TABLES

Table 1.1 Principal steroid hormones in humans.....	3
Table 2.1 Standard vector primers used for sequencing and colony PCR screens .....	47
Table 2.2 Zebrafish and mammalian naming conventions.....	53
Table 2.3 Antibodies for Western Blotting.....	65
Table 2.4 LC-MS/MS parameters for the detection and quantification of cortisol and pregnenolone-oxime, androgen and their internal standards cortisol-d4 and pregnenolone-oxime-d4.....	69
Table 3.1 Oligonucleotides for cloning of zebrafish ferredoxin paralogues .....	77
Table 3.2 Oligonucleotides for cloning of zebrafish mitochondrial redox partners into pET22b	78
Table 3.3 Oligonucleotides for RT-PCR expression analysis of the <i>fdx1</i> and <i>fdx1b</i> genes.....	80
Table 3.4 Sequences of the anti-sense morpholinos used for the transient knockdown of <i>fdx1</i> and <i>fdx1b</i> genes .....	81
Table 3.5 Oligonucleotides for the amplification of <i>fdx1</i> and <i>fdx1b</i> coding sequences with T7 polymerase recognition sequences and a polyadenylation signal.....	82
Table 3.6 Classification of the phenotype of <i>fdx1</i> morphants at 10 hpf.....	82
Table 3.7 Phenotypic classification of the <i>fdx1b</i> morphants at 120 hpf.....	83
Table 4.1 Oligonucleotides for PCR amplification P450scc cDNA .....	110
Table 4.2 Oligonucleotides for the PCR amplification and cloning of P450scc cDNA .....	111
Table 4.3 Oligonucleotides for RT-PCR expression analysis of the <i>cyp11a</i> paralogue genes.....	112
Table 4.4 Sequences of the anti-sense morpholinos used for the transient knockdown of <i>cyp11a</i> paralogs.....	113
Table 4.5 Classification of the phenotype of <i>cyp11a2</i> -Spl morphants at 120 hpf.....	114
Table 4.6 Missense mutation identified in Cyp11a1 in different wild-type strains.....	121
Table 4.7 Missense mutation identified in Cyp11a2 in different wild-type strains.....	121

Table 5.1 Primer sequences for screening TALEN construction plasmids. ....	148
Table 5.2 Sequences of the primers used for genotyping PCR for <i>fdx1b</i> and <i>cyp11a2</i> null alleles by restriction digest .....	151
Table 5.3 PCR Primers used for genotyping for <i>fdx1b</i> and <i>cyp11a2</i> null alleles by high resolution melting curve analysis.....	152
Table 6.1 Oligonucleotides for the RT-PCR amplification of 11 $\beta$ -hydroxylase from zebrafish cDNA .....	190
Table 6.2 Additional oligonucleotides used for RT-PCR amplification of <i>cyp11c1</i> from different ATG start sites .....	192
Table 6.3 Primer sequences used for RT-PCR expression analysis of <i>cyp11c1</i> .....	193
Table 6.4 Oligonucleotide sequences to generate <i>cyp11c1</i> genomic targeting guide RNAs .....	193
Table 6.5 Sequences of the primers used for genotyping PCR for <i>cyp11c1</i> indels by high resolution melting curve analysis .....	195

## LIST OF ABBREVIATIONS

ACE	angiotensin covering enzyme
ACTH	adrenocorticotropic hormone
AR	androgen receptor
AT1R	angiotensin II receptor type I
CAGE	cap analysis gene expression
cDNA	complementary DNA
CRH	corticotrophin-releasing hormone
CRISPR	Clustered regularly interspaced short palindromic repeat
CYP enzyme	Cytochrome P450 enzyme
CYP11A	cholesterol side-chain cleavage; P40scc
CYP11B1	11 $\beta$ -hydroxylase
CYP11B2	aldosterone synthase
CYP17A1	17-hydroxylase
CYP21	21-hydroxylase
dpf	days post fertilisation
DHEA	dehydroepiandrosterone
DOC	11-deoxycorticosterone
ER	oestrogen receptor
FAD	flavin adenine dinucleotide
FDX	ferredoxin
FDXR	ferredoxin reductase
GR	glucocorticoid receptor
gRNA	guide RNA
HSD enzyme	hydroxysteroid dehydrogenase enzyme

HSD3B2	3 $\beta$ -hydroxysteroid dehydrogenase type 2
HPA axis	hypothalamus-pituitary-adrenal axis
hpf	hours post fertilisation
HPI axis	hypothalamus-pituitary-interrenal axis
HRM	high resolution melting curve
LC-MS/MS	liquid chromatography tandem mass spectrometry
MC2R	melanocortin II receptor
mRNA	messenger RNA
MSH- $\alpha$	$\alpha$ -melanocyte stimulating hormone
NADPH	nicotinamide adenine dinucleotide phosphate
POMC	pro-opiomelanocortin
POR	P450 oxidoreductase
RAAS	renin-angiotensin-aldosterone system
RT-PCR	reverse transcriptase polymerase chain reaction
RVD	repeat variable dinucleotide
SF1	steroidogenic factor 1
SNP	single nucleotide polymorphism
StAR	steroid acute regulatory protein
TALEN	transcription activator-like effector nuclease
WT1	Wilms tumour suppressor 1

# ***Chapter One***

---

## ***General Introduction***

## **1.0 GENERAL INTRODUCTION**

### *Part One: Redox regulation of steroid hormone synthesis*

## **1.1 Steroid hormones**

Steroid hormones are essential for vertebrate development and normal physiology. The main classes of steroid hormones include glucocorticoids, mineralocorticoids, the sex steroids encompassing androgens (testosterone, dihydrotestosterone), oestrogens (oestrone, oestradiol) and progestins (progesterone), and the calciferols (1,25-dihydroxy vitamin D). These five classes of steroid hormones (Miller and Auchus, 2011) and the closely related 1,25-dihydroxy vitamin D (a sterol) (Feldman et al., 2014) are involved in many physiological processes including development, sex differentiation and maintaining homeostasis throughout life. Endogenous steroid hormones are produced in steroidogenic tissues and secreted into the circulation to act in an endocrine fashion. Steroid hormones modulate many physiological processes through genomic and non-genomic pathways. Classically they bind specific receptors in target tissues to modulate gene transcription to influence cellular processes (Table 1.1). Specifically, glucocorticoids, such as cortisol, have key roles in maintaining metabolic homeostasis in response to stress by binding the glucocorticoid receptor (GR). Individual sex steroids function through specific receptors to modulate sex differentiation, sexual maturation and reproductive functions. Aldosterone is the main mineralocorticoid and acts via the mineralocorticoid receptor (MR) to control osmoregulation and blood pressure (Miller and Auchus, 2011). Finally, 1,25-dihydroxy vitamin D binds the vitamin D receptor to regulate bone health and immunity (Feldman et al., 2014).

**Table 1.1 Principal steroid hormones in humans**

	<b>Mineralocorticoids</b>	<b>Glucocorticoids</b>	<b>Sex Steroids</b>	<b>Calciferols</b>
<b>Steroids</b>	Aldosterone	Cortisol	Testosterone, Oestradiol, Progesterone	1,25-dihydroxy vitamin D
<b>Origin</b>	Zona glomerulosa	Zona fasciculata	Gonads Placenta, Zona reticularis	Liver/Kidney
<b>Function</b>	Blood pressure Cardiovascular effects	Protein, carbohydrate, lipid and nucleic acid metabolism Stress and immune modulation	Sexual development Behavior Reproduction	Bone mineralisation Immune modulation
<b>Receptor</b>	Mineralocorticoid receptor (MR)	Glucocorticoid receptor (GR)	Androgen receptor (AR) Estrogen receptor (ER) Progesterone receptor (PR)	Vitamin D receptor (VDR)

## 1.2 Steroid hormone biosynthesis

Steroidogenesis is a biochemical process to synthesise active steroid hormones from cholesterol via a network of sequential enzymatic reactions (Figure 1.1). These enzymes fall into two families: cytochrome P450 (CYP) enzymes and hydroxysteroid dehydrogenase (HSD) enzymes. The inter-conversion of steroids by these enzymes involves oxidation-reduction (redox) reactions and often requires electron transporter co-factors for enzymatic activity.

Cholesterol taken up from the circulation via cholesterol receptors, or produced *de novo* from acetic acid, is transported to the inner mitochondrial membrane by an evolutionary conserved transport mechanism involving Steroid Acute Regulatory protein (StAR) and the mitochondrial translocator protein (Fan and Papadopoulos, 2013, Miller and Auchus, 2011). Subsequently, the

first and rate limiting step of steroidogenesis involves the conversion of cholesterol to pregnenolone in the mitochondrial matrix by the CYP enzyme P450 side-chain cleavage (CYP11A1; P450<sub>scc</sub>). From here the pathway diverges to produce mineralocorticoids, glucocorticoids and sex hormones, depending on the presence of steroidogenic enzymes in specific cells. Pregnenolone is translocated to the endoplasmic reticulum for further catalysis by 17-hydroxylase (CYP17A1), 3 $\beta$ -hydroxysteroid dehydrogenase (3 $\beta$ HSD2) and 21-hydroxylase (CYP21A2).

Mineralocorticoid production initially requires the activities of 3 $\beta$ -HSD2 and CYP21A2 to convert pregnenolone to progesterone and 11-deoxycorticosterone, respectively. Then 11-deoxycorticosterone is transferred to the mitochondria where the enzyme aldosterone synthase (CYP11B2) catalyses the production of aldosterone. Glucocorticoid production relies on the conversion of pregnenolone to 11-deoxycortisol by consecutive CYP17A1, 3 $\beta$ HSD2 and CYP21A2 activities. Following this 11-deoxycortisol is translocated back to the mitochondria where it undergoes 11-hydroxylation by the enzyme 11 $\beta$ -hydroxylase (CYP11B1) to generate cortisol. The synthesis of sex steroids requires the 17, 20 lyase activity of CYP17A1 to convert 17-hydroxypregnenolone to dehydroepiandrosterone (DHEA), the major precursor for both female and male sex steroids (Miller and Auchus, 2011).

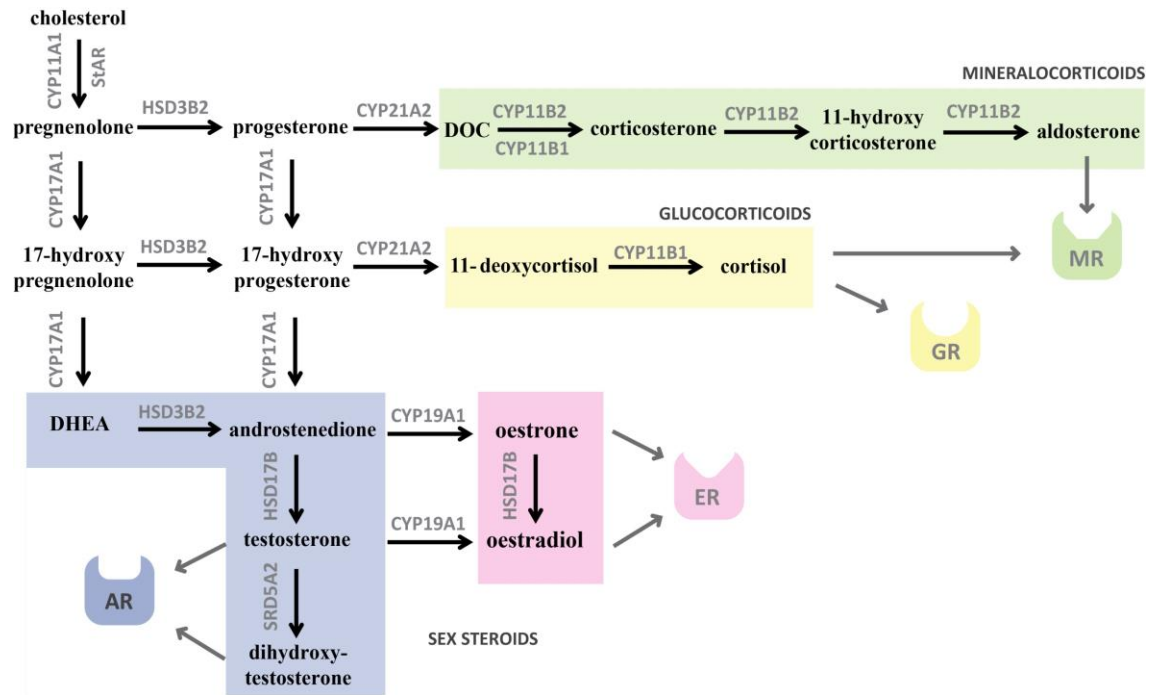


**Figure 1.1 Human steroid biosynthesis pathway**

Physiologically active steroid hormones are derived from the common precursor cholesterol. After cholesterol is transported across the mitochondrial membrane by the Steroid Acute Regulatory protein (StAR), it is converted to pregnenolone in the first step of steroidogenesis. Subsequent conversion into either glucocorticoids, mineralocorticoids or the sex steroids involves sequential enzymatic reaction catalysed by either cytochrome P450 (CYP) or hydroxysteroid dehydrogenase (HSD) enzymes. Steroids elicit physiological changes by binding to their receptor (MR, Mineralocorticoid receptor; GR, glucocorticoid receptor; AR, androgen receptor; ER, oestrogen receptor). Genes coding steroidogenic enzymes are shown in grey. *CYP11A1*, P450 side-chain cleavage enzyme; *CYP17A1*, 17-hydroxylase; *HSD3B2*, 3 $\beta$ -hydroxysteroid dehydrogenase type two; *CYP21A2*, 21-hydroxylase; *CYP19A1*, P450 aromatase; *HSD17B*, 17 $\beta$ -hydroxysteroid dehydrogenase; *CYP11B1*, 11 $\beta$ -hydroxylase; *CYP11B2*, aldosterone synthase; *SRD5A2*, steroid 5 $\alpha$  reductase; Dehydroepiandrosterone, DHEA; 11-deoxycorticosterone, DOC.

## 1.3 Classical steroid hormone producing tissues

Steroidogenic tissues are defined by their ability to convert cholesterol into pregnenolone. It was previously believed this attribute was restricted to the endocrine cells of the adrenal cortex and the gonads; specifically the Leydig cells in the testis and the Theca and Granulosa cells in the ovary (Miller and Auchus, 2011). More recently, the detection of steroidogenic enzymes in peripheral target tissues has led to the insight that the conversion of steroid precursors may be occurring locally in other tissues (Labrie et al., 1998, Labrie et al., 2000, Thiboutot et al., 2003).

### 1.3.1 *The adrenal cortex*

The adrenal cortex is the main site of steroid hormone production in humans. The adrenal glands are located above the kidneys and consist of two parts; the outer adrenal cortex and the inner adrenal medulla. While epinephrine and norepinephrine are secreted by the chromaffin cells in the medulla, the adrenal cortex is responsible for the secretion of corticosteroids; that is the glucocorticoids and mineralocorticoids and androgens (Figure 1.2). The cortex is subdivided into the outer zona glomerulosa, the middle zona fasciculata and the inner zona reticularis. Through a combination of enzyme and receptor expression each zone of the adrenal cortex is responsible for specific steroid production. While production of pregnenolone via *CYP11A1* expression is common to all three zones, the zona glomerulosa cells are positive for *CYP11B2* to facilitate aldosterone production. The middle zona fasciculata produces cortisol through *CYP11B1* expression and the zona reticularis secrete DHEA and androstenedione by expression of *CYP17A1* (Simpson and Waterman, 1988).

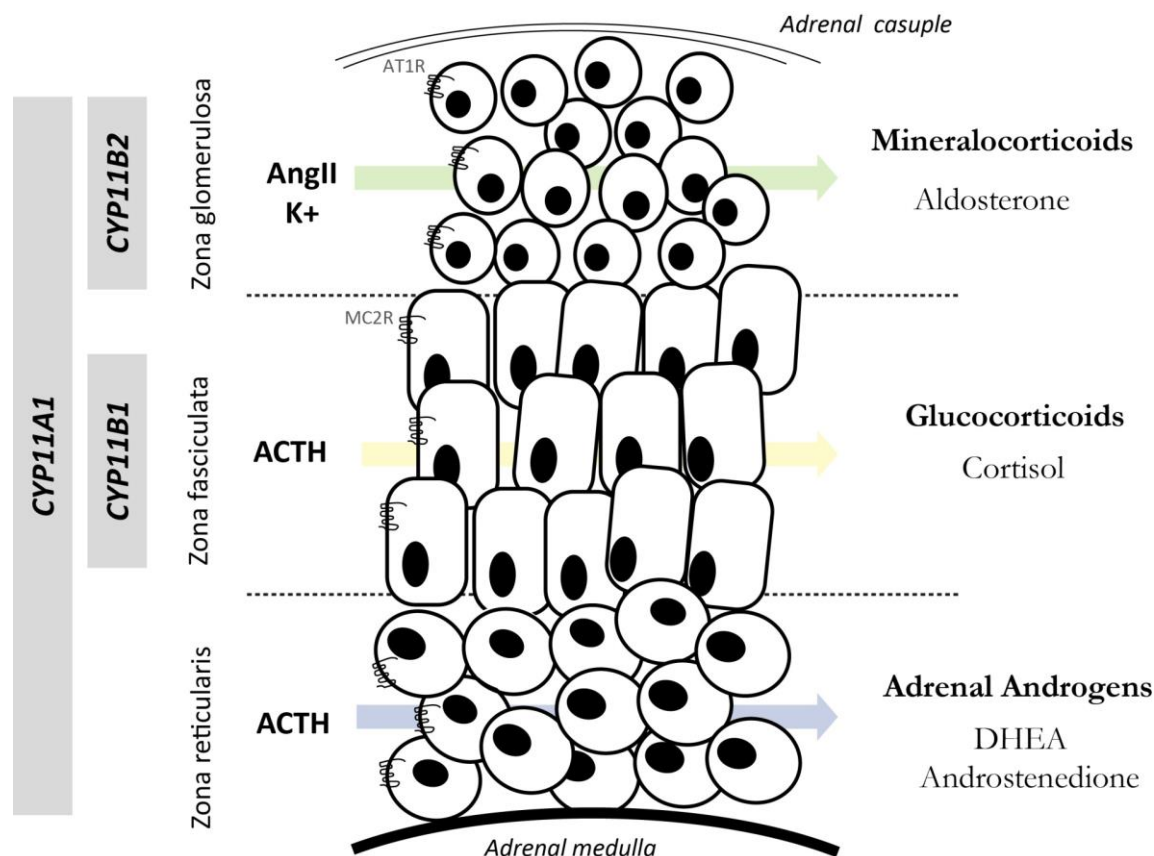


**Figure 1.2 Functional zones of the human adrenal cortex**

The adrenal cortex is the major site of steroid hormone production in humans. The outer zona glomerulosa expresses *CYP11B2* to facilitate aldosterone production in response to angiotensin II (AngII) binding to the angiotensin II receptor (AT1R) and potassium ions (K<sup>+</sup>). The zona fasciculata generates cortisol in an adrenocorticotropic hormone (ACTH) dependent manner by expressing melanocortin II receptor (MC2R) which regulates *CYP11B1* expression. Adrenal androgens dehydroepiandrosterone (DHEA) and androstenedione are synthesised from the inner zona reticularis. Expression of *CYP11A1* which generates pregnenolone required for all steroid hormone production is common to all three zones of the adrenal cortex.

## 1.4 Regulation of steroid hormones and actions

### 1.4.1 Hypothalamus-pituitary-adrenal axis

Glucocorticoid production in the adrenal cortex is regulated by the hypothalamus-pituitary-adrenal (HPA) axis (Simpson and Waterman, 1988) (Figure 1.3). Under periods of stress or as part of the diurnal rhythm, the hypothalamus secretes corticotropin-releasing hormone (CRH), which signals the pituitary to transcribe the pro-opiomelanocortin (*POMC*) gene. The POMC preprotein is cleaved to adrenocorticotrophic hormone (ACTH). ACTH promotes glucocorticoid production by binding its receptor on the adrenal cortex. Finally, circulating cortisol provides feedback to the hypothalamus and inhibits pathway stimulation, completing the HPA axis.

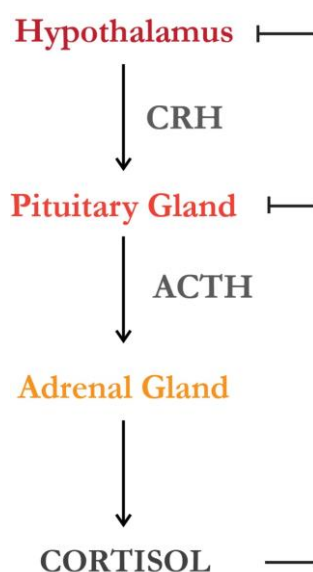


**Figure 1.3 Regulation of glucocorticoid production by the HPA axis**

The hypothalamus-pituitary-adrenal (HPA) regulates the production of cortisol. During stress or as part of the diurnal rhythm, the hypothalamus secretes corticotropin-releasing hormone (CRH), which signals the pituitary to secrete adrenocorticotrophic hormone (ACTH). ACTH binds receptors on the adrenal cortex which signal cortisol production. Circulating cortisol provides negative feedback to the hypothalamus and pituitary gland to inhibit pathway stimulation, completing the HPA axis.

ACTH promotes steroidogenesis by binding to the melanocortin II receptor (MC2R) on the zona fasciculata, which in turn activates the protein kinase A (PKA) pathway via cyclic AMP (cAMP). PKA phosphorylation of StAR causes the mobilisation of cholesterol into the mitochondria for conversion to active steroid hormones, generating an acute response to ACTH stimulation (Arakane et al., 1997, Clark et al., 1995, Stocco, 2001). Prolonged ACTH stimulation increases adrenal cortex expression of steroidogenic enzymes (mainly StAR, CYP17A1, CYP21A2 and CYP11B1) and electron transfer co-factors through cAMP element binding protein (CREB) and steroidogenic factor 1 (SF-1) transcription factors (Manna et al., 2009). This response can occur over hours or days, thus providing a sustained response to the ACTH. Chronic exposure to ACTH (weeks to months) can promote adrenal hyperplasia, excessive production of glucocorticoids and in extreme cases it can result in Cushing's syndrome (Nelson et al., 1958).

#### **1.4.2     *Renin-angiotensin-aldosterone system***

Aldosterone is a component of the renin-angiotensin-aldosterone system (RAAS) and is required for blood pressure regulation and water balance homeostasis (Figure 1.4). Low blood volume is detected by the juxtaglomerular cells in the kidneys causing them to secrete renin. Renin metabolises angiotensinogen to angiotensin I which is converted to angiotensin II by the angiotensin-converting enzyme (ACE). Angiotensin II binds the angiotensin II receptor type one (AT1R) which activates the downstream signalling pathways to increase blood pressure and volume (Guo et al., 2001). Additionally, angiotensin II increases *CYP11B2* expression from the zona glomerulosa to increase aldosterone synthesis (Bader, 2010). In turn, aldosterone stimulates sodium and water reabsorption by the kidneys through its actions via the mineralocorticoid receptor to further increase blood volume.

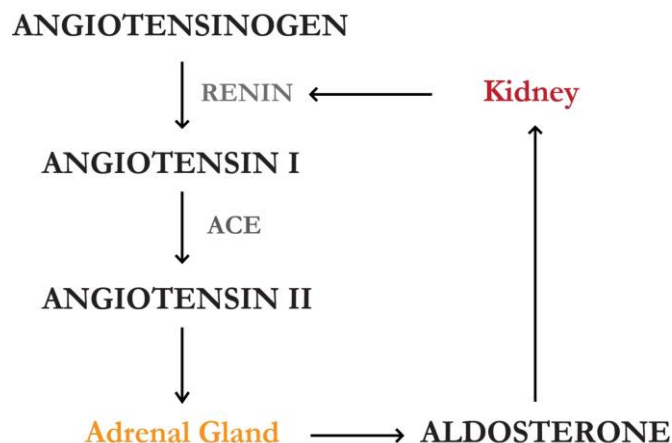


**Figure 1.4 Regulation of aldosterone production by the RAAS**

Aldosterone production in the zona glomerulosa is controlled by renin and angiotensin II through the renin-angiotensin-aldosterone system (RAAS). In response to blood pressure fluctuations, the kidney secretes renin; an enzyme which cleaves angiotensinogen into angiotensin I. Angiotensin converting enzyme (ACE) subsequently produces angiotensin II which signals to the adrenal gland to produce aldosterone. Aldosterone controls the reabsorption of sodium ions and water and secretion of potassium by the kidneys to restore blood pressure.

### **1.4.3 Mechanisms of action of steroid hormones**

The classical model of hormone action involves the steroid molecules eliciting physiological changes by binding receptors expressed by specific tissues. Nuclear steroid receptors show considerable homology to each other and consist of a carboxyl-terminal ligand binding domain; a variable amino-terminal domain that is predicted to modulate transactivation; and a central cysteine-rich domain for DNA binding (Kumar and McEwan, 2012). Ligand binding induces a conformational change in the receptor, exposing the DNA binding domain. Translocation into the nucleus enables the steroid-receptor complex to recognise and bind specific palindromic hormone response elements on genomic DNA. Regulation of steroid responsive genes is initiated through the receptor-ligand complex interacting with basal transcription complexes, activators,

repressors and transcription regulators (Beato and Klug, 2000). Steroid hormones also elicit rapid non-genomic actions. These effects involve the generation of second messengers (such as cAMP), and the activation of signalling cascades and ion fluxes to provide a dynamic response to steroid hormone signalling (Losel and Wehling, 2003).

## **1.5 Cytochrome P450 enzymes and steroid hormone production**

CYP enzymes are a diverse family of proteins which catalyse the oxidative activation or inactivation of endogenous and exogenous chemicals. This, in turn, has impact on normal and disease physiology. Typically, these evolutionary conserved enzymes are about 55 kDa in size, contain a single haem group and derive their name from their ability to absorb light maximally at 450 nm (Gonzalez, 1988). Eukaryotic CYP enzymes can be classified into two distinct groups based on their location within the cell. Class I CYP enzymes are located within the mitochondria and class II reside in microsomes. Along with their different cellular location, each class of CYP enzyme relies on different electron transfer systems for their catalytic activity. The microsomal type II enzymes receive electrons from nicotinamide adenine dinucleotide phosphate (NADPH) through P450 oxidoreductase (POR) and sometimes in conjunction with cytochrome b<sub>5</sub> (Miller, 2005). Conversely, all mitochondrial type I CYP enzymes receive electrons from NADPH via the redox co-factors ferredoxin reductase (FDR) and ferredoxin (FDX1). It is the redox regulation of mitochondrial CYP enzymes which is the focus of this study and will be discussed in detail below.

### **1.5.1 Mitochondrial steroid hormone synthesis**

Of the nine CYP enzymes involved in the synthesis of steroid hormones and 1,25-dihydroxy vitamin D, five are located in the mitochondria and rely on the ferredoxin electron transport chain for activity. The first reaction in steroid hormone production is catalysed by CYP11A1 and occurs in the mitochondria. Additionally, the final steps of glucocorticoid and mineralocorticoid synthesis are achieved by the mitochondrial CYP enzymes CYP11B1 and CYP11B2, respectively (Miller, 2013). As these reactions are essential for glucocorticoid and mineralocorticoid production it is imperative that the activity of these enzymes is tightly regulated to maintain normal physiology.

### **1.5.2 CYP11A1: The Cholesterol Side Chain-Cleavage Enzyme**

P450<sub>scc</sub> or CYP11A1 is a mitochondrial P450 enzyme which catalyses cholesterol to pregnenolone in the first step of steroid synthesis (Figure 1.5). Cholesterol is transported to the inner mitochondrial matrix by StAR before CYP11A1 catalyses three sequential monooxygenase reactions to generate pregnenolone. P450<sub>scc</sub> catalyses two hydroxylation reactions of cholesterol to produce 22R-hydroxycholesterol and then 20 $\alpha$ ,22R-dihydroxycholesterol. The final step involves the cleavage of the side chain to produce pregnenolone. Each reaction requires two electrons as reducing equivalents which are received from NADPH via the ferredoxin electron transport chain (Section 1.5.5) P450<sub>scc</sub> is encoded by the *CYP11A1* gene located on chromosome 15q23. Regulation of *CYP11A1* expression and P450<sub>scc</sub> activity is of particular importance for normal physiology. Expression of *CYP11A1* is stimulated by ACTH in all zones of the adrenal cortex, with additional regulation by angiotensin II in the zona glomerulosa. Cholesterol conversion to pregnenolone by CYP11A1 is a slow reaction which contributes to it being the rate-limiting step of steroid hormone production (Miller, 2013).

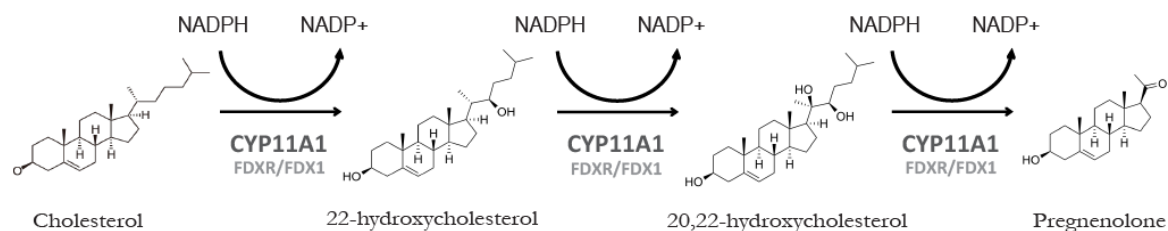


**Figure 1.5 Catalytic activity of Cholesterol P450 side chain-cleavage enzyme**

Cholesterol side-chain cleave enzyme (CYP11A1) catalyses the conversion of cholesterol to pregnenolone in three subsequent reactions. Initially, hydroxylation of cholesterol produces 22R-hydroxycholesterol and then 20 $\alpha$ ,22R-dihydroxycholesterol. The final step involves the cleavage of the side-chain to produce pregnenolone. Each monooxygenase step requires two electrons which are transferred from NADPH via the ferredoxin redox chain involving ferredoxin reductase (FDXR) and ferredoxin (FDX1).

### 1.5.3 *CYP11B1: The steroid 11 $\beta$ -hydroxylase enzyme*

CYP11B1 is a mitochondrial CYP enzyme which catalyses the final steps of cortisol synthesis (Figure 1.6). It is encoded by the *CYP11B1* gene and is located on chromosome 8q22, adjacent to its isozyme *CYP11B2*. CYP11B1 is the more abundant of the two *CYP11B* isozymes found in humans, and it is expressed in the zona fasciculata and somewhat in the zona reticularis of the adrenal cortex. It primarily converts 11-deoxycortisol to cortisol, but can also generate corticosterone from 11-deoxycorticosterone. Expression of *CYP11B1* is induced by ACTH via cAMP and can be suppressed by glucocorticoids.

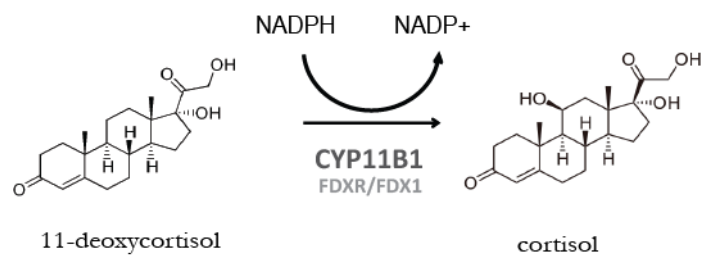


**Figure 1.6 Catalytic activity of 11 $\beta$ -hydroxylase enzyme**

The CYP enzyme 11 $\beta$ -hydroxylase converts 11-deoxycortisol into cortisol within the mitochondrial of cells in the zona fasciculata. For this reaction it requires electrons which are transferred from NADPH via the ferredoxin reductase (FDXR) and ferredoxin (FDX1).

#### **1.5.4 *CYP11B2: Aldosterone synthase***

The mitochondrial CYP enzyme aldosterone synthase is, as its name suggests, required for aldosterone production. It is localised to the zona glomerulosa of the adrenal cortex where it catalyses the final three steps in aldosterone synthesis; 11 $\beta$ -hydroxylation of 11-deoxycorticosterone to corticosterone, followed by 18-hydroxylation and 18-oxidation to produce aldosterone (Figure 1.7). Aldosterone synthase is encoded by the *CYP11B2* gene located 40 kb away from *CYP11B1* gene. These two human isozymes share 93 % amino acid identity, but unlike *CYP11B1*, expression of *CYP11B2* is regulated by potassium and angiotensin II.

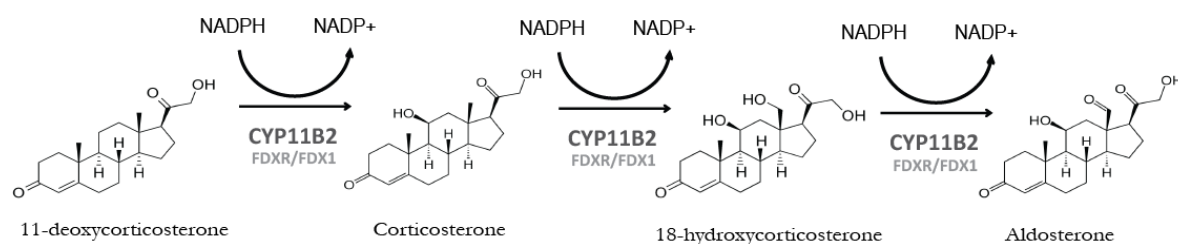


**Figure 1.7 Catalytic activity of aldosterone synthase**

The mitochondrial CYP enzyme aldosterone synthase (CYP11B2) catalyses the final three reactions required for mineralocorticoid synthesis. Two successive hydroxylations of deoxycorticosterone produce corticosterone and 18-hydroxycorticosterone. Subsequently, CYP11B2 oxidase activity converts 18-hydroxycorticosterone to aldosterone. Each step requires electrons from NADPH via the mitochondrial redox co-factors ferredoxin reductase (FDXR) and ferredoxin (FDX1).

### 1.5.5 *The mitochondrial redox electron transport chain*

Redox partner proteins are required for the transfer of electrons from NADPH to the haem centre of CYP enzymes. *In vitro* studies conclude that electron transfer co-factors regulate CYP catalytic activities by more than just their electron transfer. Since mitochondrial CYP enzymes rely on their redox partners for activity the nature of this interaction is of considerable importance for normal physiology.

#### 1.5.5.a. *Ferredoxin Reductase*

Human ferredoxin reductase (FDXR; adrenodoxin reductase; ADXR) is a 54-kDa flavoprotein which forms the first component of the electron transport to mitochondrial CYP enzymes. It is encoded by the *FDXR* gene on chromosome 17q24-q25 (Sparkes et al., 1991) and is alternatively spliced to generate two mRNA transcripts that differ by 18 nucleotides, but only the protein

encoded by the shorter mRNA is active in steroidogenesis (Brandt and Vickery, 1992). Although it is ubiquitously expressed, highest levels of expression occur in classical steroidogenic tissues, namely, the adrenal cortex, gonads and placenta (Brentano et al., 1992).

Unlike most steroidogenic genes, the promoter for *FDXR* contains the SP1 transcription binding sites which are typically found in “housekeeping genes” (Lin et al., 1990, Miller and Auchus, 2011). Additionally, cAMP from ACTH stimulation does not regulate transcription of the *FDXR* gene (Brentano et al., 1992). This suggests that dynamic changes in *FDXR* expression are not required for acute steroid hormone production. The electron transfer pathway begins when *FDXR* receives a pair of electrons from NADPH via its flexible carboxyl-terminal flavin adenine dinucleotide (FAD) domain (Kimura and Suzuki, 1967, Ziegler et al., 1999). It is loosely associated with the inner mitochondrial membrane where it interacts with ferredoxin, the second component of the mitochondrial redox chain.

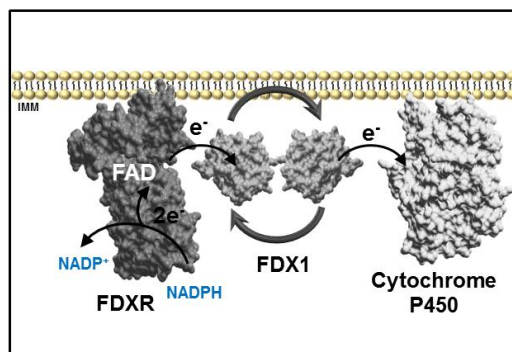


**Figure 1.8 The mitochondrial electron transfer system**

NADPH donates a pair of electrons (e<sup>-</sup>) to the FAD moiety of ferredoxin reductase (FDXR). FDXR interacts with ferredoxin 1 (FDX1) via charge-charge interactions and subsequently reduces it by transferring electrons to its Fe/S cluster. FDX1 then dissociates from FDXR and interacts via the same region with the mitochondrial cytochrome P450 enzyme. The electrons are transferred to the haem ring of the P450 enzyme, allowing it to mediate its catalytic conversion of the bound substrate. (IMM: Inner mitochondrial membrane).

#### **1.5.5.b. Ferredoxin**

Ferredoxins are iron-sulphur proteins which act as electron donors for a variety of fundamental reactions catalysed by mitochondrial CYP enzymes. The human ferredoxin 1 (FDX1; adrenodoxin; ADX) is a small (14 kDa) protein which resides in the mitochondrial matrix or closely associated with the inner mitochondrial membrane. It is involved in various metabolic processes including the synthesis of steroid hormones, vitamin D and bile acids (Meyer, 2008). The *FDX1* gene is located on chromosome 11q22 and spans over 30 kb. In humans, FDX1 is ubiquitously expressed; however, it is most abundant in steroidogenic tissue including the adrenal gland and the gonads (Picado-Leonard et al., 1988). Humans have two ferredoxin genes, *FDX1* and *FDX2* (previously termed *fdx1-like*) however, only FDX1 activity supports steroidogenic mitochondrial CYP enzymes (Sheftel et al., 2010). Electron transfer from FDX1 is critical for the catalytic activity of all mitochondrial CYP enzymes including CYP11A1, CYP11B1 and CYP11B2 (Miller and Auchus, 2011). Therefore, it is hypothesised that FDX1 plays a key role in regulating the steroid hormone producing capacities of a cell.

#### **1.5.6 Regulation of the mitochondrial electron transfer chain**

Currently little is known about the physiological importance of mitochondrial redox partner interactions in regulating steroid hormone production. Since this electron transfer mechanism was discovered in 1965 (Kimura and Suzuki, 1965, Suzuki and Kimura, 1965), the effects of FDX1 on CYP enzymatic activity has been the focus of several *in vitro* studies. Cumulatively, these studies show the amino acid sequence, redox potential, concentration of FDX1 as well as its amiability to phosphorylation can influence CYP enzyme activity (Figure 1.9).

The concentration of FDX1 in the mitochondria is hypothesised to influence the activity of CYP enzymes. Lambeth and Kriengsiri (1985) suggested CYP11A1 reduction was not dependent on

FDX1 concentration. However, more recent studies show a correlation between increasing FDX1 concentrations and increasing CYP enzyme activity (Beckert and Bernhardt, 1997). Discrepancies between these results is not clear, but it is suggested different reaction conditions and advances in data processing allow for more sensitive evaluation of measurements in the recent study (Ewen et al., 2011). Both FDX1 and FDXR transcription is regulated by SF1 (Imamichi et al., 2013, 2014) the main transcription factor regulating steroid hormone production; however, only FDX1 expression is up-regulated upon treatment of ovarian Granulosa cells with cAMP indicating FDX1 is required for dynamic changes in steroid hormone production (Imamichi et al., 2013). Given the similarity in transcriptional regulation between FDX1 and steroidogenic CYP enzymes, together with the latest functional activity data, it is likely that increases in FDX1 is a mechanism to increase CYP450 functional activity via the promotion of electron transfer.

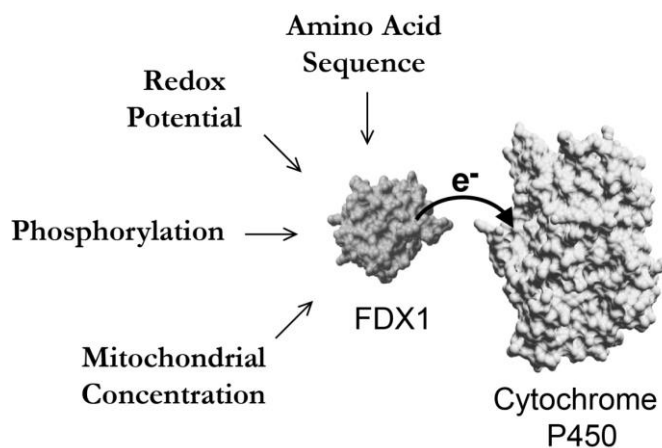


**Figure 1.9 Modulation of Fdx1 dependent CYP enzymatic reactions *in vitro***

The ability to transfer electrons is critical for FDX1 function. *In vitro* data suggests increased concentrations of FDX1 can directly affect the catalytic rate of CYP enzymes. In addition phosphorylation, amino acid sequence and redox potential are all capable of modifying FDX1 binding behaviour to its redox partners, and subsequently alters CYP activity.

Moreover, the efficiency of the interaction between redox partners can influence the catalytic rate of mitochondrial CYP enzymes. The transfer of electrons occurs during the protein-protein interaction between the electron donor and acceptor (Beratan et al., 1992). Using stop flow kinetic studies to determine the rate of electron transfer, the limiting step of the of the FDXR/FDX1/CYP11A1 redox chain was the interaction between FDX1 and CYP11A1 (Schiffler et al., 2011); highlighting the importance of this interaction. The bovine FDX1 Ser112Trp mutant has increased affinity to CYP11A1 and causes enhanced pregnenolone production from cholesterol (Schiffler et al., 2001). Furthermore, phosphorylation of bovine FDX1 at Thr71 causes enhanced affinity for CYP11A1, but not CYP11B1, which in turn improves pregnenolone production *in vitro* (Bureik et al., 2005). Given CYP11A1 is the first and rate limiting step of steroidogenesis, its interaction with FDX1 is likely to have consequences for *in vivo* steroid hormone production.

Finally, changes in redox potential can also influence CYP catalytic activity. The redox potential of a protein refers to its ability to acquire and donate electrons. FDX1 mutants with differing redox potentials can affect CYP catalytic activity *in vitro*. The bovine mutants FDX1 4-114 and FDX1 4-108 display increased electron transfer properties. Through their interaction with CYP11B2, these mutants increase the synthesis of corticosterone and aldosterone (Cao and Bernhardt, 1999). Furthermore, many *in vitro* studies (including the ones performed in this study) are routinely used with a mutant form of bovine adrenal Fdx1 (Fdx1 4-108) (Uhlmann et al., 1994). The truncation causes Fdx1 to have a more negative redox potential which results in increased CYP catalytic activity and improved substrate conversion (Ewen et al., 2012). The redox potential of ferredoxins is a critical factor in their ability to shuttle electrons from FDXR to mitochondrial CYP enzymes. All-in-all comprehensive *in vitro* studies have shown modulation of

FDX1 can influence the catalytic activity of CYP enzymes. However, the physiological *in vivo* consequences of FDX1 interactions remain undetermined.

## **1.6 Deregulation of mitochondrial steroid production causes disease**

### **1.6.1 *CYP11A1* deficiency**

CYP11A1 deficiency is an autosomal recessive condition caused by mutations in the *CYP11A1* gene. Several patients have been described with *CYP11A1* mutations rendering partial or complete inactivity of P450<sub>scc</sub> (Hiort et al., 2005, Kandari et al., 2006, Katsumata et al., 2002, Kim et al., 2008, Parajes et al., 2012, Parajes et al., 2011, Rubtsov et al., 2009, Sahakitrungruang et al., 2011, Tajima et al., 2001). These patients suffer from impairment of glucocorticoid and mineralocorticoids synthesis causing adrenal insufficiency. Interestingly, CYP11A1 deficiency is the only inborn error of steroidogenesis leading to adrenal atrophy, even in partial deficiencies (Parajes et al., 2011), rather than to hyperplasia of the adrenal cortex (Kim et al., 2008, Parajes et al., 2012, Parajes et al., 2011). Since the electron transfer between FDX1 and CYP11A1 *in vitro* is only 66 to 75 % efficient (Miller and Auchus, 2011) it is hypothesised the remaining electrons contribute to reactive oxygen generation. This reactive oxygen species production is predicted to induce apoptosis of the adrenal cortex and is likely to represent an exaggerated form of adrenal ageing. However, such mechanism cannot be determined by *in vitro* studies, and require *in vivo* analysis.

### **1.6.2 *CYP11B1 deficiency and deregulation***

Functionally disrupting *CYP11B1* mutations are the second most common cause of congenital adrenal hyperplasia in most populations (approximately 5–8% of all cases) (White et al., 1994). A lack of cortisol production in these patients results in an up regulation of the HPA axis, causing increased cortisol steroid precursors which are metabolised to adrenal androgens. The excess production of androgens leads to abnormalities in sexual development. Conversely, genetic variation in *CYP11B1* has also been linked with hypertension and primary hyperaldosteronism (Freel et al., 2008, Zhang et al., 2010). Patients with elevated levels of cortisol have been associated with cardiovascular risk factors such as components of metabolic syndrome (Fraser et al., 1999, Whitworth et al., 2005), accelerated atherosclerosis (Dekker et al., 2008), depression and subsequent increases in morbidity and mortality (Rosmond, 2005).

### **1.6.3 *CYP11B2 deficiency and deregulation***

Deficiencies in aldosterone synthases from mutations within *CYP11B2* cause excessive sodium excretion and potassium retention resulting in hyponatremia, hyperkalemia and metabolic acidosis. The complete absence of aldosterone synthases generally results in salt-wasting crisis in infancy (Peter et al., 1995), whereas patients with partially inactivating mutations in *CYP11B2* present with milder phenotypes in childhood or adulthood (Hui et al., 2014, Kayes-Wandover et al., 2001). Conversely, the excessive production of aldosterone is implicated in the pathogenesis of hypertension and heart disease. The *CYP11B2* C344T polymorphism (rs1799998) is associated with higher levels of aldosterone production, hypertension and primary aldosteronism (Kumar et al., 2003). Primary aldosteronism is due to an excessive and autonomous secretion of aldosterone and is associated with a significant increase in cardiovascular morbidity and mortality in hypertensive patients. Therefore, specific inhibition of *CYP11B2* is being investigated as a potential target for the treatment of hypertension, renal disease and heart failure (Liu et al., 2014).

#### **1.6.4 Mitochondrial redox co-factors in disease**

To date there have been no patients described with FDX1 or FDXR deficiencies. Furthermore, knockout mouse models have not been generated, limiting *in vivo* studies thus far. *Drosophila* knockouts of the FDXR homologue gene *dare* undergo developmental arrest due to lack of steroid hormone production; supporting the idea the mitochondrial redox pathway is functionally important for early development (Freeman et al., 1999). It is suggested that a human foetus deficient in FDX1 would result in spontaneous abortion around six to seven week gestation, due to loss in pregnenolone synthesis (Miller, 1998). However, given *CYP11A1* deficient patients have survived, it is feasible that *FDX1* mutations leading to partial loss of function would be compatible with life.

Mutations in the electron donor of microsomal CYP enzymes, POR, are known to result in multiple clinical manifestations (Pandey and Fluck, 2013). Although *POR* knockout mice are embryonic lethal (Otto et al., 2003), humans with complete *POR* deficiency can present with a disorder of steroidogenesis associated with Antley-Bisler skeletal malformation syndrome. Additionally, mild *POR* mutations were present in phenotypically normal adults with infertility (Scott and Miller, 2008). The identification of mutations in *POR* highlights the importance of redox cofactors in disease and normal physiology.

Numerous *in vitro* studies have shown that modulation of FDX1 can influence steroid hormone production through modifying CYP enzymatic activity, suggesting the deregulation of redox co-factors may have pathophysiological consequences. Indeed, FDX1 has been identified in whole genome association studies as a genetic risk factor of obesity (Xu et al., 2013b). Furthermore, it is hypothesised the deregulation in FDX1 may be a cause of common disease such as hypertension or cardiac disease through increased production 18-hydroxycorticosterone

and aldosterone (Cao and Bernhardt, 1999). However, the precise impact of how this mitochondrial redox protein impacts physiological or pathological conditions requires further *in vivo* studies.

## *Part Two: Zebrafish - An emerging model for endocrine disease*

### **1.7 Zebrafish**

The zebrafish (*Danio rerio*) is a small tropical freshwater fish naturally found in rivers throughout South Asia. It is a member of the teleost class along with other bony fish such as the medaka (*Oryzias latipes*), the three-spined stickleback (*Gasterosteus aculeatus*) and pufferfish species (*Takifugu rubripes* and *Tetraodon nigroviridis*). Zebrafish have commonly been used in developmental biology studies, however its popularity has now extended into other fields including translational research, cancer, toxicology and drug discovery (Ablain and Zon, 2013).

#### ***1.7.1 Advantages of zebrafish as a vertebrate model system***

Zebrafish have several advantages lending it to be amenable for biomedical research. Particularly, external fertilisation prevents many of the problems associated with other *in vivo* models which develop *in utero* and provides easy collection of fertilised eggs for genetic manipulation by microinjection. Additionally, offspring can be generated in large numbers compared to other vertebrate models, making them particularly ideal for high throughput screening studies. Pharmacological studies can be easily performed by altering media conditions (Zon and Peterson, 2005) and embryos are small enough to fit in 96-well or 384-well plates facilitating high throughput screening of chemical libraries (Peterson et al., 2000, Xu et al., 2013a). Moreover, embryos are transparent making them ideal for visualisation studies, and by fluorescently marking specific cells, researchers can track precise cells during development. Finally, zebrafish have rapid organ development and tissue maturation, with the majority of systems functional within the first 48 hours post fertilisation (hpf). With the exception of few tissues (notably lungs, prostate and mammary gland) most organs in humans are present in zebrafish making them ideal for developmental and translational studies (Kari et al., 2007).

### **1.7.2      *Studying vertebrate gene function in zebrafish***

To effectively translate zebrafish studies to human development and disease it is important to recognise how zebrafish genes relate to orthologous human genes. Analysis of the zebrafish genome sequence revealed 70 % of human genes have counterparts in zebrafish (Howe et al., 2013). Between 305 and 450 million years ago, the common teleost ancestor underwent a whole genome duplication (Amores et al., 1998, Postlethwait et al., 1998, Woods et al., 2000). This resulted in 26 % of zebrafish genes being present as a duplicate copy (Howe et al., 2013). During evolution, these paralogues can undergo subfunctionalisation (Force et al., 1999), where duplicate genes diverge in function or expression (Kassahn et al., 2009). Often the combined mechanisms of the zebrafish paralogues are equivalent to the single orthologue in other vertebrates (Schartl, 2014). Studying duplicated genes, either via changes in regulatory control or via changes in protein function, can contribute to the understanding of how genes evolve and provide insight into regulatory mechanisms or new functional adaptations. Additionally, subfunctionalisation can also allow for the study of genes involved in disease development in adult fish without effecting early development.

#### **1.7.2.a.      *Antisense morpholino knockdown strategies***

Gene knockdown by antisense RNA interference is a technique commonly used both in *in vitro* and *in vivo* model systems. The most widely used method to study a gene function in zebrafish is by antisense morpholino. Morpholinos are 25 base-pair oligonucleotides typically designed to inhibit protein translation by binding the region surrounding the start methionine codon, or disrupt splicing of the precursor mRNA by binding a splice junction site (Figure 1.10). Commonly, morpholinos are injected into single cell embryos where they effectively bind RNA transcripts during development. As the cells divide and the embryo rapidly grows the morpholino

becomes diluted and subsequently less effective, resulting in a transient knockdown. However, as most tissues, including the endocrine system is developed with the first few days after fertilisation (Lohr and Hammerschmidt, 2011), transient knockdown is usually sufficient to investigate gene function. A major advantage of using morpholino to study gene function is their ease of use. Coupled with the high fecundity of zebrafish, morpholinos can be easily injected into several hundred embryos for a single experiment making high throughput gene analysis studies possible.

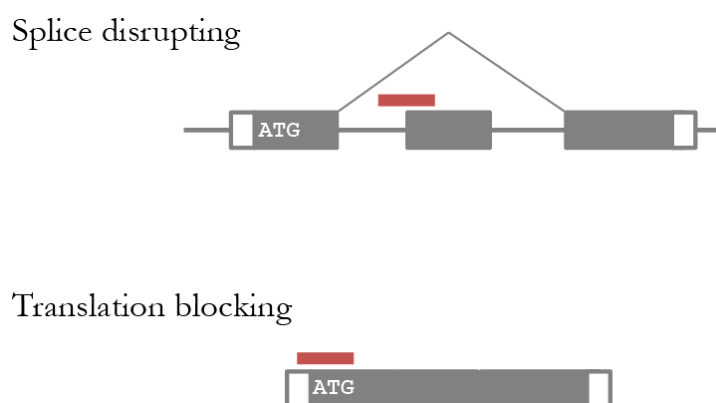


**Figure 1.10 Mechanism of action by antisense morpholino oligonucleotides**

Antisense morpholino oligonucleotides (shown in red) knock-down gene expression disrupting splicing of the pre-mRNA or blocking translation of mRNA into functional protein. Morpholinos are 25 nucleotides long and are designed to bind over intron-exon splice junctions or over the ATG start codon of the targeted gene.

Despite their prevalence among zebrafish researchers, morpholinos often elicit off-target effects which are not associated with the loss of the targeted gene. These artefacts are difficult to separate from those caused by the binding the specific RNA (Eisen and Smith, 2008), and often present as developmental delay, pericardial oedema, neural toxicity, or craniofacial defects (Bedell

et al., 2011, Schulte-Merker and Stainier, 2014). Often specificity of a phenotype is confirmed by comparing with a separate morpholino targeting the same gene, injection of a control morpholino or by rescuing the phenotype with co-injection of targeted mRNA. However, even with stringent controls several morpholino studies do not correlate with zebrafish harbouring a loss-of-function genetic mutation (den Broeder et al., 2009, Law and Sargent, 2014, Nichols et al., 2013). In light of these studies and the recent development of alternative reverse genetic approaches (Section 1.7.2.b), many researchers are opting for the generation of specific genetic knockouts over the transient knockdown morpholino approach (Schulte-Merker and Stainier, 2014).

#### ***1.7.2.b. Genomic editing in zebrafish***

Over the past decade major advances have been made in the area of genome engineering techniques. These methods have allowed for fast, easy and efficient modification of endogenous genes in a range of cell types and model organisms. To date, several classes of adaptive DNA binding tools have been developed, including: Zinc-finger nucleases (ZFNs) developed from eukaryotic transcription factors (Bibikova et al., 2003, Urnov et al., 2005), transcription activator-like effector nucleases (TALENs) (Cermak et al., 2011, Huang et al., 2011, Sander et al., 2011) (Chapter 5.0) and the more recently developed clustered regulatory interspaced short palindromic repeat (CRISPR)/Cas9-based RNA-guided DNA endonucleases (Jiang et al., 2013, Pattanayak et al., 2013b) (Chapter 6.0). These technologies are now widely available to researchers and are rapidly becoming routine molecular biology techniques.

All of the available genome engineering methods rely on the principal of making targeted chromosomal breaks. In an effort to maintain chromosomal integrity these breaks are repaired via endogenous cellular repair mechanisms: non-homologous end joining (NHEJ) or homology

directed (HD) repair to generate desired genetic modifications (Figure 1.11) (Wyman and Kanaar, 2006). NHEJ is the major chromosomal repair pathway in mammals and involves the ligation of chromosomal ends without a homologous template (Liang et al., 1998). This repair method is error prone and can lead to the insertion/deletion (commonly termed indels) of nucleotides which disrupt the translational reading frame of a protein or interrupt the binding site for trans-acting factors within their promoters. Subsequently, an out-of-frame mutation rendering a non-functional protein or impaired gene expression creates a null allele. Alternately to NHEJ, HD-mediated repair uses recombination with an exogenously supplied donor template carrying the specific insertion or mutation. HD has traditionally been used to generate knockin and knockout animal models by altering the genome of embryonic stem cells. Still, with the efficiency of recombination being low (one in  $10^6$  to  $10^9$ ) (Capecchi, 1989), large scale applications of gene targeting is challenging. Chromosomal breaks increase the efficiency HD-mediated repair in mammalian cells (Choulika et al., 1995). Genomic editing methods are now being used to create genomic insertions of functional elements in zebrafish; including loxP recombination sites (Bedell et al., 2012) and fluorescent proteins (eGFP) (Zu et al., 2013). Therefore, targeted chromosomal breaks in combination with donor templates can facilitate precise modifications of genomic regions in zebrafish.

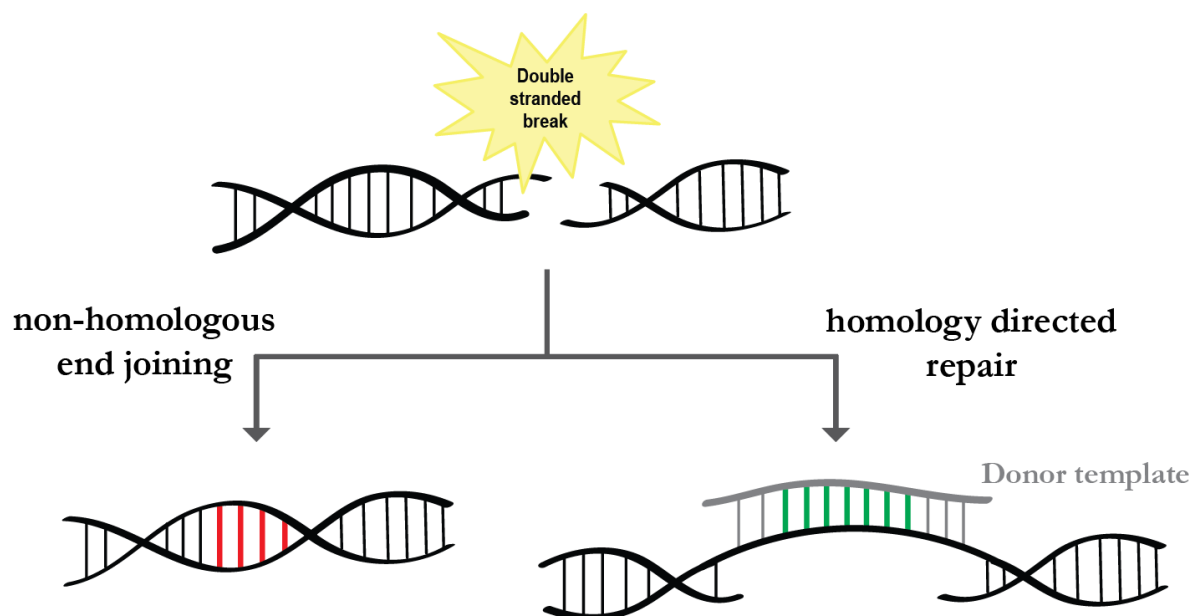


**Figure 1.11 Cellular repair mechanisms of chromosomal breaks**

Double stranded DNA breaks (DSB) can be repaired by two mechanisms; non-homologous end joining (NHEJ) and homology directed (HD) repair. NHEJ is error prone and generates insertions or deletions (red) which generate out-of-frame mutations to disrupt protein function. HR requires a homologous donor template which guides the repair. By providing an exogenous donor template with a specific mutation (green) flanked by homologous ends, specific sequences can be inserted at precise loci within the genome.

### ***1.7.3 Translational research and modelling genetic diseases in zebrafish***

Zebrafish are becoming an increasing prevalent model for human genetic diseases due to the high degree of conservation of molecules and pathways between the two species. Genome analysis showed more than 75 % of human genes implicated in disease have counterparts in the zebrafish. This has allowed zebrafish to be a valuable model for a number of human genetic conditions including, neurological and psychiatric disorders, cancer, heart defects, foetal alcohol syndrome and kidney disorders (Phillips and Westerfield, 2014). Only recently has the benefit of zebrafish

been used to study endocrine physiology and disease. Characterisation of the endocrine system between humans and zebrafish revealed it is well conserved (McGonnell and Fowkes, 2006). Importantly, the development of the endocrine system is complete and functional by five days post fertilisation (dpf). Therefore, it is possible to model human endocrine diseases and developmental physiology, taking full advantage of this *in vivo* model system. Even with the apparent differences between zebrafish and humans, using zebrafish for disease modelling, chemical screening and gene function discovery is becoming more prevalent and generating new insights in understanding pathogenesis of human disease at a molecular and cellular level.

## **1.8 Conservation of steroid hormone pathway in zebrafish**

### ***1.8.1 Glucocorticoid production in zebrafish***

Like humans, cortisol is the main glucocorticoid in zebrafish and its production relies on conserved steroidogenesis genes. Glucocorticoid synthesis begins with the import of cholesterol into the mitochondria where the zebrafish P450<sub>scc</sub> enzymes, Cyp11a1 or Cyp11a2 produce pregnenolone (Hsu et al., 2006, Parajes et al., 2013). Successively, the 17 $\alpha$ -monooxygenase isozymes (Cyp17a1 and Cyp17a2), the 3 $\beta$ -hydroxysteroid dehydrogenase (3 $\beta$ Hsd1 and 3 $\beta$ Hsd2) and the single cytochrome 21-hydroxylase enzyme produce 17-pregnenolone, 17-hydroxypregnenolone and 11-deoxycortisol, respectively. A final step catalysed by the single 11 $\beta$ -hydroxylase isozyme converts 11-deoxycortisol to cortisol (Mommsen et al., 1999) (Figure 1.12).

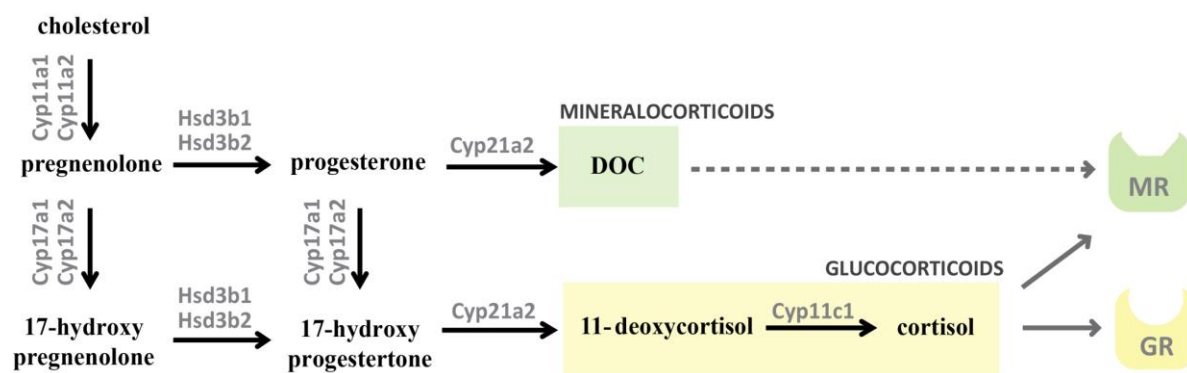


**Figure 1.12** The postulated pathway for glucocorticoid production in zebrafish

Like humans, cortisol is the main glucocorticoid in zebrafish and it is synthesised from cholesterol. Many of the steroidogenic enzymes are duplicated in zebrafish, including the first step by the P450 side chain cleavage orthologues, Cyp11a1 and Cyp11a2. Pregnenolone is successively converted by the 17 hydroxylase enzymes (Cyp17a1 and Cyp17a2), the  $3\beta$ -hydroxysteroid dehydrogenase enzymes (Hsd3b1 and Hsd3b2) and the single 21-hydroxylase enzyme (Cyp21a2). Cyp11c1 is the single  $11\beta$ -hydroxylase enzyme which generates cortisol from 11-deoxycortisol. Cortisol performs both glucocorticoid and mineralocorticoid actions through binding of glucocorticoid receptor (GR) and the mineralocorticoid receptor (MR) on targeted tissues, respectively. 11-deoxycorticosterone, DOC.

As in humans, cortisol in zebrafish is produced in response to stress and in a circadian rhythm under the regulation of the hypothalamus and the pituitary (Alsop and Vijayan, 2008, Fuzzen et al., 2011, To et al., 2007). The primary targets of cortisol are the gills, brain, intestine, muscles and liver to help mobilise energy stores to cope with stressors (Lin et al., 2011, Lohr and Hammerschmidt, 2011). Furthermore, GR null fish are chronically stressed and exhibit behavioural changes indicative of depression, suggesting glucocorticoids have additional roles in behaviour and brain function (Ziv et al., 2013). Like in a number of other species cortisol is present in unfertilised eggs and is necessary for development of the embryo (Nesan and Vijayan,

2013, Pikulkaew et al., 2011). Inhibition of early cortisol action leads to defects in mesoderm formation (Pikulkaew et al., 2011), muscle development (Nesan et al., 2012), craniofacial development (Hillegass et al., 2008) and cardiac performance (Nesan and Vijayan, 2012) in the developing zebrafish. Overall, studies have revealed that cortisol mechanisms of action are essential for embryonic development and adult life and it provides a useful model for further insight into the role of glucocorticoids in development and disease.

In addition to its glucocorticoid actions, cortisol controls ionic and osmotic regulation in teleost fish. In order to maintain hypertonic body fluids in a fresh water environment, zebrafish absorb ions; a process thought to be regulated predominantly by cortisol (Kumai et al., 2012, Laurent and Perry, 1990, Lin et al., 2011). The human MR has two physiological ligands, aldosterone and cortisol (Fuller et al., 2012). It is generally accepted that teleost fish are unable to synthesise the mineralocorticoid aldosterone, despite having a highly conserved MR (Pippal et al., 2011). Although less potent than aldosterone and deoxycorticosterone (Colombe et al., 2000), cortisol can bind and activate the zebrafish MR *in vitro* suggesting this hormone can regulate mineralocorticoid physiological actions in zebrafish (Pippal et al., 2011). Conversely, others have hypothesised that 11-deoxycorticosterone might be the ligand for the teleost mineralocorticoid receptor (Bury and Sturm, 2007, Gilmour, 2005, Prunet et al., 2006, Sturm et al., 2005). Deoxycorticosterone is present in teleost fish in significant concentrations and binds the MR (Pippal et al., 2011, Sturm et al., 2005). However, the zebrafish's adaption to hypertonic environments was not mediated by 11-deoxycorticosterone (McCormick et al., 2008). Regardless, teleost corticosteroids (cortisol and/or deoxycorticosterone) have critical roles in electrolyte homeostasis, possible roles in energy metabolism and ion regulation (Gilmour, 2005). However, evidence on the specific role of mineralocorticoids in zebrafish is considerably less than its glucocorticoids counterparts and requires further investigation.

## **1.9 The regulation of glucocorticoid production in zebrafish**

### ***1.9.1 The zebrafish interrenal***

The zebrafish interrenal is the equivalent of the mammalian adrenal gland (Hsu et al., 2003, Liu, 2007). Structurally, the interrenal is located within the anterior part of the zebrafish kidney. It is imbedded amongst the chromaffin cells within the kidney head, rather than a distinct organ on top of the kidneys like in the mammal. However, like the mammalian adrenal gland, the zebrafish interrenal shares its origins from the kidney and gonadal primordia under the regulation of Wilms' tumour suppressor 1 (WT1) transcription factor (Bandiera et al., 2013, Hsu et al., 2003, Luo et al., 1994). WT1 causes differentiation of the interrenal cells through regulating expression of the transcriptional activator Ff1b, the homologue to the mammalian SF1. Both *ff1b* deficient zebrafish (Hsu et al., 2003) and *SF1* knockout mice (Lala et al., 1995, Luo et al., 1995) fail to develop interrenal tissue or adrenal glands, respectively. Additionally, the functional role of the interrenal is also well conserved. It is the primary site of steroid synthesis in teleost fish (Grassi Milano et al., 1997). It expresses genes required for steroid hormone synthesis, including *StAR*, *cyp11a2*, and *3 $\beta$ -hsd* which are required for interrenal function (Hsu et al., 2003, Keegan and Hammer, 2002, Parajes et al., 2013). Although the structural organisation of the endocrine gland is different between teleost fish and mammals, the development during organogenesis and functional capabilities are highly conserved.

### ***1.9.2 Hypothalamus-pituitary-interrenal axis***

Zebrafish have proved to be an excellent model to gain insights into the corticoid stress axis in vertebrates. In higher vertebrates, CRH from the hypothalamus drives *POMC* expression in the pituitary, giving rise to ACTH to regulate glucocorticoid production in the adrenal glands. Although two *POMC* genes have been identified in zebrafish (de Souza et al., 2005, Gonzalez-

Nunez et al., 2003b), only one is capable of generating ACTH (Gonzalez-Nunez et al., 2003a). Additionally, zebrafish have a single *CRH* gene capable of generating the mature CRH peptide which is highly conserved with the human orthologue (Chandrasekar et al., 2007) (Figure 1.13).

### ***1.9.3 Development of the hypothalamus-pituitary-interrenal axis***

Whole-mount *in situ* hybridisation of established markers for the hypothalamus and pituitary show these structures are present in the developing zebrafish larvae from 24 hpf (Alsop and Vijayan, 2009). Furthermore, by 97 hpf interrenal function is dependent of pituitary signals indicating a functioning HPI axis (Alsop and Vijayan, 2009, To et al., 2007). Upon stress (Alsop and Vijayan, 2009) or prior to the peak of cortisol during the diurnal rhythm (Dickmeis, 2009), CRH is secreted by the hypothalamus which signals the pituitary gland to produce ACTH (Alsop and Vijayan, 2009). Subsequent glucocorticoid synthesis occurs when circulating ACTH binds the MC2R on the surface of the interrenal cells (Alderman and Bernier, 2009, Alsop and Vijayan, 2008). On the whole, the molecular mechanisms and development of the HPI axis in zebrafish is analogous to the mammalian HPA axis, and therefore zebrafish provide a suitable model to investigate the regulation of steroid hormone production.

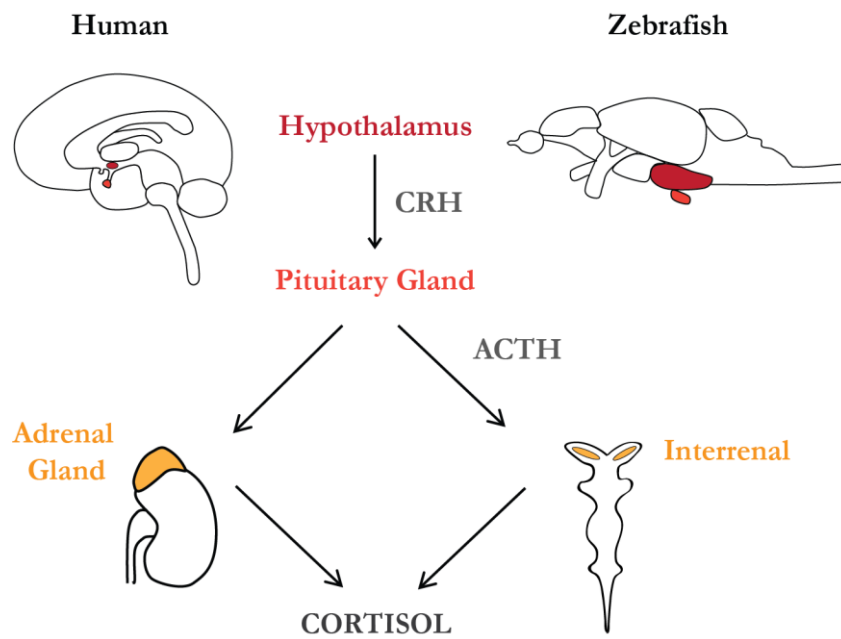


**Figure 1.13 Comparison of cortisol production between humans and zebrafish**

In humans, the hypothalamus and pituitary gland regulate cortisol production from the adrenal gland. Corticotropin releasing hormone (CRH) is produced by the hypothalamus in the brain in response to stress. It signals to the pituitary gland which produces adrenocorticotropic hormone (ACTH). ACTH signals to the adrenal gland to synthesise cortisol. Although structural different the same regulatory pathway is conserved in zebrafish. The zebrafish interrenal is the counterpart of the mammalian adrenal gland. It consists of endocrine cells imbedded within the kidney head.

## 1.10 The role of mitochondrial CYP genes in zebrafish

Zebrafish are a comprehensive model which allows the *in vivo* investigation into gene function, development and disease. Despite the evolutionary distances between mammals and fish, the developmental programming, key enzymes and physiological functions of endocrine signalling are highly conserved (Chai et al., 2003, Hsu et al., 2003). Due to the whole genome duplication of the common teleost ancestor, many zebrafish steroidogenesis genes exist in two copies; however, to date there is limited information on expression or function of individual paralogues.

### 1.10.1 Cholesterol Side Chain-Cleavage Enzyme

In humans, P450<sub>scc</sub> (encoded by the *CYP11A1* gene) converts cholesterol to pregnenolone during the first reaction of steroidogenesis. Zebrafish have duplicated *CYP11A* genes termed *cyp11a1* and *cyp11a2* (Goldstone et al., 2010). To date, work has largely focused on the *cyp11a1* paralogue (Hsu et al., 2006). This gene is expressed as a maternal transcript and by the zygote during embryonic development. Cyp11a1 facilitates the synthesis of pregnenolone which stabilises the microtubules. The dynamic changes in the microtubule network are essential for the coordinated movement of the blastoderm around the yolk during epiboly (Lee, 2014). Consequently, Cyp11a1 is essential for early zebrafish development (Hsu et al., 2006). Until this current study the functional capabilities and developmental role of Cyp11a2 remained unknown. We showed *cyp11a2* expression coincides with the development of the interrenal tissue. Additionally, in adults, its expression is restricted to the steroidogenic tissues of the interrenal, gonads and brain. Furthermore, knockdown of *cyp11a2* impairs *de novo* pregnenolone and subsequent cortisol production, which suggests Cyp11a2 is the functional orthologue of human CYP11A1 (Parajes et al., 2013) (Chapter 4.0).

### **1.10.2 Steroid 11 $\beta$ hydroxylase**

The relationship between zebrafish and human genes is often defined in terms of orthologues in which genes share the same ancestral gene. Zebrafish have a single identified Cyp11b-like gene, termed *cyp11c1* (Goldstone et al., 2010). Studies suggest mammalian *CYP11B1* evolved from *cyp11c1* of fish (Nelson et al., 2013), however, zebrafish *cyp11c1* does not share synteny with any tetrapod *Cyp11b* genes (Goldstone et al., 2010). With the exception of rainbow trout all teleost fish have retained a single *cyp11c* gene after the whole genome duplication event. Cyp11c1 is required for cortisol production, however, whether teleost Cyp11c1 has dual 11- and 18-hydroxylase activity for mineralocorticoid production remains undetermined. Located on chromosome 16, zebrafish *cyp11c1* expression is up regulated between 24 and 48 hpf coinciding with the beginning of *de novo* steroidogenesis (Wang and Orban, 2007, Wilson et al., 2013). Furthermore, both the treatment of embryos with an 11 $\beta$ -hydroxylase inhibitor (Metyrapone) and morpholino knockdown of Cyp11c1 impair cortisol production in zebrafish embryos (Wilson et al., 2013).

Most research to date on the functional characteristics of Cyp11c1 has focused on its role in androgen production. Cyp11c1 is required for the synthesis of 11-ketotestosterone, the main androgen in teleost fish (Fuzzen et al., 2011, Kusakabe et al., 2002). In zebrafish, testosterone is hydroxylated by 11 $\beta$ -hydroxylase to produce 11 $\beta$ -hydroxytestosterone, which is the substrate for 11 $\beta$ -Hsd2 to produce 11-ketotestosterone (Figure 1.14). Cyp11c1 is implicated in gonadal differentiation and it is highly expressed in the androgen producing Leydig cells of the adult testis (Sreenivasan et al., 2008, Wang and Orban, 2007).

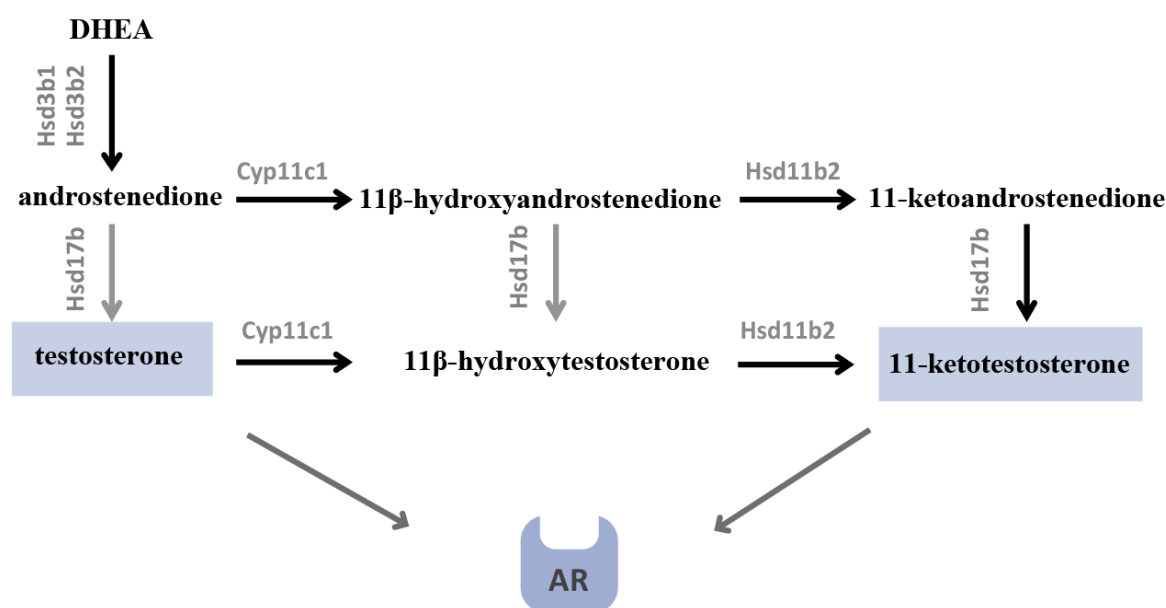


**Figure 1.14 Androgen production in zebrafish**

The principal androgen in zebrafish is 11-ketotestosterone. It is primarily synthesised in the testis from conversion of androstenedione to 11 $\beta$ -hydroxyandrostenedione and subsequent production of 11-ketoandrostenedione. 11-ketotestosterone and the less abundant testosterone are capable of binding and transactivating the androgen receptor (AR) and are predicted the most physiologically relevant androgens. Steroidogenic enzymes are shown in grey. Cyp11c1, 11 $\beta$ -hydroxylase; Hsd11b2, 11 $\beta$ -hydroxysteroid dehydrogenase type 2; Hsd17b, 17 $\beta$ -hydroxysteroid dehydrogenase.

### **1.10.3 Mitochondrial electron transport chain**

It is well established that ferredoxins are evolutionary well conserved (Ewen et al., 2012), however information of this redox pathway in teleost fish is limited. A single study identified an adrenodoxin-like peptide in the interrenal of the closely related sea bass (*Lates calcarifer*) and tilapia (Sampath-Kumar, 1994). This suggests the mitochondrial redox co-factors involved in steroidogenesis are conserved in the teleost lineage. Furthermore, gene expression profiling of zebrafish treated with androgen receptor antagonists (Flutamide and Vincolzolin), showed a

significant suppression in *fdx1* transcripts in males, along with other genes involved in androgen biosynthesis (Martinovic-Weigelt et al., 2011). This advocates a possible role in regulating sex steroid synthesis. To date the characterisation of the specific zebrafish paralogues and their functional roles has not been reported and will be one of the objectives of this current study.

## *Part Three: Project rational*

### **1.11 Rational for work**

The year 2015 will mark 50 years since the isolation of human FDX1, however, the detailed mechanisms of how this protein works are still poorly understood (Omura, 2011, Suzuki and Kimura, 1965). Furthermore, the significance of mitochondrial redox co-factor regulation in health and disease remains unknown. Given the dependence of mitochondrial CYP enzymes for electron transfer through FDX1, this interaction is of particular importance. *In vitro* discoveries have highlighted that FDX1 modifications can influence steroid hormone synthesis. In contrast, the impact of redox regulation on mitochondrial CYP enzymes has not been studied *in vivo*.

The zebrafish represents a cost-effective vertebrate system to study for the first time the mitochondrial redox regulation of steroid hormone production. The high conservation of steroidogenic enzymes and pathways between zebrafish and humans make them ideal for investigating the regulation of steroidogenesis. The transparency of the embryo together with the ease of performing knockdown or knockout studies, mean zebrafish are an ideal model for studying specific gene functions and will help in understanding the pathogenesis of human endocrine diseases.

#### ***1.11.1 Hypothesis and aims***

We hypothesise that FDX1 mutations or changes in its expression will have significant impact on steroid hormone production, which could lead to pathophysiological consequences. Furthermore, it is proposed that changes in the ferredoxin electron transport chain might be a cause of common diseases such as hypertension through influencing steroid hormone production. To test

this hypothesis, zebrafish will be used as an *in vivo* model system to investigate the mitochondrial redox regulation of steroidogenesis. The following objectives will be addressed:

- To comprehensively characterise zebrafish mitochondrial steroidogenic CYP enzymes and their redox co-factors.
- To establish zebrafish as an *in vivo* model for endocrine development and its disorders.
- Investigate the influence of mitochondrial redox reactions on steroid hormone synthesis *in vivo* by using zebrafish as a vertebrate model system.

The proposed project will support our understanding of the physiological processes regulating steroid hormone synthesis. Additionally, it will provide insights into zebrafish physiology and develop it as a translational model for human pathophysiology. These results will broaden the knowledge of CYP enzymes and co-factor regulation in general, and highlight the functional importance of redox regulation in health and disease.

# ***Chapter Two***

---

## ***General materials and methodologies***

## 2.0 GENERAL MATERIALS AND METHODOLOGIES

Chemical reagents were supplied by Sigma Aldrich (Dorset, United Kingdom) unless otherwise stated. Restriction enzymes and T4 DNAse ligase were provided by New England Biolabs (Hitchin, United Kingdom). Oligonucleotides were synthesised by Sigma Aldrich at 0.025  $\mu\text{mol}$  and purified by desalting. Dried oligonucleotides were resuspended in nuclease free water to a concentration of 100  $\mu\text{M}$  and stored at  $-20\text{ }^{\circ}\text{C}$ .

## 2.1 Molecular biology materials and methodologies

### 2.1.1 *Standard solutions*

Luria Bertani (LB) media	12.5 g LB powder was made up to 500 mL with deionise water, and sterilised by autoclave.
LB agar plates	7.5 g agar per 500 mL of LB media, sterilised by autoclave, poured into Petri dishes and cooled.
1 X TBE	40 mM Tris-acetate (pH 8.3), 1 mM diamino ethanetetra-acetic acid, disodium salt (EDTA).
DEPC treated water	0.1 % diethyl pyrocarbonate (DEPC) water was treated overnight and autoclaved to remove DEPC.
1M IPTG	IPTG in 50 % ethanol, stored at $-20\text{ }^{\circ}\text{C}$ .
20mg/ml X-Gal	200 mg X-Gal in 10 ml dimethylformamide, stored at $-20\text{ }^{\circ}\text{C}$ .

### 2.1.2 *Transformation of E. coli by heat shock*

The naturally occurring process of transformation allows bacteria to uptake circular plasmid DNA. Molecular biology techniques can manipulate this process by allowing competent bacteria to uptake plasmids containing genes of interest. As the bacteria replicate they make copies of the recombinant plasmid which can be purified for future work.

Typically, bronze efficiency competent DH5 $\alpha$  *Escherichia coli* (*E. coli*) cells (Bioline; London, United Kingdom) were transformed by incubating with a recombinant plasmid and using a heat shock method. One microlitre of DNA was added to 40  $\mu$ L of competent cells. The mixture was placed on ice for 20 minutes before heat shocking at 42 °C for one minute and then returned to ice for five minutes. Two hundred microlitres of LB media was added to the cells and incubated for 20 minutes at 37 °C. Finally, the cell suspension was plated onto LB agar plates containing the appropriate antibiotic for selection. The agar plates were incubated at 37 °C for 16 hours.

### **2.1.3 Plasmid DNA preparation**

Plasmid DNA preparation is a method that allows the extraction and purification of plasmid DNA from bacteria. Plasmids were prepared using the QIAprep Spin Miniprep kit as per the manufacturer's instructions (Qiagen; Venlo, Netherlands). This kit uses an alkaline lysis method of bacterial cells and allows the plasmids to bind onto a silica column. Typically, a single *E. coli* colony was used to inoculate 5 mL of LB media containing the appropriate antibiotic for selection. They were cultured at 37 °C for 16 hours at 250 rpm. The culture was centrifuged at 3,000 rpm for five minutes to pellet the bacteria. The cells were then resuspended in 250  $\mu$ L Qiagen Buffer P1 (50 mM Tris-Cl, pH 8.0; 10 mM EDTA; 100  $\mu$ g/mL RNase A). The bacteria were lysed using 250  $\mu$ L Qiagen Buffer P2 (200 mM NaOH, 1 % SDS [w/v]) and neutralised by adding 350  $\mu$ L of acetate containing Qiagen Buffer N3. Samples were then centrifuged for 10 minutes at 13,000 rpm. The remaining supernatant was added to the QIAprep Spin Column and centrifuged for one minute to allow plasmid DNA to bind to the column. The column was washed by adding 750  $\mu$ L of ethanol containing PE Buffer and centrifuged for one minute. After centrifugation for an additional minute to remove residual wash buffer, the purified plasmid DNA was eluted by adding 50  $\mu$ L of DEPC treated water to the column and centrifuged for one minute. Plasmid concentration and purity was determined and samples were stored at -20 °C.

### **2.1.4 Reverse transcription**

Reverse transcription (RT) is a methodology that allows for the generation of complementary DNA (cDNA) from a purified RNA sample. cDNA was prepared from total RNA using SuperScript III Reverse Transcriptase (Invitrogen). Before the RT reaction RNA was treated with DNase to remove any residual genomic DNA contamination from the RNA purification. One microgram of RNA was combined in 1x DNaseI buffer with 1 U of DNaseI amplification grade and incubated for one hour at 37 °C. DNase activity was inhibited by adding of 1 µL of 25 mM EDTA solution and heating 10 minutes at 65 °C. One microlitre of Oligo(dT)<sub>20</sub> primers and 1 µL of 10 mM dNTP mix was added to the pre-treated RNA in a final volume of 13 µL. Samples were incubated at 65 °C for five minutes and cooled on ice to allow annealing of the oligonucleotides to the RNA. Four microlitres of Invitrogen's 5x First strand buffer was added to the RNA mix with 1 µL of 0.1 M DTT and 1 µL RNaseOUT Recombinant RNase Inhibitor to prevent RNA degradation by RNases. Finally, 1 µL of SuperScript III Reverse Transcriptase was added and the samples were incubated at 50 °C for one hour. The enzymes were inactivated by incubating at 70 °C for 15 minutes and stored at -20 °C until required.

### **2.1.5 General expression plasmids**

#### **2.1.5.a. pGEMt-easy**

The pGEM-T Easy vector system (Promega; Madison, United States of America) is a linearised vector with single three-prime terminal thymidine residues to allow easy cloning of PCR products with compatible deoxyadenosine overhangs. It contains both T7 and SP6 RNA polymerase promoters flanking the multiple cloning site. It is amenable for blue/white screening due to the presence of the β-galactosidase gene.

**2.1.5.b. *pcDNA6-V5/His***

The pcDNA6-V5 (Life Technologies; Carlsbad, United States of America) drives expression of cloned cDNA in mammalian cells via the human cytomegalovirus (CMV) promoter. Additionally, it contains a V5 epitope and a polyhistidine (His-tag) metal-binding peptide at the carboxyl-terminal which allows detection of the protein via Western blot using appropriate antibodies. A T7 promoter site is located upstream of the multiple cloning site to permit RNA synthesis by T7 polymerase.

**2.1.5.c. *pCS2+***

The pCS2+ plasmid is a multipurpose expression vector which was primarily used for *in vitro* RNA transcription. It contains a SP6 promoter, upstream of the first multiple cloning site followed by a poly-A signal. By directionally cloning cDNA into the first multiple cloning site, SP6 RNA polymerase can be used to synthesise messenger RNA *in vitro*. A second multiple cloning site is located after the poly-A signal and permits vector linearisation prior to mRNA transcription which prevents transcription of the full plasmid.

**2.1.5.d. *pET22b+***

The pET22b+ vector (Merck Millipore; Billerica, United States of America) was used for bacterial expression for protein purification. This plasmid has an amino terminal *pelB* signal sequence for periplasmic localisation of the desired protein and an additional carboxyl terminal His-tag sequences for protein purification. It contains a T7 RNA polymerase promoter upstream of the multiple cloning site for RNA synthesis.

### 2.1.6 *Quantification of nucleic acids*

Purified DNA and RNA samples were all quantified using the NanoDrop ND-1000 spectrophotometer (Thermo Fisher Scientific; Waltham, United States of America). Typically, DEPC water was used to determine a background level and then 2.0  $\mu$ L of sample was applied onto the spectrophotometer. For nucleic acid samples, a ratio of A260/280 was used to determine purity. A ratio between 1.8 and 2.2 was considered acceptable to use in future experiments.

### 2.1.7 *DNA sequencing*

DNA sequencing was performed by the sequencing facility at the Genomics Facility at the School of Biosciences within the University of Birmingham (United Kingdom). Typically, 6.4 pmol of sequence primer and 400-1000 ng of double stranded plasmid DNA were supplied in 10  $\mu$ L of DEPC water. At this facility they perform BigDye terminator sequencing and the samples are run on the capillary sequencer ABI 3730 to produce read lengths up to 1,000 base-pairs. Assembled sequence data was viewed and analysed by CLC Main workbench software (Qiagen). Standard vector primers were routinely used for sequencing plasmids and are shown in Table 2.1.

**Table 2.1 Standard vector primers used for sequencing and colony PCR screens**

<i>Primer</i>	<i>Sequence (5-prime to 3-prime)</i>
<b>T7</b>	TAATACGACTCACTATAGGG
<b>SP6</b>	ATTTAGGTGACACTATAG
<b>T7 pIRES</b>	GTAATAATACGACTCACTATAG
<b>M13 Forward</b>	GTAAAACGACGGCCAGT

### **2.1.8     *Agarose gel electrophoresis***

Electrophoresis of DNA was carried out at room temperature using 0.7 - 3.0 % (w/v) TBE agarose gels. Agarose gels were prepared by heating and dissolving the required amount of agarose in TBE buffer. After the solution was cooled to approximately 50 °C, 1x SYBR® Safe DNA gel stain (Life Technologies) was added for visualisation of DNA products under ultraviolet (UV) excitation. The DNA samples were mixed with DNA loading buffer (Thermo Fisher Scientific) and electrophoresis carried out in 1x TBE buffer at 100 volts. Samples were run concurrently with Hyperladder I or Hyperladder V (Bioline) as a molecular weight marker for product size determination. The DNA bands were visualised under UV transillumination at 300 nm.

### **2.1.9     *Enzymatic restriction digests***

Bacterial restriction enzymes cut double stranded DNA at specific recognition sites. Restriction digest reactions were performed to confirm ligation of cDNA into plasmids or to linearise plasmids prior to mRNA transcription. One to 6 µg of plasmid DNA or purified PCR product was incubated in 10 or 50 µL reactions with the appropriate buffer. Reactions were carried out using 1 U of enzyme per microgram of DNA. Samples were typically incubated at 37 °C for at least one hour to ensure complete digestion. After digestion samples were either purified by QIAquick PCR Purification Kit (Qiagen) or run on an agarose gel to with undigested control to confirm complete digestion.

### **2.1.10    *Alkaline phosphatase treatment of linearised vectors***

Linearised plasmids were dephosphorylated using calf intestinal alkaline phosphatase (CIP) (New England Biolabs) to avoid recirculation after restriction digestion. For this purpose, 10 U CIP

was added to the restriction digestion reaction and incubated for one hour at 37 °C. Enzyme deactivation was performed by incubating the mix at 75 °C for ten minutes.

### ***2.1.11 DNA purification***

Purification of DNA from enzymatic reactions such as PCR or restriction digests was carried out using the QIAquick PCR Purification Kit according to the manufactures instructions (Qiagen). Briefly, five volumes of Buffer PB were added to one volume of reaction mix. To ensure correct pH for DNA binding to the silica column, 10 µL of 3 M sodium acetate was also added. The mix was added to the QIAquick silica column and centrifuged 13,000 rpm to bind the DNA. The column was washed adding 750 µL of Buffer PE and centrifuging 13,000 rpm for one minute. An additional centrifugation for one minute was performed before the DNA was eluted in 40 µL of DEPC water. Samples were stored at -20 °C until required.

### ***2.1.12 Agarose gel DNA purification***

Purification of DNA fragments from agarose gels fragments was performed by QIAquick Gel Extraction Kit (Qiagen). After samples were separated by agarose gel electrophoresis, the desired DNA fragment was excised from the gel using a scalpel and transferred to a 1.5 mL microcentrifuge tube. Samples were weighed and three volumes of Buffer QG were added for each volume of gel slice. To help the Buffer QG solubilises the agarose gel, samples were incubated at 50 °C for ten minutes. Optimal pH for DNA binding the silica column was achieved by adding 10 µL of 3 M sodium acetate (pH 5.0). Subsequently, one volume of isopropanol was added and the samples were mixed. The DNA was bound to the QIAquick silica column by centrifuging at 13,000 rpm for one minute. The column was washed in 750 µL of Buffer PE and centrifuged at 13,000 rpm for one minute. After an additional centrifugation for a minute to

remove residual wash solution, the samples were eluted in 40  $\mu\text{L}$  of DEPC water. Samples were stored at  $-20\text{ }^{\circ}\text{C}$  until required.

### **2.1.13 *T4 DNA ligation***

The T4 DNA ligase enzyme catalyses the formation of a phosphodiester bonds between the five-prime phosphate and three-prime hydroxyl termini of DNA, allowing the joining of double stranded DNA fragments. Typically, a ratio of five moles of insert to one mole of vector was used for ligation reactions. Ten microlitre reactions containing, digested and purified plasmid and an insert with compatible ends, were combined with 1x T4 DNA Ligase buffer and 1  $\mu\text{L}$  of T4 DNA ligase enzyme. Reactions were mixed gently and incubated overnight at  $4\text{ }^{\circ}\text{C}$ . The following day, 10  $\mu\text{L}$  ligation reactions were used to transform 50  $\mu\text{L}$  of gold efficiency competent DH5 $\alpha$  *E. coli* cells (Bioline) by the standard transformation protocol.

### **2.1.14 *pGEMT-easy ligation***

The pGEM-T Easy vector system (Promega) allows for cloning of PCR products with three-prime adenosine overhangs. A ratio of five moles of insert to one mole of pGEM-Teasy vector was used in 1x ligase buffer with 3 U of T4 DNA ligase enzyme. Reactions were mixed gently and incubated overnight at  $4\text{ }^{\circ}\text{C}$ . The following day, 10  $\mu\text{L}$  ligation reactions were used to transform 50  $\mu\text{L}$  of gold efficiency competent DH5 $\alpha$  *E. coli* cells (Bioline) by the standard transformation protocol.

### **2.1.15 *Colony Polymerase Chain Reaction***

Colony PCR is a method to screen transformed bacteria for presence of a specific plasmid DNA construct. The initial melting step of the PCR bursts the bacteria, making the plasmid DNA

available to act as a template for primers. Twenty-five microlitre reactions were performed using BIOTAQ DNA polymerase (Bioline). Briefly, a mix of 1x  $\text{NH}_4$  reaction buffer, 4 mM  $\text{MgCl}_2$ , 1 mM of dNTPs, and 0.2  $\mu\text{M}$  each of forward and reverse oligonucleotides were used. Either gene specific oligonucleotides were used or if direction specificity of the insert was required, a vector targeting oligonucleotide (Table 2.1) with a gene specific oligonucleotide was used. Using a pipette tip, individual colonies were scraped off the LB agar plates and combined with the PCR. The pipette tip was left to inoculate 100  $\mu\text{L}$  of LB media. PCR consisted of an initial 10 minutes at 94 °C followed by 35 cycles of 94 °C for 30 seconds, a 30 second anneal step and a 72 °C extension step. A final seven minute extension step completed the PCR. Reactions were then run on an agarose gel to determine positive clones. Once positive clones were identified the corresponding 100  $\mu\text{L}$  of LB media was used as a starter culture for plasmid purification

### **2.1.16 RNA extraction**

RNA extraction is a procedure which allows for the isolation of RNA from a biological sample and therefore providing a snapshot of the genes being actively transcribed at that the respective time point. RNA was isolated from dissected zebrafish tissues or a pool of zebrafish embryos using TRI-Reagent. Samples were washed in phosphate buffered saline (PBS) before 1 mL of TRI-Reagent was added. Tissues were homogenised using a micropestle (Eppendorf; Hamburg, Germany). Two hundred microlitres of chloroform was added to the samples and they were mixed vigorously. Samples were incubated at room temperature for 10 minutes and centrifuged at 13,000 rpm for 20 minutes. The upper aqueous phase containing the RNA was transferred to a fresh microcentrifuge tube. The RNA was precipitated at -20 °C overnight using 500  $\mu\text{L}$  of cold isopropyl alcohol. The following day, RNA was pelleted by centrifugation at 13,000 rpm for 10 minutes at 4 °C and washed in 70 % ethanol. After a further centrifugation step at 13,000 rpm

for 10 minutes at 4 °C the supernatant was removed and the RNA was allowed to dry. RNA was then resuspended in RNase-free water, quantified and stored at -20 °C.

### ***2.1.17 Reverse Transcriptase Polymerase Chain Reaction (RT-PCR)***

Semi-quantitative reverse transcriptase polymerase chain reaction (RT-PCR) was used to investigate gene expression by using Megamix-Blue (Microzone Ltd; West Sussex, United Kingdom). Typically, 0.6 µM of specific forward and reverse oligonucleotides were combined with 1.5 µL of cDNA in a 25 µL reaction volume of Megamix-Blue. Reactions were run with an initial denaturing step of 95 °C and then 40 cycles consisting of a 95 °C for 30 seconds, 30 seconds for annealing at the appropriate temperature for the primers and extension at 72 °C for one minute per 1,000 base-pairs of product. A final extension of 72 °C for seven minutes completed the PCR. For visualisation of PCR products, 12 µL of the reactions were run on DNA agarose gel.

For amplification of full length coding sequences of zebrafish genes, Expand High Fidelity PCR System (Roche; Basel, Switzerland) was used. Specific oligonucleotides were designed typically with endonuclease restriction sites for direct cloning into the required plasmid. Fifty microlitre reactions consisted of 1x Expand High Fidelity PCR system buffer, 2 mM MgCl<sub>2</sub>, 0.4 µM of dNTPs, 0.3 µM of each forward and reverse oligonucleotides, 1.5 µL of cDNA and 2.6 U of polymerase mix. Reactions were performed using a single denaturing step at 94 °C for five minutes, 40 cycles consisting of 94 °C for 30 seconds, annealing temperature between 52 °C and 58 °C (depending on the oligonucleotide melting temperature) and an extension time of one minute per 1,000 base-pairs at 68 °C. A final extension of 72 °C for seven minutes completed the PCR cycle.

## 2.2 In silico protein analysis

### 2.2.1 Multiple sequence alignments

Multiple protein alignments and homology analyses were performed using ClustalW2 software under default parameters (URL: <http://www.ebi.ac.uk/Tools/msa/clustalw2/>). Typically, ENSEMBL (version Zv9) protein sequences were imported in FASTA format for analysis. Phylogenetic analyses of protein sequences were performed with the PhyML software under the SH-like likelihood-Ratio test parameters (URL: <http://www.phylogeny.fr/>) (Dereeper et al., 2008). Scaled phylogenetic tree was drawn with TreeDyn software.

## 2.3 Zebrafish husbandry and methodologies

### 2.3.1 Zebrafish nomenclature

Nomenclature used throughout this thesis is consistent with the current guidelines based on the *Trends in Genetics* Genetic Nomenclature Guide for Zebrafish (Mullins, 1995). Typically, zebrafish genes are named after the mammalian orthologue and written italicised and in lower case. Zebrafish protein symbols are the same as the gene symbol, but not italicised and the first letter is uppercase. A comparison between different species naming conventions is shown in Table 2.2.

**Table 2.2 Zebrafish and mammalian naming conventions**

<i>Species</i>	<i>Gene</i>	<i>Protein</i>
zebrafish	<i>fdx1</i>	Fdx1
human	<i>FDX1</i>	FDX1
mouse/bovine	<i>Fdx1</i>	FDX1

### **2.3.2 Standard solutions**

E3 Media	5 mM NaCl, 0.17 mM KCl, 0.33 mM CaCl <sub>2</sub> , 0.33 mM MgSO <sub>4</sub> made up in dionised water and supplemented with 2 µg/mL gentamycin.
DNA extraction buffer	10 mM Tris-HCl (pH 8.0), 1.0 mM EDTA and 200 µg/mL Proteinase K.
Phenylthiourea (PTU)	0.003 % 1-phenyl 2-thiourea in E3 media.
Pronase solution	Protease Type XIV from <i>Streptomyces griseus</i> was diluted in DEPC water to a concentration of 10 mg/mL and stored at -20 °C.
Rhodamine dextran solution	4 % (w/v) 10,000 MW rhodamine dextran in 0.2 mol/L potassium chloride.

### **2.3.3 Zebrafish maintenance**

All zebrafish work was performed under project licence PPL 40/3681 and personal licence ICB7ED2A1 in accordance with the HOME Office Animal (Scientific Procedures) Act 1986. The zebrafish wild-type AB strain was maintained in a recirculating system (Tecniplast; Kettering, United Kingdom) at 28.5 °C with a 10:14 hour dark:light photoperiod. Adults were fed three times per day with granule fish food and brine shrimp (ZMSystems; Hampshire, United Kingdom). Embryos were obtained by natural spawning and incubated at 28.5 °C in E3 medium. To prevent pigment formation embryos required for imaging were incubated with E3 medium supplemented with PTU from 24 hours post fertilisation (hpf). The developmental stages were determined according to hpf and morphological features as previously described by Kimmel et al. (1995).

### ***2.3.4 Breeding strategy to generate knockout zebrafish lines***

To generate several zebrafish lines harbouring mutations in specific steroidogenic genes I used Transcription Activator-Like Effector Nucleases (TALENs) (Chapter 5.0) or the Clustered regularly interspaced short palindromic repeats and Cas9 nuclease (CRISPR/Cas9 system) (Chapter 6.0). The following strategy was used to generate knockout embryos (Figure 2.1). The TALEN or CRISPR/Cas9 RNA was injected into single-cell embryos. During cleavage and blastula phases, the RNA and subsequent protein is dispersed throughout the blastomere. The mutations generated from the TALENs or CRISPR/Cas9 is different in each cell, creating mosaic embryos which were raised to adulthood. Adult zebrafish harbouring mutations within the germ-cells, and therefore capable of transmitting mutations to the next generation (F1), were identified by out-crossing to a wild-type and screening the off-spring for genomic disruption. Embryos from positive clutches were raised to adults. These adults were genotyped from fin clips and sequenced to identify the specific mutation. Once adults harbouring a mutation were identified they were out-crossed to wild-type zebrafish, producing the F2 generation which would contain embryos heterozygous for the same mutation (50 % of embryos with Mendelian inheritance). These embryos were raised to adults. Heterozygous adults were identified by genotyping fin clips, and were in-crossed to produce the F3 generation. With Mendelian inheritance, 25 % of F3 embryos were expected to be homozygous for the specific mutation.

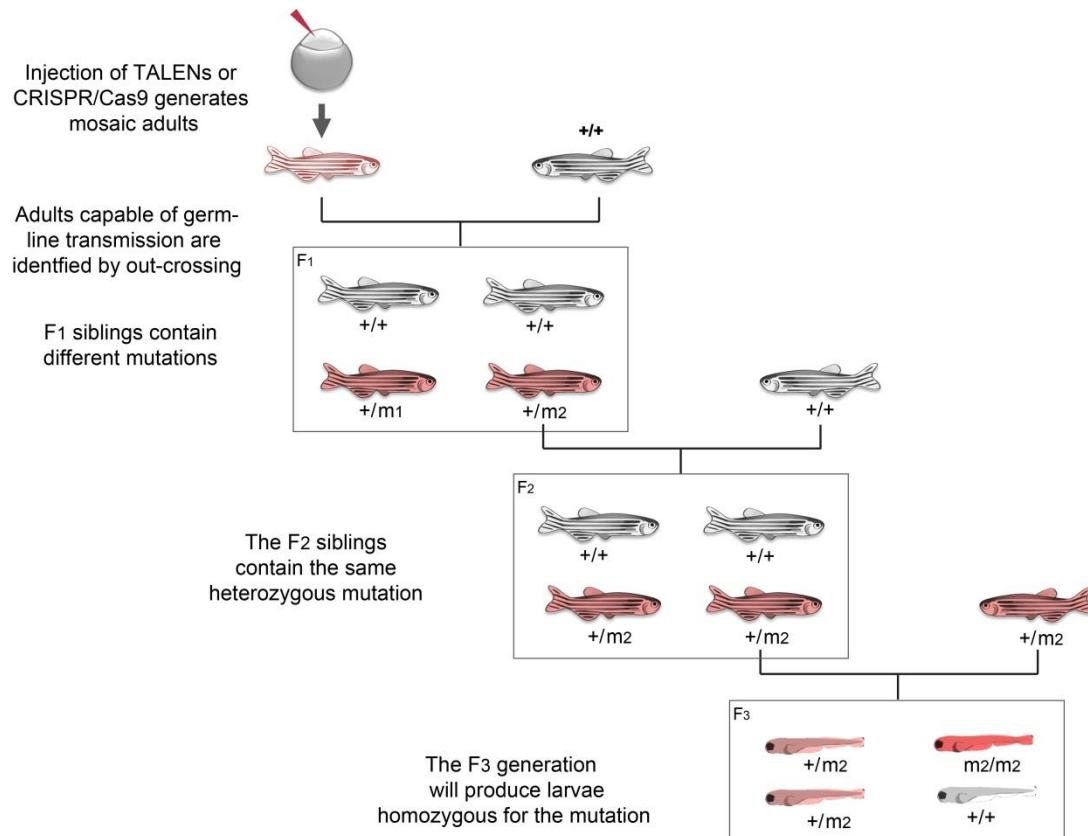


**Figure 2.1 Breeding strategy to generate homozygous mutant zebrafish lines**

To generate knockout stable lines single-cell embryos were subjected to genome editing by injecting TALEN or CRISPR/Cas9 RNA. As the blastomere grows and divides the genome editing occurs. Adults raised from these injections are mosaic for different mutations (m). Out-crossing injected adults identifies fish capable of germ-line transmission of genetic mutations. F1 generation siblings may have different mutations (m1 or m2) as the parent is mosaic. Out-crossing of individual F1 adults produces the F2 generation which are heterozygous (+/m2) for the same mutation. In-crossing of two heterozygotes will generate embryos homozygous for the mutation (m2/m2).

### **2.3.5     *Embryo collection***

For zebrafish embryo collection, a sexually mature male and female adult were placed in three litre breeding tanks separated by a baffle. Each breeding tank has an internal raised tank with a latticed bottom which allowed externally fertilised eggs to fall through to the bottom of the tank preventing adult fish from consuming them and ensuring easy collection. Zebrafish naturally spawn shortly after dawn and each female can produce 100 to 300 eggs each week. To make spawning as natural as possible, the following morning the baffles were removed shortly after the facility lights were turned on. Upon detection of eggs, adult zebrafish were transported to a new tank and the eggs were collected in a small sieve and transferred to a petri dish with a Pasteur pipette. The collected eggs were sorted and checked for fertilisation and vitality under a dissection microscope and incubated in E3 Media at 28.5 °C until the desired time point was reached.

### **2.3.6     *Dechoriation of zebrafish embryos***

Naturally, zebrafish develop inside a chorion, which is a tough outer membrane that protects the developing embryo for the first three days of development. Observations of zebrafish development can be made through the chorion; however, for some techniques such as imaging, it is beneficial to remove the chorion. When raised at 28.5 °C in E3 medium embryos can develop normally outside of their chorion. After 18 hpf chorions can be removed manually by using Dumont No. 5 forceps to tear it and allowing the embryo to fall out.

Chorions can also be chemically digested using pronase. Single cell embryos were placed in a Petri dish and incubated in pronase solution. When the chorions begin to collapse, embryos were transferred to a one litre glass beaker containing fish water. Embryos were gently washed at least four times in one litre of fish water to remove excess pronase and chorions. Finally, using a

transfer pipette embryos were placed in agarose coated Petri dishes contain E3 medium. Dechorionated embryos were continually submerged in media, as exposure to air causes the embryos to burst.

### ***2.3.7 In vitro mRNA synthesis***

In order to perform rescue experiments, full length coding sequences were cloned into the pCS2+ plasmid. The SP6 RNA polymerase promoter allows for *in vitro* transcription of sequences cloned into the polylinker one site. It also generates a polyadenylation tail (pA) via the SV40 polyadenylation site down stream of the cloned gene. In a 50  $\mu$ L reaction, 5  $\mu$ g of pCS2+ plasmids was linearised by a unique restriction enzyme in polylinker two. This linearisation prevents continuous mRNA synthesis of plasmid DNA by the RNA polymerase. Complete digestion was confirmed by running 2  $\mu$ L of the reaction on a 1 % DNA agarose gel and the remainder was purified using QIAquick PCR Purification Kit (Qiagen).

*In vitro* mRNA synthesis was performed using mMessage mMachine Kit (Life Technologies). The 20  $\mu$ L transcription reactions were assembled at room temperature using 1  $\mu$ g of linearised DNA template, 1x SP6 transcription buffer, 1x NTP/CAP ribonucleotides, and 2  $\mu$ L of SP6 RNA polymerase. After mixing, reactions were incubated at 37 °C for two hours. Subsequent treatment at 37 °C for 15 minutes with 1  $\mu$ L of TURBO DNase removed the DNA template.

*In vitro* derived mRNA was then purified using the GenElute Mammalian Total RNA Miniprep Kit (Qiagen). Elution solution was used to make the final volume RNA mix to 100  $\mu$ L. Three hundred and fifty microlitres of fresh lysis Solution/2-mercaptoethanol mixture was added and the solution mixed thoroughly. Subsequently, 250  $\mu$ L of 100 % ethanol was added to the solution. After mixing, the RNA sample was added to the RNA binding column and centrifuged

at 13,000 rpm for 15 seconds. The binding column was transferred to a new tube and washed twice with Wash 2 solution by centrifuging at 13,000 rpm. After a final centrifugation to remove residual wash solution, the RNA was eluted into a fresh tube by adding 30  $\mu$ L of nuclease-free water to the column and centrifuging at 13,000 rpm for one minute. Typically, the concentration and quality was determined by spectrophotometer and running the samples on an agarose gel, respectively. Aliquots of RNA were stored at -80 °C until required.

### **2.3.8 *In vivo knockdown by antisense morpholino***

Antisense morpholino oligonucleotides were synthesised by Gene Tools, LLC (Philomath, United States of America). Morpholinos are synthetic oligonucleotides similar to DNA oligonucleotides, except they have a morpholine ring and a non-charged phosphorodiamidate backbone, making them resistant to nucleases (Nasevicius and Ekker, 2000). They were designed to bind either the initiating methionine codon on mRNA to block formation of translational machinery or over splice site junctions to disrupt correct splicing of mRNA. Each morpholino comprised of a 25 base-pair antisense sequence of approximately 50 % guanine/cytosine nucleotide content without any predicted internal hairpins. Candidate sequences were then screened for representation elsewhere in the zebrafish genome by performing a BLASTn database search (URL: <http://www.ncbi.nlm.nih.gov/BLAST/>). Control morpholinos were also synthesised by creating a five nucleotide mismatch to the targeting site to determine off-target effects. Morpholinos were resuspended in DEPC water to a concentration of 1 mM and stored at -20 °C until required.

### **2.3.9 *Morpholino microinjection of single cell zebrafish embryos***

The morpholino stock solution was diluted to working concentrations of 0.5 - 6 ng/nL in DEPC water containing 0.05 % phenol red. Two microlitres of 4 % rhodamine dextran was also added

to the 10  $\mu$ L injection mixes as a fluorescent tracer. Approximately 2 nL of the working solution was microinjected into the yolk of single cell embryos. Phenol red served as a visible marker for injections. Approximately, four hours after injection embryos were screened for rhodamine dextran fluorescence to identify effectively injected embryos using a 554 nm laser on a fluorescence microscope (SMZ1500-P-FLA2, Nikon UK Limited; Surrey, United Kingdom).

### ***2.3.10 Fin clipping adult zebrafish***

Adult zebrafish were anaesthetised by immersion in 0.004 % in Tricaine Methanesulfonate (MS-222) pH 7.2 until gill movement is slowed and the fish had stopped swimming. Fish were transferred to a Petri dish and the fin was clipped using a sterile scalpel. The fish was immediately transferred to a tank containing 1.5 L of fresh system water and monitored while swimming ability was regained. Post fin clipping, fish were housed in individual holding tanks while genetic DNA was isolated for the purposes of genotyping.

### ***2.3.11 Genomic DNA extraction***

The extraction of genomic DNA from either pooled embryos or adult fin clips was performed to determine genomic alterations after genome editing or for sequencing specific loci. Embryos or fin clips were incubated overnight in 30  $\mu$ L of DNA extraction buffer. Subsequently, the proteinase K was inactivated by heating samples to 95 °C for 15 minutes. Debris was pelleted by centrifuging 4,000 rpm for 10 minutes. The supernatant containing the genomic DNA was transferred to a clean microcentrifuge tube and stored at -20 °C until required.

## 2.4 Cell biology materials and methodologies

### 2.4.1 *Standard solutions*

5x SDS Loading Buffer	250 mM Tris-HCl pH 6.8, 50 % glycerol, 10 % sodium dodecyl sulphate (SDS), 1 % $\beta$ -mercaptoethanol, 0.25 % bromophenol blue.
PBST	PBS with 0.1 % Tween 20.
Blocking buffer	10 % skim milk in PBST.
RIPA buffer	150 mM sodium chloride, 1.0 % Triton X-100, 0.5 % sodium deoxycholate, 0.1 % SDS (sodium dodecyl sulphate), 50 mM Tris, pH 8.0.

### 2.4.2 *Mammalian cell culture*

The COS-7 cell line was isolated from the kidney of the African Green Monkey (*Cercopithecus aethiops*) and is commonly used for enzyme activity assays. Cells were grown in Dulbecco's Modified Eagle's medium (DMEM) high glucose and glutamine (4 mM) (Life Technologies), supplemented with 10 % foetal bovine serum, 100 U/mL penicillin and 0.1 mg/mL streptomycin. Cells were maintained at a density of  $2 \times 10^3$  to  $1 \times 10^4$  cells/cm<sup>2</sup> in a 5 % carbon dioxide, 37 °C humidified incubator. Harvesting of the cells was performed using trypsin digestion using Tryple Express (Life Technologies) and cells subcultured using a 1:4 to 1:8 split.

### 2.4.3 *Transfection of mammalian cell lines*

Transfection is a process whereby DNA is deliberately introduced into a eukaryotic cell. Often in molecular biology, transfection of a plasmid containing a cloned cDNA sequence allows the over-expression of the gene by a highly expressing promoter. Twenty-four hours before transfection, cells were seeded at 300,000 cells per well of a six-well plate. A ratio of 3  $\mu$ L of X-treamGene HP Reagent to 1  $\mu$ g of plasmid DNA was mixed in 100  $\mu$ L of DMEM. After

incubation at room temperature for 15 minutes to form transfection complexes, 100  $\mu$ L was added drop-wise to each well. Subsequently, fresh media with bovine serum and antibiotics was added after six hours.

#### **2.4.4 *In vitro* enzyme activity assay**

##### **2.4.4.a. *22R-hydroxycholesterol conversion assay***

The enzyme activity of the zebrafish Cyp11a1 and Cyp11a2 was assessed by measuring the conversion of 22R-hydroxycholesterol into pregnenolone. The intermediate product 22R-hydroxycholesterol does not rely on StAR-mediated transport to enter the mitochondria; therefore, enzymatic activity can be measured independent of StAR activity. Forty-eight hours after transfection cells were subjected to conversion assays. Cells were incubated for four or 24 hours at 37 °C with 1,000  $\mu$ L of DMEM containing 2  $\mu$ M 22R-hydroxycholesterol and 200  $\mu$ M of NADPH. Ethanol was added to cells as a negative control. After the incubation, media was collected separately in sylinised test tubes (Fisher Scientific; Loughborough, United Kingdom) and subjected to cell media steroid extraction.

##### **2.4.4.b. *11-deoxycortisol conversion assay***

Enzymatic activity of zebrafish Cyp11c1 was assessed by measuring the conversion of 11-deoxycortisol to cortisol. Functional activity assays were performed 48 hours after transfection. Cells were treated with 1,000  $\mu$ L of 2.5  $\mu$ M of 11-deoxycortisol, 5  $\mu$ M of 18 $\beta$ -glycyrrhetic acid (an 11 $\beta$ -hydroxysteroid dehydrogenase inhibitor to prevent the 11 $\beta$ -hydroxysteroid dehydrogenase type 2 activity endogenous to COS7 cells), and 200  $\mu$ M of NADPH and incubated for six or 24 hours at 37 °C in a humidified incubator. Ethanol was

added to cells as a negative control cells. After the incubation steroid were extracted from cell media.

#### **2.4.5 Protein extraction**

Media was aspirated and COS7 cells were washed twice in 10 mL ice-cold PBS before being harvested. Cells were harvested in 1 mL of Radio Immunoprecipitation Assay buffer (RIPA buffer) supplemented with a protease inhibitor (Complete Mini Tablets; Roche). Cells were removed by scraping and collected in a microcentrifuge tube. The cell solution was vortexed for 10 seconds followed by incubation at  $-20^{\circ}\text{C}$  for 30 minutes. Debris was pelleted by centrifugation at 13,000 rpm for ten minutes at  $4^{\circ}\text{C}$ . The supernatant containing the proteins was then collected in a fresh microcentrifuge tube for protein quantification.

#### **2.4.6 Protein quantification**

Protein concentrations were determined the Bio-Rad DC Protein Assay according to the manufactures instructions (Bio-Rad Laboratories, Inc.; Hercules, United States of America). Prior to the assay, a small aliquot of harvested protein was diluted in distilled water. A fresh mix was made containing 20  $\mu\text{L}$  of Reagent S for each millilitre of Reagent A required of the assay. Five microlitres of each sample was added to a well of a 96-well plate followed by 25  $\mu\text{L}$  of Reagent A (supplemented with Reagent S). Then 200  $\mu\text{L}$  Reagent B was added and the plate was mixed. Finally, after 15 minutes absorbance were read at 750 nm using the Victor<sup>3</sup> plate reader (Perkin Elmer; Turku, Finland) using Wallac 1420 software (Perkin Elmer). Concentrations of proteins were derived by comparison of a standard curve ranging from 0.2 mg/mL to 2.0 mg/mL of protein using bovine serum albumin diluted in the same buffer as the proteins. Blank samples containing no bovine serum albumin were also used to determine background absorbance.

#### **2.4.7 *SDS Poly Acrylamide Gel Electrophoresis***

Sodium dodecyl sulphate polyacrylamide gel electrophoresis or SDS PAGE, is a method that allows for the separation of proteins based on size. Typically, 10 µg of protein sample was mixed with 1x loading buffer in a final volume of 20 µL. Samples were heated at 95 °C for five minutes and cooled on ice. Samples were loaded on a 10 % NuPAGE Novex Tris-Bis precast gel (Invitrogen) and run at 200 volts for one hour in 1x NuPAGE Buffer (Invitrogen).

#### **2.4.8 *Protein transfer using the iBlot Blotting System***

Upon completion of gel electrophoresis proteins were transferred to nitrocellulose membranes using the iBlot 7-Minute Blotting System (Invitrogen) consisting of the iBlot Gel Transfer Device and iBlot Gel Transfer Stacks. SDS PAGE gels were rinsed in deionised water and placed on top of the iBlot Anode Stack containing the nitrocellulose membrane. Filter paper pre-soaked in deionised water was placed on top of the acrylamide gel and any air bubbles were removed. The iBlot cathode stack was positioned with the electrode side facing up. After completion of the Gel Transfer Stack a seven minute dry transfer at 23 volts was performed using the iBlot Gel Transfer Device.

#### **2.4.9 *Western Blot***

Western Blot is a technique that uses specific antibodies to detect proteins of interest which have previously been separated based on their size by SDS PAGE. Antibodies used for western blotting analysis were purchased from Abcam (Cambridge, United Kingdom) and are detailed in Table 2.3.

**Table 2.3 Antibodies for Western Blotting**

<i>Antibody</i>	<i>dilution</i>	<i>Catalogue number</i>
<b>mouse-anti-V5</b>	<i>1:1000</i>	ab9137
<b>mouse-anti-<math>\beta</math>-actin-HRP</b>	<i>1:1000</i>	ab20272
<b>Anti-mouse-HRP</b>	<i>1:20,000</i>	ab97046

Initially, nitrocellulose membranes were blocked for one hour at room temperature in blocking buffer. The membranes were incubated overnight at 4 °C with primary antibody (mouse-anti-V5) at the required dilution in blocking buffer. The following day the membranes were washed three times for five minutes in PBST. The secondary antibody (Anti-mouse-HRP) was diluted to the appropriate concentration in blocking buffer and incubated with the membrane for one hour. Finally, the membrane was washed three times for five minutes in PBST. Following antibody incubation, the blot was developed using ECL detection kit (GE health care; Little Chalfont, United Kingdom) according to the manufactures instructions and developed on Kodak film. To establish equal loading mouse anti- $\beta$ -actin-HRP was used 1:20,000 dilution. After blocking, membranes were incubated with the antibody for one hour, washed and develop as described above.

## 2.5 Biochemical materials and methods

### 2.5.1 *Standard Solutions*

Internal Standards                      Deuterated cortisol (Cortisol-d4), 11-deoxycortisol (11-deoxycortisol-d2), corticosterone (corticosterone-d8), testosterone (testosterone-d3), Dihydroxytestosterone (DHT-d3), Dehydroepiandrosterone (DHEA-d6), 17-hydroxyprogesterone (17OHP-d8), progesterone (progesterone-d9), pregnenolone (pregnenolone-d4), and 17-hydroxypregnenolone (17OHPreg-d3) were combined to make a stock solution containing 1 µg/mL of each steroid.

### 2.5.2 *Steroid hormone extraction from zebrafish*

To determine the steroid hormone profiles of zebrafish embryos, a steroid hormone extraction method was developed to quantify cortisol and pregnenolone by liquid chromatography/tandem mass spectrometry (LC-MS/MS). Typically, 300 zebrafish embryos were collected for each time point of development. Dechorionated embryos and larvae were gently washed twice in 1x Dulbecco's modified PBS and kept in 1 mL 1x Dulbecco's modified PBS at -20 °C until required.

To extract steroid hormones, zebrafish embryos were thawed at 55 °C, followed by addition of 10 ng of deuterated steroid internal standards. After samples were frozen and thawed three more times, they were homogenised for one minute using a PowerGen 125 homogeniser using small stainless-steel blades (Fisher Scientific Ltd.; Leicestershire, United Kingdom). Between samples, blades were rinsed with 1 mL 1x Dulbecco's modified PBS, which was combined with the homogenised samples. Steroid hormones were extracted via liquid/liquid extraction four times from the homogenates in 5 mL dichloromethane. Organic phases were combined and dried under a nitrogen stream at 55 °C. Samples were resuspended and vortexed in 400 µL of a 1:3 methanol:water solution. Samples were passed through a Phree phospholipid removal plate

(Phenomenex; Cheshire, United Kingdom) to remove residual proteins and lipids. Each Phree phospholipid extraction column was equilibrated with 1.2 mL methanol containing 0.1 % formic acid. Zebrafish extracts were subsequently added to the columns and the plate was vortexed for two minutes. Using a vacuum manifold the solutions passed through the columns under pressure. The eluent containing the steroid fraction was collected and evaporated to dryness under a nitrogen stream at 55 °C. Samples were then reconstituted in 125 µL of 50:50 methanol:water for LC-MS/MS analysis.

### ***2.5.3 Steroid hormone extraction from cell media***

To analyse specific enzyme catalytic activity, COS7 cells were transfected with the specific enzyme of interest and subjected to steroid hormone treatments. All steroids were extracted using a liquid/liquid extraction regardless of the substrate. Typically, 1 mL of culture media was transferred to a silylised test tube. Twenty nanograms of deuterated internal standard stock were added to each sample prior to extraction. Three millilitres of MTBE was then added and the samples were vortexed. Samples were then frozen for at least an hour at -20 °C. Using a glass Pasture pipette, the top layer was transferred to 96-well plate (Thermo-Fisher Scientific) and allowed to evaporate to dryness at 55 °C under nitrogen stream in a 96-well plate evaporator (TurboVap, Biotage, United Kingdom). Samples were reconstituted in 125 µL of 50:50 methanol:water for analysis.

#### ***2.5.4 Liquid Chromatography/Tandem mass spectrometry (LC-MS/MS) System Setup***

Steroids were identified and quantified using a Waters Xevo TQ mass spectrometer with an ACQUITY ultra high-pressure liquid chromatography (uPLC) system, fitted with a HSS T3 1.8  $\mu\text{m}$  2.1 x 50 mm column (Waters Corporation, Milford, United States of America). The Waters Xevo was fitted with an electrospray ionisation source, operated in positive mode. Twenty microlitres of each sample was injected into the mass spectrometer for analysis. Steroid hormones were eluted from the column using a methanol/water gradient system, solvent A was water with 0.1 % formic acid, and B was methanol with 0.1 % formic acid. Three different gradient systems were used in these experiments for the analysis of cortisol, pregnenolone-oxime and the analysis of zebrafish androgens. For positive identification of a steroid within a sample, two identical mass transitions and an identical retention time in comparison to an authentic steroid standard was required (Table 2.4). To quantify each steroid each method included a calibration series ranging from 0.5 to 500 ng/mL. TargetLynx software was used to process the mass spectrometry data (Masslynx 4.1; Waters Corporation).

##### ***2.5.4.a. Cortisol analysis by LC-MS/MS***

Cortisol analysis was completed using a gradient system starting at 45 % methanol (0.1 % formic acid), followed by four linear increases to 47 % at one minute, 57 % at two minutes, 70 % at 2.5 minutes and 98 % at four minutes. Detection of cortisol in a zebrafish sample relative to an authentic steroid standard can be seen in Figure 2.2.

**Table 2.4 LC-MS/MS parameters for the detection and quantification of cortisol and pregnenolone-oxime, androgen and their internal standards cortisol-d4 and pregnenolone-oxime-d4.**

Steroid	Retention Time (min)	Mass Transitions	Cone Voltage (CV)	Collision Energy (CE)
Cortisol	1.26	363 > 121	26	30
		363 > 97 <sup>&amp;</sup>	26	23
Cortisol-d4	1.24	367 > 121	24	24
		367 > 331 <sup>&amp;</sup>	24	16
Pregnenolone-oxime	2.66	332 > 86	36	26
		332 > 300 <sup>&amp;</sup>	36	24
Pregnenolone-oxime-d4	2.66	336 > 90	36	26
		336 > 304 <sup>&amp;</sup>	36	24
11-ketoandrostenedione	1.70	303 > 121	30	24
		302 > 265 <sup>&amp;</sup>	30	18
11-ketotestosterone	1.48	303 > 121	34	26
		303 > 91 <sup>&amp;</sup>	34	50
11- $\beta$ OH androstenedione	2.66	303 > 267	26	18
		303 > 145 <sup>&amp;</sup>	26	26
11- $\beta$ OH testosterone	2.66	305 > 269	26	16
		305 > 121 <sup>&amp;</sup>	26	22

<sup>&</sup>Qualifier ions

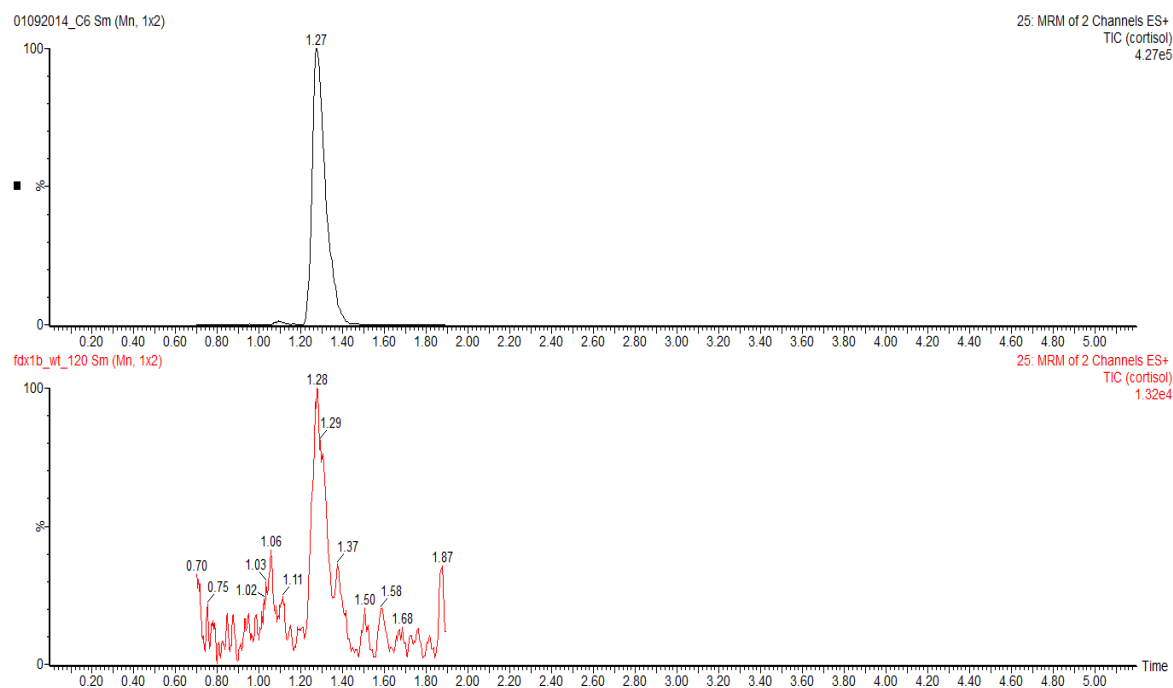


**Figure 2.2 LC-MS/MS detection of cortisol in whole zebrafish extracts**

Representative chromatogram showing positive identification of cortisol from whole zebrafish embryo extracts. Top is authentic reference standard, and bottom is cortisol from zebrafish embryos. The chromatogram is a sum of the two mass transitions defined in Table 2.4.

#### **2.5.4.b. Pregnenolone Analysis by LC-MS/MS: Oxime Derivatisation**

To increase LC-MS/MS sensitivity to lipophilic pregnenolone, an oxime derivatisation method was used. Following cortisol analysis, the samples and calibration series were evaporated to dryness under nitrogen at 55 °C. Oxime derivatisation was conducted by adding 100  $\mu$ L 2% hydroxylamine hydrochloride solution in pyridine (w/v) to the dried samples. The mixture was vortexed then incubated at 60 °C for one hour. Oxime-derivatised samples were

subsequently dried under nitrogen at 55 °C then reconstituted in 125 µL of 50:50 methanol:water. Reconstituted samples were analysed by LC-MS/MS and quantified as described in Section 2.5.4.

The optimised chromatography method started at a gradient of 50 % methanol (0.1 % formic acid) which was held for one minute. Following this, there were three linear increases to 55 % methanol (0.1 % formic acid) at one minute, 70 % at two minutes and 90 % at five minutes. Detection of pregnenolone-oxime in a zebrafish sample relative to an authentic steroid standard can be seen in Figure 2.3.

#### **2.5.4.c. Androgen analysis by LC-MS/MS**

Androgen analysis was completed using a gradient system starting at 45 % methanol (0.1 % formic acid), followed by four linear increases to 47 % at one minute, 57 % at two minutes, 70 % at 2.5 minutes and 98 % at four minutes. These chromatographic conditions allowed for simultaneous detection of the zebrafish androgens (see Chapter 6.0).

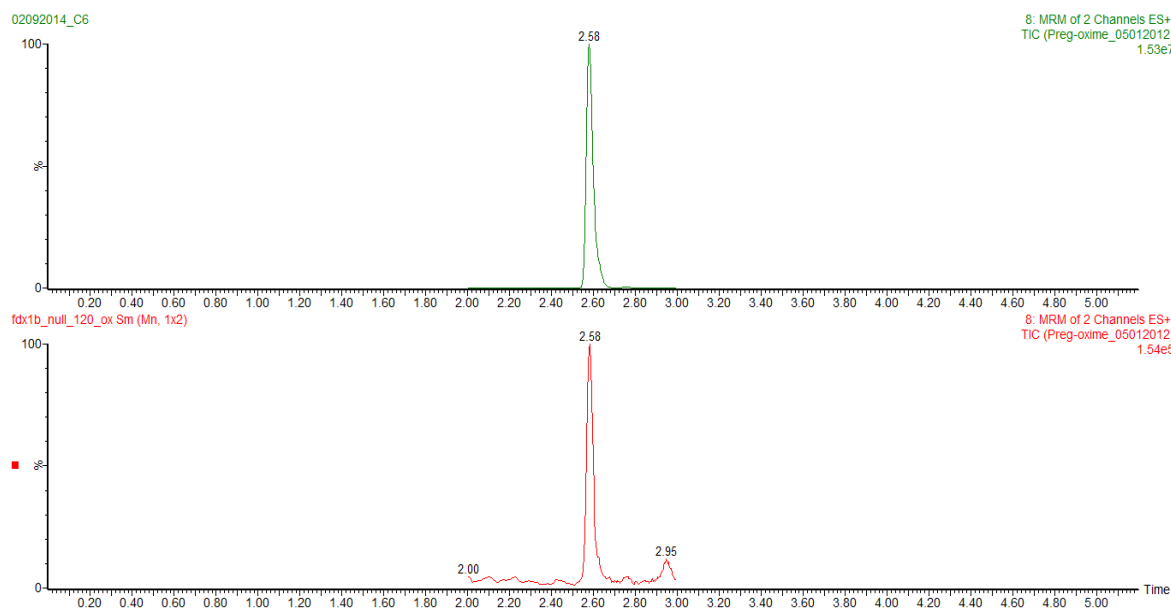


**Figure 2.3 LC-MS/MS detection of pregnenolone-oxime in whole zebrafish extracts**

Representative chromatogram showing positive identification of pregnenolone-oxime from whole zebrafish embryo extracts. Top is authentic reference standard, and bottom is pregnenolone-oxime from zebrafish embryos. The chromatogram is a sum of the two mass transitions defined in Table 2.4.

### 2.5.5 *Statistical analysis of steroid hormone measurements*

#### 2.5.5.a. *Whole zebrafish extracts*

Steroid measurements from whole zebrafish extracts are expressed as the mean in pg per embryo or larva  $\pm$  standard deviation (SD). Experiments were performed in triplicate, unless stated otherwise and plotted using GraphPad Prism v.6.0 software (GraphPad Software, Inc.; La Joya, United States of America). Comparison between steroid profiles of morpholino knockdowns and controls were performed using unpaired student t-test. Rescue experiments were compared

using one-way analysis of variance (ANOVA) following Dunnett's multiple comparisons test. Statistically significant differences are noted with asterisks.

**2.5.5.b. Enzymatic assays**

Enzymatic assays were performed in triplicate and data is presented from three independent experiments. Enzyme activities are expressed as percentage of the appropriate human orthologue and are represented as the mean  $\pm$  SD and plotted using GraphPad Prism v.6.0 software. Statistical significance was determined by ANOVA following Dunnett's multiple comparisons test. Statistically significant differences are noted with asterisks.

## ***Chapter Three***

---

***The duplicated mitochondrial  
ferredoxin Fdx1b regulates  
glucocorticoid production in  
zebrafish***

### **3.0 THE DUPLICATED MITOCHONDRIAL FERREDOXIN FDX1B REGULATES GLUCOCORTICOID PRODUCTION IN ZEBRAFISH**

#### **3.1 Introduction**

Ferredoxins are iron-sulphur (Fe/S) proteins which act as electron donors for a variety of fundamental reactions catalysed by mitochondrial CYP enzymes. The human ferredoxin 1 (FDX1; adrenodoxin; ADX) is a 14 kDa protein loosely associated with the inner mitochondrial membrane and is involved in various metabolic processes including the synthesis of steroid hormones (Meyer, 2008), bile acids and vitamin D (Ewen et al., 2012). In these biochemical pathways, the flavoprotein ferredoxin reductase (FDR) receives electrons from nicotinamide adenine dinucleotide phosphate (NADPH) and in turn reduces FDX1. FDX1 then transfers these electrons to CYP enzymes allowing them to perform their catalytic functions (Miller, 2005, Miller and Auchus, 2011). In steroidogenic tissues, FDX1 transfers electrons to the P450 side-chain cleavage enzyme, CYP11A1, which facilitates the conversion of cholesterol into pregnenolone first step of steroid hormone biosynthesis (Miller and Auchus, 2011). In addition, the mitochondrial CYP enzymes 11 $\beta$ -hydroxylase (CYP11B1) and aldosterone synthase (CYP11B2) also require FDR/FDX1 electron transfer to catalyse the reactions required for glucocorticoid and mineralocorticoid synthesis, respectively.

Currently, little is known about the physiological importance of mitochondrial redox partner interactions or their ability to modulate steroid hormone production in the adrenal glands. *In vitro* studies show that modifying the available concentrations of FDX1 or FDX1 mutants harbouring different redox potentials can influence CYP catalytic activity (Bureik et al., 2005, Grinberg et al., 2000). However, to date there are no *FDX1* human mutations identified or *Fdx1* knockout animals to investigate the whole system consequences of such changes.

## 3.2 Rational for work

Previous *in vitro* studies established FDX1 can influence steroid hormone production through regulating CYP enzymatic activity. However, the *in vivo* impact of these changes remains undetermined. My project aimed to develop zebrafish as an *in vivo* model to study mitochondrial redox reactions. Additionally, we intended to investigate the influence of redox reactions on mitochondrial CYP enzymes and establish the effect on a whole-system. The objective of this current study was to characterise the FDX1 paralogues in zebrafish and determine, *in vivo*, how ferredoxin deficiency affects embryonic development and influences steroidogenic capacity.

### 3.3 Methods

#### 3.3.1 PCR amplification and cloning of zebrafish ferredoxin paralogues

The *fdx1* and *fdx1b* coding sequences were amplified and sequenced from cDNA derived from an ovary of an adult female zebrafish. Oligonucleotides were designed based on sequences annotations from ENSEMBL Zv9 genomic database. For the amplification of *fdx1*, all oligonucleotides were designed with BamHI restriction sites to allow direct cloning into pCS2+ and pCDNA6-V5. Reverse oligonucleotides were used to generate products with (XR-BamHI) and without (R-BamHI) a stop codon to allow the three prime end to be tagged with a V5 epitope. The same strategy was implemented for amplification of *fdx1b*, except primers were designed with flanking EcoRI restriction sites (Table 3.1). RT-PCR was performed using a high fidelity polymerase. After PCR purification, digestion of the PCR product and ligation into the required plasmid were performed using the standard protocols. Directionally of insert was screened using T7 vector primer with an appropriate insert primer.

**Table 3.1 Oligonucleotides for cloning of zebrafish ferredoxin paralogues**

<i>Gene</i>	<i>Primer</i>	<i>Sequence (5-prime to 3-prime)</i>
<i>fdx1</i>	<i>fdx1</i> -F-BamHI	TACCGAGCTCGGATCCATGTCTGCGTGTGTTTTAAGAG
	<i>fdx1</i> -XR-BamHI <sup>a</sup>	CTGGACTAGTGGATCCTTATATTTTGGGTGGGGCTGT
	<i>fdx1</i> -R-BamHI	CTGGACTAGTGGATCCTATTTTGGGTGGGGCTGTG
<i>fdx1b</i>	<i>fdx1b</i> -F-EcoRI	CAGTGTGGTGGAAATTCATGGCATATCGTATGTGTGTGC
	<i>fdx1b</i> -XR-EcoRI <sup>a</sup>	GATATCTGCAGAATTCTCATTTGCTGCTCACAGCCT
	<i>fdx1b</i> -R-EcoRI	GATATCTGCAGAATTCATTTGCTGCTCACAGCCT

<sup>a</sup>Reverse oligonucleotides contain a stop codon.

### 3.3.2 *PCR amplification and cloning of zebrafish mitochondrial redox partners for expression assays*

For protein expression and purification of the zebrafish mitochondrial redox proteins, each coding sequence was cloned into pET22b vector. The sequences were amplified in the mature form without the predicted mitochondrial targeting sequence (mitochondrial targeting sequences were predicated by alignment conservation). Oligonucleotides used for amplification and ligation are listed in Table 3.2.

**Table 3.2 Oligonucleotides for cloning of zebrafish mitochondrial redox partners into pET22b**

<i>Gene</i>	<i>Primer</i>	<i>Sequence</i> (5-prime to 3-prime)
<i>fdx1</i>	p.46-F-NdeI	CAGTGTGGTGGCATATGTCACATAGGGCTGAAGAGAAG
	XR-EcoRI	CCATCGATTTCGAATTCCTTTGGGTGGGGCTGTG
<i>fdx1b</i>	p.46-F-NdeI	CAGTGTGGTGGCATATGGGTTCTTCAAGCTCTAAAGTGCT
	XR-EcoRI	CCATCCGATTTCGAATTCCTTTGCTGCTCACAGCCT
<i>cyp11a1</i>	p.36-F	ATGCAAAACTCCACTGTCCAGCC
	R	GCATCTCTGCTTTCTGCTGGCA
<i>cyp11a2</i>	p.36-F	ATGCAAGACTCCACTGTACGGC
	R	TCTCTGCTTTCTGCTGGAG
<i>cyp11c1</i>	p.138-F-NdeI	CAGTGTGGTGGCATATGCAAAGCTCAGATCCGCTG
	R-EcoRI	CCATCGATTTCGAATTCGAGTGCTGGTGTGTGAGTGT
<i>fdxR</i>	p.56-F-NdeI	CAGTGTGGTGGCATATGCAGCTACTGAAGGCTCGA
	R-NotI	CCATCGATTTCGCGGCCGCGGACCAGGCGATCTTCAG

Zebrafish *cyp11a1* and *cyp11a2* were cloned within NdeI and EcoRI sites of pET22b via blunt end cloning due to the presences of an NdeI site in the coding sequences. Cloning into the NdeI restriction site was required for all genes as it removes the *pelB* signal sequence required for periplasmic localisation. *fdxR* and *cyp11c1* were also cloned into NdeI and EcoRI using restriction digest of the PCR product and direct ligation into the vector. All cytochrome P450 enzymes and FdxR were cloned in-frame with the carboxyl polyhistadine tag to purification of the protein. Mature *fdx1* and *fdx1b* were directionally cloned using NdeI and EcoRI restriction sites without the carboxyl terminal polyhistadine tag as it was predicated to interfere with redox potential.

### **3.3.3 Alignment and phylogenetic analyses of zebrafish Fdx isozymes**

Coding sequences were used to infer Fdx1 and Fdx1b protein sequences. Zebrafish Fdx1 and Fdx1b protein sequences were then compared to vertebrate Fdx1 protein sequences, including human (*Homo sapiens*; ENSP00000260270), gorilla (*Gorilla gorilla gorilla*; ENSGGOP00000023526), bovine (*Bos Taurus*; ENSBTAT00000033850), mouse (*Mus musculus*; ENSMUSP00000034552), medaka (*Oryzias latipes*; ENSORLP00000005248), and stickleback (*Gasterosteus aculeatus*; ENSGACP00000018745). Alignment and homology analyses were performed as described in Section 2.2.1.

### **3.3.4 Characterisation of Fdx1 and Fdx1b expression**

The spatial and temporal expression of *fdx1* and *fdx1b* were determined by RT-PCR. A 694 nucleotide fragment of the *fdx1* gene was amplified using 3' UTR F and R primers (Table 3.3) and 25 ng of cDNA as previously described under the following conditions: initial denaturation at 95 °C for five minutes, followed by 40 cycles at 95 °C for 30 seconds, 58 °C for 40 seconds and 72 °C for 40 seconds; and a final incubation at 72 °C for 7 minutes. To define the expression of *fdx1b*, a 159 nucleotide fragment was amplified with e3 F and e5 R primers (Table 3.3) under the

conditions described above. As a control for cDNA quality and equal loading, a 102 nucleotide fragment of the  $\beta$ -actin gene (*actb1*, ENSEMBL Gene ID ENSDARG00000037746) was amplified using e4 F and e4 R primers (Table 3.3).

**Table 3.3 Oligonucleotides for RT-PCR expression analysis of the *fdx1* and *fdx1b* genes.**

<i>Gene</i>	<i>Primer</i>	<i>Sequence</i> (5-prime to 3-prime)
<i>fdx1</i>	3' UTR F	AGTCAAACCAGAGCGTTTCC
	3' UTR R	CAGCTACAGGCATATCTGCAA
<i>fdx1b</i>	e3 F	GAGCAGCGTATTTGTACACAGA
	e5 R	ACCATTGGCTCCAGTTTGTCA
<i>actb1</i>	e4 F	CGAGCAGGAGATGGGAACC
	e4 R	CAACGGAAACGCTCATTGC

### 3.3.5 Zebrafish *fdx1b* knockdown studies

To analyse the role of the two zebrafish ferredoxin paralogues during development I performed transient knockdowns with specific anti-sense morpholinos as previously described in Section 2.3.9. Translation of *fdx1* mRNA was blocked using 9 ng morpholino per embryo directed to the start ATG codon (*fdx1*-ATG<sup>MO</sup>). Additionally, a five base-pair mismatched control morpholino (*fdx1*-Ctl<sup>MO</sup>) and 9 ng of *fdx1*-Spl<sup>MO</sup> targeting the splice acceptor site of exon two were also used. For *fdx1b* disruption, 6 ng of ATG morpholino (*fdx1b*-ATG<sup>MO</sup>), and 6 ng of a splice morpholino (*fdx1b*-Spl<sup>MO</sup>) targeting the splice acceptor site of exon four were used. A five base-pair mismatch of the ATG morpholino was injected as a control (*fdx1b*-Ctl<sup>MO</sup>). Sequences of the morpholinos and mismatch controls are listed in Table 3.4.

**Table 3.4 Sequences of the anti-sense morpholinos used for the transient knockdown of *fdx1* and *fdx1b* genes**

<i>Gene</i>	<i>Morpholino</i>	<i>Sequence</i> (5-prime to 3-prime)
<i>fdx1</i>	<i>fdx1</i> -ATG <sup>MO a</sup>	CTCTTAAAACACACGCAGACATTGC
	<i>fdx1</i> -CtI <sup>MO</sup>	CTGTTAAAAGACACGGACACATTCC
	<i>fdx1</i> -Spl <sup>MO</sup>	TCTCTTCAGCCCTGCATAGAAACAC
<i>fdx1b</i>	<i>fdx1b</i> -ATG <sup>MO a</sup>	GCACACACATACGATATGCCATGCT
	<i>fdx1b</i> -CtI <sup>MO</sup>	GCAGACAGATACGTTATGCGATGGT
	<i>fdx1b</i> -Spl <sup>MO b</sup>	GCTCCTAATATAGACACACACATGC

<sup>a</sup>ATG morpholinos impair initiation of mRNA translation

<sup>b</sup>Splice morpholinos induce abnormal splicing of the mRNA

Underlined letters highlight base-pair mismatches between ATG or splice morpholinos and controls.

### 3.3.6 mRNA rescues of *fdx1* and *fdx1b* morphants

To confirm specificity of the phenotype of *fdx1* and *fdx1b* morpholino knockdown, co-injection with mRNA of *fdx1* or *fdx1b* was performed. Five-prime oligonucleotides were designed containing five base-pair synonymous mutations with the morpholino binding site and a T7 polymerase recognition sequence. A reverse oligonucleotide was designed to include a polyadenylation signal (Table 3.5). PCR was performed using high fidelity polymerase using the methodology previously described and using previously cloned *fdx1* or *fdx1b* as a template. After purification of the PCR product, mRNA was synthesised containing a 7-methyl guanosine five prime cap and a polyadenylated tail by *in vitro* transcription as detailed in Section 2.3.7.

**Table 3.5 Oligonucleotides for the amplification of *fdx1* and *fdx1b* coding sequences with T7 polymerase recognition sequences and a polyadenylation signal**

<i>Gene</i>	<i>Primer</i>	<i>Sequence</i> (5-prime to 3-prime)
<i>fdx1</i>	T7-mm F	GAAGGTAATACGACTCACTATAGGGAGAGCAATGTC <u>AGCCTG</u> TGTATT <u>GAGGG</u>
<i>fdx1b</i>	T7-mm F	GAAGGTAATACGACTCACTATAGGGAGAATGGCTT <u>TACCGAAT</u> GTGC <u>GTCC</u>
	R-polyA	TCACTAAAGGGAACAAAAGTGG

Underlined letters highlight base-pair mismatches between ATG morpholinos and amplified mRNA.

### 3.3.7 Phenotypic classification of embryos and larvae

After morpholino injection of *fdx1*-ATG<sup>MO</sup>, *fdx1*-Spl<sup>MO</sup> or *fdx1*-Ctl<sup>MO</sup> embryos were screened for rhodamine incorporation into the embryo proper between 64 and 572 cell stages. At 10 hpf embryos were scored based on the percentage of epiboly completed and detection of embryonic shield (Table 3.6).

**Table 3.6 Classification of the phenotype of *fdx1* morphants at 10 hpf**

Class I	Class II	Class III	Class IV
normal epiboly movement	delay in epiboly	serve delay in epiboly and no shield	dead

Similarly, embryos injected with *fdx1b*-ATG<sup>MO</sup> and *fdx1b*-Spl<sup>MO</sup> and *fdx1b*-Ctl<sup>MO</sup> were screened for rhodamine incorporation into the embryo after injection. At 120 hpf, larvae were classified into four groups based on the inflation of the swim bladder, the size of the yolk sac, oedema of the pericardial sac and size of the head (Table 3.7).

**Table 3.7 Phenotypic classification of the *fdx1b* morphants at 120 hpf**

Phenotype	Class I	Class II	Class III	Class IV
<b>Swim bladder</b>	inflated	inflated	none	none
<b>Yolk sac</b>	normal	enlarged	enlarged	enlarged
<b>Pericardial sac</b>	normal	normal	normal	oedema
<b>Head</b>	normal	normal	small	shortened snout

## 3.4 Results

### 3.4.1 *Zebrafish Fdx1 and Fdx1b homology with other vertebrate Ferredoxins*

Two *FDX1* paralogues were identified in zebrafish and these are termed *fdx1* and *fdx1b*. Protein sequences of our zebrafish wild-type strain were deduced by directly sequencing RT-PCR products amplified from ovary cDNA. No polymorphisms were identified in either gene when compared to the annotated sequences on the ENSEMBL genome database (Zv9). Protein sequence analysis was performed *in silico* to determine evolutionary conservation of the two identified ferredoxin paralogues. The pre-processed zebrafish ferredoxins; Fdx1 and Fdx1b are 175 and 168 amino acids in length, respectively, and share 43 % protein identity. Additionally, the predicted mature proteins (after cleavage of the mitochondrial signalling peptide) share 60 % protein identity. Fdx1 was most similar to other teleost species with 57 % and 51 % identity with medaka and stickleback.

Conservation of known functional amino acids and motifs was observed in both zebrafish paralogues. Motif one and motif three collectively contain the four cysteine residues required for Fe/S binding and are present in both zebrafish paralogues. The negatively charged motif two, which contains amino acids required for the interaction with redox partners, was also conserved. Many other functionally important amino acids were identified, including, Gly26, His56 and Pro108 (Grinberg et al., 2000) which are present in all vertebrate ferredoxins, and Thr49 (Hannemann et al., 2001) and Thr54 (Uhlmann and Bernhardt, 1995) which are both involved in modulating the redox potential of the protein. Notably, at amino acid 14, Fdx1b has a glutamine amino acid rather than the well conserved arginine. Additionally, at the corresponding amino acids for Thr71 in motif two, Fdx1 has a serine and Fdx1b contains a valine (Figure 3.1).



### **3.4.2 Tissue distribution and temporal expression of *fdx1* and *fdx1b***

The expression of *fdx1* and *fdx1b* genes was investigated during early zebrafish development and in adult fish. *fdx1* was expressed as a maternal transcript (present from one-cell stage) and is sustained by the zygote throughout development (Figure 3.2). Expression of *fdx1b* started weakly during late segmentation period (28 hpf) and became prominent from 32 hpf up to 120 hpf (Figure 3.2A). In adults, *fdx1* expression was detected in all tissues tested including the gonads, kidney, brain, liver, intestine and heart. Zebrafish *fdx1b* expression was identified in the kidney head, brain, ovary and testis (Figure 3.2). No sexual dimorphism in the expression pattern of either gene was observed.

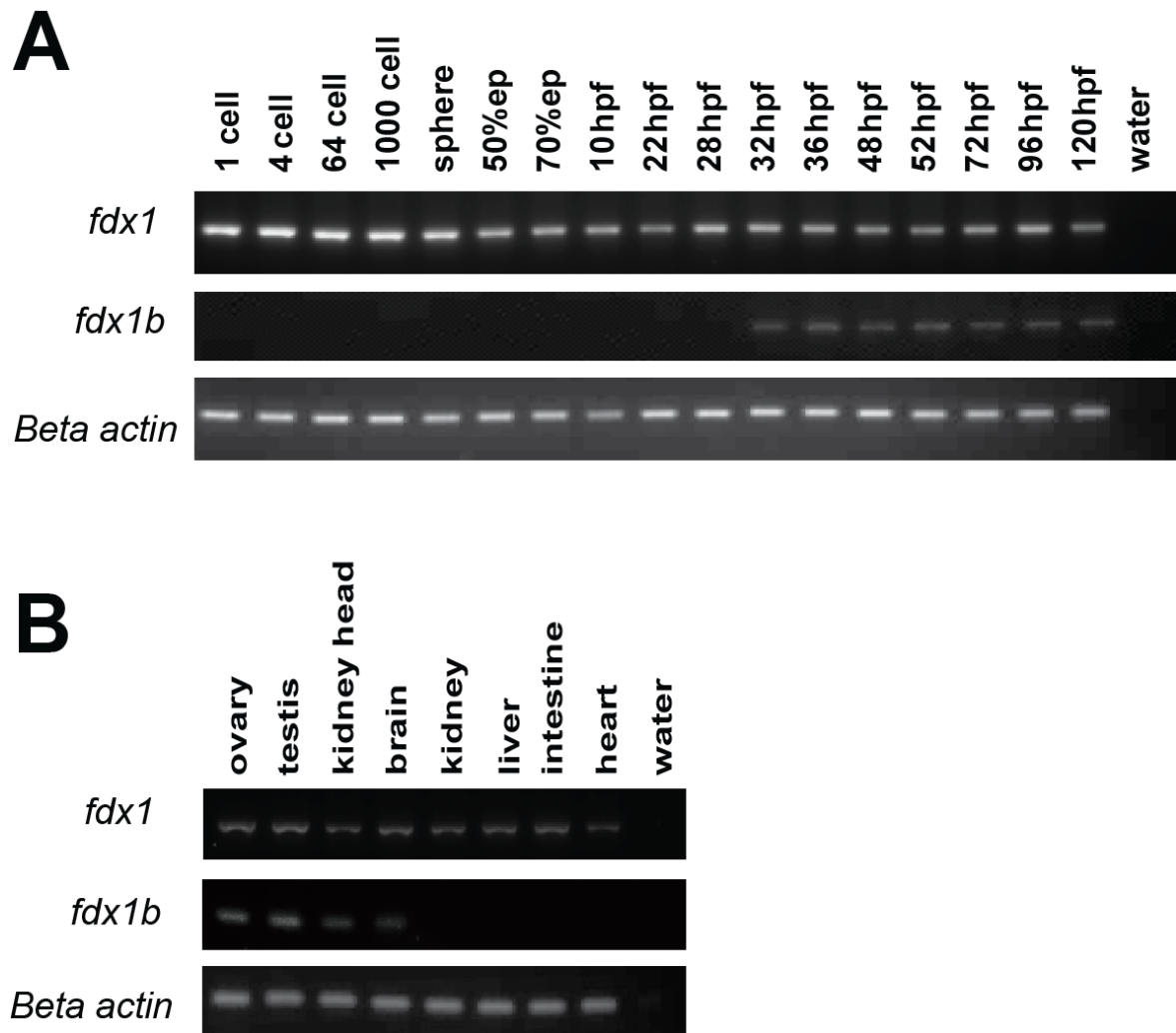


**Figure 3.2 Temporal expression and tissue distribution of zebrafish *fdx1* and *fdx1b* transcripts.**

Expression of *fdx1* and *fdx1b* was characterised in zebrafish embryos and larvae (**A**) and in adult tissues (**B**). Beta actin was used as a loading control.

### **3.4.3 Defining the role of Fdx1 in early zebrafish development**

To determine the role of Fdx1 in zebrafish development transient knockdown studies were performed using anti-sense morpholinos. Microinjection of the *fdx1*-ATG<sup>MO</sup> resulted in a phenotype during the gastrula phase consisting of delayed epiboly and a grainy cellular appearance. An initial titration injection of 3 ng, 6 ng and 9 ng of *fdx1*-ATG<sup>MO</sup> per embryo was performed to establish the toxicity of the morpholino. Increasing concentration showed increased severity of the phenotype observed at 10 hpf (Figure 3.3). As there were no adverse effects with the *fdx1*-Ctl<sup>MO</sup> at any concentration (data not shown), 9 ng was used for subsequent experiments. By 10 hpf, 69 % of *fdx1* morphants showed a class II phenotype consisting of a delay in epiboly (the movement of cells over the yolk during gastrulation) and a thickening of the dorsal blastoderm. Additionally, 18 % of *fdx1* morphants showed a class III phenotype where a severe delay in epiboly was observed, together with a grainy appearance of the cells of the blastoderm and no shield was detected. In contrast, 97 % of control injected embryos showed a typical Class I phenotype with normal developmental progression through epiboly. The observed phenotype in the *fdx1*-ATG<sup>MO</sup> injected embryos was partially reproduced by injecting with the *fdx1* splice disrupting morpholino (*fdx1*-Spl<sup>MO</sup>), with 40 % of embryos showing either Class II (19 %), Class III (9 %) or failing to thrive (12 %) by 10 hpf. Furthermore, co-injection of the *fdx1* five base-pair mismatched mRNA with *fdx1*-ATG<sup>MO</sup> partially restored the mutant phenotype. Of the rescued embryos, 65 % showed a normal Class I phenotype compared 8 % of *fdx1*-ATG<sup>MO</sup> injected embryos (Figure 3.3).

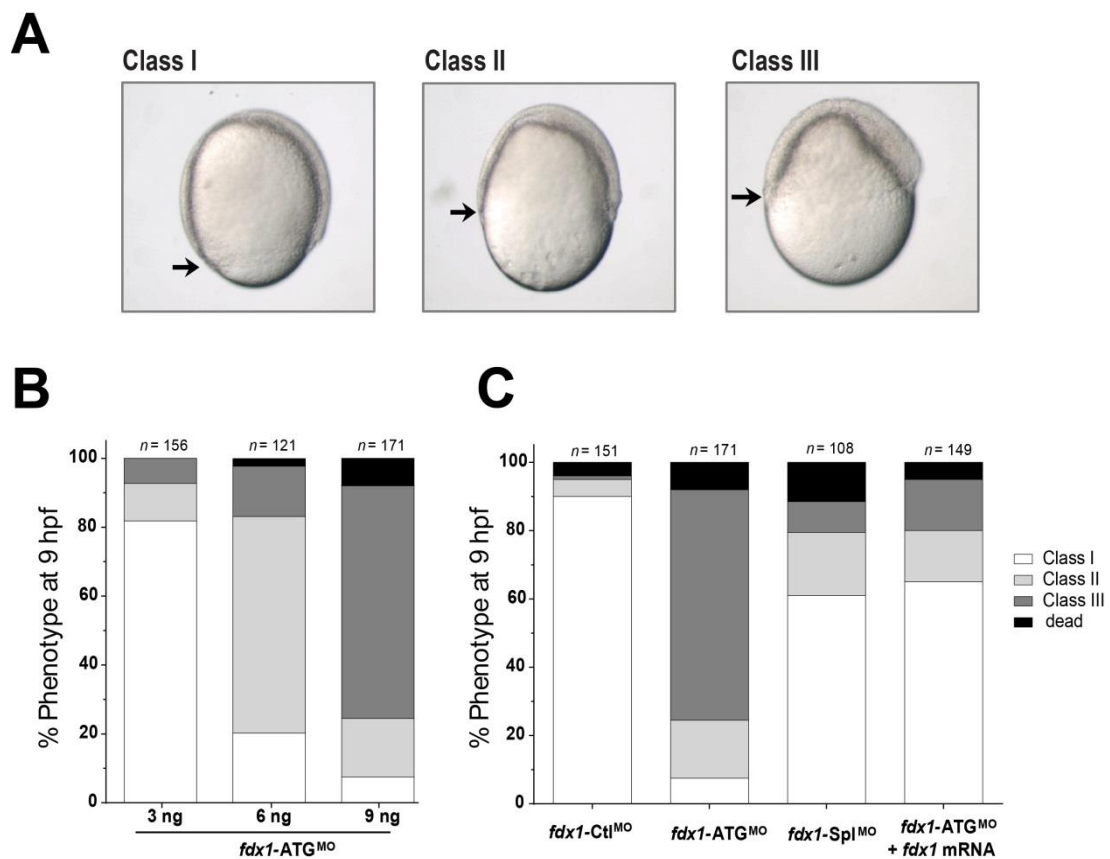


**Figure 3.3 Morphological phenotype of embryos injected with Fdx1 morpholino at 9 hpf**

**(A)** Embryos injected with *fdx1*-ATG<sup>MO</sup>, *fdx1*-Spl<sup>MO</sup> or *fdx1*-Ctl<sup>MO</sup> were classified based on their progression of epiboly at 9 hpf. Class I represents a normal epiboly, and class II and class III represent delayed movement as indicated by the black arrow. **(B)** A titration of *fdx1*-ATG<sup>MO</sup> of 3 ng, 6 ng and 9 ng showed increasing in the severity of morphological phenotype. **(C)** Injection of 9 ng of *fdx1*-Ctl<sup>MO</sup> showed 95 % of the normal Class I phenotype compared to *fdx1*-ATG<sup>MO</sup> injected embryos which had 68.9 % Class II and 18 % Class III. Embryos injected with 9 ng with *fdx1*-Spl<sup>MO</sup> to target zygotic transcripts had 40 % of embryos with Class II, Class II or failing to thrive. Co-injection of with *fdx1* mRNA with *fdx1*-ATG<sup>MO</sup> partially restored embryos to a Class I phenotype.

### 3.4.4 Pregnenolone synthesis in *Fdx1* morphants

To determine if Fdx1 was required for early pregnenolone steroid synthesis in the developing embryo, steroids were extracted and analysed by LC-MS/MS at 10 hpf from *fdx1*-ATG<sup>MO</sup> and *fdx1*-Ctl<sup>MO</sup> injected embryos. No difference was observed in pregnenolone concentration between *fdx1* morphants and controls. Pregnenolone concentrations of *fdx1*-ATG<sup>MO</sup> injected embryos were 0.65 pg per embryo compared *fdx1*-CTL<sup>MO</sup> embryos with 0.64 pg per embryo (Figure 3.4).

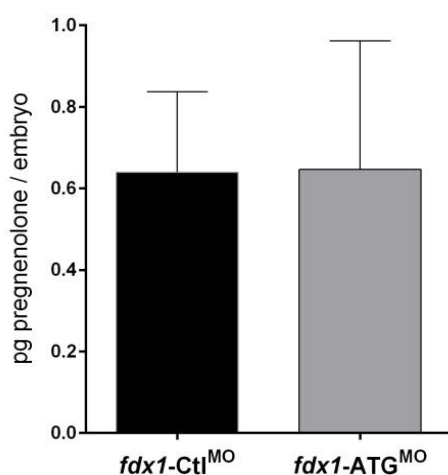


**Figure 3.4** Pregnenolone concentrations of *fdx1* morphants and controls at 10 hpf

Embryos were injected with either *fdx1*-Ctl<sup>MO</sup> (black) or *fdx1*-ATG<sup>MO</sup> (grey) and pregnenolone concentrations were calculated from amounts measured by LC-MS/MS in zebrafish extracts. *fdx1*-ATG<sup>MO</sup> injected embryos had 0.65 (± 0.32) pg per embryo while *fdx1*-CTL<sup>MO</sup> injected embryos had 0.64 (± 0.20) pg per embryo. Graph represents mean ± SD from three independent experiments.

### ***3.4.5 Identifying the role of Fdx1b during zebrafish development***

The expression of *fdx1b* was disrupted by injecting an anti-sense morpholino targeting its transcriptional start codon (*fdx1b*-ATG<sup>MO</sup>). Injected embryos developed normally up to 48 hpf. A late onset phenotype was observed from 52 hpf and was most obvious at 120 hpf. *fdx1b* morphants showed a delay in the absorption of the yolk sac, smaller heads, jaw malformations and cardiac oedema when compared to control injected embryos (Figure 3.5). At 120 hpf, the majority *fdx1b*-ATG morphants showed Class II (54 %) morphology consisting of a large yolk sac and no inflation of the swim bladder, or Class III (27 %) which had additional jaw malformation. In comparison, the majority of *fdx1b*-Ctl<sup>MO</sup> injected larvae showed a normal Class I phenotype (94 %). To determine the specificity of the morphological phenotype, mRNA rescues were performed by co-injection of *fdx1b*-ATG<sup>MO</sup> and *fdx1b* mRNA. A partial rescue of the morphological phenotype was observed with 47 % of larvae having a Class I phenotype at 120 hpf compared with 18 % of larvae injected with *fdx1b*-ATG<sup>MO</sup> only. However, there was an increase in the severe Class IV morphology with 6 % of mRNA rescued larvae compared to 1 % of *fdx1b*-ATG<sup>MO</sup> only.

A second morpholino targeting exon four splice acceptor site of *fdx1b* (*fdx1b*-Spl<sup>MO</sup>) was used to confirm gene disruption by RT-PCR. At 72 hpf, *fdx1b* transcript could not be detected in *fdx1b*-Spl<sup>MO</sup> injected larvae using the primer pair *fdx1b* e3F and e3R (Figure 3.6). By 96 hpf transcript levels begin to be detected and by 120 hpf no difference can be seen between the control and the *fdx1b*-SPL<sup>MO</sup> injected larvae. These morphants showed a similar, but less prominent, morphology compared to the translational blocking morpholino with 30 % and 18 % of larvae having a Class II or Class III phenotype, respectively.

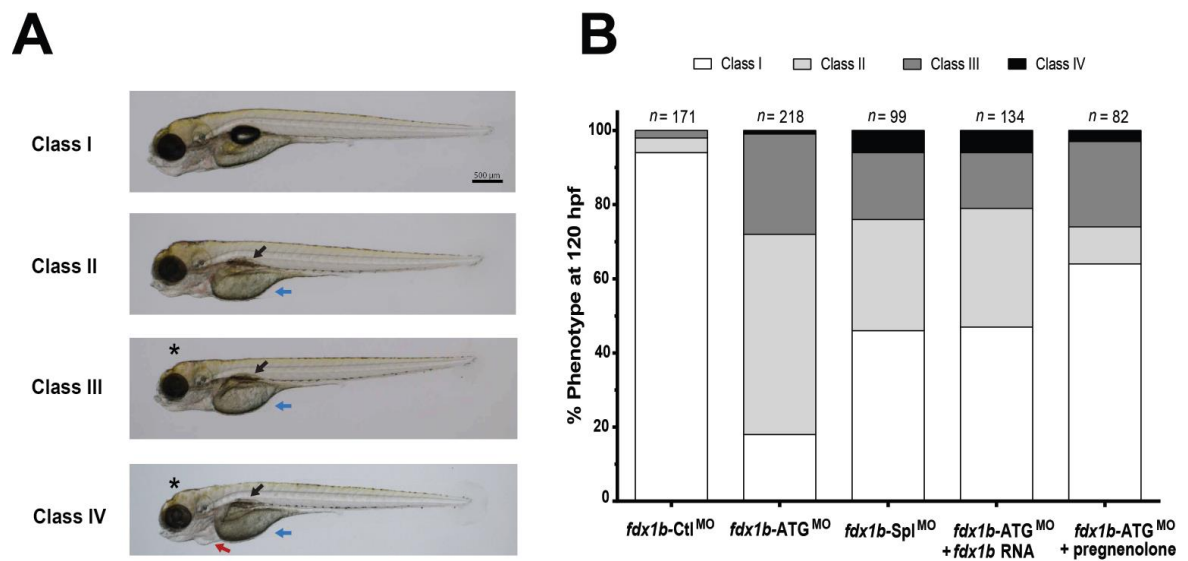


**Figure 3.5 Morphological characterisation of *fdx1b* morphants at 120 hpf.**

**(A)** At 120 hpf larvae were categorised into four different classes depending on inflation of the swim bladder (black arrow), size of the yolk sac (blue arrow), head size (black asterisks) and pericardial oedema (red arrow) (Table 3.7). Class I represents a wild-type phenotype. **(B)** The phenotypic spectrum observed in *fdx1b-Ctl*<sup>MO</sup>, *fdx1b-ATG*<sup>MO</sup> and *fdx1b-Spl*<sup>MO</sup> injected embryos. Additionally, embryos co-injected with *fdx1b-ATG*<sup>MO</sup> and *fdx1b* mRNA were also assessed for phenotypic abnormalities.

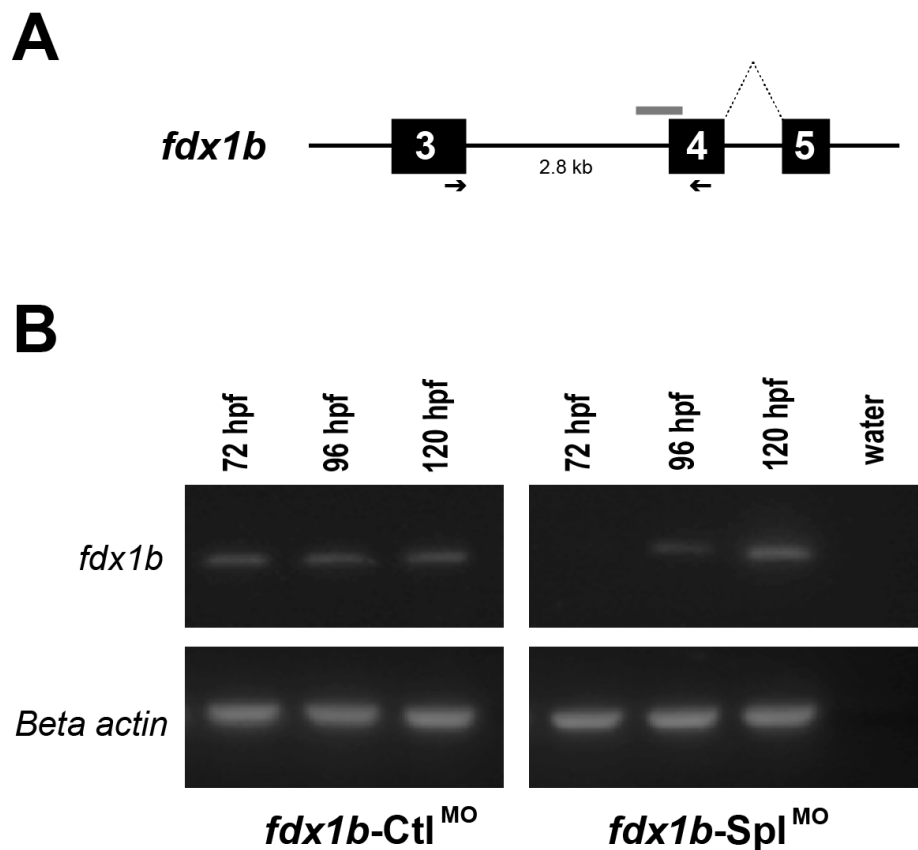


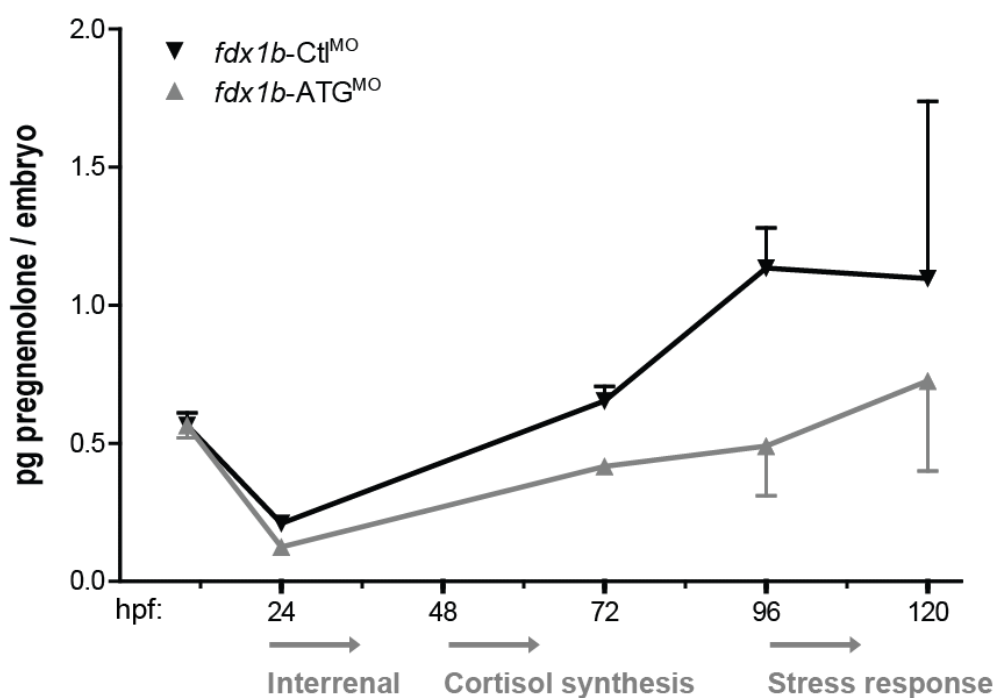
**Figure 3.6** The *fdx1b* splice morpholino (*fdx1b-Spl<sup>MO</sup>*) effectively disrupts the *fdx1b* mRNA transcript

(A) The *fdx1b-Spl<sup>MO</sup>* binds to the splice acceptor site of exon 4, causing inclusion of the enclosed intron in the *fdx1b* mRNA. (B) RT-PCR analysis confirmed disruption of the *fdx1b* mRNA in the splice morphants but not in embryos injected with the control morpholino (*fdx1b-Ctl<sup>MO</sup>*). Black arrows indicate the binding sites of the primers used for RT-PCR analysis to confirm missplicing of *fdx1b* mRNA; grey line represents *fdx1b-Spl<sup>MO</sup>* binding site at the splice acceptor site of exon 4. Beta actin was used as a loading control.

### **3.4.6      *The effects of fdx1b deficiency on zebrafish steroidogenesis***

Pregnenolone and cortisol concentrations were measured in *fdx1b*-ATG<sup>MO</sup> and *fdx1b*-Ctl<sup>MO</sup> injected embryos at five developmental stages to investigate the influence of Fdx1b on the zebrafish steroidogenic pathway (Figure 3.7). No differences in pregnenolone concentrations were observed between *fdx1b*-ATG morphants and controls at 10 hpf or 24 hpf. At 72 hpf, *fdx1b*-ATG morphants had pregnenolone concentrations of 0.42 pg per larva compared to 0.65 pg per larva in the controls. Fdx1b morphants maintained lower pregnenolone concentrations at 72 hpf and 96 hpf and at 120 hpf were detected having 0.73 pg in contrast to the control injected embryos with 1.10 pg.

As a measure of steroid hormone biosynthesis capabilities, cortisol was determined from both *fdx1b*-ATG and *fdx1b*-Ctl morphants during development. At 10 hpf and 24 hpf there was no difference in cortisol concentrations between *fdx1b*-ATG and *fdx1b*-Ctl embryos. However, at 72 hpf cortisol levels were undetectable in *fdx1b*-ATG<sup>MO</sup> injected larvae while control larvae were detected having 2.5 pg of cortisol per larva. By 120 hpf *fdx1b*-ATG morphants regained some steroidogenic capacity producing 0.9 pg cortisol per larva, but still remained drastically reduced compared to 15.25 pg in the controls (Figure 3.8). Additionally, embryos injected with *fdx1b*-Spl<sup>MO</sup> were analysed at 72 hpf and showed cortisol concentrations of 0.4 pg per larva, 3.6 times less than control larvae at the same time point (data not shown).

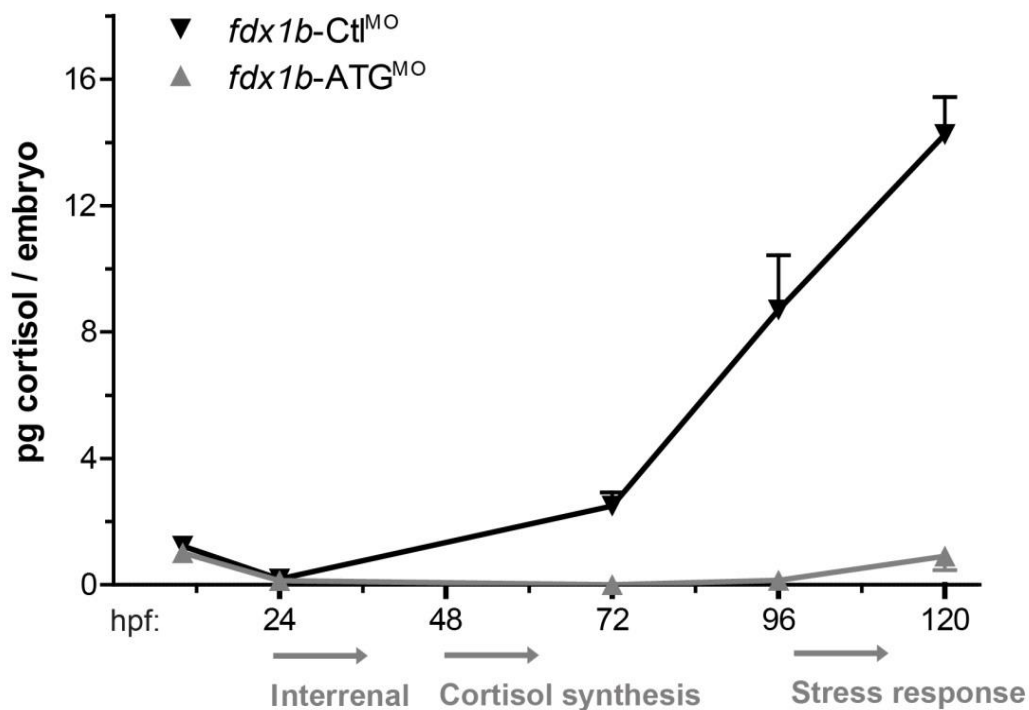


**Picograms pregnenolone per embryo / larva**  
mean ( $\pm$ SD)

	10 hpf	22 hpf	72 hpf	96 hpf	120 hpf
<i>fdx1b-ATG</i> <sup>MO</sup>	0.57 (0.06)	0.13 (0.01)	0.42 (0.03)	0.49 (0.23)	0.73 (0.57)
<i>fdx1b-CTL</i> <sup>MO</sup>	0.57(0.07)	0.21 (0.01)	0.65 (0.09)	1.14 (0.21)	1.10 (1.11)

**Figure 3.7 Pregnenolone concentrations of Fdx1b morphants and controls during development**

Pregnenolone concentrations were measured over development in *fdx1b-ATG*<sup>MO</sup> (grey) and *fdx1b-Ctl*<sup>MO</sup> (black). Picograms of pregnenolone per embryo or larva were calculated from concentrations measured by LC-MS/MS in zebrafish extracts. Data represents concentrations from at least two independent experiments and was plotted against developmental stages as mean  $\pm$  SD.



**Picograms cortisol per embryo / larva**  
mean ( $\pm$ SD)

	10 hpf	22 hpf	72 hpf	96 hpf	120 hpf
<i>fdx1b-ATG</i> <sup>MO</sup>	1.01 (0.19)	0.14 (0.19)	0.0 (0.0)	0.14 (0.24)	0.90 (0.75)
<i>fdx1b-CTL</i> <sup>MO</sup>	1.53 (0.21)	0.19 (0.26)	2.50 (0.59)	8.70 (3.00)	15.25 (2.63)

**Figure 3.8 Cortisol concentrations of Fdx1b morphants and controls during development**

Cortisol concentrations were measured over development in zebrafish injected with *fdx1b-ATG*<sup>MO</sup> (grey) or *fdx1b-CTL*<sup>MO</sup> (black). Picograms of cortisol per embryo or larva were calculated from concentrations measured by LC-MS/MS in zebrafish extracts. Data represents concentrations from at least two independent experiments and was plotted against developmental stages as mean  $\pm$  SD.

### **3.4.7 mRNA and steroid rescues of *fdx1b* deficient embryos**

Rescue experiments were performed with the co-injection of five base-pair mismatched Fdx1b mRNA with *fdx1b*-ATG<sup>MO</sup> and steroid extraction was performed at 72 hpf. Co-injection of mRNA partially restored pregnenolone concentrations to 0.60 (SD  $\pm$  0.21) pg per larvae, which were similar to control injected embryo levels of 0.65 (SD  $\pm$  0.09) pg per larvae, however this change was not significant. Additionally, cortisol levels remained undetected in larvae co-injected with *fdx1b*-ATG<sup>MO</sup> and *fdx1b* mRNA (Figure 3.9). To further elucidate the role of Fdx1b in zebrafish steroidogenesis, zebrafish injected with *fdx1b*-ATG<sup>MO</sup> were supplemented with pregnenolone or vehicle (ethanol) and cortisol was measured at 72 hpf. Despite there being an excess pregnenolone detected in the embryos (1.92 pg - data not shown), cortisol levels remained undetected (Figure 3.9).

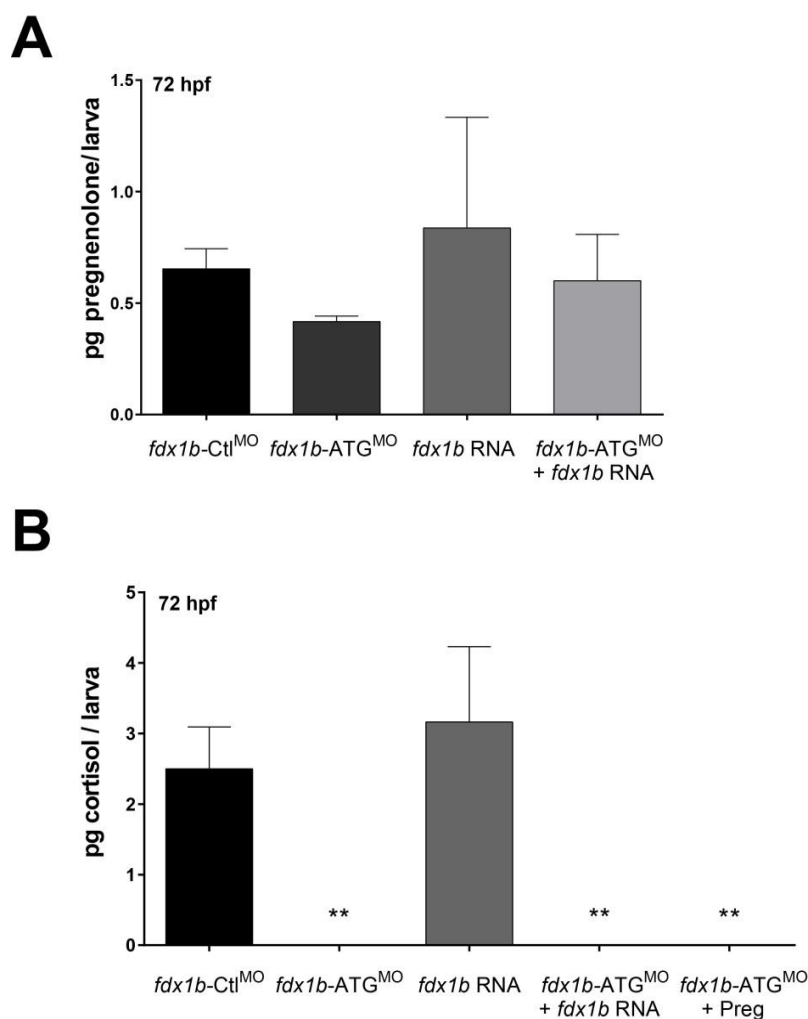


**Figure 3.9 Pregnenolone and cortisol measurements in *fdx1b* rescued larvae.**

Steroids concentrations were measured in embryos injected with *fdx1b-Ctl*<sup>MO</sup>, *fdx1b-ATG*<sup>MO</sup>, *fdx1b* mRNA and *fdx1b-ATG*<sup>MO</sup> with *fdx1b* mRNA. **(A)** Pregnenolone concentrations of embryos showed no difference between the injected groups. **(B)** Cortisol concentrations were similar in embryos injected with *fdx1b* mRNA compared to control injected embryos. In comparison, co-injection of *fdx1b-ATG*<sup>MO</sup> and *fdx1b* mRNA could not restore cortisol levels. Additionally, incubation of embryos with 50 nM pregnenolone also failed to synthesise cortisol. Concentrations were measured at 72 hpf from three independent experiments. Concentrations are expressed as picograms per larva (mean  $\pm$  SD), calculated from concentrations measured by LC-MS/MS. Statistical analysis was performed using one-way ANOVA followed by Dunnett's multiple comparisons test. \*\* P<0.01

## 3.5 Discussion and prospective studies

### 3.5.1 *Evolutionary conservation of the ferredoxin electron transport system*

It is well established that ferredoxins are evolutionary well conserved (Ewen et al., 2012). Interestingly, zebrafish is the only teleost that retained both duplicated ferredoxin genes after the genome duplication of the common teleost ancestor. This provides a unique opportunity to investigate amino acid changes in the duplicated genes and correlate these with functional capabilities. Although the zebrafish ferredoxin pre-proteins share 43 % amino acid identity, there are notable differences which may provide insights into functionally important amino acids of ferredoxins.

Post translational modifications of ferredoxins can alter activities of the interacting CYP enzymes. Thr71 is located within the interaction domain which is the interface for redox partner recognition. *In vitro*, phosphorylation of bovine FDX1 at position Thr71 increases CYP11A1 enzymatic activity, but not CYP11B1 activity (Bureik et al., 2005) suggesting an important regulatory mechanism impacting on mitochondrial CYP enzyme function. Interestingly, zebrafish Fdx1 has a serine at this position which is capable of being phosphorylated, whereas Fdx1b has a valine residue, which is not amenable to phosphorylation. The mechanistic importance of phosphorylation of redox partners during *in vivo* steroidogenesis has not yet been elucidated. It would be hypothesised phosphorylation of zebrafish Fdx1 at Ser71 would improve the interaction and catalytic activity of some its redox CYP enzymes. Fdx1 is predicted to be the mitochondrial redox partner of Cyp11a1 during early zebrafish embryo development. Therefore, phosphorylation may be an important mechanism for regulating pregnenolone production during zebrafish development. Importantly, phosphorylation capability at this position has no effect on

interactions with FDXR (Bureik et al., 2005) suggesting that both Fdx1 and Fdx1b can interact with the single zebrafish FdxR protein independent of their phosphorylation status.

Another notable difference in amino acid conservation is the replacement of Arg14 with a polar uncharged glutamine residue in the zebrafish Fdx1b protein. The biochemical properties of this amino acid position is highly conserved in bacterial, plant and vertebrate ferredoxins and typically carries a positive charged amino acid (arginine, lysine or histidine) (Grinberg and Bernhardt, 1998). In the mature bovine FDX1, crystallography studies show amino acid Arg14 forms a hydrogen bond with the conserved Pro108. Elimination of this hydrogen bond decreases stability of the protein at physiological temperatures, but has no effect on redox potential or protein interactions (Grinberg and Bernhardt, 1998). The zebrafish Fdx1b protein is likely to have decreased stability compared to other ferredoxins due to a glutamine residue at position 14; however, the significance of this currently remains unknown. *In silico* sequence comparison of the two zebrafish FDX1 proteins suggests differences in regulation and stability. However, further studies are required to determine the protein stability of each zebrafish paralogue and to gain insights into their individual functional roles during zebrafish development.

### ***3.5.2 The role of Fdx1 in zebrafish development***

Expression analysis of the zebrafish *fdx1* revealed it was present from the one-cell stage as a maternal transcript and was maintained by the zygote during zebrafish development. In concordance with human *FDX1* (Picado-Leonard et al., 1988, Voutiainen et al., 1988) zebrafish *fdx1* expression was detected in all tissues tested. Knockdown of Fdx1 by antisense morpholino showed a strong cellular defect with abnormal epiboly. Further analysis is required to determine if these cellular defects are cellular necrosis, apoptosis, from a general developmental delay in the embryo. To confirm the phenotype of *fdx1* knockdown, the *fdx1*-Spl<sup>MO</sup> was used. This

morpholino also caused epiboly delay and similar cellular defects; however, it was less severe, as splice disrupting morpholinos only affect zygotic pre-RNA (i.e. not maternally derived mRNA). Co-injection of *fdx1*-ATG<sup>MO</sup> with *fdx1* mRNA could restore 65 % of the embryos to the normal Class I phenotype, suggesting the morphological and developmental changes observed resulted from the loss of Fdx1 protein in the developing embryo. Additionally, rescue with *fdx1b* mRNA (data not shown) could also restore the phenotype suggesting functional conservation between the two paralogues. However, the functional role of Fdx1 in the developing zebrafish embryo remains undetermined.

Morpholino knockdown of Cyp11a1 causes a delay in epiboly resulting from decreased pregnenolone synthesis and subsequent destabilisation of microtubules (Hsu et al., 2006). It was hypothesised that Fdx1 would be the redox partner of Cyp11a1 in the yolk syncytial layer. To address this, pregnenolone was measured by LC/MS-MS in *fdx1*-ATG<sup>MO</sup> and *fdx1*-Ctl<sup>MO</sup> injected embryos and no difference was observed. To fully exclude that Fdx1 does not have a role in pregnenolone production, it would be recommended to incubate *fdx1*-ATG<sup>MO</sup> with media supplemented with 50 nM pregnenolone as previously described (Hsu et al., 2006, Parajes et al., 2013), to determine if the epiboly phenotype can be restored. It cannot be excluded that Fdx1 is interacting with other mitochondrial CYP enzymes at this developmental stage. Although, data from transcript microarray profiling of zebrafish CYP enzymes during development, suggest Cyp11a1 is the most likely candidate based on its high expression levels during cleavage and gastrula stages (Goldstone et al., 2010).

In addition to the epiboly phenotype, a distinct, yet uncharacterised, cellular phenotype was observed in Fdx1 deficient embryos. It is hypothesised that disruption of the mitochondrial electron chain, through loss of Fdx1 causes cellular damage. Electron leakage from the

mitochondrial CYP redox chain can contribute to reactive oxygen species (ROS) production (Hanukoglu, 2006). At low concentration ROS is involved in many cellular processes, however, imbalances in the oxidative state of a cell can lead to cell damage and cell death (Prasad et al., 2014). Additionally, changes in redox homeostasis within the adrenal cortex can affect steroidogenesis and has implications for steroidogenic disease (Meimaridou et al., 2012). It remains undetermined if a knockdown of electron transport chain proteins, such as in the *fdx1* morphants, causes cellular defects from the production of mitochondrial ROS. Further investigations are required into the *fdx1* morphant phenotype to identify if the loss of ferredoxin can generate ROS and how the mitochondrial redox pathway affects cellular processes.

### ***3.5.3 Fdx1b expression is required for steroid hormone synthesis in the adult zebrafish***

Alternative to *fdx1*, *fdx1b* expression was restricted to steroidogenic tissues of the kidney head (containing the interrenal gland), brain, ovary and testis. Additionally, *fdx1b* transcripts were up-regulated between 24 and 28 hpf, coinciding with the development of the interrenal gland. (Chai et al., 2003, To et al., 2007). This expression mirrors that of zebrafish *cyp11a2*, the side-chain cleavage enzyme facilitating *de novo* interrenal steroidogenesis in larvae and adults (Parajes et al., 2013) (Chapter 4.0). Therefore, it was hypothesised that Fdx1b is the ferredoxin regulating mitochondrial steroid hormone production in the interrenal.

Transient loss of Fdx1b using morpholino knockdown showed a late on-set phenotype characterised by increased yolk size, small heads, jaw malformations along with a delay in inflation so the swim bladder. This phenotype is consistent with other studies of adrenal insufficiency and glucocorticoid resistance, including the transient knockdown of *cyp11a2* (Parajes et al., 2013) (Chapter 4.0), *ff1b* (orthologue of mammalian steroidogenic factor 1, SF1) (Hsu et al.,

2003), the SF1 transcriptional regulator *dax1* (Zhao et al., 2006) and glucocorticoid receptor (Pikulkaew et al., 2011). This consistency in the morphological phenotype supports the hypothesis that Fdx1b is the ferredoxin regulating glucocorticoid synthesis in the interrenal of larvae and adults.

To determine if *fdx1b* morphants were capable of synthesising glucocorticoids, cortisol measurements were assessed over the first five days of development. Similar to control embryos, *fdx1b*-ATG<sup>MO</sup> injected embryos showed maternal cortisol stores in the yolk were almost depleted after 24 hpf. In wild-type embryos, *de novo* cortisol synthesis begins at 48 hpf (Alsop and Vijayan, 2008). Cortisol synthesis was observed in *fdx1b*-CTL<sup>MO</sup> larvae. However, *fdx1b*-ATG<sup>MO</sup> injected embryos fail to synthesise cortisol at 72 hpf and 96 hpf. Minimal cortisol was detected by 120 hpf, but was still 98 % less than the concentrations observed in the control larvae. This lack of cortisol production at 72 hpf was also observed in the *fdx1b*-Spl<sup>MO</sup> larvae. The inability of Fdx1b deficient embryos to produce cortisol is similar to larvae deficient in Cyp11a2 (Parajes et al., 2013) (Chapter 4.0).

### ***3.5.4 Fdx1b is essential for cortisol synthesis through interactions with Cyp11c1 and possibly Cyp11a2***

The regulation of cortisol synthesis is highly conserved between zebrafish and mammals. In the adult interrenal gland zebrafish have two mitochondrial CYP enzymes required for glucocorticoid production, Cyp11a2 and Cyp11c1. Cyp11a2 is required for the first step of steroidogenesis when pregnenolone is produced from cholesterol (Parajes et al., 2013). To determine if Fdx1b was affecting pregnenolone synthesis, pregnenolone was measured in *fdx1b*-ATG<sup>MO</sup> injected embryos and larvae. Compared to control injected embryos, Fdx1b deficient embryos had less pregnenolone synthesis after interrenal steroid synthesis begins at 48 hpf. This suggests Fdx1b is

interacting with Cyp11a2 in the interrenal gland to impair pregnenolone synthesis. Pregnenolone concentrations were higher in Fdx1b deficient embryos (0.73 pg per larva at 120 hpf) when compared to Cyp11a2 morphants (0.33 pg per larva at 120 hpf). Although this is likely due to different efficacies of the individual morpholinos, it cannot be excluded that the ubiquitously expressed Fdx1 may be capable of supplying electrons, although with less efficiency, to partially restore Cyp11a2 activity. Further studies are required to investigate the efficiencies of interaction and electron transfer between the different ferredoxin and CYP enzymes.

Cyp11c1 is the only identified Cyp11b-like enzyme identified in zebrafish (Goldstone et al., 2010). It is required for cortisol (Wilson et al., 2013) and androgen (de Waal et al., 2008) synthesis in zebrafish. To establish the requirement of Cyp11c1 on electron transport from Fdx1b, Fdx1b deficient embryos were incubated with pregnenolone (to restore any loss resulting from disrupted Cyp11a2 activity) and the subsequent cortisol level was measured. Despite pregnenolone substitution, Fdx1b morphants failed to produce cortisol, suggesting Fdx1b regulates glucocorticoid production through Cyp11c1. As the Fdx1b deficient larvae morphologically resembles glucocorticoid resistance zebrafish models, the phenotype of *fdx1b* morphants is likely from impaired glucocorticoid synthesis during development rather than androgen synthesis deficiency.

### ***3.5.5 Stability of zebrafish ferredoxin proteins and mRNA***

Ferredoxins are regulated at many levels including the stability of at the mRNA and protein levels. In humans the functional *FDX1* gene on chromosomal 11q22 encodes several alternatively splice transcripts which differ in their three-prime untranslated region, and predicted to have different mRNA half-lives (Picado-Leonard et al., 1988). Additionally, vertebrate ferredoxin proteins are known to have extremely low conformational stability. Studies show

bovine FDX1 has low thermodynamic stability ( $\Delta_dG = 21$  kJ/mol at 25°C and pH 8.5) (Burova et al., 1995), compared to most of globular proteins ( $\Delta_dG$  values of 25 – 60 kJ/mol) (Privalov, 1979). It is likely that the general lack of protein stability of ferredoxins and possible mRNA instability makes mRNA rescues technically challenging. Additionally, a lack of zebrafish specific antibodies, makes determining individual paralogue protein concentrations difficult. Currently, nothing is known about the stability of the zebrafish paralogues. However, it would of interest to compare the related paralogues, especially in contrast with the loss of Arg14 in Fdx1b as mentioned above.

### ***3.5.6 Investigating the interaction between zebrafish ferredoxins and CYP enzymes***

We have shown that the zebrafish ferredoxin, Fdx1b, is involved in the production of cortisol in the zebrafish larvae, most likely through electron transfer with Cyp11c1 and possibly Cyp11a2. One major question that remains is the efficiency of interaction and electron transfer between each ferredoxin paralogue and specific CYP enzymes. In collaboration with Professor Rita Bernhardt (Institute of Biochemistry, University of the Saarland, Germany) the interaction affinities and stability of the zebrafish redox proteins will be investigated. Professor Bernhardt's laboratory established a method to express and purify bovine ferredoxin (Uhlmann et al., 1992), which has since been optimised and modified to investigate the interactions and structure of these proteins. I have cloned mature forms of zebrafish *fdx1* and *fdx1b*, together with *cyp11a1*, *cyp11a2*, *cyp11c1* and the only identified *fdxr* gene into pET22b for bacterial expression and purification. *In vitro* analysis will provide further information about efficiency of electron transfer between these proteins as well as specific protein-protein interactions. Furthermore, specific functional differences between the ferredoxin paralogues will provide information on how mitochondrial steroidogenesis can be influenced by redox partners.

## *Chapter Four*

---

### *Redefining cytochrome P450 side-chain cleavage activity in zebrafish development*

## ***Forward***

Results from this chapter were published in the May 2013 issue of the journal *Endocrinology*. This chapter outlines the work which I completed as part of this project. The full publication can be found in Appendix One (page 224).

## **4.0 REDEFINING CYTOCHROME P450 SIDE-CHAIN CLEAVAGE ACTIVITY IN ZEBRAFISH DEVELOPMENT**

### **4.1 Introduction**

The human *CYP11A1* gene encodes the P450 side-chain cleavage enzyme (P450<sub>scc</sub>; CYP11A1) which catalyses the first and rate limiting step of steroidogenesis. Many of the key enzymes for steroid hormone synthesis and signalling are conserved in zebrafish, including CYP11A1 reactions. A zebrafish gene encoding *cyp11a1* was identified on chromosome 25 and consists of nine coding exons and two five-prime located non-coding exons (Hsu et al., 2009). Several studies show *cyp11a1* is expressed in zebrafish embryos and larvae (Chai et al., 2003, Hsu et al., 2002, Hu et al., 2004, To et al., 2007, Xie et al., 2008). Consistently, zebrafish *cyp11a1* has shown to be expressed as a maternal transcript and maintained in the yolk syncytial layer. Functionally, this early expression of *cyp11a1* facilitates pregnenolone synthesis, which stabilises microtubules via accessory proteins and promotes the epiboly movement required for zebrafish development (Hsu et al., 2006, Weng et al., 2013).

During larva development, expression of *cyp11a1* was shown in the interrenal primordial cells and has been suggested to be present between 24 and 120 hours post fertilisation (hpf) (Chai et al., 2003, Hsu et al., 2003, To et al., 2007, Xie et al., 2008). However, others failed to demonstrate *cyp11a1* expression in zebrafish larvae between three to 14 days post fertilisation (dpf) (Hsu et al., 2002, Hu et al., 2004), despite reported *de novo* steroidogenesis at these stages (Alsop and Vijayan, 2008). Whole transcriptome microarray analysis focusing on the expression of cytochrome P450 enzymes in zebrafish identified a second *cyp11a* gene; *cyp11a2* (Goldstone et al., 2010). The *cyp11a2* gene consists of nine coding exons and is also located on chromosome 25, approximately

9 Kb upstream of the *cyp11a1* gene. This newly proposed *cyp11a* paralogue remained uncharacterised in terms of function and expression in the zebrafish.

## **4.2 Rational for work**

Zebrafish are becoming an increasingly popular model to study steroid hormone synthesis, signalling and action. In order to investigate the redox interactions between the ferredoxin and mitochondrial CYP proteins in zebrafish we first had to comprehensively characterise these enzymes. Therefore, we aimed to determine the functional roles of each zebrafish Cyp11a paralogue during zebrafish development.

## 4.3 Methodology

### 4.3.1 PCR amplification of zebrafish *cyp11a1* and *cyp11a2*

The nucleotide sequences for zebrafish *cyp11a1* and *cyp11a2* were determined by amplifying the cDNA sequences from the ovary of an adult AB female. Oligonucleotides were designed based on sequences annotations from ENSEMBL Zv9 genomic database (Table 4.1) and RT-PCR was performed using a high fidelity polymerase. After PCR purification, the PCR product was ligated into pGEM-T Easy vector using the standard protocols and sequenced.

**Table 4.1 Oligonucleotides for PCR amplification P450scc cDNA**

<i>Gene</i>	<i>Primer</i>	<i>Sequence (5-prime to 3-prime)</i>
<i>cyp11a1</i>	<i>cyp11a1</i> -F	GTGATGGCCCTCTGGAATG
	<i>cyp11a1</i> -XR <sup>a</sup>	CATCTCTGCTATCTGCTGGCA
<i>cyp11a2</i>	<i>cyp11a2</i> -F	CAATGGCCCTCTGGAGTC
	<i>cyp11a2</i> -XR <sup>a</sup>	GTACCGACCCAACTGTACCG

<sup>a</sup>Reverse oligonucleotides contain a stop codon

### 4.3.2 Alignment and phylogenetic analysis of *Cyp11a* sequences

Amplified PCR sequences were used to infer amino acid sequences of the Cyp11a paralogues. Zebrafish Cyp11a1 and Cyp11a2 protein sequences were compared to vertebrate Cyp11a1 protein sequences from the ENSEMBL database, including human (*Homo sapiens*; ENSP00000268053), gorilla (*Gorilla gorilla gorilla*; ENSGGOP00000006378), tilapia (*Oreochromis niloticus*; ENSONIP00000019362), fugu (*Takifugu rubripes*; ENSTRUP00000035273), tetraodon (*Tetraodon nigroviridis*; ENSTNIP00000011253), and

stickleback (*Gasterosteus aculeatus*; ENSGACP00000006220). Alignment and homology analyses were performed using ClustalW2 software as previously described.

### 4.3.3 PCR amplification and cloning of zebrafish P450-scc paralogues

The *cyp11a1* and *cyp11a2* coding sequences from AB, Tubingen, Casper and Nacre wild-type strains were amplified and sequenced from an ovary of an adult female. For both genes, oligonucleotides were designed with BamHI restriction sites to allow direct cloning into pCS2+ and pCDNA6-V5. Additionally, reverse oligonucleotides were used to generate products with (XR-BamHI) and without (R-BamHI) a stop codon to allow the three-prime end to be tagged with a V5 epitope (Table 4.2). RT-PCR was performed using Expand High Fidelity PCR system. After PCR purification, digestion of the PCR product and ligation into the required plasmid was performed using the standard protocols. The correct directionality of the insert was screened by colony PCR using T7 vector primer with an appropriate insert primer.

**Table 4.2 Oligonucleotides for the PCR amplification and cloning of P450scc cDNA**

<i>Gene</i>	<i>Primer</i>	<i>Sequence</i> (5-prime to 3-prime)
<i>cyp11a1</i>	<i>cyp11a1</i> -F-BamHI	TACCGAGCTCGGATCCGTGATGGCCCTCTGGAATG
	<i>cyp11a1</i> -XR-BamHI <sup>a</sup>	CTGGACTAGTGGAATCCCATCTCTGCTATCTGCTGGCA
	<i>cyp11a1</i> -R-BamHI	CTGGACTAGTGGATCCGCATCTCTGCTTTCTGCTGGCA
<i>cyp11a2</i>	<i>cyp11a2</i> -F-BamHI	TACCGAGCTCGGATCCCAATGGCCCTCTGGAGTC
	<i>cyp11a2</i> -XR-BamHI <sup>a</sup>	CTGGACTAGTGGATCCGTATCTCTGCTATCTGCTGGAG
	<i>cyp11a2</i> -R-BamHI	CTGGACTAGTGGATCCGTATCTCTGCTTTCTGCTGGAG

<sup>a</sup> Reverse oligonucleotides contain a stop codon.

#### 4.3.4 Characterisation of *cyp11a1* and *cyp11a2* expression

The spatial and temporal expression of *cyp11a1* and *cyp11a2* was determined by RT-PCR as previously described. Specifically, a 76 nucleotide fragment of the *cyp11a1* gene was amplified using MegaMix-Blue reaction mix containing *cyp11a1* e9F and e9/10R primers. To characterise *cyp11a2* expression, a 902 nucleotide fragment was amplified with e1F and e3R primers (Table 4.3). As a control for mRNA quality, a 102 nucleotide fragment of the  $\beta$ -actin gene was amplified using e4F and e4R primers (Table 3.3 Table 3.3 Oligonucleotides for RT-PCR expression analysis of the *fdx1* and *fdx1b* genes.).

**Table 4.3 Oligonucleotides for RT-PCR expression analysis of the *cyp11a* paralogue genes**

<i>Gene</i>	<i>Primer</i>	<i>Sequence (5-prime to 3-prime)</i>
<i>cyp11a1</i>	e9F	GCAATGAGTCTTCCAAGGTTC
	e9/10R	GAACTAAAGTCCCTGCTGGAA
<i>cyp11a2</i>	e1F	GAGCACCTGCAATCGGACT
	e3R	TCCCCTGCACCTTCGGAG
	e5/6R	TGTTATAGCCGTCGTGTCCACT

#### 4.3.5 Transient knockdown of *cyp11a1* and *cyp11a2* in zebrafish embryos

To analyse the role of each zebrafish P450<sub>scc</sub> enzyme during development, transient knockdowns were performed with specific anti-sense morpholinos. The *cyp11a1* morpholino was previously described by Hsu et al. (2006) and was directed to the transcriptional start codon (*cyp11a1*-ATG<sup>MO</sup>). A five base-pair mismatched morpholino (*cyp11a1*-Ctl<sup>MO</sup>) was used as a

control. For *cyp11a2*, two different morpholinos were designed to disrupt gene expression; an ATG morpholino (*cyp11a2*-ATG<sup>MO</sup>), and a splice morpholino (*cyp11a2*-Spl<sup>MO</sup>) against the splice acceptor site of exon four. A five base-pair mismatch for the translation blocking morpholino (*cyp11a2*-Ctl<sup>MO</sup>) and the splice morpholino (*cyp11a2*-Ctl2<sup>MO</sup>) were used as controls. Sequences of the morpholinos and mismatch controls are listed in Table 4.4

**Table 4.4 Sequences of the anti-sense morpholinos used for the transient knockdown of *cyp11a* paralogs**

<i>Gene</i>	<i>Morpholino</i>	<i>Sequence</i> (5-prime to 3-prime)
<i>cyp11a1</i>	<i>cyp11a1</i> -ATG <sup>MO</sup> <sup>a</sup>	GCCATCACA <u>C</u> ACTCTCTCTCTCTACTT
	<i>cyp11a1</i> -Ctl <sup>MO</sup>	G <u>C</u> GAT <u>G</u> ACACT <u>G</u> TCTCTCT <u>G</u> TAGTT
<i>cyp11a2</i>	<i>cyp11a2</i> -ATG <sup>MO</sup> <sup>a</sup>	GCCATTGC <u>A</u> CTCTCTCTGTCTCTGC
	<i>cyp11a2</i> -Ctl <sup>MO</sup>	G <u>C</u> GAT <u>T</u> <u>C</u> CACTCT <u>G</u> T <u>G</u> T <u>G</u> TCTGC
	<i>cyp11a2</i> -Spl <sup>MO</sup> <sup>b</sup>	ATTGGAAGACGTTGCTTACTTCAGC
	<i>cyp11a2</i> -Ctl2 <sup>MO</sup>	ATTG <u>C</u> AAGAG <u>G</u> TTGGTTACATC <u>A</u> CC

<sup>a</sup> ATG morpholinos impair initiation of mRNA translation

<sup>b</sup> Splice morpholinos induce abnormal splicing of the mRNA

Underlined letters highlight base-pair mismatches between ATG or splice morpholinos and controls.

#### 4.3.6 Phenotypic characterisation of *cyp11a* morphants

Zebrafish embryos injected with 3 ng of morpholino were raised to the desired developmental stage and observed on a stereomicroscope. At 10 hpf all morphants and controls were categorised into three classes based on normal epiboly, abnormal epiboly or dead. At 5 dpf *cyp11a2*-Spl morphants and *cyp11a2*-Ctl2 larvae were categorised into four classes depending on the observed morphology. Class I were considered to have normal development and Class IV

were the most severe. Class I larvae were subdivided into Class Ia and Class Ib, depending on inflation or no inflation of the swim bladder, respectively.

**Table 4.5 Classification of the phenotype of *cyp11a2*-Spl morphants at 120 hpf.**

Phenotype	Class Ia <sup>a</sup>	Class Ib <sup>a</sup>	Class II	Class III	Class IV
Swim bladder	inflated	none	inflated	none	none
Yolk sac	normal	normal	enlarged	enlarged	enlarged
Pericardial sac	normal	normal	normal	normal	oedema
Head	normal	normal	normal	small	shortened snout

<sup>a</sup>Phenotype of class Ia and Ib zebrafish larvae represent the wild-type phenotype.

#### **4.3.7 Rescue experiments of *cyp11a2* morphants with pregnenolone**

At 10 hpf zebrafish *cyp11a2*-Spl morphants were incubated in E3 media supplemented with 50 nM pregnenolone or vehicle (ethanol). Treatments were changed every 24 hours over the first five days of development. At 120 hpf, the morphological phenotype was assessed based on the classifications outlined in Table 4.5 In addition, 300 larvae injected with *cyp11a2*-Spl<sup>MO</sup> that were treated with pregnenolone or ethanol and were collected at 72 hpf for cortisol analysis. Rescue experiments with pregnenolone were performed in duplicate and represented as mean  $\pm$  SD for each embryo treatment.

## 4.4 Results

### 4.4.1 Homology of Cyp11a isozymes with vertebrate orthologues

Protein sequence comparison between the two identified Cyp11a isozymes and other vertebrate orthologues was performed *in silico* to elucidate the evolution and conserved functional domains of the recently identified Cyp11a2 enzyme (Goldstone et al., 2010). Zebrafish were the only vertebrate with two identified *cyp11a* genes. Evolutionary analysis revealed that teleost Cyp11a enzymes grouped together on their own clade distinct from other mammals. The phylogenetic analysis indicates both zebrafish Cyp11a isozymes share a common ancestor with other teleost fish (Figure 4.1).

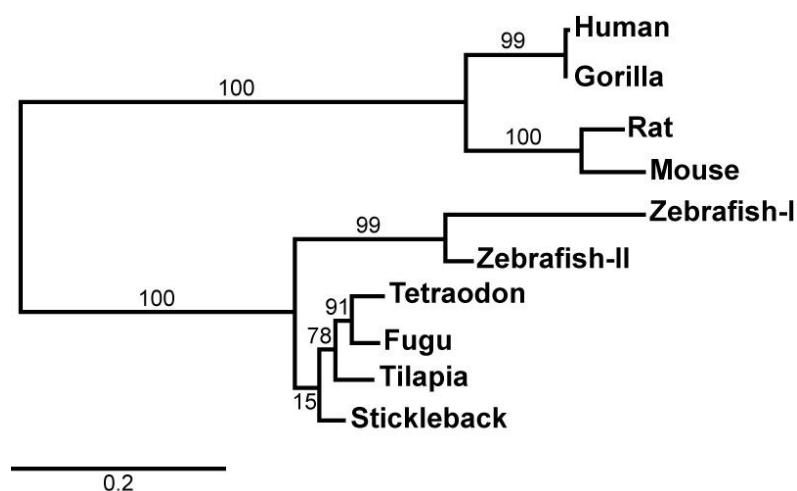


**Figure 4.1 Evolution of Cyp11a paralogs**

Maximum likelihood phylogenetic analyses of vertebrate Cyp11a protein sequences were conducted using the PhyML software under the SH-like likelihood-Ratio test parameters. Scaled phylogenetic tree was drawn with TreeDyn software. Branch support values are represented in %. Zebrafish-I and Zebrafish-II refer to Cyp11a1 and Cyp11a2 isozymes, respectively.

Comparison between the two zebrafish Cyp11a proteins showed 80 % protein sequencing identity. Cyp11a1 and Cyp11a2 have 509 and 512 amino acids, respectively, and both share typical cytochrome P450 functional domains. Notably, the redox-interaction domain is conserved, as well as the oxygen-binding and substrate binding domains, ExxR motif and the meander sequence (Hasemann et al., 1995, Strushkevich et al., 2011). Alignment of the protein sequences showed zebrafish Cyp11a2 has higher homology with other vertebrate cytochrome P450scc enzymes than its paralogue enzyme Cyp11a1. Specifically, in comparison to other teleost fish, Cyp11a2 had highest identity with stickleback and tetraodon (73 %), followed by fugu and tilapia (72 %). Alternatively, Cyp11a1 had most identity with stickleback and fugu (66 %) followed by tetraodon (65 %) and tilapia (64 %). In comparison to mammalian orthologues Cyp11a2 showed 46 % identity with human and gorilla and 44 % identity with rat and mouse. Cyp11a1 had 45 % identity with human, gorilla, rat and mouse.





---

**Figure 4.2 ClustalW alignment of Cyp11a paralogs**

The protein sequence of human, gorilla, rat, mouse, tilapia, fugu, tetraodon, stickleback, zebrafish Cyp11a enzymes were aligned using ClustalW under default parameters. Black lines and arrows annotate  $\alpha$ -helices and  $\beta$ -sheets, respectively, of the secondary protein structure of human CYP11A1, based on the crystallographic structure (<http://www.rcsb.org/pdb/home/home.do>, PDB code 3NA0). The haem-binding domain is highlighted in red, the oxygen-binding domain in brown, the meander in light grey, and the ExxR in blue. Residues from the substrate-binding domain are coloured in green (residues directly binding to the substrate) and yellow (residues stabilizing the  $3\beta$ -hydroxyl of cholesterol). Residues participating in redox interaction are coloured in orange. Zebrafish-I and Zebrafish-II refers to Cyp11a1 and Cyp11a2, respectively.

#### **4.4.2 Identification of polymorphisms in zebrafish *cyp11a1* and *cyp11a2* genes**

The *cyp11a1* and *cyp11a2* full length cDNA was amplified from wild-type AB fish by high fidelity polymerase and sequenced to confirm PCR amplification without mutations. Comparison of our amplified sequences to the annotated ENSEMBL database sequences identified eight non-synonymous single nucleotide polymorphisms (SNPs) in the amplified *cyp11a1*. These included F8L, E165D, L328M, Y273C, I297V, F390Y, T392N and K437D. Repeat amplification and sequencing confirmed the presence of these SNPs. To compare the prevalence of these mutations, *cyp11a1* coding sequences were amplified from other wild-type strains including Nacre, WIK and Casper, and compared to the available Tübingen sequence and the previously published *cyp11a1* sequence (Hsu et al., 2009). A ClustalW alignment the corresponding proteins were used to compare the amino acid sequences. Each Cyp11a1 contained several mutations which are summarised in Table 4.6.

Similarly, the cloned *cyp11a2* sequence from wild-type AB fish had three non-synonymous SNPs when compared to the ENSEMBL reference sequence. These point mutations were confirmed by repeat amplification of the *cyp11a2* cDNA, suggesting it was not PCR error. These mutations included T191N, N341H and K402N (Table 4.7). As there was no other annotated sequences for *cyp11a2* the presence of the missense mutation was confirmed by repeating the amplification from other wild-type zebrafish. Only the T191N mutation was not present in other strains. However, the conservation of a polar uncharged amino acid at this position across all vertebrates, and the high polymorphic variability of these genes I continued with functional testing our AB Cyp11a2 sequence.

**Table 4.6 Missense mutation identified in Cyp11a1 in different wild-type strains**

<b>Mutation</b>	<b>Reference<sup>a</sup></b>	<b>AB<sup>b</sup></b>	<b>WIK<sup>c</sup></b>	<b>Hsu<sup>d</sup></b>	<b>Tub<sup>b</sup></b>	<b>Nacre<sup>b</sup></b>	<b>Casper<sup>b</sup></b>
F8L	F	L	L	L	F	F	F
E165D	E	D	D	D	E	E	E
K197R	K	K	K	R	K	K	K
Y273C	Y	C	C	C	Y	Y	Y
I297V	I	V	V	I	I	I	I
L328M	L	M	M	L	L	L	L
F390Y	F	Y	Y	Y	F	F	F
T392N	T	N	N	T	T	T	T
K437N	K	N	N	N	K	K	K
Δ451L/452E	LE	LE	LE	LE	Δ	LE	LE

<sup>a</sup> ENSEMBL annotated sequence<sup>b</sup> PCR amplified from University of Birmingham stocks<sup>c</sup> NCBI annotated from sequence<sup>d</sup> Previously published by (Hsu et al., 2009)**Table 4.7 Missense mutation identified in Cyp11a2 in different wild-type strains**

<b>Mutation</b>	<b>Reference<sup>a</sup></b>	<b>AB<sup>b</sup></b>	<b>Tub<sup>b</sup></b>	<b>Nacre<sup>b</sup></b>
T191N	T	N	T	T
N341H	N	H	H	N
K402N	K	N	N	K

<sup>a</sup> ENSEMBL annotated sequence<sup>b</sup> PCR amplified from University of Birmingham stocks

#### **4.4.3      *Functional in vivo assays of cyp11a1 and cyp11a2 paralogues***

Amplified *cyp11a1* and *cyp11a2* from the AB wild-type strain were directionally cloned into the pcDNA6-V5 mammalian expression vector. After transfection into COS7 cells, catalytic assays were used to determine the conversion of 22ROH-cholesterol to pregnenolone. The zebrafish Cyp11a2 showed 114 % ( $\pm 11.1$ ) activity of the human homologue, CYP11A1. In comparison, zebrafish Cyp11a1 only had 0.1 % ( $\pm 0.03$ ) of human CYP11A1 activity (Figure 4.3). To determine if this was from the identified mutations in the AB amplified sequence, *cyp11a1* coding sequences from Tubingen and Nacre were also directionally cloned into the mammalian expression vector for functional testing. Similarly, the wild-type Tubingen and Nacre Cyp11a1 had minimal conversion of 22ROH-cholesterol to pregnenolone. Additionally, AB *cyp11a1* and *cyp11a2* were cloned with a V5-tag to confirm protein levels. Western blot using a V5 antibody showed decreased Cyp11a1 protein compared to Cyp11a2. Beta-actin protein levels were used to confirm equal protein loading.

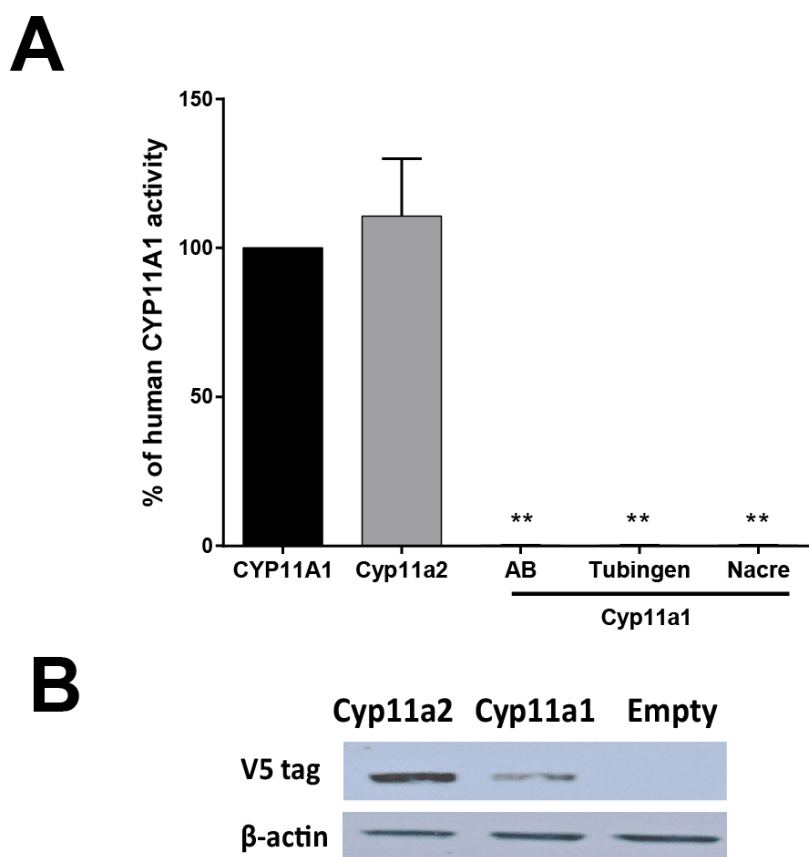


**Figure 4.3** *In vitro* activity of zebrafish Cyp11a paralogues

**(A)** COS7 cells were transfected with human *CYP11A1*, zebrafish *cyp11a2* from AB strain or zebrafish *cyp11a1* from AB, Tubingen or Nacre wild-type strains. Cells were then incubated with 22ROH-cholesterol for StAR independent conversion to pregnenolone. Zebrafish Cyp11a2 had 114% ( $\pm 11.1$ ) activity compared to human CYP11A1. All zebrafish Cyp11a1 had 0.1% ( $\pm 0.03$ ) activity of the human paralogue. **(B)** Western blot of V5 tagged Cyp11a2 and Cyp11a1 proteins show decreases in Cyp11a1 protein levels compared to Cyp11a2. Beta-actin was used to show equal loading. Experiments were performed in triplicate and the mean  $\pm$  SD is shown for each paralogue. . Statistical analysis was performed using one-way ANOVA followed by Dunnett's multiple comparisons test. \*\* P<0.01

#### **4.4.4 Tissue distribution and temporal *cyp11a* expression**

The developmental expression of each *cyp11a* paralogue was determined by RT-PCR. *cyp11a1* was expressed as a maternal transcript as it was detected at the single-cell stage. Expression was maintained to the segmentation periods (up to 22-24 hpf) with only residual expression being detected at 28 hpf. Alternatively, *cyp11a2* transcripts were not detected at these early developmental stages and were only weakly detected during late segmentation period (28 hpf). By 32 hpf expression of *cyp11a2* became prominent and was maintained to 120 hpf (Figure 4.4).

To determine spatial expression in adults, RT-PCR was performed using cDNA extracted from adult tissues. *cyp11a1* expression was highest in the ovary, and was also detected in the testis kidney head (containing the interrenal gland), kidney and intestine. In contrast, *cyp11a2* expression was restricted to the kidney head, gonads and the brain. No sexual dimorphism in the expression pattern was observed (Figure 4.4).

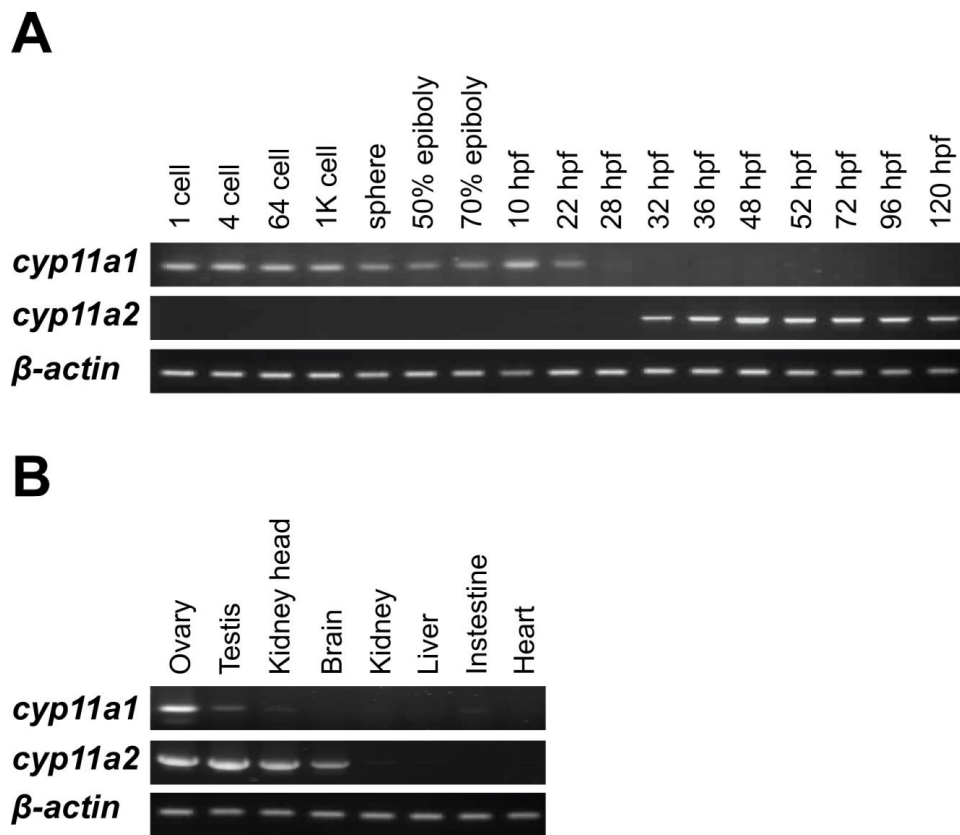


**Figure 4.4 Temporal expression and tissue distribution of zebrafish *cyp11a1* and *cyp11a2* genes**

Expression of *cyp11a1* and *cyp11a2* was characterised in zebrafish embryos and larvae (**A**) and in adult tissues (**B**). Beta-actin was used as a loading control.

#### 4.4.5 Confirmation of *cyp11a1* function during early zebrafish development

To determine the specific roles of Cyp11a1 and Cyp11a2 during zebrafish development, each paralogue was knocked down using anti-sense morpholinos. Microinjection of *cyp11a1*-ATG<sup>MO</sup> resulted in a similar phenotype observed in previous studies (Hsu et al., 2006). At 10 hpf, 68 % of morphants (n = 300) had incomplete epiboly, and 29 % had died during these early

developmental stages. In contrast, 97 % of *cyp11a1*-Ctl<sup>MO</sup> injected embryos (n = 300) had completed epiboly. Pregnenolone concentrations were determined from 300 *cyp11a1*-Ctl<sup>MO</sup> and surviving *cyp11a1*-ATG<sup>MO</sup> at 10 hpf. Control morphants had pregnenolone concentration of 0.19 ( $\pm$  0.05) pg per embryo. In comparison, *cyp11a1* deficient embryos showed a decrease to 0.1 ( $\pm$  0.08) pg per embryo at 10 hpf (Figure 4.5).

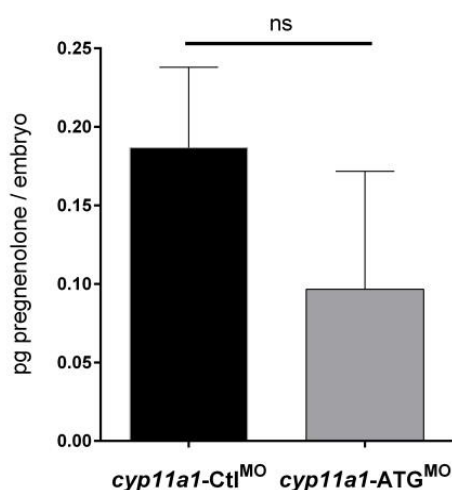


**Figure 4.5 Pregnenolone concentrations in *cyp11a1* deficient embryos at 10 hpf**

Pregnenolone concentrations were determined in *cyp11a1*-Ctl<sup>MO</sup> (black) and *cyp11a1*-ATG<sup>MO</sup> (grey) injected embryos at 10 hpf. Picograms of pregnenolone per embryo were calculated from concentration measured by LC-MS/MS from whole zebrafish extracts. *cyp11a1*-Ctl<sup>MO</sup> injected embryos showed a pregnenolone concentration of 0.19 ( $\pm$  0.05) pg per embryo. In comparison, *cyp11a1*-ATG<sup>MO</sup> embryos had 0.1 ( $\pm$  0.08) pg per embryo. Mean  $\pm$  SD from three independent experiments is shown.

Microinjection of *cyp11a2*-ATG<sup>MO</sup> resulted in a similar phenotype at 10 hpf. Of the injected embryos 45 % (n = 60) had not completed epiboly, with 18 % failing to thrive. In contrast, the *cyp11a2*-Ctl<sup>MO</sup> did not alter normal development and allowed 93 % (n = 49) of embryos to complete epiboly by 10 hpf (Figure 4.6). Our expression data demonstrated that only *cyp11a1* is expressed from one cell to 10 hpf. The *cyp11a2* cDNA region which is targeted by the *cyp11a2*-ATG<sup>MO</sup> has 72 % homology (18 out of 25 base-pairs) with *cyp11a1* with the highest identity being around the ATG start codon. Unspecific binding of the *cyp11a2*-ATG<sup>MO</sup> to *cyp11a1* mRNA would explain the abnormal epiboly observed in the *cyp11a2*-ATG morphants within the first 10 hours of development. Given the high nucleotide identity between the zebrafish *cyp11a* paralogues around the translation initiating start codon, it was not possible to design a specific morpholino blocking the ATG codon. The splice disrupting morpholino targeting *cyp11a2* (*cyp11a2*-Spl<sup>MO</sup>) did not recapitulate the epiboly delays observed with the *cyp11a2*-ATG<sup>MO</sup> injections, suggesting it was not targeting *cyp11a1*. The nucleotide identity between the *cyp11a2*-Spl<sup>MO</sup> with *cyp11a1* was 44 % (11 out of 25 base-pairs) and the mismatches are distributed over the entire morpholino binding region. Thus, unspecific binding of the *cyp11a2*-Spl<sup>MO</sup> to *cyp11a1* mRNA was not expected.

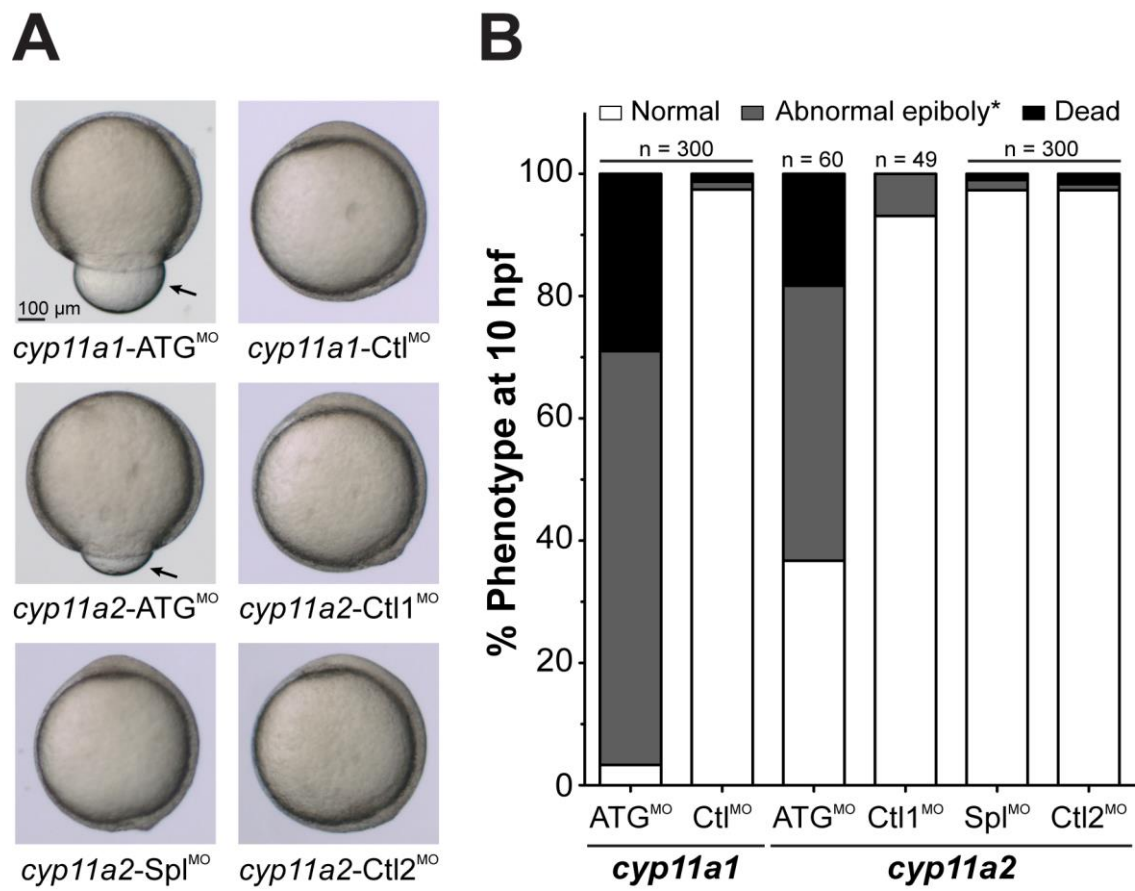


**Figure 4.6 Morphological phenotype of Cyp11a morphants at 10 hpf**

**(A)** Abnormal epiboly (black arrow) was observed in *cyp11a1*-ATG and *cyp11a2*-ATG morphants at 10 hpf. Phenotype of *cyp11a2*-Spl morphants and controls was normal. **(B)** Frequency of normal development, abnormal epiboly and mortality in zebrafish morphants and controls at 10 hpf.

\*Abnormal epiboly refers to the inability of the blastoderm to move normally towards the vegetal pole of the embryo during gastrulation.

#### 4.4.6 Determining the specific roles of *cyp11a2* during early development

Confirmation of splice disruption of the *cyp11a2* RNA transcript by the *cyp11a2*-Spl<sup>MO</sup> was performed by RT-PCR. The injection of *cyp11a2*-Spl<sup>MO</sup> into single-cell embryos efficiently induced abnormal splicing of *cyp11a2* intron 2. Amplification of a cDNA fragment extending from exon 1 to 3 of *cyp11a2* showed a 240 base-pair band in the *cyp11a2*-Spl morphants, indicating the loss of exon two (Figure 4.7). A dilution effect of *cyp11a2*-Spl<sup>MO</sup> was noted at 96 and 120 hpf, as indicated by the presence of the correctly spliced 396 base-pair band. The *cyp11a2*-Ctl2<sup>MO</sup> did not disrupt splicing of *cyp11a2*, as indicated by the single 396 base-pair product.

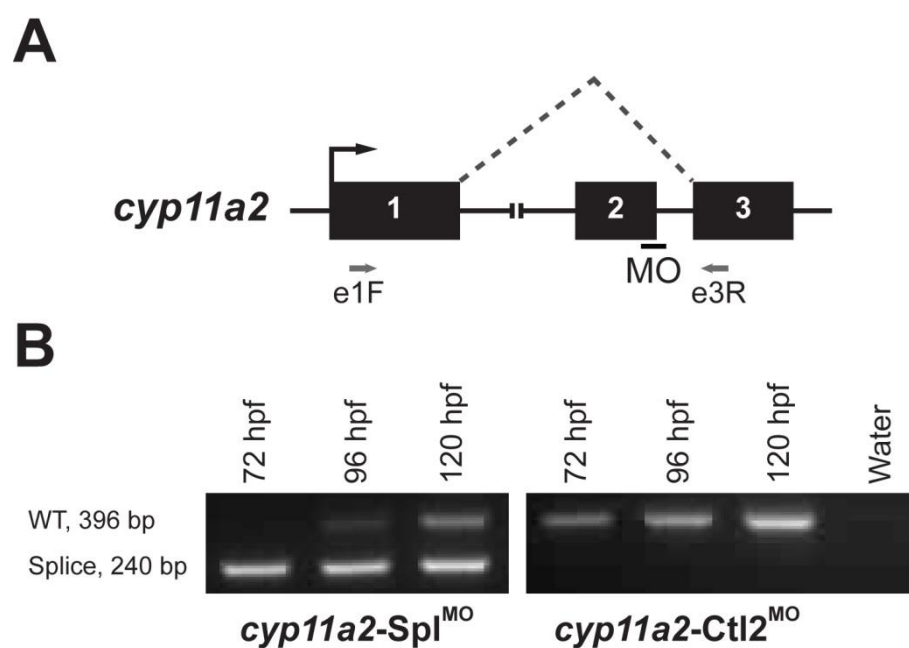


**Figure 4.7 Confirmation of disruption of *cyp11a2* splicing**

(A) *cyp11a2*-Spl<sup>MO</sup> binds to the donor splice site of intron 2, inducing a deletion of exon 2 in mature *cyp11a2* mRNA. (B) RT-PCR analysis confirmed loss of exon 2 in *cyp11a2* morphants but not in the controls. MO, indicates *cyp11a2*-Spl<sup>MO</sup> binding site. Black arrow shows transcription initiation site. Black line represents *cyp11a2*-Spl<sup>MO</sup> binding site. Grey arrows indicate the binding sites of the primers used for RT-PCR analysis to confirm missplicing of *cyp11a2* mRNA.

Embryos microinjected with *cyp11a2*-Spl<sup>MO</sup> developed normally up to 24 hpf. At 52 hpf, 55 % of *cyp11a2*-Spl morphants (n = 193) had delayed absorption of the yolk in contrast to 32 % of the controls (n = 182). Pericardial oedema was observed in 6 % of *cyp11a2* splice morphants compared to 1 % in control injected embryos. As zebrafish embryos grow and develop, the yolk is absorbed and metabolised, however, in *cyp11a2*-Spl morphants the enlarged yolk persisted in half the embryos by 96 hpf. In control injected embryos only 10 % showed a slightly enlarged yolk at the same time point (data not shown). At 120 hpf injected embryos were classified based on their morphological phenotype. In *cyp11a2*-Spl<sup>MO</sup> injected embryos the prominent phenotype was Class II (58 %) followed by Class III (21 %). Approximately, 80 % of *cyp11a2* morphants (Class II, III and IV) had a large yolk sac. In control injected embryos only Class Ia (56 %) and Ib (44 %) phenotypes were observed at 120 hpf (n = 173) (Figure 4.8). Chemical rescues were performed by incubating morpholino injected embryos in E3 media supplemented with 50 nM pregnenolone. Treated *cyp11a2*-Spl<sup>MO</sup> injected larvae were classified based on their morphology at 120 hpf. Sixty-six per cent of *cyp11a2* morphants had a normal Class I phenotype (59 % class Ia, 7 % class I b) at 120 hpf (n = 59).

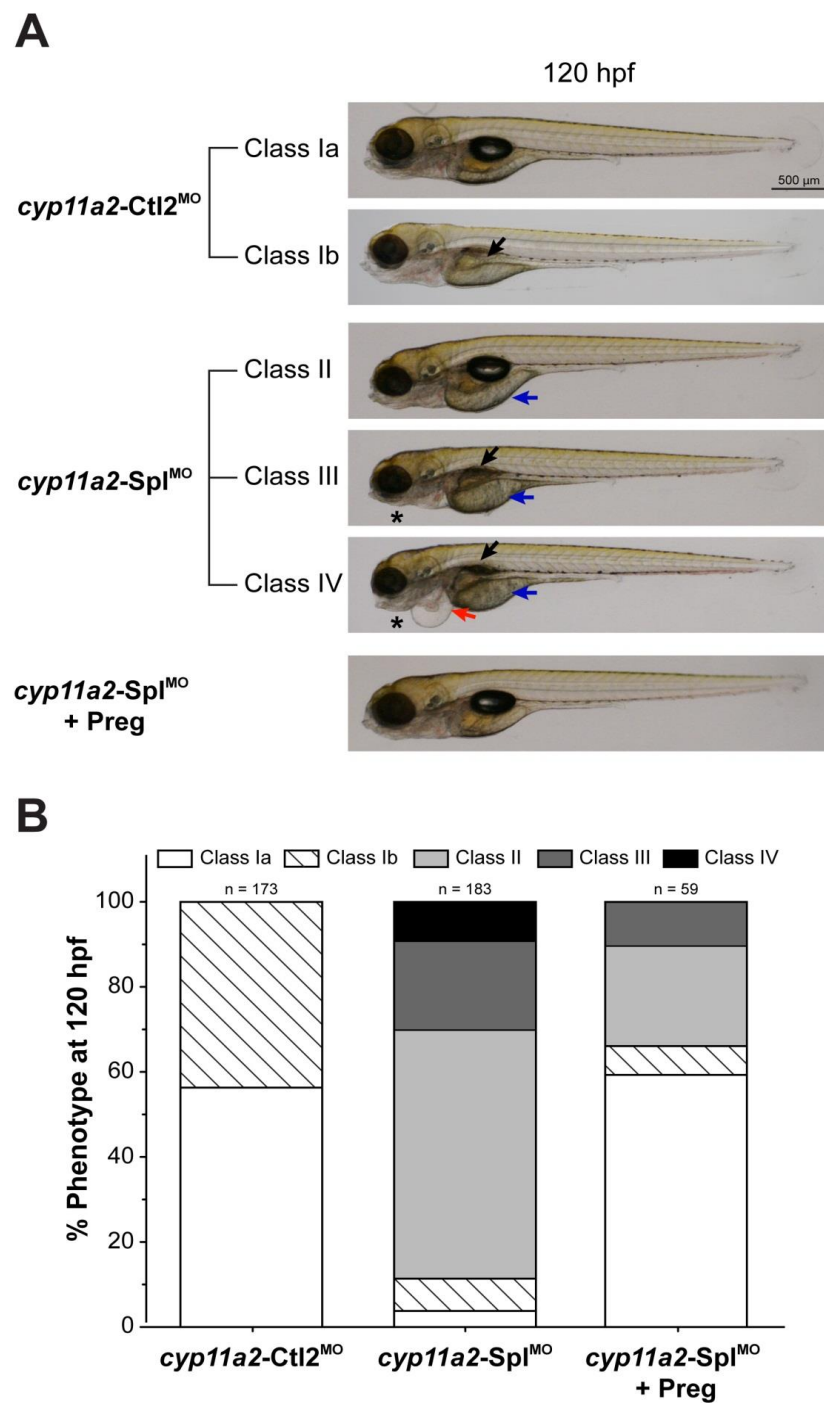


**Figure 4.8 Classification of *cyp11a2* deficient embryos at 120 hpf**

**(A)** At 120 hpf larvae were categorised into five different classes depending on the swim bladder (black arrow), yolk sac (blue arrow), pericardial sac (red arrow) and head (black asterisks) phenotype (Table 4.5). Class Ia (inflated swim bladder) and Ib (not inflated swim bladder) represent a wild-type phenotype. **(B)** Phenotypic spectrum observed in controls, untreated *cyp11a2-Spl* morphants, and *cyp11a2-Spl* morphants supplemented with pregnenolone.

#### **4.4.7 Steroid profiles of *cyp11a2* deficient embryos**

To determine the effect of Cyp11a2 on pregnenolone synthesis, pregnenolone concentrations were measured in *cyp11a2*-Spl<sup>MO</sup> and *cyp11a2*-Ctl2<sup>MO</sup> injected embryos at 10, 22, 72, 96 and 120 hpf. At 10, 22 and 72 hpf there was no difference observed between *cyp11a2* deficient embryos and controls. At 96 hpf and 120 hpf the *cyp11a2*-Spl<sup>MO</sup> larvae had 48 % and 80 % less pregnenolone when compared to the controls (Figure 4.9).

Cortisol measurements in embryos were also determined at each time point as an indication of *de novo* interrenal steroid hormone production. Both *cyp11a2*-Spl<sup>MO</sup> and *cyp11a2*-Ctl2<sup>MO</sup> injected embryos had similar cortisol concentration at 10 and 22 hpf. By 72 hpf, cortisol concentrations were 90 % lower in *cyp11a2*-Spl morphants compared to the controls. This decrease was maintained at 96 and 120 hpf with *cyp11a2* deficient embryos showing a 70 to 80 % decrease in cortisol concentrations (Figure 4.9). Additionally, cortisol was measured from 300 larvae to determine if pregnenolone supplementation could restore steroid hormone production. At 72 hpf, pregnenolone treated *cyp11a2*-Spl morphants had 1.47 pg per larvae cortisol which was comparable to untreated *cyp11a2*-Ctl2 morphants whose cortisol levels were 1.53 pg per larvae.

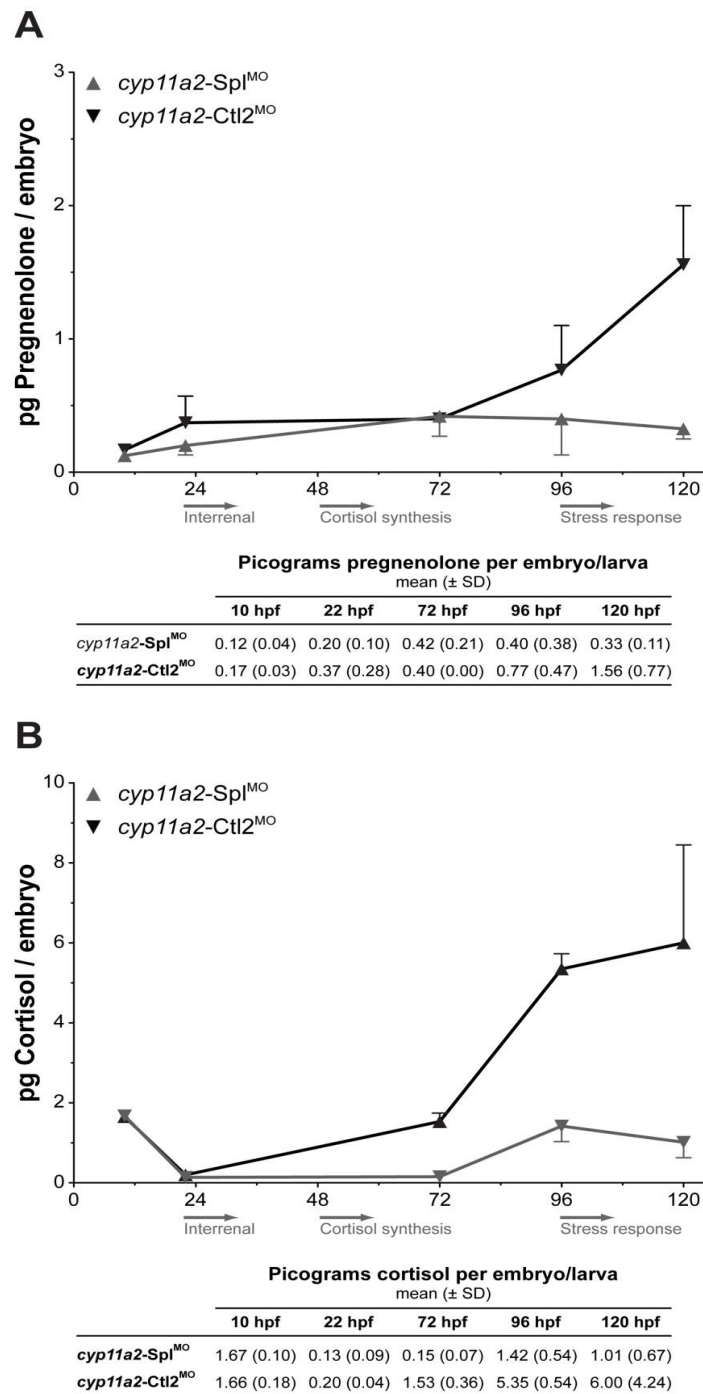


**Figure 4.9 Pregnenolone and cortisol concentrations in *cyp11a2* deficient embryos**

(A) Pregnenolone and (B) cortisol concentrations were determined in *cyp11a2-Spl*<sup>MO</sup> (grey) and *cyp11a2-Ctl2*<sup>MO</sup> (black) during the first five days of development. Picograms of pregnenolone and cortisol per embryos or larvae were calculated from concentrations measured by LC-MS/MS from whole zebrafish extracts. Mean  $\pm$  SD was plotted against developmental stages. Grey arrows show interrenal primordial formation (22 hpf), and initiation of *de novo* cortisol synthesis (48 hpf) and active stress response (96 hpf).

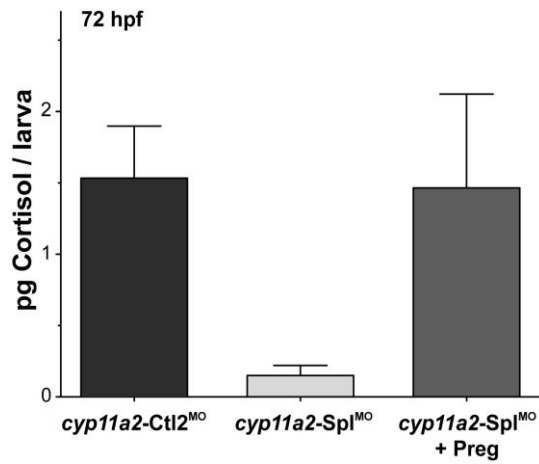


**Figure 4.10 Cortisol concentrations of *cyp11a2-Spl* morphants supplemented with pregnenolone**

*cyp11a2-Spl* morphants were incubated in E3 medium containing 50 nM pregnenolone or vehicle from 10 hpf. Cortisol concentrations were measured in 72 hpf zebrafish larvae from two independent experiments. Cortisol concentrations expressed as picograms per larvae were calculated from concentrations measured by LC-MS/MS in zebrafish extracts. Mean  $\pm$  SD was plotted against embryo treatment.

## 4.5 Discussion and prospective studies

It was previously reported that *cyp11a1* was the only identified *CYP11A1* orthologue in zebrafish. However, with the newly identified *cyp11a2*, the specific functional roles of these enzymes during zebrafish development remained to be determined. We have comprehensively characterised both *cyp11a* paralogues in zebrafish. Subsequently, we confirmed previous studies that Cyp11a1 is required during gastrulation stages for completion of epiboly and is therefore essential for embryo development. Additionally, we have shown that Cyp11a2 is required for pregnenolone production in the interrenal gland.

### 4.5.1 *Cyp11a1 has low catalytic activity in vitro*

PCR amplification of *cyp11a1* identified amino acid mutations when compared to the ENSEMBL annotated sequences. Functional activity analysis performed in mammalian cells identified zebrafish Cyp11a1 had 0.1 % of human CYP11A1 activity. This low level activity was confirmed with different zebrafish Cyp11a1 sequences amplified from other wild-type strains. In comparison, zebrafish Cyp11a2 showed 114 % of human activity. Western blot showed decreased levels of Cyp11a1 protein in comparison to Cyp11a2 which may explain the decrease in activity. During characterisation of the zebrafish Cyp17a paralogues, we identified Cyp17a1 has rapid protein turnover compared to its isozyme Cyp17a2 (Parajes et. al. *unpublished*). Work is continuing to assess the stability of Cyp11a1 by performing *in vitro* assays with proteasome inhibitors, to inhibit Cyp11a1 degradation. Nevertheless, it is plausible that protein stability might be a common mechanism of regulating steroid production during early zebrafish development. Furthermore, despite the detected low level of *in vitro* functional activity, transient knockdown studies confirmed the importance of Cyp11a1 for zebrafish embryogenesis.

#### ***4.5.2 Maternal expression of *cyp11a1* is essential for embryogenesis***

Our *in vivo* knockdown investigations confirmed previous studies showing that Cyp11a1 is essential for early embryo development (Hsu et al., 2006). The early onset morphological phenotype in *cyp11a1* deficient embryos is consistent with its early expression pattern and highlights the importance of Cyp11a1 activity for early zebrafish development. Pregnenolone is the main product of Cyp11a1 and it was confirmed by LC-MS/MS a non-significant decrease in pregnenolone per embryo in *cyp11a1*-ATG morphants compared to controls. Steroid profiles were analysed only from embryos which had survived to 10 hpf. It is hypothesised that embryos with the most efficient *cyp11a1* knockdown were not viable at this stage and therefore it is expected that pregnenolone concentrations would be even more decreased in *cyp11a1* deficient embryos. Pregnenolone can directly bind to microtubule plus end-tracking proteins which subsequently help stabilise the microtubules (Weng et al., 2013). Cyp11a1 activity is therefore essential for zebrafish development through promotion of epiboly via microtubule polymerisation. Although I did not detect *cyp11a2* expression during early gastrulation stages, injection of the *cyp11a2*-ATG<sup>MO</sup> caused a similar abnormal epiboly movement as seen with the *cyp11a1*-ATG<sup>MO</sup>. These findings were in contrast with the late onset *cyp11a2*-Spl<sup>MO</sup> phenotype. We accredited the different phenotype observed between the translation blocking and splice disrupting morpholinos to unspecific binding of the *cyp11a2*-ATG<sup>MO</sup> to the *cyp11a1* mRNA.

#### ***4.5.3 Transition of *cyp11a1* to *cyp11a2* expression correlates to the initiation of de novo steroidogenesis***

The expression of *cyp11a1* was strongest in embryos from fertilisation to 24 hpf with minimal expression detected at 28 and 48 hpf. This expression is in agreement with previous results obtained by RT-PCR (Hu et al., 2004) and microarray analysis (ZF-espresso 0.7.5 alpha, URL: zf-

espresso.tuebingen.mpg.de). However, other studies detected *cyp11a1* expression at later stages by whole mount *in situ* hybridisation (Hsu et al., 2003, To et al., 2007). Discrepancies were also noted when comparing expression in adult tissues. Our study showed *cyp11a1* expression was confined to the adult gonads, and was minimally detected or absent in the kidney head (containing the interrenal gland) and brain. This result is not consistent with earlier studies which detect high *cyp11a1* expression in all these tissues (Diotel et al., 2011, Hsu et al., 2003, Tong et al., 2010). It was speculated that the discrepancies observed with other reported expression data are due to non-specific detection of the previously uncharacterised *cyp11a2*.

We have for the first time characterised the *cyp11a1* paralogue gene, *cyp11a2*. The two zebrafish P450scc enzymes share 85 % identity of the coding nucleotide sequence and 80 % at the amino acid level. A transition between *cyp11a1* and *cyp11a2* expression was observed by RT-PCR between 28 and 48 hpf. Interestingly, this transition also coincides with development of the interrenal and *de novo* cortisol production. Furthermore, *cyp11a2* was maintained as the only P450scc enzyme expressed during larval development stages. In adult tissues, *cyp11a2* was restricted to steroidogenic tissues, including the kidney head, brain and gonads. *cyp11a2* is expressed in the early larvae when cortisol synthesis begins, and in the adult steroidogenic tissues. Coupled with its observed functional *in vitro* activity, it suggests *cyp11a2*, rather than *cyp11a1*, is required to initiate and maintain *de novo* steroidogenesis.

#### **4.5.4      *Deficiency in cyp11a2 impairs interrenal steroidogenesis***

The synthesis of cortisol is highly conserved between zebrafish and mammals. As in wild-type embryos (Alsop and Vijayan, 2008), the *cyp11a2*-Spl morphants and controls showed the maternal cortisol stores were almost depleted by 24 hpf. At 72 hpf, active steroid hormone synthesis was confirmed in control injected embryos by detecting a seven fold increase in whole embryo

cortisol levels. At 96 hpf the HPI axis becomes active which corresponded to a three-fold increase in cortisol concentration in control larvae. At this time, the larvae are capable of synthesising cortisol in response to stress (Alsop and Vijayan, 2008, 2009, To et al., 2007). However, Cyp11a2 deficient larvae showed impaired pregnenolone and *de novo* cortisol synthesis at 72, 96 and 120 hpf. At 96 and 120 hpf minimal cortisol was detected, which can be attributed to dilution of the morpholino as the larvae grow. Supplementation of *cyp11a2* morphants with pregnenolone was able to restore cortisol production, confirming that the observed cortisol deficiency was from impaired pregnenolone synthesis from a loss of *cyp11a2*. This clearly shows that Cyp11a2 is essential for active steroid hormone biosynthesis in early larvae.

The morphology of *cyp11a2*-Spl was consistent with other zebrafish morphants which lack glucocorticoid production or response. Larvae deficient in *cyp11a2* have delayed metabolism of the yolk and less frequently pericardial oedema from 52 hpf. By 120 hpf, the phenotype was more pronounced compared to the controls. The most severely affected embryos had additional craniofacial abnormalities and pericardial oedema. Previous studies show the morpholino knockdown of the glucocorticoid receptor (Pikulkaew et al., 2011) or a zebrafish model of interrenal insufficiency due to loss of *ff1b* (orthologue of the mammalian SF1) (Chai et al., 2003) have a similar phenotypes. Similarly, the *dax1* (SF1 transcription regulator) deficient zebrafish (Zhao et al., 2006) and chemical inhibition of P450<sub>sc</sub> (Chai et al., 2003) are both reported to have similar morphological phenotypes.

In contrast to zebrafish models of glucocorticoid resistance and interrenal insufficiency, *cyp11a2* deficient embryos showed no changes in the inflation of the swim bladder. Inflation of the swim bladder begins at 96 hpf. At 96 hpf the *cyp11a2*-Spl<sup>MO</sup> had lost efficacy from being diluted and minimal cortisol production can be detected. Cortisol levels were not measured in previous

zebrafish models of glucocorticoid deficiencies, so a direct comparison cannot be made. However, our study would suggest that low cortisol production is sufficient for inflation of the swim bladder, as reported by inflation of the swim bladder at 120 hpf with partial glucocorticoid resistance. Notably, supplementation of *cyp11a2* deficient embryos with pregnenolone caused an increase in swim bladder inflation. This supports the role of glucocorticoids in swim bladder inflation. However, it should not be ruled out that the swim bladder inflation maybe a secondary phenotype from lethargy and reduced swimming from a decreased metabolic rate. Thus further studies are required to determine the role of glucocorticoids in development.

## 4.6 Conclusion

By comprehensively characterising the zebrafish P450<sub>scc</sub> enzymes we were able to demonstrate that Cyp11a2, rather than Cyp11a1 is the functional orthologue of human CYP11A1 in larvae and adult zebrafish. Both Cyp11a1 and Cyp11a2 have distinct functional roles and both are critical for zebrafish development. We confirmed that pregnenolone synthesised by Cyp11a1 is functionally important for microtubule polymerisation and stabilisation to promote epiboly. Additionally, Cyp11a2 is critical for pregnenolone production during *de novo* steroidogenesis and is expressed in steroidogenic tissues in the adults. Overall, we were able to redefine the initiation and maintenance of zebrafish steroid hormone synthesis.

## *Chapter Five*

---

### *Genomic disruption of *fdx1b* and *cyp11a2* with transcription activator-like effector nucleases*

## **5.0 GENOMIC DISRUPTION OF *FDX1B* AND *CYP11A2* WITH TRANSCRIPTION ACTIVATOR-LIKE EFFECTOR NUCLEASES**

### **5.1 Introduction**

#### ***5.1.1 Genomic engineering with TALENs***

Transcription activator-like effectors (TALEs) are naturally occurring proteins from the plant pathogenic bacterium *Xanthomonas*. During infection, the bacterium secretes TALE proteins which enter the nucleus and regulate promoter sequences to enhance the bacterial colonisation of the plant cell. The TALE recognises specific plant DNA sequences through a central repeating domain consisting of 34 amino acids. Nucleotide specificity is achieved by two critical amino acids at positions 12 and 13 of the repeating domain; these are known as the repeat variable diresidues (RVD) (Figure 5.1). Simultaneously, two groups identified the correlation between the two amino acid residues of the RVD and the DNA nucleotide it recognised (Boch et al., 2009, Moscou and Bogdanove, 2009). Subsequent studies further refined the nucleotide binding specificity code of individual RVDs (Cong et al., 2012, Streubel et al., 2012). By following this code, researchers can now engineer specific TALEs to recognise desired nucleotide sequences and subject them to genomic editing.

Being able to target specific DNA sequences through the modification of the RVD in the TALE has been critical in developing recent genome engineering methodologies. TALEs have been fused to protein recombinases (Mercer et al., 2012), as well as transcriptional repressors (Cong et al., 2012) or activators (Maeder et al., 2013) to turn off or on endogenous gene expression, respectively. Additionally, TALEs have been fused to nucleases to generate transcription activator-like effector nucleases or TALENs, which are capable of introducing chromosomal breaks (Christian et al., 2010, Li et al., 2011, Mahfouz et al., 2011, Miller et al., 2011). With the

straightforward one-to-one RVD to nucleotide association code (NH binds guanine, NG binds thymine, NI bind adenine, and HD binds cytosine), TALE DNA-binding domains have rapidly become a promising platform to create a variety of molecular tools.

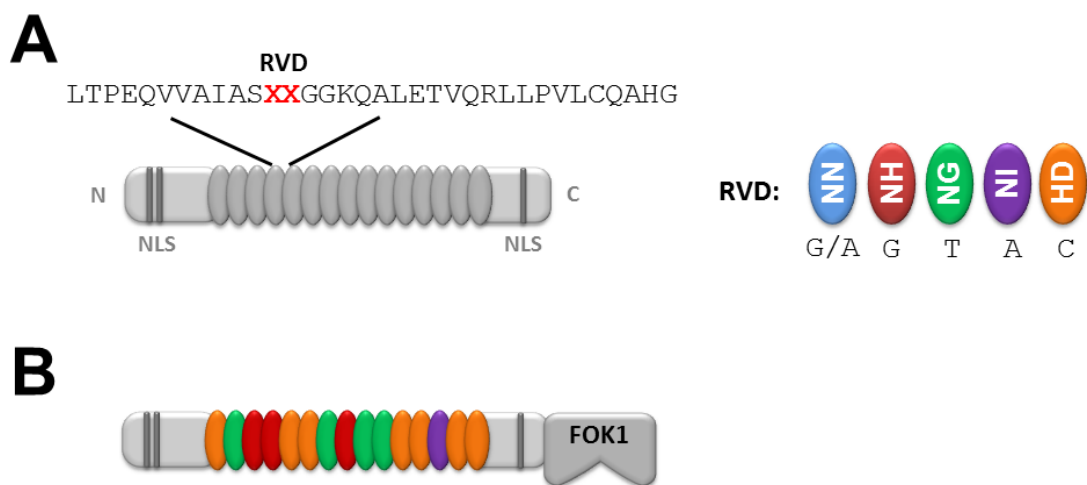


**Figure 5.1 Transcription Activator-Like Effector Nuclease (TALEN) architecture**

**(A)** Transcription Activator-Like Effectors (TALEs) contain a central tandem 34 amino acid repeating module. Each module is capable of recognising a single DNA nucleotide through the repeat variable diresidue (RVD) at amino acid position 12 and 13 (red x). By specifying the RVD of each repeating domain specific DNA sequences can be targeted. The RVD to nucleotide association code is: NN binds guanine or adenine, NH binds guanine, NG binds thymine, NI bind adenine, and HD binds cytosine. **(B)** TALE nucleases (TALENs) consist of specifically assembled TALEs linked to the nuclease domain of the Fok1 restriction enzyme (NLS; nuclear localisation signal).

### 5.1.2 Generating targeted DNA breaks using TALENs

TALENs are becoming an increasing predominant tool in generating genomic modifications through their ability to produce loci specific chromosomal breaks. Typically, the TALE is linked to the DNA cleavage domain of FokI enzyme, to generate the TALEN. As the FokI domain requires dimerisation for activity, TALENs function as a pair. Individual TALENs bind to each strand of DNA which is separated by a spacer region where the FokI nuclease dimerises. Dimerisation of the FokI motifs induces nuclease activity resulting in chromosomal breaks, which are repaired by the endogenous cellular repair mechanisms. The generation of null alleles relies on the error prone non-homologous end joining (NHEJ) for chromosomal repair. The insertion or deletion of nucleotides (collectively known as indels) at the site of repair causes amino acid changes or frame-shift mutations rendering a non-functional protein (Figure 5.2).

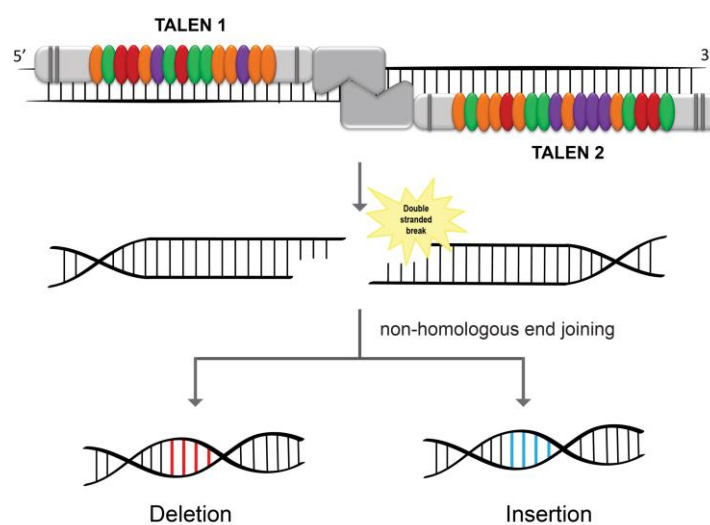


**Figure 5.2 TALEN induced genetic disruption by non-homologous end joining**

TALENs recognise specific DNA sequences through the RVD. Dimerisation of the FokI nuclease domains induces nuclease activity which causes double stranded chromosomal breaks. Repair by the error prone non-homologous end joining method results in nucleotide deletions (red) or insertions (blue) commonly referred to as indels. Indels cause amino acid changes or frame-shift mutations rendering a non-functional protein.

### **5.1.3 Genome editing with TALENs in zebrafish**

Since the first use of TALENs for genomic manipulation (Christian et al., 2010, Miller et al., 2011), there are a growing number of model organisms and cell types which have been amenable by TALENs; and zebrafish has been no exception. Zebrafish lack the conventional genomic modifications methods made by homologous recombination in embryonic stem cells which are well established in other translational models such as mice. Traditionally, zebrafish studies have relied on transient knockdown by targeted antisense morpholino oligonucleotides or mutagenesis screens (Eisen and Smith, 2008, Lieschke and Currie, 2007). With recent advances in gene editing technology, researchers can now specifically target endogenous zebrafish loci to make genetic mutations.

Simultaneously, two independent groups first described the use of TALENs in zebrafish. Sander et al. (2011) described the presence of indels generated from TALENs in somatic zebrafish cells, while Huang et al. (2011) reported the generation of heritable mutations in zebrafish. Since these initial studies, many groups have published optimised strategies and methodologies to successfully use TALENs in zebrafish. Different platforms have been developed to enable fast assemble of TALEN plasmids including the GoldenGate cloning (Cermak et al., 2011), high-throughput solid-phase assembly (Reyon et al., 2012), and ligation-independent cloning techniques (Schmid-Burgk et al., 2013). Additionally, several groups have confirmed the generation of allele disruption in zebrafish due to indels from NHEJ chromosomal repair (Auer and Del Bene, 2014). The fast and efficient assembly, together with the site specific genome engineering offered by TALENs, has significantly expanded the usefulness of zebrafish as a translational model for development and disease studies.

#### **5.1.4      *Rational for work***

Morpholinos are widely used to study gene function in zebrafish; however, they only provide transient knockdown in the early embryo. Therefore, this study aimed to generate loss-of-function alleles in zebrafish genes *fdx1b* and *cyp11a2* using TALENs. It was hypothesised that these lines would show a correlation between the observed morpholino phenotypes and provide a useful tool for future experiments investigating the impact of mitochondrial redox regulation on steroidogenesis.

## 5.2 Methodology

### 5.2.1 *GoldenGate TALEN assembly method*

GoldenGate TALEN and TAL Effector Kit 2.0 was first published by Cermak et al. (2011) as a method for the easy assembly of custom TALENs. As the name suggests, this assembly method is based on GoldenGate cloning principals which uses type II restriction endonucleases (such as BsaI and Esp3I), whose recognition sites are distal to their cleavage sites. Additionally, they produce nonpalindromic, four nucleotide five-prime overhangs. As the cleavage site and recognition site are separated, any desired five-prime overhang can be generated for ligation. Furthermore, upon ligation, the enzyme recognition site will be absent; hence ligated products cannot be recut allowing restriction digestions and ligations to occur in a single reaction.

#### 5.2.1.a. *GoldenGate reaction one*

Each TALEN is created via two rounds of digestion and ligation steps. In the first reaction, ten repeat units containing the desired RVDs are cloned into an intermediate pFUS plasmid. Each pFUS vector can only be used for 10 repeats, therefore, TALENs with 11 or more repeat units require separate ligations into a second pFUS vector. The 20  $\mu$ L reaction contains 150 ng of the appropriate pFUS plasmid, 150 ng of each module plasmids (containing the appropriate RVD for the specific position), 1x T4 DNA ligase buffer, 1  $\mu$ L of T4 DNA ligase, 2  $\mu$ g BSA and 1  $\mu$ L of BsaI restriction enzyme. The single digest-ligation reaction consisted of 10 cycles of 37 °C for five minutes followed by 16 °C for 10 minutes. A final incubation of 50 °C for five minutes and enzyme inactivation at 80 °C for five minutes completed the reaction. For each GoldenGate reaction, 1  $\mu$ L of 10 mM ATP and 1  $\mu$ L of Plasmid-Safe Nuclease (Epicentre Biotechnologies; Madison, United States of America) was added and subsequently incubated for one hour at 37 °C to digest all unligated plasmids. Next, 5  $\mu$ L of each reaction was used to transform 50  $\mu$ L of

DH5 $\alpha$  gold competent *E. coli* as per the stranded protocol. Transformations were plated out on LB agar plates containing 50  $\mu$ g/mL of spectinomycin with X-gal and IPTG and incubated overnight. White colonies containing RVD modules were screened by colony PCR using pCR8\_F1 and pCR8\_R1 oligonucleotides (Table 5.1) as per the standard protocol. Upon plasmid purification, the sequence of RVD amino acids was confirmed by sequencing with pCR8\_F1 and pCR8\_R1 primers (Table 5.1).

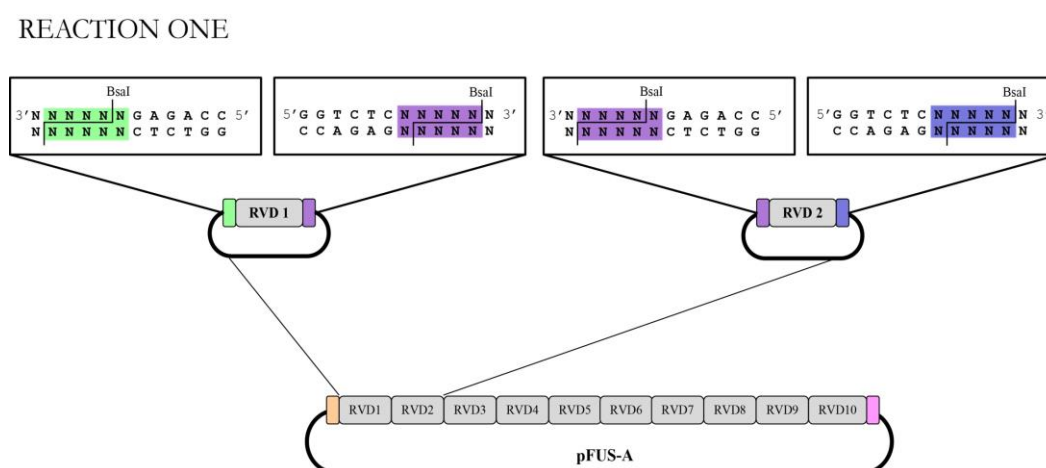


**Figure 5.3 GoldenGate TALEN assembly reaction one**

GoldenGate assembly of customised TALENs involves the digestion and ligation of specific modules containing the repeating domains into specific plasmids. In reaction one, the type IIS restriction endonucleases BsaI is used to create unique overhangs to ligate repeat modules containing the desired repeat variable diresidues (RVD) in order. This single step reaction involves the generation of up to 10 repeats into an intermediate pFUS plasmids. The schematic depicts the ligation of repeat domains one and two containing the required RVDs into pFUS-A. For repeat domains between positions 11 and 20 of the TALEN a separate reaction is used to ligate them into the intermediate pFUS-B vector.

**5.2.1.b. GoldenGate reaction two**

The second GoldenGate reaction ligates the intermediate pFUS plasmids into the final destination vector containing the last module and the *fok1* nuclease coding sequence. After digestion with Esp3I, the TALE containing the desired RVD sequences will be ligated in-frame with the FokI nuclease domain. The final destination vectors are the second generation pCS2TAL3-DD or pCS2TAL3-RR (Dahlem et al., 2012) (Figure 5.4).

**Table 5.1 Primer sequences for screening TALEN construction plasmids.**

<i>Primer</i>	<i>Sequence (5-prime to 3-prime)</i>
pCR8_F1	TTGATGCCTGGCATGGCCCT
pCR8_R1	CGAACCGAACAGGCTTATTGT
TAL_F1	TTGGCGTCGGCAAACAGTGG
TAL_R2	GGCGACGAGGTGGTCGTTGG
SeqTALEN_5-1	CATCGCGCGCAATGCACTGAC

In the second reaction 150 ng of each pFUS intermediate vector was added to 150 ng of the pLR vector containing the last repeating module and the destination vector (either pCS2+TAL3-DD or pCS2+TAL3-RR). These were mixed in a 20  $\mu$ L reaction contacting 1x T4 DNA ligase buffer, 1  $\mu$ L of T4 DNA ligase, and 1  $\mu$ L of Esp3I restriction enzyme. A single incubation series of 37 °C for 10 minutes, 16 °C for 15 minutes and 37 °C for 15 minutes was followed by enzyme inactivation at 80 °C for five minutes. Five microlitres of each reaction was used to transform 50  $\mu$ L of DH5 $\alpha$  gold competent *E. Coli* as per the stranded protocol. Transformations were plated out on LB agar plates containing 100  $\mu$ g/mL of Carbenicillin with X-gal and IPTG and incubated overnight at 37 °C.

The following day four white colonies were picked to be screened by colony PCR using TAL\_F1 and TAL\_R primers (Table 5.1). The PCR cycle consisted of 35 cycles of annealing at 55 °C and extension step of three minutes. Reactions were run on a 1 % agarose gel to identify correct clones to start an overnight culture for plasmid purification. Following purification, the plasmid was sequenced using SeqTALEN 5-1 and TAL\_R2 (Table 5.1). After sequencing confirmation of the correct order of the RVDs, the final plasmids were stored at -20 °C until required for *in vitro* mRNA generation.

#### REACTION TWO

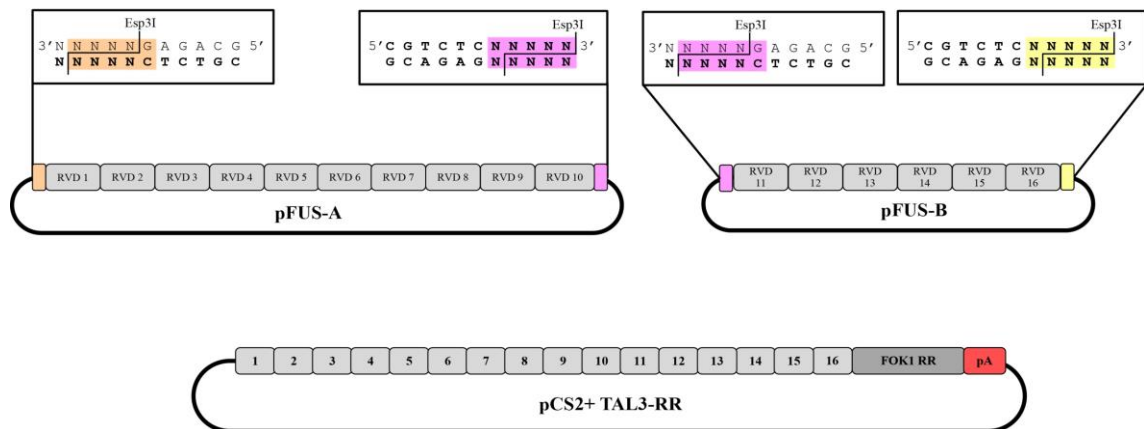


**Figure 5.4 GoldenGate TALEN assembly reaction two**

Reaction one involves the ligation of the desired repeats into the intermediate pFUS plasmids (pFUS-A or pFUS-B). In reaction two, the type IIS restriction endonucleases Esp3I is used to create unique overhangs to ligate the pFUS plasmids containing the desired repeat variable diresidues (RVDs) in order. They are simultaneously ligated into the final destination vector, pCS2+TAL3. The schematic depicts the generation of a single TALEN plasmid of containing 16 repeat domains in-frame with the fok1-RR domain with a poly adenylation signal (pA). The pCS2+ backbone allows for *in vitro* mRNA synthesis of the TALEN through a SP6 promoter prior to injection into the zebrafish embryo.

### **5.2.2      *Generation of TALEN RNA for microinjection***

The constructed customised TALEN plasmids were used as templates for *in vitro* mRNA transcription. Prior to mRNA synthesis 5 µg of plasmid DNA was linearised with NotI-HF and purified. TALEN mRNA was generated using SP6 polymerase and purified using the GenElute Mammalian Total RNA Miniprep Kit. Five microlitres of purified mRNA was run on an agarose gel to confirm RNA integrity.

### **5.2.3      *Microinjection of TALEN mRNA***

Microinjection into the single cell embryo is the most effective way to transmit the TALEN mRNA into the developing embryo. Upon injection the mRNA will be translated by the zebrafish's endogenous translational machinery to produce the TALEN protein. Initially, single cell embryos were microinjected with 50 to 150 pg of TALEN mRNA. After microinjections, embryos were screened to identify TALEN induced indels. mRNA concentrations showing over 50 % of embryos survival were used.

### **5.2.4      *Genotyping by restriction digest***

Initially, detection of indels was performed by loss of restriction site within the TALEN spacer region. Injected embryos were genotyped by PCR with primers flanking the predicted cut site and subsequent restriction digest of the amplified product. It was assumed that loss of the restriction site would be caused by the presence of indels from NHEJ repair of the chromosomal break. Genomic DNA was extracted from injected embryos as previously described. PCR amplification was performed using Megamix-Blue (Microzone Ltd.), 0.6 µM of specific forward and reverse oligonucleotides (Table 5.2) were combined with 3 µL of genomic DNA in a 50 µL reaction volume. PCR cycles consisted of an initial denaturing step of 95 °C for five minutes and then 40

cycles consisting of 95 °C for 30 seconds, 58 °C for 30 seconds for annealing and extension step at 72 °C for 15 seconds. A final step of seven minutes at 72 °C completed the PCR cycle. Following the PCR, the amplified product was subjected to a restriction digest. Typically, in a 25 µL reaction, 2.5 µL of restriction enzyme buffer was added with 1 µL of enzyme with 21.5 µL of PCR. After incubation 20 µL was run on an agarose gel for visualisation of the production.

**Table 5.2 Sequences of the primers used for genotyping PCR for *fdx1b* and *cyp11a2* null alleles by restriction digest**

<i>Gene</i>	<i>Primer</i>	<i>Sequence (5-prime to 3-prime)</i>	<i>Restriction enzyme</i>
<i>fdx1b</i>	TALEN F	GTGTCTATATTAGGAGCATGCT	Tsp451
	TALEN R	TTCCGTAAGCCAAATCCAGC	
<i>cyp11a2</i>	TALEN F	GGTTGGATTCTATGAAAGTGTGA	DraI
	TALEN R	CCCAACCTCATCCAGAAGG	

### **5.2.5 Genotyping by high resolution melting curve (HRM) analysis**

High resolution melting curve (HRM) analysis is a PCR method which detects indels, including single base-pair changes. HRM was performed using two sets of primers designed around the TALEN binding region. *fdx1b* primer pairs HRM1 forward (F) and reverse (R), and HRM2 forward (F) and reverse (R), gave products of 110 and 74 base-pairs, respectively. *cyp11a2* primer pairs HRM1 forward (F) and reverse (R), and HRM2 forward (F) and reverse (R), gave products of 143 and 90 base-pairs, respectively (Table 5.3).

HRM analysis was performed using 7900HT Fast Real-Time PCR system (Applied Biosystems) using 384-well block module. Ten microlitre reactions were performed in duplicate containing 1x SYBRGreen Master Mix (Applied Biosystems), 150 nM each of the forward and reverse primer and 3  $\mu$ L of genomic DNA. An initial holding stage for enzyme activation at 95 °C for 10 minutes was followed by 40 cycles of denaturing at 95 °C for 15 seconds and annealing and extending at 60 °C for one minute. Finally, the dissociation phase was performed consisting of denaturing at 95 °C for 10 seconds, annealing and extension for one minute at 60 °C, high resolution melting at 95 °C for 15 seconds with a ramp rate of 1 % and a final annealing step of 60 °C for 15 seconds. Amplification was confirmed by analysis of cycle threshold (Ct) values. To detect indels, changes in the dissociation curve shape and melting temperature ( $T_m$ ) of PCR products were compared to uninjected wild-type controls.

**Table 5.3 PCR Primers used for genotyping for *fdx1b* and *cyp11a2* null alleles by high resolution melting curve analysis.**

<i>Gene</i>	<i>Primer</i>	<i>Sequence (5-prime to 3-prime)</i>
<i>fdx1b</i>	HRM1 F	CTATATTAGGAGCATGCGAGG
	HRM1 R	CATGTCAATCTCTTCATCCACC
<i>fdx1b</i>	HRM2 F	AGGGCACTCTGGCCTGTTC
	HRM2 R	CACCATTGGCTCCAGTTTGTC
<i>cyp11a2</i>	HRM1 F	AGGTTGGATTCTATGAAAGTGTG
	HRM1 R	AGGCAGTCCATGCGTCAATG
<i>cyp11a2</i>	HRM2 F	GAAAGTGTGAACATCATCAAGCC
	HRM2 R	CATGCGTCAATGGTGAGTCTC

### **5.2.6      *Visualisation mediated background adaptation assessment***

This method assesses the larvae's ability to adjust their pigmentation in order to adapt to changes in the background environment. Five day old larvae were maintained in a dark environment for 45 minutes. Following this larvae were kept under fluorescent illumination for at least 20 minutes to light-adapt. Larvae were sorted on their melanin pigmentation.

## 5.3 Results

### 5.3.1 Strategic design of *fdx1b* and *cyp11a2* TALENs

TALENs were designed using TAL Effector-Nucleotide Targeter 2.0 (Doyle et al., 2012). Several parameters were considered in the design of the TALENs including preference for a thymidine nucleotide at the five-prime end of the target site (Moscou and Bogdanove, 2009), presence of a unique restriction site within the spacer region, a spacer region of 15 to 24 nucleotides and to include 15 to 20 RVDs per TALEN (Cermak et al., 2011). Specifically, *fdx1b* binding TALENs were designed to target the conserved motif 1 region which contains the cystine residues essential for haem binding and critical for protein function. Secondly, nucleotide similarity with its paralogues *fdx1* and *fdx1l* was also considered in the design. Initially, *fdx1b* targeting TALEN 1 and TALEN 2 was comprised of 20 and 17 repeating domains, respectively, and separated by a 24 base-pair spacer that included a Tsp45I enzymatic restriction site for genotyping (Figure 5.5). Alternatively, given *cyp11a2* has 80 % nucleotide identity to its paralogue *cyp11a1* (Parajes et al., 2013), the *cyp11a2* targeting TALENs were designed in the region which was most dissimilar to its paralogue gene. A region was chosen including exon 2 which encodes a conserved  $\beta$ -helix. Initial design constraints also meant the *cyp11a2* targeting TALENs were designed flanking a DraI enzymatic restriction site (Figure 5.5B). Given the similarity between *cyp11a1* and *cyp11a2*, and the fact they lie adjacent on chromosome 25, it was essential to ensure specific targeting to *cyp11a2* while considering the best chance to generate a non-functional protein.



### **5.3.2 Assembly of customised TALEN repeat arrays**

In total, seven TALENs were generated during this project; four specifically targeting *fdx1b* and three targeting *cyp11a2*. Each TALEN was constructed by two rounds of digestion and ligation. The initial round of TALEN assemble ligates the first 10 repeating domains of each TALEN into one intermediate plasmid (pFUS-A) and the remaining domains in a second intermediate plasmid (pFUS-B). After the ligation and transformation, eight bacterial colonies from each reaction were screened by colony PCR (Figure 5.6). Due to the repetitive nature of the repeats, a smear like pattern and low molecular weight laddering is expected when screening. A single positive colony was amplified, purified and sequenced to confirm the correct order of RVDs for each plasmid (Figure 5.6)

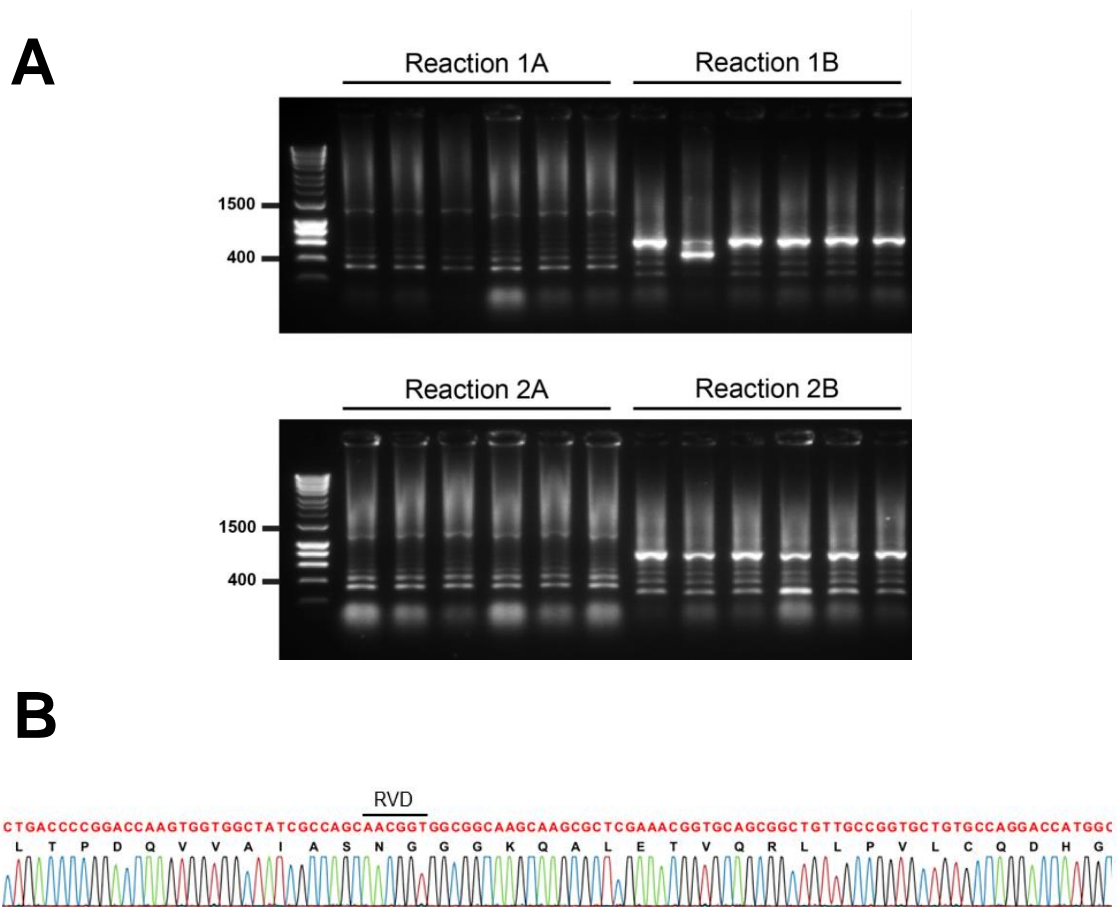


**Figure 5.6 Confirmation of correct ligation of reaction one of the GoldenGate TALEN assembly**

**(A)** A representative agarose gel showing the colony PCR from GoldenGate reaction one. Reaction A and B of each TALEN generates the intermediate pFUS plasmids (pFUS-A or pFUS-B) which will be further ligated in reaction two to generate either TALEN 1 or TALEN 2. Eight colonies from each reaction were screened using pCR8\_F1 and pCR8\_R1 primers. The presence of a bright band around the expected molecular weight and a smear indicates a correct ligation. **(B)** Representative sequencing trace shows one 34 amino acid repeating domain with and NG RVD. Sequencing of each intermediate pFUS plasmid confirmed the order of the RVDs (underlined).

Following confirmation of the two intermediate pFUS plasmids, the second round of digestion and ligation was performed. After transformation of each ligation reaction, three bacterial colonies were screened by colony PCR to confirm the final ligation. Similar to reaction one, the presence of a smear pattern typically indicates a correct clone (Figure 5.7). Additional sequencing of each TALEN was performed as confirmation (Figure 5.8). After validation of the TALEN construction, the final plasmids were used to synthesis mRNA for microinjection into single-cell zebrafish embryos.

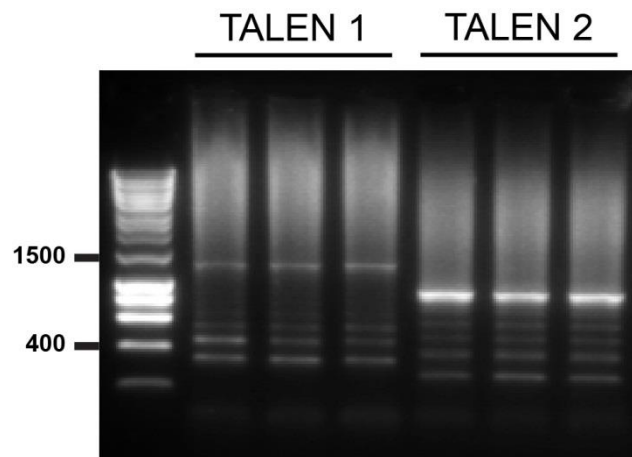


**Figure 5.7 Confirmation of TALEN assembly from GoldenGate reaction two**

After the second ligation step three bacterial colonies for TALEN 1 and TALEN 2 were screened by colony PCR using TAL\_F1 and TAL\_R2. PCR products were run on a 1 % agarose gel. A representative agarose gel is shown from TALEN 1 and TALEN 2 which target the *fdx1b* locus. Due to the repetitive nature of the TALEN, a smear like pattern with a low molecular weight laddering typically indicates the presence of the correct clone. A single clone was picked for each TALEN to confirm with sequencing.

***fdx1b* TALEN 1**

Position:	1	2	3	4	5	6	7	8	9	10	11	12	13	14	15	16	17	18	19	20
RVD residue:	NN	HD	NN	NI	NN	NN	NN	HD	NI	HD	NG	HD	NG	NN	NN	HD	HD	NG	NN	NG
Target:	G	C	G	A	G	G	G	C	A	C	T	C	T	G	G	C	C	T	G	T

***fdx1b* TALEN 2**

Position:	1	2	3	4	5	6	7	8	9	10	11	12	13	14	15	16	17
RVD residue:	NG	NG	NN	NG	HD	NI	NI	NI	HD	NI	HD	NI	NG	NG	HD	NG	HD
Target:	T	T	G	T	C	A	A	A	C	A	C	A	T	T	C	T	C

***cyp11a2* TALEN 1**

Position:	1	2	3	4	5	6	7	8	9	10	11	12	13	14	15	16	17
RVD residue:	HD	NI	NI	NN	HD	HD	NG	NN	NI	NI	NN	NI	NG	NN	HD	NG	NN
Target:	C	A	A	G	C	C	T	G	A	A	G	A	T	G	C	T	G

***cyp11a2* TALEN 2**

Position:	1	2	3	4	5	6	7	8	9	10	11	12	13	14	15	16	17
RVD residue:	NN	NN	NG	NN	NI	NN	NG	HD	NG	HD	NG	NG	NG	NN	NN	NI	NG
Target:	G	G	T	G	A	G	T	C	T	C	T	T	T	G	G	A	T

**Figure 5.8 Sequencing confirmation of the RVD amino acids for each TALEN**

Sequencing of TALENs after assembly confirmed the order of the repeat variable diresidues (RVD) at the positions within the repeating domains. Above are the confirmed RVD sequences from the first set of TALEN assembly for *fdx1b* and *cyp11a2*, with their position within the TALEN and the corresponding nucleotide they recognise.

### 5.3.3 *Microinjection and validation of in vivo TALEN activity by PCR digest*

Once the correct sequence for each *fdx1b* and *cyp11a2* TALEN plasmids was confirmed, mRNA was synthesised *in vitro* for microinjection. Paired TALEN mRNAs were injected into single-cell embryo with a rhodamine tracer as per the standard injection procedure. Initially, 2 nL injections were performed at concentrations of 25, 75 and 150 pg/TALEN/embryo. The following day embryos were screened for normal development. High levels of RNA toxicity and abnormal

development was observed at the highest concentration of mRNA, therefore, these embryos were not used for further analysis. At 72 hpf, genomic DNA was extracted from pools of five embryos to determine if the TALEN pair was capable generating indels. This was initially performed by restriction digest as described by Bedell et al. (2012).

### **5.3.3.a. *Fdx1b* genotyping by restriction digest**

For *fdx1b* genotyping, *fdx1b* TALEN forward (F) and reverse (R) primers (Table 5.2) were used to produce a product of 133 base-pairs. Tsp451 restriction digest of the PCR product produces a 97 and a 46 nucleotide fragment in the wild-type allele. Restriction digests showed the presence of undigested PCR products, suggesting a loss of restriction site from the generation of indels (Figure 5.9). No difference in the proportion of embryos positive for indels was observed between the different concentrations of mRNA injected. Remaining larvae from positive clutches were grown to adults.

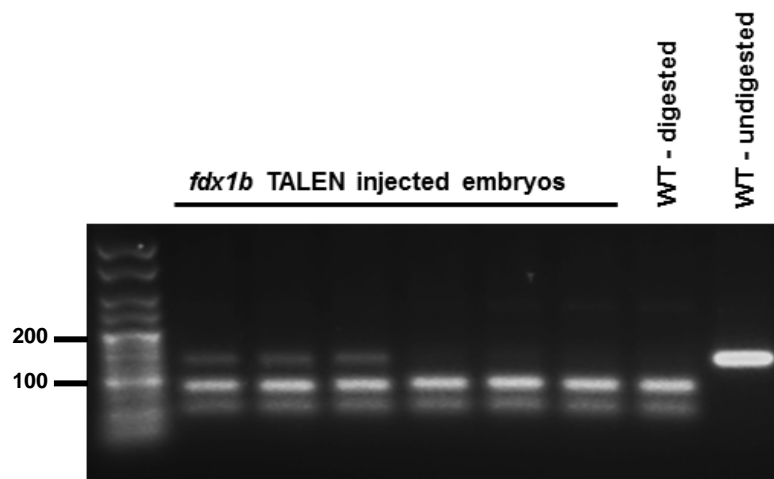


**Figure 5.9 Confirmation of *in vivo* *fdx1b* TALEN activity by restriction digest**

Genomic DNA was extracted from pools of *fdx1b* TALEN injected embryos at 72 hpf. PCR with *fdx1b* TALEN F and R primers produced a product of 133 base-pairs and subsequent digest with Tsp451 generated products of 97 and 46 base-pairs. The presence of undigested product (133 base-pairs) in the *fdx1b* TALEN injected indicates loss of the restriction site from indels produced from TALEN activity.

Once raised to adults (approximately four months), injected zebrafish were outcrossed to wild-type fish. Ten to 15 pools of four embryos from each adult were genotyped by PCR and restriction digest. No embryos were identified to have genomic disruption of the Tsp451 restriction site (Figure 5.10). Hence, no adult fish were capable of germ-line transmission of indels. Following this, the *fdx1b* targeting TALENs were redesigned based on optimised design strategies.

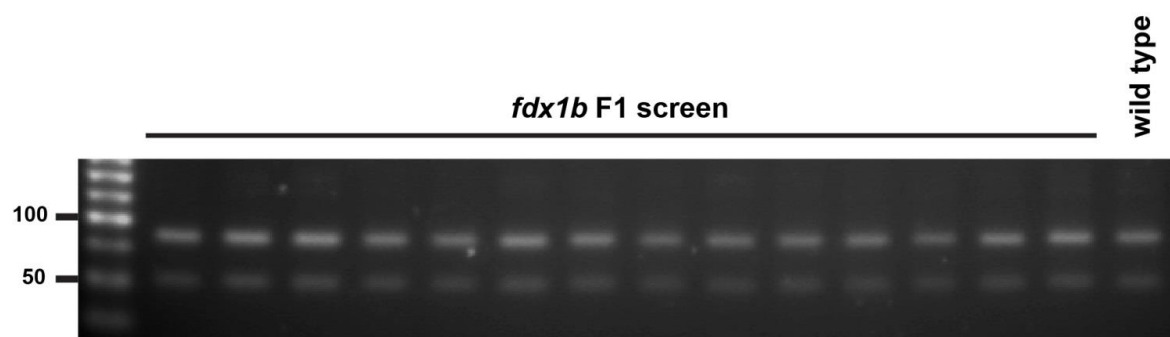


**Figure 5.10 Screening F1 generation for *fdx1b* indels**

Embryos injected with *fdx1b* TALENs were raised to adults. Upon sexual maturation they were out-crossed with wild-type zebrafish. Pools of four F1 generation embryos were screened for indels by PCR and restriction digest to determine adults capable of transmitting indels to the F1 generation. Image shows a representative agarose gel of the *fdx1b* F1 screen. All embryos tested showed complete digest of the *fdx1b* PCR product suggesting a wild-type genotype. No adults capable of transmitting indels to the F1 generation were identified.

### **5.3.3.b. *Cyp11a2* genotyping by restriction digest**

At 72 hpf genomic DNA was extracted from embryos injected with the *cyp11a2* TALEN. PCR with *cyp11a2* TALEN forward (F) and reverse (R) primers (Table 5.2) amplified a 316 base-pair region which would produce two fragments of 60 and 256 base-pair upon treatment with DraI

restriction enzyme. At all concentrations of RNA tested, there was no loss of restriction site (Figure 5.11). This suggests that the first version of *cyp11a2* targeting TALEN was not introducing chromosomal breaks and subsequently needed to be redesigned.

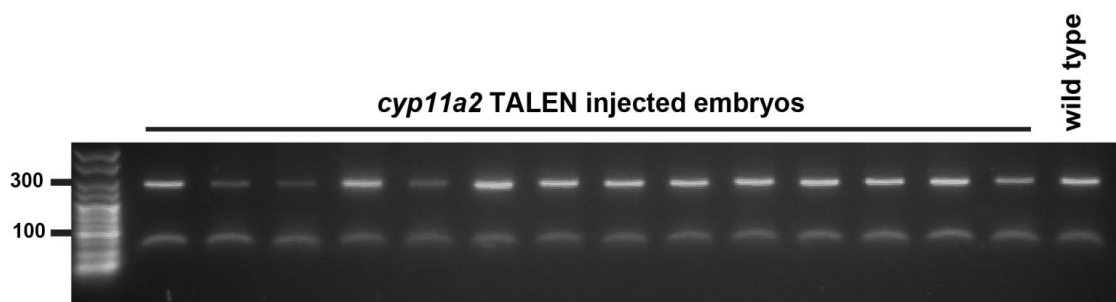


**Figure 5.11 Determining *cyp11a2* TALEN activity *in vivo***

Genomic DNA was extracted from pools of *cyp11a2* TALEN injected embryos at 48 hpf. PCR with *cyp11a2* TALEN F and R primers produced a product of 316 nucleotides and subsequent digest with *DraI* generated products of 256 and 60 base-pairs. No undigested product (316 base-pairs) was observed in the *cyp11a2* TALEN injected indicates suggesting there is no *cyp11a2* TALEN activity.

### 5.3.4 Redesign of *fdx1b* and *cyp11a2* TALENs

We observed that the first versions of TALENs targeting *fdx1b* and *cyp11a2* were not inducing indels as anticipated and subsequent redesign was required. During the time when the first TALENs were synthesised and tested and when the new TALENs were required, several studies were published to optimise TALEN efficiency. During July 2012, two individual groups demonstrated that the diresidue asparagine histidine (NH) targets the nucleotide guanosine with

more specificity and with good affinity than the previously described asparagine asparagine (NN) RVD (Cong et al., 2012, Streubel et al., 2012). Additionally, shorter spacer lengths were considered based on the newly proposed optimal distance for FokI dimerisation and nuclease activity (Ma et al., 2013). Considering these optimal constraints, new TALENs were generated targeting *fdx1b* and *cyp11a2*. For *fdx1b*, TALENs were redesigned to encompass a spacer region of 15 base-pairs and NN diresidues were replaced by NH to increase specificity and affinity. Additionally, only *cyp11a2* TALEN 2 was remade to incorporate a smaller spacer region of 15 nucleotides (Figure 5.12). The second generation TALENs were synthesised as described above and the RVDs were confirmed by sequencing (Figure 5.13).



***fdx1b* TALEN 1**

Position:	1	2	3	4	5	6	7	8	9	10	11	12	13	14	15
RVD residue:	HD	NG	NH	NH	HD	HD	NG	NH	NG	NG	HD	HD	NI	HD	HD
Target:	C	T	G	G	C	C	T	G	T	T	C	C	A	C	C

***fdx1b* TALEN 2**

Position:	1	2	3	4	5	6	7	8	9	10	11	12	13	14	15	16	17	18	19	20
RVD residue:	NG	NG	NH	NG	HD	NI	NI	NI	HD	NI	HD	NI	NG	NG	HD	NG	HD	HD	NG	HD
Target:	T	T	G	T	C	A	A	A	C	A	C	A	T	T	C	T	C	C	T	C

***cyp11a2* TALEN 2**

Position:	1	2	3	4	5	6	7	8	9	10	11	12	13	14	15	16	17	18	19	20
RVD residue:	HD	NG	NG	NG	NH	NH	NI	NG	NI	NI	NG	NH	NI	HD	HD	NG	NG	HD	NH	NH
Target:	C	T	T	T	G	G	A	T	A	A	T	G	A	C	C	T	T	C	G	G

**Figure 5.13 Sequencing confirmation of RVD of second generation TALENs**

Sequencing of TALENs after assemble confirmed the order of the repeat variable diresidues (RVD) at the positions within the TALEN repeating domains. The confirmed RVD sequences from the second round of TALEN assembly are shown for *fdx1b* and *cyp11a2* with their position within the TALEN and the corresponding nucleotide sequence they recognise. Two new TALENs targeting *fdx1b* were synthesised. Only TALEN 2 was redesigned for *cyp11a2* and it was paired with TALEN 1 from the first TALEN assembly.

### 5.3.5 *Development of high resolution melting curve analysis for genotyping*

A genotyping method using high resolution melting curve (HRM) analysis was established to detect indels. For HRM, real time PCR is performed using SYBRGreen followed by dissociation curve analysis. Changes in the dissociation curve represent changes in the melting temperate of the PCR product, which corresponds to differences in nucleotide sequence. To determine if the in-house real-time PCR machine and software was sensitive enough to detect individual

nucleotide changes, a trial HRM was performed using *cyp11a2* cDNA extracted from AB and Tubingen. From previous *Cyp11a2* studies, a SNP was identified in the AB wild-type strain which was not present in the Tubingen strain (Chapter 4.0). PCR amplification of 143 nucleotides using *cyp11a2* HRM1 forward and reverse primers confirm specificity by amplification of a single dissociation peak when using these primers. Additionally, changes in the dissociation curve and subsequent  $T_m$  between the two zebrafish strains confirmed the method was sensitive enough to detect single base-pair differences (data not shown). All subsequent detection of indels was carried out using this method.

### **5.3.6 Microinjection and validation of *in vivo* TALEN activity by HRM**

As per the previous TALEN mRNA injections, concentrations of 25 and 75 pg of each TALEN mRNA per embryo was microinjected into single cell embryos. After 48 hpf, genomic DNA was extracted from pools of five embryos and used for HRM analysis. Two different primers pairs were used for each pool of genomic DNA and each sample was performed in duplicate.

#### **5.3.6.a. Confirmation of TALEN induced *fdx1b* indels**

After *fdx1b* TALENs were injected, embryos were screened by HRM to determine if the newly designed TALENs were capable of generating indels. Genomic DNA was screened using *fdx1b* HRM1 primers and confirmed with HRM2 primers (Table 5.3). A change in the dissociation curve was observed in embryos injected with both concentrations of *fdx1b* TALENs when compared with uninjected embryos (Figure 5.14).

**5.3.6.b. Confirmation of TALEN induced *cyp11a2* indels**

HRM was used to determine if the redesigned *cyp11a2* TALENs were capable of producing indels in the targeted genomic region. Genomic DNA was extracted from pools of injected embryos which were then screened for indels by HRM using *cyp11a2* HRM1 (Table 5.3). Dissociation curves showed two peaks suggesting the presence of indels in the injected embryos. This was in contrast to uninjected embryos where only a single peak was observed. Confirmation of changes in the dissociation curve was confirmed by a second set of *cyp11a2* HRM2 primers.

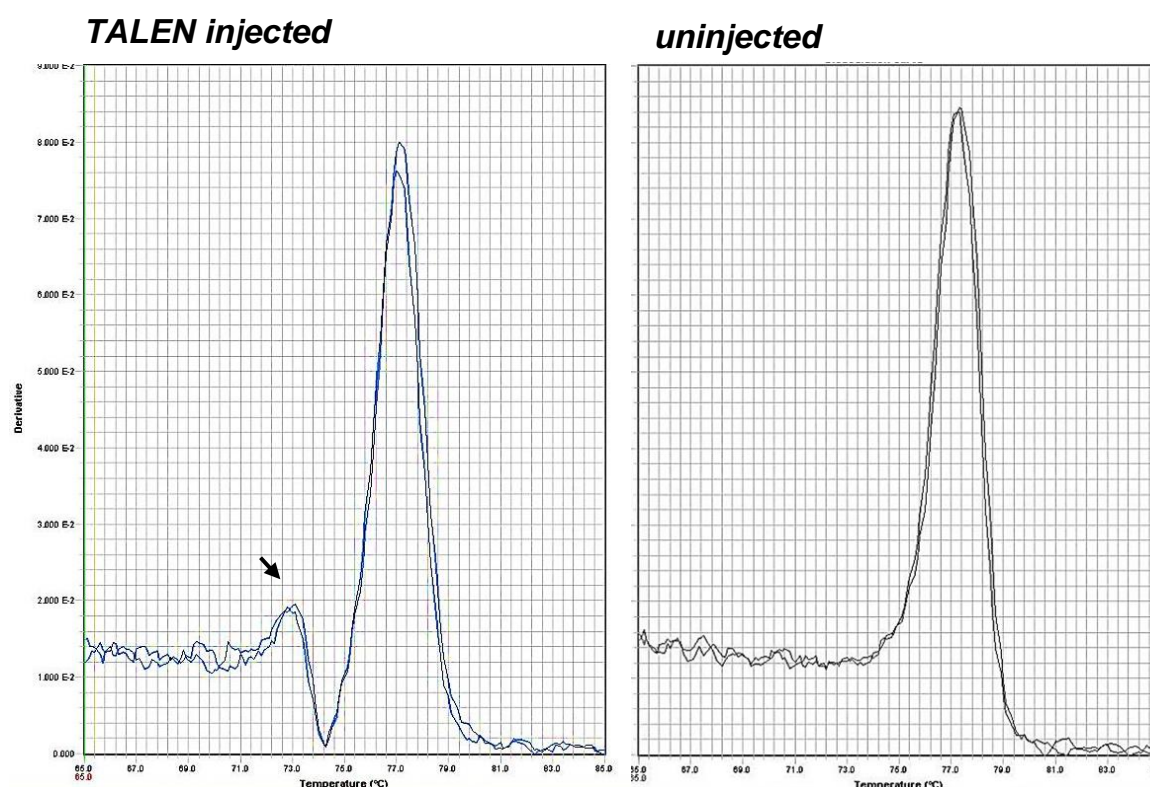


**Figure 5.14 HRM dissociation curves of TALEN injected embryos**

A representative high resolution melting (HRM) dissociation curve of embryos injected with TALENs targeting *fdx1b*. A 110 base-pair fragment of *fdx1b* was amplified with SybrGreen and subjected to dissociation curve analysis. In uninjected embryos a single peak was observed suggesting PCR amplification of a single product. In TALEN injected embryos two peaks were observed, one corresponding to the wild-type product and a second smaller product which is likely the result of generated indels (arrow). The presence of two peaks suggests disruption of the wild-type allele.

### 5.3.7 Identification of heritable mutations

After TALENs were confirmed to successfully induce indels, positive clutches were grown to adults. It was anticipated that each adult zebrafish would be a mosaic of different indels as the TALEN would cut and repair differently in each cell. Once sexual maturity was reached

(approximately four months) injected adult fish were outcrossed with wild-type fish. Individual embryos from these crosses were screened by HRM at 72 hpf to identify adults capable of germ-line transmission of indels. F1 generation embryos from positive founder adults were grown to adulthood. Adults not capable of producing offspring with disrupted alleles were sacrificed.

**5.3.7.a. *Fdx1b* heritable indels**

Using the strategy outlined above, four (from 15 screened) adult zebrafish which were previously injected with TALENs targeting *fdx1b* were capable of germ-line transmission (26.6 %). To confirm that the observed changes in the dissociation curve correlated with disruption of *fdx1b* allele an individual embryo was sequenced. A change in sequencing trace was observed within the spacer region flanked by the TALENs (Figure 5.15) Clutches of embryos from positive *fdx1b* TALEN injected founder zebrafish were raised (F1 generation).

**5.3.7.b. *Cyp11a2* heritable indels**

To determine if adults previously injected with *cyp11a2* targeting TALENs were capable of transmitting indels to the next generation, they were out-crossed with wild-type zebrafish and the embryos were screened by HRM. Four female adults were identified (from 22 screened) as capable of producing offspring with changes in the *cyp11a2* genomic region (18 %). To confirm the HRM findings, an individual embryo was sequenced. Heterozygous sequencing traces were identified starting from within in the spacer region flanked by the TALENs (Figure 5.15). Clutches of larvae from positive founders were raised to adults (F1 generation).



**Figure 5.15 Sequencing confirmation of *fdx1b* and *cyp11a2* TALEN induced deletion**

To confirm the presence of mutations in the F1 generation, individual embryos which showed a positive or negative peak for indels (**A**) *fdx1b* and (**B**) *cyp11a2* was sequenced. The arrow indicates the repair site within the spacer region where the TALEN was designed.

### 5.3.8 Outcrossing and establishing lines harbouring indels

Due to the mosaic nature of the TALEN injected generation each individual founder fish is capable of producing offspring with different indels. Additionally, each individual founder would produce a different percentage of off-spring harbouring indels depending on how proficient the

original TALEN cut and repair was. Clutches from individual founders were grown to adults. Heterozygote adults from the F1 generation were identified by extracting genomic DNA from a fin clip and performing HRM analysis.

#### **5.3.8.a. Establishing *fdx1b* null lines**

Fin clipping and subsequent HRM analysis of the F1 generation adults identified 12 fish which were heterozygous for individual mutations within *fdx1b*. To identify the exact indels *fdx1b* genomic DNA was amplified by PCR using *fdx1b* TALEN forward and reverse primers (Table 5.2) and six were subjected to sequencing (Figure 5.16). From the six heterozygotes sequenced, four different mutations were identified. Line one and two showed the same two base-pair deletion and lines four and five had the same 12 base-pair deletion. Line three and line six had unique indels. Once the heterozygote F1 adults were identified and confirmed, lines three, four and five were maintained by outcrossing to wild-types zebrafish and growing up the offspring (F2 generation).

#### **5.3.8.b. Establishing *Cyp11a2* null lines**

The F1 generation, previously confirmed to contain indels within *cyp11a2*, were raised to adults and subjected to fin clipping and HRM analysis to identify those heterozygote adults. From 43 adults screened, no fish harbouring *cyp11a2* indels was identified. Additionally, only a single *cyp11a2* founder fish had survived.



**Figure 5.16 Sequencing confirmation of F1 heterozygotes for mutations in *fdx1b***

Twelve F1 generation adults that were heterozygote for mutations in *fdx1b* were initially identified by high resolution melting curve analysis from fin clips. **(A)** PCR of the region of the where the TALEN was targeted shows the presence of two bands in some fish. **(B)** Sequencing of six lines identify the precise mutations. Outcrossing of these F1 fish was performed to establish the F2 generation harbouring the same mutation.

### 5.3.9 *Genotyping and characterisation of generation *fdx1b* F2 TALEN lines*

After identification of individual heterozygote carrying genomic disruptions in *fdx1b*, lines three, four and five were maintained as heterozygotes for future experiments. These F1 adults were

outcrossed to wild-type fish and individual F2 clutches harbouring the same indel were raised to adults. It was anticipated that indels would be inherited by traditional Mendelian inheritance and therefore, 50 % of the F2 generation would be heterozygous. To identify heterozygotes, adult F2 zebrafish were fin clipped and genotyped by regular PCR. Heterozygotes were identified by PCR using TALEN forward and reverse primers (Table 5.2). Heterozygotes were identified and kept for future experiments.

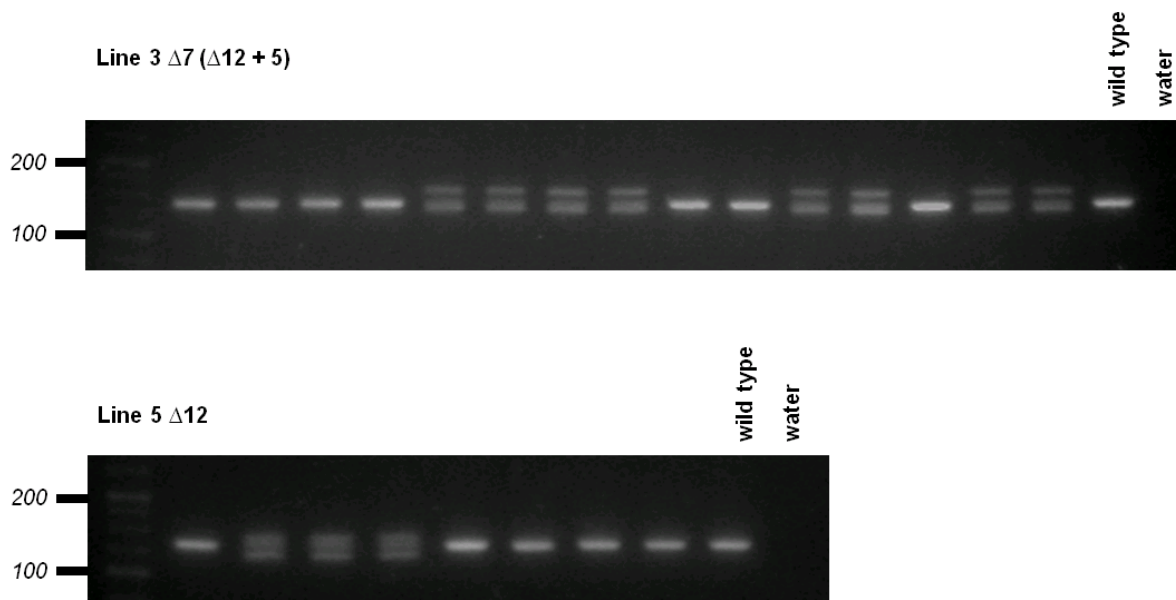


**Figure 5.17 Identification of *fdx1b* null alleles by PCR of F2 generation**

An F2 generation was established for line three, four and five. To identify heterozygous fish, adults were screened by PCR from genomic DNA extracted from fin clips. A representative agarose gel from screening line three and line five is shown. Wild-type genomic DNA was used as a positive PCR control.

### **5.3.10 Preliminary characterisation of *fdx1b* null zebrafish embryos**

Once F2 heterozygote adults had been identified from each line, they were in-crossed to generate *fdx1b* knockouts. Preliminary data suggest *fdx1b* null larvae are morphologically indistinguishable from wild-type siblings during the first five days of development. When subjected to visually mediated background adaptation assessment, 38 of 132 larvae (28.8 %) showed a darker appearance after 20 minutes. Genotyping of larva that had pigmentation adaption and no pigmentation adaptation showed *fdx1b* genetic disruption in five out of six larvae without a pigmentation change. Only the wild-type or heterozygous allele was present in larva capable of background adaption. Larvae were sorted based on their ability to adjust to lighter background environments and their steroid hormones were analysed at five days. Preliminary results ( $n = 1$ ) showed *fdx1b* mutants have cortisol levels of 0.76 pg per larva while their wild-type siblings have 12.96 pg per larva (Figure 5.18).

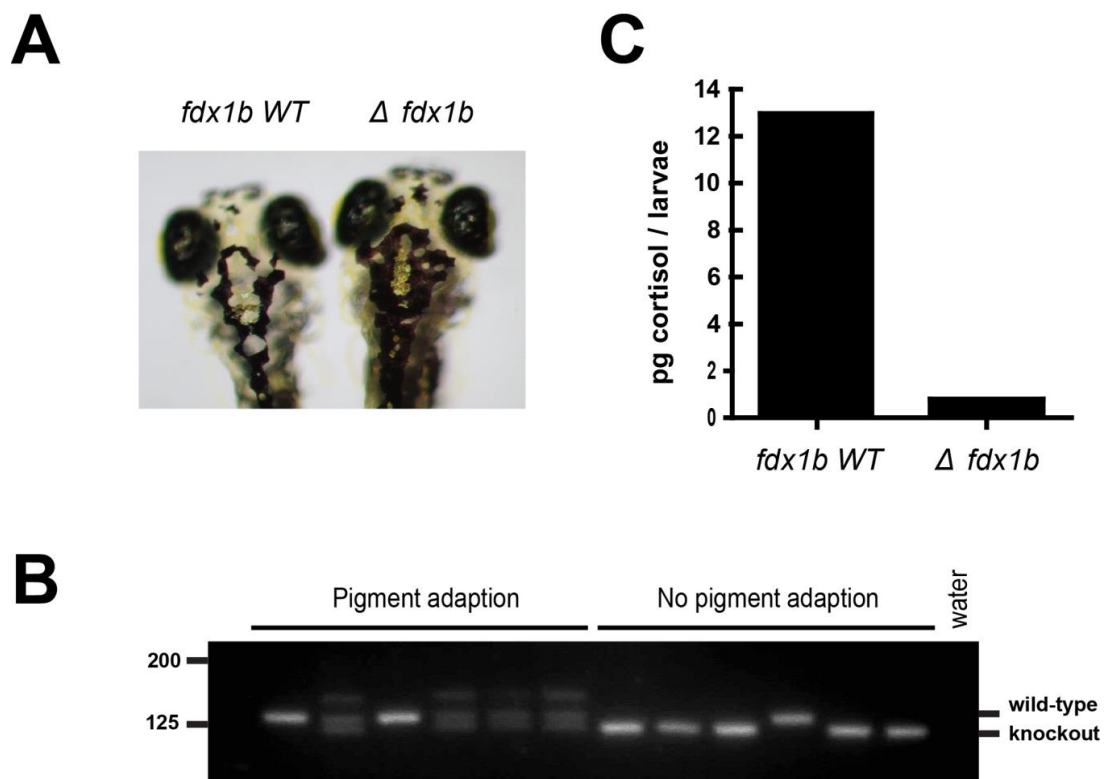


**Figure 5.18 Phenotypic characterisation of *fdx1b* null larvae (line five)**

**(A)** Visual mediated adaption assessment shows *fdx1b* mutant larvae ( $\Delta$  *fdx1b*) are unable to contract their melanin granules when exposed to a bright environment when compared with wild-type siblings. **(B)** Phenotype/genotype correlation between larvae showing pigment adjustment and no pigment adjustment during visual mediated adaptation. Larvae capable of pigmentation adjustment showed either wild-type or heterozygous genotype. Five out of six larva with no pigment adjustment were homozygous for a 12 base-pair deletion in *fdx1b*. Line five heterozygotes produce a higher molecular weight band as a result of PCR amplification of this locus. **(C)** At 120 hpf cortisol concentrations of *fdx1b* null larvae were 0.76 pg per larvae compared to 12.96 pg per larva for their wild-type siblings ( $n = 1$ ).

## 5.4 Discussion and prospective studies

### 5.4.1 *Using TALENs as an alternative to traditional morpholino knockdown studies*

Zebrafish lack the traditional genome knockout methodologies which have been widely used in mammalian model organisms since 1989 (Capecchi, 1989). Therefore, gene functional studies in the zebrafish have typically relied on antisense morpholino oligonucleotides as an effective, gene-specific knockdown technology. Morpholinos target the endogenous mRNA and disrupt translation or splicing to generate an aberrant protein. However, morpholinos allow for transient knockdown only. As the cells divide and the embryo grows, the morpholino becomes diluted and used up which allows for functional endogenous expression to be restored during development. Additionally, morpholino oligonucleotides are known to be toxic and bind to unstipulated RNAs, resulting in non-specific phenotypes (Eisen and Smith, 2008). Common non-specific phenotypes include developmental delay, defects in organ asymmetry and pericardial oedema, which are often attributed to loss of a specific gene. TALENs are a new genome editing method that allows for targeted genetic disruption. In comparison to the traditional morpholino methods, this methodology is considered a more reliable and feasible option to determine gene function in zebrafish (Schulte-Merker and Stainier, 2014). Generating knockouts omits many of the limitations of morpholino knockdowns and should be considered as a method to accurately determine the physiological importance of genes of interest in zebrafish.

### 5.4.2 *Designing and optimisation of TALENs targeting *fdx1b* and *cyp11a2**

During the TALEN design process it was necessary to consider several features to give the highest chance of generating null alleles while limiting off-target effects. For each targeted gene,

design considerations included; spacer sequence length, number of repeating domains containing the RVD, target site similarity with other genes in the genome, and the inclusion of a unique restriction site around the predicted cut site for genotyping.

Given the similarity to its paralogue gene, *cyp11a1*, target site specificity was of particular importance when designing *cyp11a2* targeting TALENs. It was suggested that a difference of two base-pairs within the targeting sequence was enough to lose TALEN binding ability (Cade et al., 2012). Given the high homology, a region which was most dissimilar between the two genes was chosen to design the TALENs. When compared to *cyp11a1* sequence, the successful second *cyp11a2* TALEN pair had mismatches of 2/17 and 7/20 nucleotides for TALEN 1 and TALEN 2, respectively. Given previous studies, these mismatches would allow sufficient targeting to *cyp11a2*, without disrupting *cyp11a1*.

Optimisation of the spacer region length proved critical for efficient FokI dimerisation and subsequent generation of chromosomal breaks. Initial studies reported TALEN induced double stranded breaks with spacer regions ranging from 12 to 31 base-pairs (Cermak et al., 2011, Li et al., 2011, Miller et al., 2011, Mussolino et al., 2011). Given this, our first generation TALENs were synthesised with 24 and 26 spacers regions for *fdx1b* and *cyp11a2*, respectively. Neither the *fdx1b* nor *cyp11a2* TALENs were able to conclusively show *in vivo* activity. However, a recent study by Ma et al. (2013) reported increased TALEN efficiency in zebrafish embryos when the spacer length was between 13 and 19 base-pairs. In the second generation TALENs, the spacer regions were shortened to 15 nucleotides for both genes. Subsequently, the newly designed TALENs successfully produced chromosomal breaks and subsequent indels within the spacer region and consequently disrupted the *fdx1b* or *cyp11a2* coding sequence.

### ***5.4.3 Optimisation of high resolution melting curve analysis for genotyping***

Initial detection of indels relied on the loss of restriction site within the spacer region between the two TALENs. However, there are several limitations of genotyping by loss of restriction site. Firstly, TALEN design is restricted to flanking locations which harbour a unique restriction site in the spacer region. This eliminates TALEN targeting sites which do not fit such requirements. Additionally, relying on a loss of restriction site can lead to false negatives being detected if indels occur outside of the restriction enzymes recognition domain. Furthermore, detection of false positives may also occur due to incomplete digestion of the PCR product. It is likely that false positives were detected in the initial screening of the *fdx1b* targeting TALENs, and would explain why no indels were observed in the F1 generation.

Along with optimising TALEN design, new methods to successfully detect indels were also established. Apart from restriction digest analysis, other methods including HRM analysis (Dahlem et al., 2012), PCR based approaches (Yu et al., 2014), hetero-duplex analysis (SURVEYOR assay) (Guschin et al., 2010) or LacZ recovery/disruption assay (Christian et al., 2010) have all been applied as methods to test for TALEN activity. As an alternative to the loss of restriction digest method, HRM analysis was used to detect indels for the second round of TALEN injection. Using specific oligonucleotides to generate small PCR products (<300 base-pairs), single nucleotide mutations can be detected by HRM (Reed and Wittwer, 2004). In the initial trial experiments, the detection of a SNP from different zebrafish strains was possible by observing changes in dissociation curve. Therefore, HRM provided a more robust and sensitive method in which to screen TALEN injected zebrafish. Despite the detection of false negatives when using HRM (data not shown), HRM permits a large number of injected embryos to be screened for indels in a single efficient reaction (Dahlem et al., 2012). Furthermore, HRM allows

TALENs to be targeted more specifically within the desired locus, as it does not rely on the presence of a unique restriction site within the spacer region. By implementing the HRM analysis, I was able to successfully detect different indels within *fdx1b* and *cyp11a2*, thus confirming the activity of our TALENs *in vivo*.

#### **5.4.4      *Generating zebrafish Fdx1b null alleles***

To complement our morpholino knockdown studies, TALENs were designed and assembled to successfully engineer genomic disruption of *fdx1b*. Furthermore, through screening and out-crossing different lines containing heterozygote alleles were established. Line four and five have the same 12 base-pair deletion. This produces an in-frame deletion of a conserved cysteine residue required for stabilising the Fe/S cluster. It is predicted this deletion would generate a non-functional protein as mutations of any cysteine residues have proven critical for ferredoxin activity *in vivo* (Grinberg et al., 2000). Line three contains a seven base-pair indel generating a frame-shift. The mutation is predicted to generate a truncated 135 amino acid pre-protein, where there is an additional 34 amino acids after Lys101. This protein would lack conserved motifs two and three required for functional activity.

#### **5.4.5      *Preliminary data suggests fdx1b knockouts lack glucocorticoid production***

In-crossing *fdx1b* heterozygotes resulted in the generation of *fdx1b* knockout embryos. Preliminary characterisation of the *fdx1b* knockouts showed no obvious morphological differences between *fdx1b* deficient embryos and wild-type siblings. This is in contrast to our *fdx1b* morpholino studies, which suggest loss of *fdx1b* gives a morphological phenotype consistent with glucocorticoid resistance and adrenal insufficiency (Chapter 3.0). However,

preliminary steroid hormone analysis suggests *fdx1b* knockouts have a cortisol deficiency. This biochemical phenotype is consistent with the knockdown phenotype and suggests the morphological characteristics are, at least in part, due to non-specific morpholino effects. As zebrafish genetic disrupting methods become more prevalent, there are several cases where knockout studies do not recapitulate morpholino knockdown data (Law and Sargent, 2014, van Impel et al., 2014), and highlight the importance in distinguishing specific from non-specific phenotypes in morpholino studies (Schulte-Merker and Stainier, 2014). Further characterisation of the of *fdx1b* knockout larvae is required to determine the physiological importance of *fdx1b* during development.

When five day old larvae were subjected to lighter environments, *fdx1b* knockout embryos were darker in appearance compared to their wild-type siblings. Zebrafish larvae are capable of background adaptation, which involves changing their colour to blend into the surrounding environment. This rapid and reversible physiological process is functional from 96 hpf and involves the distribution or aggregation of melanin within the melanophore (Logan et al., 2006). Larvae were separated based on their melanosome pigmentation and collected at 120 hpf for steroid analysis. Cortisol concentration in *fdx1b* knockouts was decreased compared to siblings. However, there was some cortisol detected, which may be from false *fdx1b* knockouts being present. Further characterisation of the *fdx1b* knockout line is required to confirm the phenotype-genotype correlation.

The *fdx1b* larvae were darker than wild-type siblings from dispersed melanin pigment in the melanosomes. This hyperpigmentation phenotype is likely to be caused by the up-regulation of the HPI axis, and subsequent increased expression of *pomc*. In humans, the POMC protein is cleaved to give rise to multiple proteins including, ACTH which increases cortisol production,

and  $\alpha$ -melanocyte-stimulating hormone (MSH- $\alpha$ ), which regulates the production of melanin (Figure 5.19). Hyperpigmentation in humans is often associated with a number of diseases including adrenal insufficiency and excessive ACTH production (Arlt and Allolio, 2003). In a similar way, this pathway has previously been implicated in regulating the camouflage behaviour of zebrafish (Wagle et al., 2011, Ziv et al., 2013) and is consistent with larvae deficient in the glucocorticoid receptor (Ziv et al., 2013). Although further characterisation of the *fdx1b* mutant lines is required, it is hypothesised the observed decrease in cortisol causes an up-regulation of the HPI axis and results in hyperpigmentation.

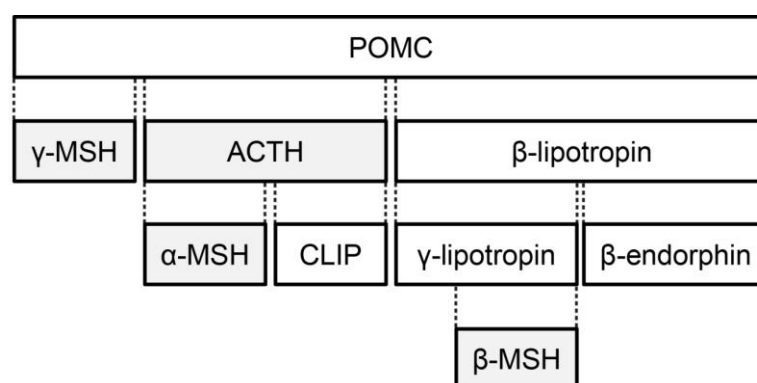


**Figure 5.19 Cleavage of pro-opiomelanocortin (POMC) protein**

Pro-opiomelanocortin (POMC) is a precursor polypeptide which undergoes cleavage to adrenocorticotrophic hormone (ACTH), which stimulates cortisol production and melanocyte-stimulating hormones (MSH), which stimulate the production and release of melanin by melanocytes in the skin.

#### **5.4.6      *Establishing cyp11a2 null lines***

Despite being able to successfully show gene disruption of *cyp11a2* and identify founder fish capable of transmitting these indels to their offspring, no heterozygote F1 adults were identified. The reason for this result is currently under investigation. It is possible that *cyp11a2* heterozygotes have decreased viability compared to wild-types. CYP11A1 mutations in humans have been described in patients with adrenal insufficiency and disordered sex development (Hiort et al., 2005, Kandari et al., 2006, Katsumata et al., 2002, Kim et al., 2008, Parajes et al., 2012, Parajes et al., 2011, Rubtsov et al., 2009, Sahakitrungruang et al., 2011, Tajima et al., 2001); however, humans who are heterozygotes are reported as healthy and able to reproduce (Miller and Auchus, 2011). Therefore, it is unlikely heterozygote *cyp11a2* fish show a phenotype; however, further characterisation of heterozygous adult zebrafish would be required. Additionally, it is unclear if the *cyp11a2* TALENs are targeting the highly homologous paralogue *cyp11a1*. Currently, the off-target effects generated by our TALENs are unknown. Typically, off-target mutations can be eliminated by out-crossing the founder to wild-types for several generations. Given *cyp11a1* and *cyp11a2* lie adjacent on chromosome 25 it is unlikely these mutations can be eliminated as they are closely linked. Embryos recently re-injected with the *cyp11a2* targeting TALENs are currently being raised and survival rates are being monitored to establish possible off-target effects of the *cyp11a2* TALENs.

## **5.5      Conclusions**

In summary, this study has successfully established the use of TALENs for the genome editing of zebrafish within our laboratory. Specifically, TALENs were designed and assembled to successfully generate chromosomal breaks and subsequent indels which caused genetic disruption to the endogenous *fdx1b* and *cyp11a2* genes. The successful generation and future development of

the *fdx1b* and *cyp11a2* null alleles will serve as useful tools for investigating the mitochondrial redox regulation of steroidogenesis.

In the case of *fdx1b*, heritable mutations were generated and several lines which contain disruption in the *fdx1b* gene were established. Zebrafish are the only teleost to retain duplicated ferredoxins. Due to this uniqueness, I was able to disrupt redox transfer in the late larvae without disrupting early development. Over 30 mutants of ferredoxin have been described and explored via *in vitro* assays (Grinberg et al., 2000), however, no *in vivo* models have been established. The generation of the *fdx1b* null zebrafish is the first ferredoxin *in vivo* knockout model system and preliminary results suggest a direct impact on steroid hormone synthesis. The further characterisation of these lines and its use in future studies will allow for direct *in vivo* analysis of redox regulation of steroidogenesis and its impact.

## *Chapter Six*

---

### *Characterising the role of steroid 11 $\beta$ -hydroxylase in zebrafish*

## 6.0 CHARACTERISING THE ROLE OF MITOCHONDRIAL CYP11C1

### 6.1 Introduction

#### 6.1.1 *11 $\beta$ -steroid hydroxylase in zebrafish*

Like most teleosts, zebrafish have a single *CYP11B* homologue, termed *cyp11c1*. Teleost Cyp11c1 has conserved motifs required for Cyp11b activity including binding sites for steroids, oxygen, and haem (Kusakabe et al., 2002, Wang and Orban, 2007). Specifically, zebrafish *cyp11c1* is located on chromosome 16 and is expressed as a maternal transcript and maintained throughout development (Alsop and Vijayan, 2008). To date, defining the physiological importance of Cyp11c1 in teleosts has primarily focused on its role in androgen synthesis. In the testis, Cyp11c1 hydroxylates testosterone to produce 11-hydroxytestosterone. Subsequent metabolism of 11-hydroxytestosterone by 11 $\beta$ -Hsd2 generates 11-ketotestosterone, the primary androgen in many teleost species including zebrafish (de Waal et al., 2008). The function of Cyp11c1 in androgen production has important roles in gonadal differentiation and development (Wang and Orban, 2007). Microarray analysis confirmed *cyp11c1* is highly expressed in the testis (Sreenivasan et al., 2008) and is specifically localised to the androgen producing Leydig cells. Some studies have concluded that *cyp11c1* is not expressed in the zebrafish ovary (Siegfried and Nusslein-Volhard, 2008) while others have detected *cyp11c1* transcripts by RT-PCR but not *in situ* hybridisation (Wang and Orban, 2007); suggesting *cyp11c1* has low levels of expression in the ovary.

Cortisol is the primary glucocorticoid in teleosts and requires the 11 $\beta$ -hydroxylation of 11-deoxycortisol for its production. In zebrafish, *cyp11c1* catalyses this final step in cortisol synthesis. Expression of *cyp11c1* precedes the increase in cortisol levels observed after the hatching period (Alsop and Vijayan, 2009), and a study published in 2013 showed morpholino

knockdown of *cyp11c1* results in 45 % cortisol decrease at 120 hpf (Wilson et al., 2013). However, the precise catalytic ability of teleost *cyp11c1* remains unknown. Aldosterone is the main mineralocorticoid in mammals, but often remains undetected in fish (Bern, 1967, Sandor et al., 1966), leading to the hypothesis cortisol has both mineralocorticoid and glucocorticoid actions (McCormick et al., 2008). Conversely, deoxycorticosterone has been detected in several teleost species, suggesting it may be the active mineralocorticoid (Bury and Sturm, 2007, Gilmour, 2005, Prunet et al., 2006, Sturm et al., 2005). Whether zebrafish Cyp11c1 has dual 11- and 18-hydroxylase and 18-oxidase activity required for aldosterone production remains undetermined. Further studies are necessary to determine the contribution of mineralocorticoids and/or glucocorticoids in electrolyte homeostasis and energy metabolism in fish.

### **6.1.2 CRISPR/Cas9 genome editing**

Clustered regularly interspaced short palindromic repeats (CRISPRs) and the CRISPR-associated Cas9 nuclease, function together as part of an adaptive immune system in bacteria and Archaea (Jiang et al., 2013). Naturally, the CRISPR RNA contains sequences complementary to invading viral DNA which it recognises and binds to. A second trans-activating RNA guides the Cas9 nuclease to the CRISPR RNA to direct cleavage of the viral DNA. Therefore, the CRISPR and trans-activating RNAs, in combination with the Cas9 protein, acts as an antiviral mechanism for the microbe, by introducing DNA breaks in the virus's genome (Barrangou et al., 2007). This CRISPR/Cas9 system has recently been amended for genome editing purposes and is used by many laboratories for genomic manipulation in a variety of model systems (Sander and Joung, 2014).

For genome editing, the Cas9 is guided to the target DNA by a short guide RNA combining both the CRISPR RNA and trans-activating RNA sequences. An additional component of the Cas9

system is the genomic protospacer-adjacent motif (PAM) located at the three-prime end of the DNA target site. This consensus is recognised by the Cas9 protein and signals nuclease activity exactly three nucleotides upstream. Although the precise PAM is specific for each Cas9 orthologue, the most commonly used Cas9 nuclease is from *Streptococcus pyogenes* which recognises the consensus of a single amino acid followed by two guanosine nucleotides (5'-NGG) (Figure 6.1) (Esvelt et al., 2013, Hsu et al., 2014). By designing specific guide RNAs, the Cas9 nuclease can be directed to specific loci to generate chromosomal breaks. In comparison to TALEN assembly methods (Chapter 5.0), the desired sequence for the guide can be ordered as a pair of oligonucleotides and cloned into a guide RNA expressing plasmid. Due to the quick assembly and efficient nuclease activity, the CRISPR/Cas9 system has accelerated the generation of transgenic animal models and is becoming the method of choice for genome editing for researchers (Gaj et al., 2013).

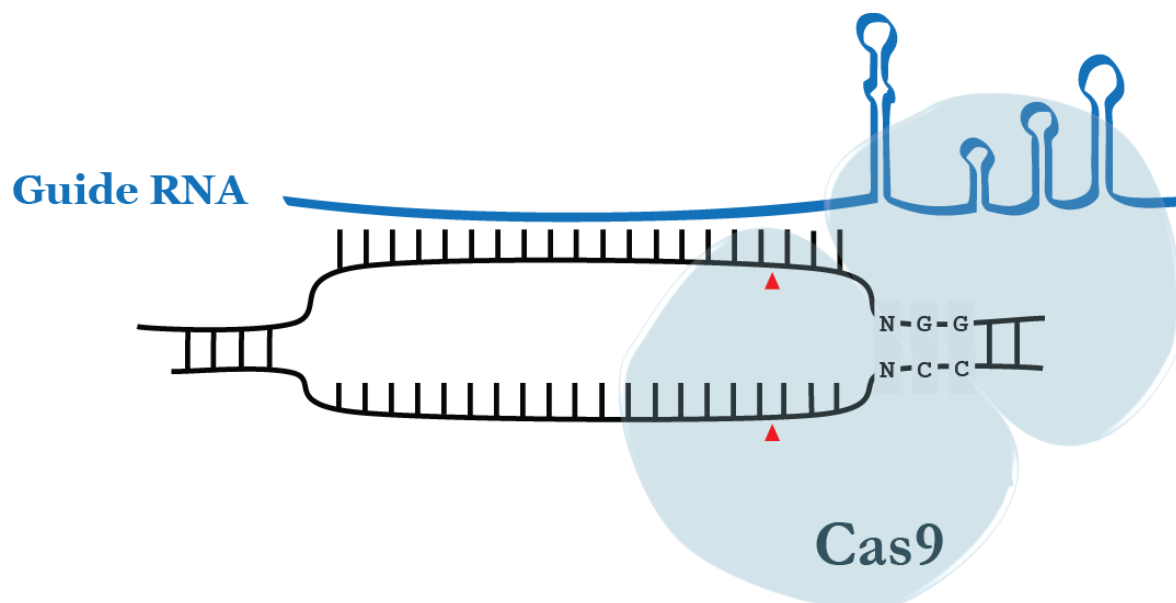


**Figure 6.1 CRISPR/Cas9 system for genomic engineering**

The Cas9 nuclease is targeted to the genomic loci by a specifically designed guide RNA. The guide RNA contains a 20 nucleotide complementary sequence linked to the trans-activating RNA sequence which recruits the Cas9 nuclease. Through recognition of the protospacer-adjacent motif (PAM), 5' NGG, Cas9 cleaves both strands of DNA three nucleotides upstream of this consensus motif (red arrow).

### **6.1.3 Rational for work**

The zebrafish mitochondrial Cyp11c1 enzyme has critical roles in glucocorticoid and androgen production through its 11 $\beta$ -hydroxylase activity. Additionally, its activity is likely to be regulated by electron transfer via the mitochondrial redox proteins Fdx1 or Fdx1b. To fully elucidate the role of this this enzyme, this study aimed to systematically characterise *cyp11c1* in zebrafish. Secondly, it aimed to establish the CRISPR/Cas9 methodology to generate *cyp11c1* loss-of-function alleles for future studies. Finally, in order to investigate the role of androgen production during zebrafish development this projected aimed to develop a specific and sensitive LC-MS/MS methodology to detect zebrafish androgens.

## 6.2 Methodology

### 6.2.1 PCR amplification and cloning of *cyp11c1*

Specific RT-PCR primers were designed based on the ENSEMBL (Zv9) *cyp11c1* sequence (ENSDART00000061572). A 1,892 nucleotide fragment containing the *cyp11c1* coding sequence was amplified with high fidelity Taq polymerase using *cyp11c1*-F and *cyp11c1*-XR oligonucleotides (Table 6.1) and cDNA from the testis of an adult male zebrafish. After confirmation of the PCR product size by agarose gel electrophoresis, the PCR was purified and sequenced. This PCR fragment was cloned into pGEMT-easy vector for plasmid amplification and subsequent sub-cloning.

**Table 6.1 Oligonucleotides for the RT-PCR amplification of 11 $\beta$ -hydroxylase from zebrafish cDNA**

<i>Gene</i>	<i>Primer</i>	<i>Sequence (5-prime to 3-prime)</i>
<i>cyp11c1</i>	cyp11c1-F	CAACAGACAGAGATGGTGA
	cyp11c1-XR <sup>a</sup>	GAACTCCAGAAGAAGCACAG

<sup>a</sup> Reverse oligonucleotides contain a stop codon

### 6.2.2 Alignment and phylogenetic analysis of zebrafish *Cyp11c1*

Our Cyp11c1 protein sequence was compared to human (*Homo sapiens*) CYP11B1 (ENST00000292427) and CYP11B2 (ENST00000323110) protein sequences, stickleback (*Gasterosteus aculeatus*; ENSGACG00000011657), tilapia (*Oreochromis niloticus*; ENSONIG00000006462) and mouse (*Mus musculus*; ENSMUSG00000022589). Alignment and homology analysis was performed using ClustalW2 software as previously described.

### **6.2.3 *In silico KOZAC sequence analysis***

The KOZAC consensus sequence is found on eukaryotic mRNA and is recognised by the ribosome as the transcriptional start site. *In silico* KOZAC sequence prediction was performed using the ATGpr program (URL: <http://www.hri.co.jp/atgpr>) (Salamov et al., 1998), using the full-length ENSEMBL *cyp11c1* cDNA annotated sequence.

### **6.2.4 *Cloning of additional zebrafish cyp11c1 constructs for in vitro studies***

Zebrafish *cyp11c1* cDNA was directionally cloned into the pcDNA6-V5 vector which permits expression in mammalian cells through the CMV promoter. As the transcription initiation site of *cyp11c1* was unclear, four separate in-frame ATG transcription initiation sites were used to test functional activity. All transcripts were amplified using high fidelity Taq polymerase, using different forward primers (Table 6.2) and the *cyp11c1*-XR reverse oligonucleotide (Table 6.1). The full-length 1,892 nucleotide *cyp11c1*-pGEMTeasy plasmid was used as a template. After confirmation of each PCR product size by agarose gel electrophoresis, the PCRs were treated with DpnI restriction enzyme to remove residual plasmid template, purified and sequenced. The PCR fragments were initially cloned into pGEMT-easy vector for plasmid amplification and subsequent sub-cloning.

**Table 6.2 Additional oligonucleotides used for RT-PCR amplification of *cyp11c1* from different ATG start sites**

<i>Gene</i>	<i>Primer</i>	<i>Sequence (5-prime to 3-prime)</i>
<i>cyp11c1-ATG2</i>	F	CAGGATGGTTCGCCCCGA
<i>cyp11c1-ATG3</i>	F	ATGTTACACCGGCAGCAAACAC
<i>cyp11c1-ATG4</i>	F	ATGTTCTTCTTCTGCGCTG

All *cyp11c1*-pGEMTeasy plasmids (i.e. full-length *cyp11c1* and *cyp11c1-ATG2*, *cyp11c1-ATG3* and *cyp11c1-ATG4* constructs) were ligated into pcDNA6 via EcoRI restriction sites. After transformation, direction of the inserts was confirmed by colony PCR using T7 (Table 2.1) and *cyp11c1* e5/6 R primers (Table 6.3). Plasmids in the correct orientation were amplified and purified for subsequent experiments.

### **6.2.5 Characterisation of *Cyp11c1* spatial and temporal expression**

The spatial and temporal expression of *cyp11c1* was characterised by RT-PCR. A 107 base-pair fragment of *cyp11c1* cDNA was amplified as previously described using forward (e5 F) and reverse (e5/6 R) primers (Table 6.3). The following PCR conditions were used: initial denaturation at 95 °C for five minutes, followed by 40 cycles at 95 °C for 30 seconds, 56 °C for 15 seconds and 72 °C for 60 seconds; and a final incubation at 72 °C for seven minutes. As a control for cDNA quality and equal loading a 102 nucleotide fragment of the  $\beta$ -actin gene was amplified using e4F and e4R primers (Table 3.3).

**Table 6.3 Primer sequences used for RT-PCR expression analysis of *cyp11c1***

<i>Gene</i>	<i>Primer</i>	<i>Sequence (5-prime to 3-prime)</i>
<i>cyp11c1</i>	e5 F	GATGAACCTGCTGCGCTTCT
	e5/6 R	AGCCCAGGTGCTCTCTGTAT

### 6.2.6 Generation of *cyp11c1* short guide RNA plasmids

In order to facilitate Cas9 directed genomic disruption, plasmids for transcribing specific guide RNAs were generated. Two individual guides targeting *cyp11c1* were synthesised and tested during the optimisation of the CRISPR/Cas9 methodology. For each guide, two specific oligonucleotides were designed (Table 6.4). Each pair of oligonucleotides was hybridised by combining 10  $\mu$ M of oligonucleotide one and two with 1x Buffer 4 (NEB) in 20  $\mu$ L of DEPC water. The oligonucleotide mix was incubated at 95 °C for ten minutes and cooled to room temperature to permit hybridisation. Hybridisation creates overhangs compatible with cloning into the BsaI linearised RNA guide synthesis vector, DR274 (Figure 6.2).

**Table 6.4 Oligonucleotide sequences to generate *cyp11c1* genomic targeting guide RNAs**

<i>Genomic target sequence</i>	<i>Name</i>	<i>Sequence (5-prime to 3-prime)</i>
GGCGCGTAACCCTGATGTGC	Oligo1	TAGGCGCGTAACCCTGATGTGC
	Oligo2	AAACGCACATCAGGGTTACGCG
GGCGTCTGGAGACCCTCTGA	Oligo1	TAGGCGTCTGGAGACCCTCTGA
	Oligo2	AAACTCAGAGGGTCTCCAGACG



**Figure 6.2 Hybridisation of oligonucleotides for cloning into DR274**

Hybridisation of oligonucleotides one and two generates five-prime over-hangs compatible with BsaI restriction digest. Directional ligation of hybridised oligonucleotides into BsaI digested DR274 plasmid, permits the specific *cyp11c1* target sequence to be inserted in the correct position within the guide RNA.

The hybridised oligonucleotides and digested DR274 were ligated together to generate the guide RNA template. Seven microlitres of hybridised oligonucleotides and 50 ng of digested DR274 were combined in a 10 µL reaction with 1x of T4 DNA ligase buffer and 1 µL of T4 DNA ligase. The reactions were incubated for 30 minutes at room temperature. Following this, 5 µL was used to transform 50 µL of Gold efficiency DH5α competent *E. coli* as per the standard protocol. Transformations were plated on 50 µg/mL kanamycin plates and incubated over night at 37 °C. The following day, two individual bacterial colonies were grown for plasmid purification. Each plasmid was screened for the inclusion of the specific oligonucleotides by sequencing with M13 forward primer (Table 2.1).

### **6.2.7 Genotyping by high resolution melting curve (HRM) analysis**

High resolution melting curve (HRM) analysis was employed for the detection of genetic disruption. This method was previously optimised for detection of indels generated by TALENs (Chapter 5.0). HRM was performed using a single set of primers designed around the Cas9 cut site. For each guide RNA targeting *cyp11c1*, unique primers were used to detect indels (Table 6.5). Specifically, for both guide RNA1 and guide RNA2, primers amplified an 84 nucleotide fragment

of *cyp11c1* for HRM analysis. HRM analysis was performed using 7900HT Fast Real-Time PCR system using parameters previously described.

**Table 6.5 Sequences of the primers used for genotyping PCR for *cyp11c1* indels by high resolution melting curve analysis**

<i>RNA</i>	<i>Primer</i>	<i>Sequence (5-prime to 3-prime)</i>
<b>gRNA1</b>	HRM1 F	GCCGTGCCGCTGCAATTTCG
	HRM1 R	TGACGACAGAACCTGCGCG
<b>gRNA2</b>	HRM2 F	GCGCAGGTTCTGTTCGTCA
	HRM2 R	GATGGTCCCCTTCAGCAGC

### **6.2.8 *In vitro* mRNA synthesis of *cyp11c1* guide RNAs**

Prior to *in vitro* RNA synthesis, the *cyp11c1* guide plasmids were linearised by DraI restriction enzyme. After purification, transcription of the guide RNA was performed using a MEGA shortscript Kit (Life Technologies) according the manufactures instructions. Specifically, 100 nM of template plasmid was combined in a 20 µL reaction with 1x Buffer and 7.5 mM of ATP, GTP, CTP and UTP each. Reactions were incubated for three hours at 37 °C. One microlitre of TURBO DNase was added to the reaction and incubated for 15 minutes to remove the DNA template.

Due to the small size of the guide RNA, it was purified using phenol chloroform liquid-liquid extraction, rather than the standard RNA column purification. Specifically, 115 µL of DEPC water was added to the RNA with 15 µL of 3 M sodium acetate and mixed. Next, 150 µL of phenol/chloroform was added and followed by an equal volume a chloroform. The top aqueous

phase containing the RNA was transferred to a new tube. RNA was precipitated by adding two volumes of cold 100 % ethanol and mixing. After incubation for one hour at -20 °C, RNA was pelleted by centrifugation for 15 minutes at 13 000 rpm at 4 °C. The supernatant was removed and the pellet was allowed to air dry. Resuspension in 80 µL of DEPC water typically resulted in concentration of 2 µg/µL. One microlitre of guide was run on a 3 % agarose gel to confirm the quality of the RNA.

### **6.2.9 Generation of Cas9 mRNA**

The plasmid to generate *cas9* mRNA (MLM3613) was linearised by PmeI restriction enzyme and purified. The mRNA was synthesised *in vitro* using a T7 polymerase mMessage mMachine kit and purified using the GenElute Mammalian Total RNA Miniprep Kit, as previously described. *cas9* RNA was aliquoted and stored at -80 °C until required.

### **6.2.10 Microinjection of CRISPR/Cas9 for genome editing**

Microinjection into the single cell embryo is the most effective way to transmit the *cas9* mRNA and the *cyp11c1* guide RNA into the developing embryo. Ten microlitre microinjection mixes were made in DEPC water with 0.05 % phenol red and 2 µL rhodamine dextran. For initial injections a titration of the guide RNA was performed using 10 pg, 20 pg and 50 pg of RNA per embryo with 50 pg per embryo of *cas9* mRNA. After microinjection, the *cas9* mRNA will be translated by the endogenous translational machinery to produce the Cas9 nuclease protein.

## 6.3 Results

### 6.3.1 Phylogenetic analysis

Alignment of teleost Cyp11b-like proteins, the single mouse Cyp11b protein and human the CYP11B1 and CYP11B2 protein sequences was performed *in silico* to elucidate the evolution and conserved functional domains of the zebrafish Cyp11c1 enzyme. Evolutionary analysis revealed that teleost Cyp11c1 enzymes grouped together on their own clade distinct from other mammals (Figure 6.3).

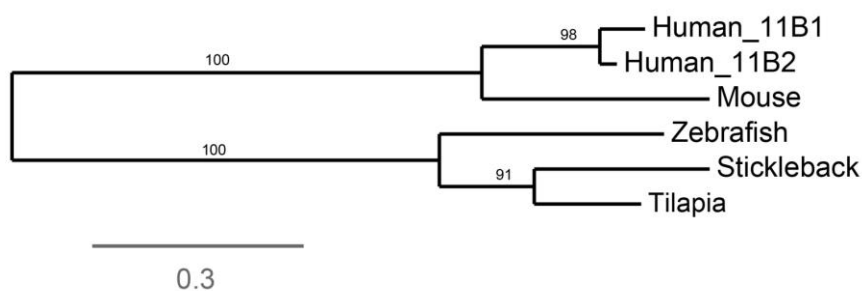


**Figure 6.3 Evolution of Cyp11b-like proteins**

Maximum likelihood phylogenetic analyses of vertebrate Cyp11b-like protein sequences were conducted using the PhyML software under the SH-like likelihood-ratio test parameters. Scaled phylogenetic tree was drawn with TreeDyn software. Branch support values are represented in %. Human CYP11B1 and CYP11B2 are represented as 11B1 and 11B2, respectively.

The zebrafish Cyp11c1 protein showed typical cytochrome P450 functional domains, including the redox-interaction domain, oxygen-binding and the ExxR motif (Kusakabe et al., 2002, Wang and Orban, 2007). In comparison to the human orthologues, zebrafish shares the highest protein identity with CYP11B2 (42 %); which is required for mineralocorticoid production in humans. Protein sequence alignment showed conservation of amino acids in teleost Cyp11c1 sequences that are functionally important for CYP11B2 activity. Additionally, zebrafish Cyp11c1 had 67 % identity with tilapia and shared a long five-prime signalling peptide, which was well conserved between the two species (Figure 6.4).





### 6.3.2 Characterisation of *cyp11c1* expression

The expression of the *cyp11c1* was investigated during early zebrafish development and in adult zebrafish tissues (Figure 6.5). *cyp11c1* showed low levels of expression from zygote to segmentation periods (from one-cell stage up to 22-24 hpf). From 28 hpf expression became more prominent and was maintained to 120 hpf. In adults, expression was detected in all tissues tested with the predominant being the testis and the kidney head. No sexual dimorphism in the expression pattern was observed.

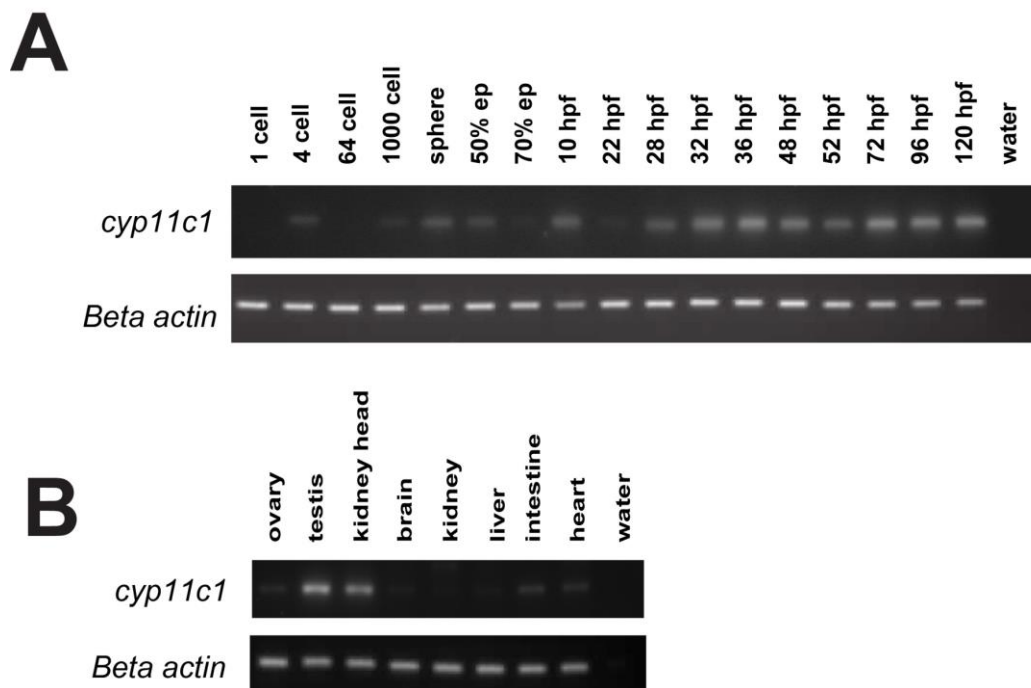


**Figure 6.5** Spatial and temporal expression of zebrafish *cyp11c1* transcripts

Expression of *cyp11c1* was characterised in zebrafish embryos and larvae (**A**) and in adult tissues (**B**). Beta actin was used as a loading control.

### **6.3.3 *Cyp11c1 functional in vitro assays***

To determine the functional activity of the zebrafish Cyp11c1 protein in comparison to human orthologues, catalytic conversion assays were performed using 11-deoxycortisol as the substrate. Initially, experiments were performed using cDNA encoding a 628 amino acid protein as annotated on the ENSEMBL genome browser (ENSDART00000061572). Functional activity showed the transcripts initiating from this start site (Met 1) had 1.2 % of enzymatic activity compared to human wild-type CYP11B1 (Figure 6.6).

Sequence homology with human CYP11B orthologues and other previous reports (Wang and Orban, 2007), predict a shorter Cyp11c1 protein which lacks amino acids at the amino terminus. Therefore, three other in-frame start methionine residues (Met 2, Met 3 or Met 4) were evaluated. Firstly, *in silico* KOZAK sequence analysis was performed to determine possible translation initiation sites. Met 1 and Met 4 were predicted to have strong KOZAK consensus sequences (cxxATGG and AxxATGt) with a reliability of 75% and 30 %, respectively. Further analysis using five-prime cap analysis gene expression (CAGE) data both Met 1 and Met 4 were shown to produce transcripts (*personal communication*). The three additional *cyp11c1* sequences with different start methionine amino acids were cloned and predicted to encode pre-proteins of 592, 565 or 518 amino acids. Catalytic activity using 11-deoxycortisol as the substrate revealed the three additional Cyp11c1 proteins all had similar functional activity compared to human CYP11B1. Specifically, Cyp11c1 Met 2, Met 3 and Met 4 proteins had 116 %, 139 % and 129 % activity of the human homologue, respectively (Figure 6.6).

**A**

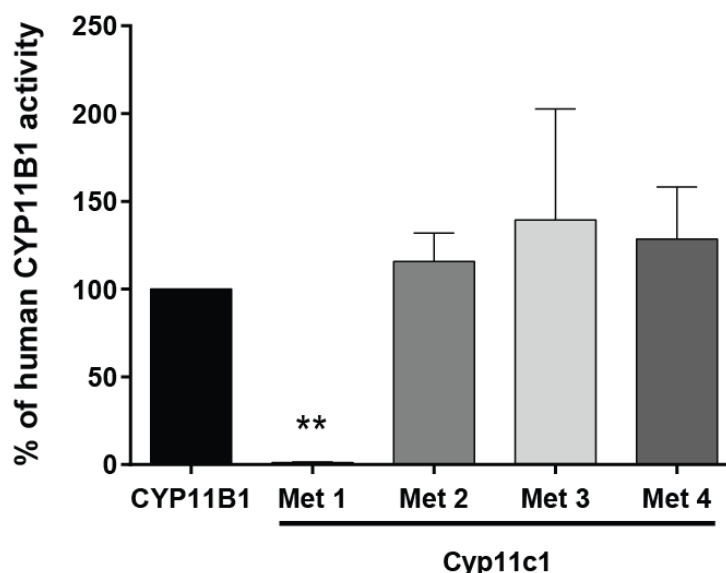
```

CYP11B2 -----
CYP11B1 -----
Cyp11c1 MRAHFRRKYQLSQNAKDSAQLRVGGKVFLSGDLARVRPDAPEKDDGFNLIRAFQGLKF 60
          Met 1                               Met 2

CYP11B2 -----
CYP11B1 -----
Cyp11c1 SGFMFTGSKHSRADKTTNEEPCRVIRRTDAQDTLLFSSSQCSVCEISIGSMFSSCAGSVC 120
          Met 3                               Met 4: : *

CYP11B2 AAPWLSLQARALG--TRAARAPRTVLPFEAMPQHPGNRWLRLQIWREQGYEHLHLEMH 69
CYP11B1 AVPWLSLQRAQALG--TRAARVPRTVLPFEAMPRRPGNRWLRLQIWREQGYEDLHLEVH 69
Cyp11c1 ARPHLCVRASVCVRPLHQSSRSAGAARLFQEIPDTGSNGWMNLLRFWRDGRFSRMHKHME 180
* * * . : : . : : : * . . . * : : * . * * . : : * : : . : * . .

```

**B**

**Figure 6.6 Catalytic conversion of 11-deoxycortisol to cortisol by Cyp11c1**

**(A)** Comparison of the zebrafish Cyp11c1 with human CYP11B1 and CYP11B2 revealed a longer amino terminal sequence. Four full-length zebrafish *cyp11c1* sequences were cloned using a different methionine start amino acid (termed Met 1, Met 2, Met 3 or Met 4). **(B)** COS7 cells were transfected with human *CYP11B1* or zebrafish *Cyp11c1* with different start sites (Met 1, Met 2, Met 3 or Met 4). Cells were then incubated with 11-deoxycortisol for conversion to cortisol. Zebrafish Cyp11c1 Met 1 had 1.2 % ( $\pm$  0.34) activity compared to human CYP11B1. While zebrafish Cyp11c1 Met 2, Met 3 or Met 4 had 115.8 % ( $\pm$  16.20), 139.4 % ( $\pm$  63.24) and 128.5 % ( $\pm$  29.67) activity of the human paralogue, respectively. Experiments were performed in triplicate-triplicate and the mean  $\pm$  SD is shown for each protein. Statistical significance was determined by ANOVA following Dunnett's multiple comparisons test  $**p < 0.01$ .

### **6.3.4 Generating *cyp11c1* null alleles using CRISPR/Cas9**

#### **6.3.4.a. Strategic design of guide RNAs**

To generate Cyp11c1 loss-of-function alleles, the CRISPR/Cas9 system was used. The Cyp11c1 CRISPR guide RNAs were designed using the ZiFiT Targeter software (URL: <http://zifit.partners.org>), which is a web tool that identifies guide RNA target sites within a particular sequence, while recognising potential off-target sites in the specified organism (Sander et al., 2010, Sander et al., 2007). The output lists possible CRISPR guides in order of their quality score ranging from 0 to 100 %, which indicates the on-target activity of each guide. Exon 10 of zebrafish *cyp11c1* was used to identify potential guides. Two guides were synthesised and tested. The first guide RNA (gRNA 1) gave a quality score of 92 %, and was predicted to have 24 off-targets sites in zebrafish; four of which were located in genes. The second guide (gRNA 2) had a quality score of 66 % and was estimated to have 135 off-target binding sites; 35 of which were contained in exons. Neither gRNA 1, nor gRNA 2 were predicted to non-specifically bind genes located on chromosome 16 where *cyp11c1* is located; thus allowing for potential off-target effects to be outbred.

#### **6.3.4.b. Construction and synthesis of short guide RNAs**

Two guide RNAs targeting *cyp11c1* were constructed by hybridisation of specific oligonucleotides and ligated into DR274 plasmid. The DR274 plasmid contains additional sequence which directs the Cas9 protein to the specific chromosomal locus. Each guide RNA was co-injected with mRNA transcribing Cas9 protein. Initial microinjections were performed with 10, 20 and 50 pg of guide RNA with 50 pg of *cas9* mRNA. Embryos were monitored for RNA toxicity, abnormal development and screened by HRM for indels. RNA toxicity was observed at 50 pg of guide RNA with 80 % of embryos showing abnormal development. At 72 hpf, 36 larvae from each

injection pool were screened for indels using HRM analysis. No indels were detected from gRNA 1 at any concentration. The second guide, gRNA 2, produced changes in the melting curve indicative of indels at all concentration tested, ranging from 50 % of 10 pg injected larvae to 85 % of 50 pg injected larvae (Figure 6.7). Embryos injected with 10 pg of gRNA 2 were raised for further screening.

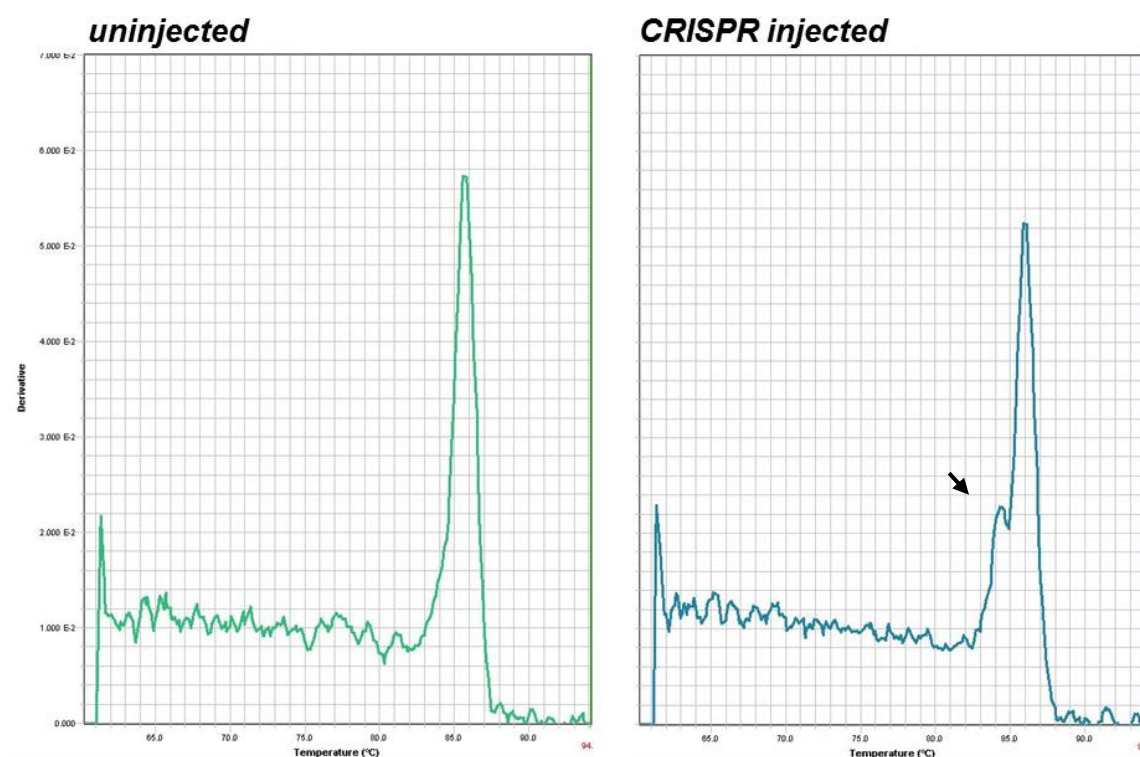


**Figure 6.7 HRM analysis of larva injected with *cyp11c1* targeting guide RNA 2**

A high resolution melting (HRM) curve obtained from a *cyp11c1* fragment amplified from genomic DNA extracted from a larva injected with guide RNA 2 (gRNA 2) and *cas9* mRNA. An 84 base-pair fragment of *cyp11c1* was amplified with SybrGreen and subjected to dissociation curve analysis. In uninjected embryos a single peak was observed indicating amplification of a single product. In gRNA 2/*cas9* injected embryos, two peaks were observed; one corresponding to the wild-type product and a second smaller product due to the generation of indels (arrow). The presence of two peaks suggests disruption of the wild-type allele.

### 6.3.5 Optimisation of androgen detection by LC-MS/MS

By using the core LC-MS/MS facility at the Centre for Endocrinology, Diabetes and Metabolism at the University of Birmingham a method was confirmed for the simultaneous detection of androgens. Initially, individual androgens were analysed to determine chromatographic peaks and analysed using the TargetLynx software. An androgen mixture containing androstenedione, testosterone, 11 $\beta$ -hydroxyandrostenedione, 11-ketoandrostenedione, 11-ketotestosterone, 11 $\beta$ -hydroxytestosterone, dihydrotestosterone and 5 $\alpha$ -androstenedione was then run to determine if individual analytes could be resolved. Chromatographic peaks for each analyte were resolved in a short LC-MS/MS method of less than three minutes (Figure 6.8).

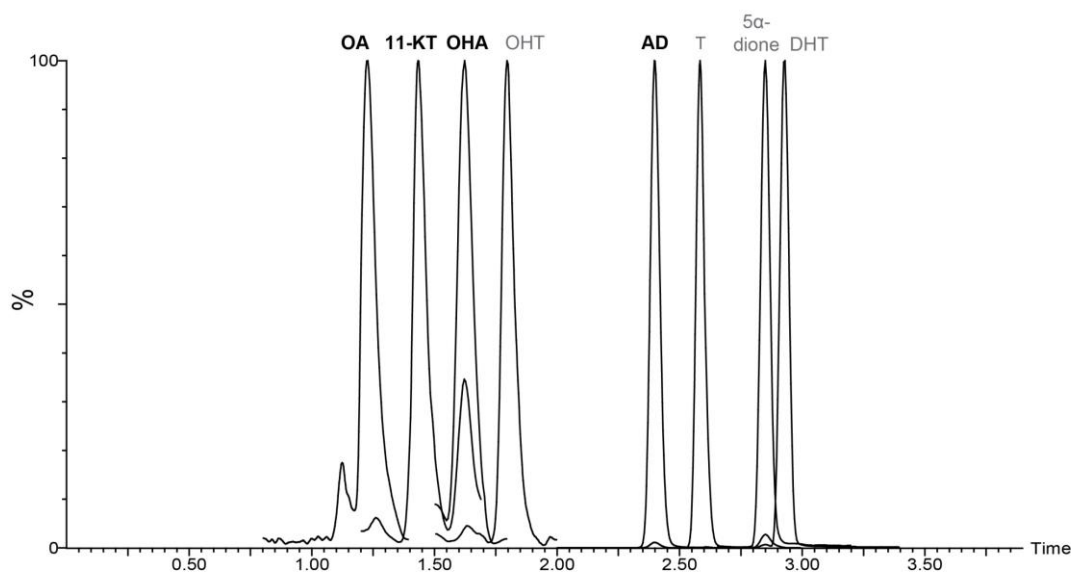


**Figure 6.8 Chromatogram showing optimise solution of the zebrafish androgens**

A LC-MS/MS method was developed to identify androgens androstenedione (OA), 11 $\beta$ -hydroxyandrostenedione (OHA), 11-ketoandrostenedione (OA), 11-ketotestosterone (11-KT), testosterone (T), 11 $\beta$ -hydroxytestosterone (OHT), dihydrotestosterone (DHT) and 5 $\alpha$ -androstenedione (5 $\alpha$ -dione). The main metabolites involved in zebrafish androgen production are shown in black.

## 6.4 Discussion and prospective studies

Our previous work exploring zebrafish as a model for steroidogenic physiology and disease has highlighted the importance of meticulous characterisation of the system before further exploring more complex physiological questions (Parajes et al., 2013). Therefore, this study aimed to comprehensively characterise the zebrafish CYP11B isozyme, Cyp11c1, and establish methods to assess its function *in vivo* and *in vitro*.

### 6.4.1 Zebrafish Cyp11c1 shares homology with human aldosterone synthase

The classical 11 $\beta$ -hydroxylase enzyme in humans, CYP11B1, hydroxylates 11-deoxycortisol to produce cortisol, as well as deoxycorticosterone to corticosterone. The production of mineralocorticoids requires the additional 18-hydroxylase and 18-oxidase activities of aldosterone synthase (CYP11B2) to generate aldosterone from corticosterone. Like most teleosts, zebrafish have a single *cyp11b-like* homologue, termed *cyp11c1*. Protein alignment with teleost Cyp11c1 and the human orthologues, CYP11B1 and CYP11B2, showed Cyp11c1 shares most protein identity with CYP11B2. Human CYP11B1 and CYP11B2 share 95 % identity (Kawamoto et al., 1990), however, specific amino acids are required for their catalytic activities. Mutation of Leu301, Glu302 and Ala320 in human CYP11B2 to the corresponding amino acids of CYP11B1 (Pro301, Asp302 and Val320, respectively), increases the 11 $\beta$ -hydroxylase activity of CYP11B2. Subsequently, this increases cortisol production from 5 % to 85 % (Bottner et al., 1998). Additionally, these substitutions impair aldosterone synthesis by up to 13 % of wild-type CYP11B2, thus indicating these amino acids are important for efficient cortisol production. The amino acid alignment reveals zebrafish Cyp11c1 shares homology with human CYP11B2 at these functional specifying amino acid positions. Although the critical amino acids for aldosterone

synthesis are conserved in Cyp11c1, it is generally accepted that teleost lack the ability to synthesise mineralocorticoids, and that the primary function of this protein is 11 $\beta$ -hydroxylase activity.

Even within mammals there are significant differences in Cyp11b enzymes. It is hypothesised that *Cyp11b2* is the ancestral gene which is capable of synthesising mineralocorticoids and glucocorticoids. However, within the mammalian lineage *Cyp11b* has undergone one or more duplication events leading to diverse functions (Colombo et al., 2006). A single bovine enzyme was identified which catalyses 11-deoxycortisol to cortisol and all three steps required to convert deoxycorticosterone to aldosterone (Ogishima et al., 1989, Sato et al., 1978). Conversely, rats (but not mice) have three *Cyp11b-like* functional genes (Mellon et al., 1995). Neither the crystal structure for CYP11B1 or CYP11B2 has been deduced, making structural-functional correlations difficult. Out sequence homology analysis of the zebrafish Cyp11c1 was not sufficient to understand the functional capabilities of this enzyme; therefore, functional *in vitro* assays were performed.

#### **6.4.2 Functional characterisation of predicated Cyp11c1 proteins**

Protein sequence alignment of the annotated Cyp11c1 revealed a long amino terminus in comparison to the human CYP11B sequences. This region of the protein contains the mitochondrial signalling peptide which is cleaved once the protein is imported into the mitochondria. Although this sequence is conserved with other teleosts, other studies based on homology analysis suggest that M111 (Met 4) of the annotated sequence is the start methionine (Wang and Orban, 2007). *In silico* analysis of the amino terminal nucleotide sequence identified KOZAK consensus sites to initiate transcription at Met 1 and Met 4. Furthermore, analysis of

five-prime CAGE tags also supported transcription from Met 1 and Met 4, suggesting *cyp11c1* has at least two alternative start sites.

We tested the functional capabilities of all four proteins in comparison to the human orthologue CYP11B1. In assessing their ability to convert 11-deoxycortisol to cortisol Met 1 showed 1 % conversion activity compared to human. This suggests the additional amino terminus residues of the 628 amino acid protein transcribed from Met 1 renders targeting sequence non-functional. The stability of different Cyp11c1 products will be assessed by Western blot using carboxyl terminal V5 tags. Additionally, by tagging a fluorescent protein with the different amino terminal mitochondrial import sequences, we can visualise the effectiveness of directing proteins to the mitochondria. *In vivo* functional studies suggest blocking translation from the annotated methionine (Met 1) by morpholino inhibits *de novo* glucocorticoid production in zebrafish (Wilson et al., 2013), and suggests the 628 amino acid protein is capable of glucocorticoid production.

The three shorter Cyp11c1 proteins exhibited catalytic activities equivalent to human CYP11B1. Despite Cyp11c1 having conserved amino acids which are predicted to promote aldosterone synthesis rather than glucocorticoid production, this enzyme is capable of producing cortisol *in vitro*. As it has retained its 11 $\beta$ -hydroxylase activity, it would be anticipated it could also generate corticosterone from deoxycorticosterone. However, further *in vitro* studies are required to determine the mineralocorticoid producing capabilities of this enzyme. Taken together the homology alignments, KOZAC consensus identification and *in vitro* data, it is suggested that Met 4 of Cyp11c1 encodes a functional 518 amino acid protein which allows for Cyp11c1 to enter the mitochondria for glucocorticoid synthesis.

### **6.4.3 *Spatial and temporal expression of cyp11c1 is consistent with its functional activities***

Characterisation of the spatial and temporal expression of Cyp11c1 is required when employing zebrafish as a model for biological processes and human disease. Expression of *cyp11c1* was detected from early stages of development and it was up-regulated between 24 and 28 hpf. This coincides with the expression of other steroidogenic genes including *cyp11a2* (Parajes et al., 2013). This result is consistent with previous reported microarray studies and reflects its role in *de novo* glucocorticoid production during larva development (Alsop and Vijayan, 2009). Although expression of *cyp11c1* was detected in all adult tissues tested, its highest expression was observed in the kidney head and testis. This expression reflects the role of Cyp11c1 in glucocorticoid and possible mineralocorticoid production in the interrenal and androgen synthesis in the testis of adults.

### **6.4.4 *Generating cyp11c1 null zebrafish line by CRISPR/Cas9***

#### **6.4.4.a. *Implementation of the CRISPR/Cas9 system for genomic engineering***

Recently, Hwang et al. (2013b) published the first report of successful implementation of the CRISPR/Cas9 system zebrafish. The co-injection of *in vitro* transcribed guide RNA and *cas9* mRNA into one-cell stage embryos led to targeted chromosomal breaks and sequence indels. Additionally, transmission rates of indels ranged from 42 to 100 % (Hwang et al., 2013a, Hwang et al., 2013b); establishing it as the most efficient genome editing method to date. Due to the recent developments in creating targeted genomic modifications in zebrafish, this study aimed to generate *cyp11c1* loss-of-function alleles by implementing the CRISPR/Cas9 system.

In comparison to TALENs, CRISPR guide RNAs are considerably easier and quicker to generate. Unlike Zinc Finger Nucleases and TALENS which preceded this method, the CRISPR/Cas9 system relies on RNA rather than proteins to recognise genomic DNA. The efficiency to generate somatic mutations in zebrafish with the CRISPR/Cas9 system is, on average, 30 %; which is comparable to TALENs (Blackburn et al., 2013). Higher indel frequencies have been reported with injection of Cas9 protein rather than mRNA (Gagnon et al., 2014), suggesting higher rates of genetic disruptions could be achieved in the future. Furthermore, a unique advantage of the CRISPR/Cas9 system is the ability to target multiple genomic loci at once. Jao et al. (2013), simultaneously targeted five loci in zebrafish embryos, eliminating the need for complicated breeding strategies to make multiple changes, and highlighting the power of this new method.

One current limitation of the CRISPR/Cas9 systems is the uncertainty of Cas9 to induce off-target cleavage events and subsequent production of unwanted indels. Several studies investigating the specificity of Cas9 have found it variable and difficult to predict the off-target cleavage events with a given guide RNA sequence (Cho et al., 2014, Fu et al., 2013, Hsu et al., 2013, Pattanayak et al., 2013a). Variants of the Cas9 protein (Shen et al., 2014), length of the guide RNA (Fu et al., 2014) and modification of the guide RNA architecture (Hsu et al., 2013) have all been used to increase the effectiveness and specificity of the CRISPR/Cas9 system. Due to the infancy of this technology, optimisation of the method is still a current topic in establishing it as a routine biotechnology tool.

#### **6.4.4.b. The genetic disruption of *cyp11c1***

For further investigation into the role of Cyp11c1 in zebrafish and to compare to previously described morpholino studies (Wilson et al., 2013) we generated a *cyp11c1* disrupted allele. The

CRISPR guide RNAs were targeted to exon 10, which contains the conserved CYP ExxR motif and predicted amino acids involved in redox partner interaction. Two separate guide RNAs targeting *cyp11c1* were trialled. The first guide (gRNA 1) was unsuccessful in generating indels in embryos when analysed by HRM. However, up to 85 % of embryos microinjected with the second guide (gRNA 2) showed disrupted melting curves by HRM analysis. At the time of this manuscript preparation the CRISPR/Cas9 injected zebrafish were being raised to adults. Upon reaching sexual maturity, adults capable of transmitting indels to offspring will be determined. Furthermore, lines harbouring heterozygous alleles from the second generation will be established for future experiments.

#### ***6.4.5 Development of LC-MS/MS methodology to identify zebrafish androgens***

Other than cortisol production, Cyp11c1 is also required for the biosynthesis of zebrafish androgens. Generally, steroid quantification in fish relies on enzyme immunoassays which can lack specificity and sensitivity. In collaboration with Dr. Angela Taylor and the core LC-MS/MS facility at the Centre for Endocrinology, Diabetes and Metabolism at the University of Birmingham, we were able to detect simultaneously zebrafish androgens from a purified mixture. The main products from zebrafish testis are 11 $\beta$ -hydroxyandrostenedione, 11-ketoandrostenedione, and 11-ketotestosterone (de Waal et al., 2008) and a corresponding peaks of each analyte were clearly resolved with our method. Future work will involve optimisation of the extraction of androgens from zebrafish embryos and larvae to determine concentrations of androgens during development and in adult tissues. This will give further insight into the role of androgens during development and in specific tissues, and also provide a biochemical analysis of future studies of zebrafish steroidogenic genes.

A quantitative method for these specific androgens is not limited to zebrafish studies. In humans,  $11\beta$ -hydroxyandrostenedione and  $11\beta$ -hydroxytestosterone are synthesised in the adrenals. Interestingly,  $11\beta$ -hydroxyandrostenedione is the second most abundant androgen in the adrenal vein of women but, its physiological functions remain unknown (Bloem et al., 2013). Both  $11\beta$ -hydroxyandrostenedione and  $11\beta$ -hydroxytestosterone can be generated from the CYP11B isoforms, suggesting that CYP11B1 and CYP11B2 have a role in adrenal derived androgens (Swart et al., 2013). Furthermore, the hydroxyl- and keto-metabolites of androstenedione and testosterone are capable of androgen receptor activation in humans (Yazawa et al 2008) and is proposed to have physiological consequences in castration resistant prostate cancer (Bloem et al., 2013).

#### **6.4.6 Summary**

CYP11B orthologues have been well conserved during the evolution of vertebrates, including within the teleost lineage. Therefore, the characterisation of this family of enzymes from lower species will help in understanding the evolution and divergence of this family. The zebrafish enzyme, Cyp11c1, is capable of synthesising cortisol (Wilson et al., 2013) and thus provides a promising and genetically amenable model system to study conserved endocrine mechanisms, including the mitochondrial redox regulation of steroidogenesis.

The CYP11B family of proteins are mitochondrial CYP enzymes and therefore rely on electron transfer from ferredoxin for catalytic activity. Our previous studies show the zebrafish ferredoxin, Fdx1b, is required for cortisol production during zebrafish development (Chapter 3.0). It was postulated that through its electron transfer interaction with Cyp11c1, Fdx1b can influence glucocorticoid and androgen production in zebrafish. For further investigation several methods to characterise the role of Cyp11c1 during zebrafish development were developed.

These included *in vitro* assays to investigate functional activity, LC-MS/MS method to simultaneously detect the main zebrafish androgens and implementation of the CRISPR/Cas9 system to generate a *cyp11c1* knockout line. Overall, the detailed characterisation of Cyp11c1 and the implementation novel methods will provide insight into the regulation of glucocorticoid and androgen production in zebrafish.

# ***Chapter Seven***

---

## ***General discussion and prospective studies***

## 7.0 GENERAL DISCUSSION AND PROSPECTIVE STUDIES

### 7.1 Characterising steroidogenic enzymes in zebrafish

Basic biomedical research relies on the study of systems which have similar physiological characteristics to humans. Traditionally, this has led to mammals, particularly rodents, being the most widely used models in medical research. Since first being pioneered as a model organism by George Streisinger (Streisinger et al., 1981), zebrafish have become a popular resource for developmental and molecular biologists. In recent years, zebrafish have become increasingly used for exploring human diseases and have extended their utility into translational research, cancer, toxicology and drug discovery (Ablain and Zon, 2013). Zebrafish represent an important model to provide significant insights into the conserved role of steroid hormones during early development, with implications in stress research, ageing and the pathophysiology of common diseases.

This project aimed to establish zebrafish as an *in vivo* model for endocrine development and steroidogenic disorders. This required comprehensive characterisation of zebrafish steroidogenic genes. A detail review of the literature identified discrepancies in the expression and functional characterisation of the zebrafish side-chain cleavage paralogue, *cyp11a1*. In **chapter three** we redefined the initiation and maintenance of interrenal steroid hormone production, through characterisation of the *cyp11a2* paralogue. Temporal expression of each zebrafish *cyp11a* gene was paralogue specific; with only *cyp11a2* being expressed after the interrenal had formed. Through the development of a LC-MS/MS method to quantify cortisol and pregnenolone from whole zebrafish embryos and larvae extracts, we were able to identify that the Cyp11a isozymes have similar enzymatic functions; that is, they are both required for pregnenolone synthesis. Overall, our data revised previous findings and identified *cyp11a2* as the functional equivalent of human

*CYP11A1*, as it is required for *de novo* steroidogenesis in zebrafish larvae. Additionally, this data highlighted the need for meticulous characterisation of the steroidogenic pathway prior to employing zebrafish as model in translational research of adrenal disease.

In **chapter six** the work in characterising the 11 $\beta$ -hydroxylase homologue, *cyp11c1*, was highlighted. Through *in silico* analysis and homology alignments I identified two alternative start sites for *cyp11c1*. Further *in vitro* functional analysis revealed only the shorter transcript had equivalent 11 $\beta$ -hydroxylase activity compared to human. The functional characterisation of zebrafish *cyp11c1* is still in its infancy. By testing *in vitro* Cyp11c1's conversion of androstenedione, testosterone and deoxycorticosterone, further information about the functional characteristics of this enzyme with regards to androgen and mineralocorticoid production will be revealed. To date, human CYP11B1 and CYP11B2 proteins have not been crystallised, therefore, the study and comparison with the zebrafish Cyp11c1 will provide insight into functional amino acids required for specific catalytic activity.

## 7.2 The study of mitochondria redox reactions *in vivo*

Previous *in vitro* studies established FDX1 can influence steroid hormone production through regulating CYP enzymatic activity. Since the relevance of *in vitro* findings is constantly being questioned, the need for *in vivo* model systems is often required (Langheinrich, 2003). This study aimed to develop zebrafish as an *in vivo* model to investigate mitochondrial redox reactions. This would provide insight into the influence of redox reactions on mitochondrial steroidogenic CYP enzymes and determine the consequences within a whole organism. During initial characterisation of the mitochondrial steroidogenesis redox pathway, two *Fdx1* zebrafish paralogues were identified. **Chapter three** details the protein sequence comparison, spatial and

temporal expression and relevance of their functional roles during zebrafish development. Upon observation that *fdx1b* expression reflects that of the zebrafish side-chain cleavage paralogue, *cyp11a2*, it was hypothesised Fdx1b has a functional role in steroid hormone production. Functional characterisation through antisense morpholino knockdown coupled with steroid analysis by LC-MS/MS showed Fdx1b is the ferredoxin required for cortisol production in larvae.

It remains to be further elucidated as to why zebrafish Fdx1 cannot compensate for the loss of Fdx1b. We hypothesise that zebrafish Fdx1b specifically interact with steroidogenic CYP enzymes while Fdx1 is required for other processes such as bile acid synthesis and vitamin D metabolism (via *Cyp24A1* and *Cyp27A* homologues) (Goldstone et al., 2010). Ferredoxin genes have bacterial origins and are well conserved through evolution; to such an extent there are several examples where bacterial CYPs can accept electrons from mammalian FDX1 (Ewen et al., 2012). Through collaboration with Professor Rita Bernhardt (Institute of Biochemistry, University of the Saarland, Germany) the interaction affinities and the electron transfer rates between each zebrafish ferredoxin and the mitochondrial CYP enzymes are currently being explored. This will provide an understanding of the mitochondrial redox regulation in zebrafish, and will also give additional insight about the specific regulation of individual CYP enzymes by their redox partners.

## 7.3 Establishing zebrafish as a model for endocrine disease and development

### 7.3.1 *Genome engineering in zebrafish*

Traditional molecular biology involves the study of genes outside the context of the genome. However, recent genomic engineering methodologies allow direct editing or modulation of the DNA sequence in their endogenous context. This has created an exciting new era in biological research which is capable of transforming basic biology, biotechnology and medical fields. There is little doubt that the recent advances in genome editing methods, such as TALENs and the CRISPR/Cas9 system will have profound consequences for disease treatments.

One of the major limitations for loss-of-function studies in zebrafish was the lack of targeted genome editing tools. Traditionally, the laboratory mouse is the most widely used *in vivo* model system primarily due to the ease of genetic manipulation of the embryonic stem-cells (Schartl, 2014). Now, with the development of the TALEN and CRISPR/Cas9 strategies it is the first time specific gene targeting can be achieved in zebrafish (Grunwald, 2013). Therefore, to develop zebrafish as a tool to investigate endocrine development and disease, several knockout lines were generated using these methods. **Chapter five** details the methodology undertaken to establish, troubleshoot and optimise the successful implantation of TALENs in zebrafish. Soon after the successful use of TALENs was first published in zebrafish (Cermak et al., 2011, Huang et al., 2011), I began generating TALENs to target *fdx1b* and *cyp11a2* using a commercially available assembly kit. As the field of genomic editing by TALENs developed, optimised strategies for design and indel detection became apparent and proved critical for our studies. The initial TALENs were unsuccessful in generating indels in *fdx1b* and *cyp11a2*. Nevertheless, incorporation of optimised methodologies allowed for successful generation of genomic lesions in both genes.

Although, the *cyp11a2* knockout zebrafish still require confirmation of germ-line indels, several different *fdx1b* knockout lines have already been established. These, *fdx1b* lines await further characterisation. Based on expression patterns of the zebrafish ferredoxin genes and the loss of cortisol observed in *fdx1b* morphants, it was hypothesised zebrafish Fdx1b specifically interacts with steroidogenic CYP enzymes. Therefore, by using TALENs I have generated a unique steroidogenic mitochondrial redox pathway specific knockout. This is in contrast to traditional tissue or global knockout models and allows for the first time the ability to investigate the role of redox regulation on steroidogenesis *in vivo*, without disruption of early zebrafish development or other mitochondrial redox regulated processes.

**Chapter six** describes the successful implementation of the CRISPR/Cas9 system in zebrafish to genetically disrupt the *cyp11c1* coding sequence. Similar to *cyp11a2*, the *cyp11c1* knockout line requires confirmation of germ-line indels. Once individual knockout lines are established we will be able to compare and contrast the physiological impact of *cyp11a2*, *cyp11c1* and *fdx1b* deficiencies and the effects on adrenal insufficiency.

Due to its simplicity of assembly and efficiency of inducing chromosomal lesions, the CRISPR/Cas9 system has taken over TALENs as the technique of choice for genome editing. However, both TALENs and CRISPRs all have unique advantages and limitations which need to be considered in the application and interpretation of genome engineering studies. From a practical standpoint, CRISPRs are easier to implement than TALENs. TALENs must be constructed individually through timely assembly of the individual modules. In comparison, CRISPRs require the exchange of 20 nucleotide sequence of the guide RNA. This can be simply ordered as a pair of oligonucleotides. The CRISPR/Cas9 system is suggested to be more effective in targeting the genome in comparison to other methods, however, such comparisons requires

systematic analysis and will only be truly reflective as these methods become optimised. One major concern in the field is the generation of off-target mutations within the cell causing unwarranted genomic disruption. Despite efforts to predict and identify the off target effects of these systems, no conclusive guidelines have been established. Further characterisation of our knockout lines and out-breeding for several more generations will insure off-target effects are mitigated.

### **7.3.2      *Development of zebrafish whole system steroid assays***

Traditionally, immunoassays have been used for the quantification of plasma steroid hormones in adult teleost fish or from whole embryo/larva extracts. However, one limitation of steroid hormone immunoassays is cross-reactivity with structurally related compounds (Krasowski et al., 2014). LC-MS/MS is an alternative method of steroid hormone analysis which provides improved specificity and increased sensitivity. In order to investigate the systemic effects of modified steroidogenesis in zebrafish we developed and optimised a LC-MS/MS to measure cortisol and pregnenolone from whole zebrafish embryos and larvae (Parajes et al., 2013). Using this methodology we were able to establish pregnenolone and cortisol concentrations during the first five days of zebrafish development (data not shown) as well as confirm steroid profiles of *fdx1*, *fdx1b*, *cyp11a1* and *cyp11a2* deficient embryos.

As the mitochondrial CYP enzyme Cyp11c1 is involved in androgen production, a sensitive method to measure specific androgens was required. To provide a biochemical readout for androgen synthesis, we developed a LC-MS/MS method to identify the primary androgens in zebrafish. Work is now continuing to optimise the extraction method from whole zebrafish. From other studies in our laboratory we confirmed the androgen receptor is required for early development. It would be beneficial to determine the composition of androgens during zebrafish

development; an achievement not currently available with immunoassay due to cross-reactivity between the steroids.

The use of LC-MS/MS methodology to investigate the steroid hormone profiles in zebrafish will enhance the usefulness of zebrafish as a model for endocrine development, physiology and pathophysiology. Furthermore, the ability to accurately identify steroids from whole embryo extracts will provide information about the role of hormones during development. Additionally, coupled with the genome editing techniques, zebrafish can be used to establish the systemic effects, both morphologically and biochemically of genetic alterations; an achievement not possible with *in vitro* assays.

## **7.4 The future of zebrafish in endocrine research**

Throughout this project we have established zebrafish as an *in vivo* model to study mitochondrial redox regulation of steroidogenesis. However, the usefulness of zebrafish as a model for endocrine research goes beyond their applications in developmental and molecular biology applications. Genomic engineering in zebrafish provides the ability to specifically generate precise mutations which are present in human endocrine pathologies. The engineering of clinically relevant mutations in zebrafish will provide useful advantages compared to other systems. These zebrafish could be used in studying genotype/phenotype correlations, molecular mechanisms of disease and disease pathology. Additionally, high-throughput drug screening offers the potential to identify novel therapeutic agents which can be developed as disease treatments.

The comprehensive characterisation of zebrafish steroidogenic genes, use of novel genome editing methods and the development of steroid analytical methods, have helped establish

zebrafish as a model to study the role of steroid hormone in development and disease. By focusing on mitochondrial steroidogenesis reactions, this study has provided insights into the mechanism of mitochondrial redox regulation. Importantly, this data forms the basis for future studies using zebrafish as a comprehensive *in vivo* model in translational research of adrenal diseases.

**8.0 APPENDIX**

**8.1 Appendix One: Redefining Cytochrome P450 side-chain  
cleavage activity in zebrafish**





















## 9.0 REFERENCES

- Ablain, J. and Zon, L.I. (2013) Of fish and men: using zebrafish to fight human diseases. **Trends Cell Biol**, 23: (12): 584-586.
- Alderman, S.L. and Bernier, N.J. (2009) Ontogeny of the corticotropin-releasing factor system in zebrafish. **Gen Comp Endocrinol**, 164: (1): 61-69.
- Alsop, D. and Vijayan, M.M. (2008) Development of the corticosteroid stress axis and receptor expression in zebrafish. **Am J Physiol Regul Integr Comp Physiol**, 294: (3): R711-719.
- Alsop, D. and Vijayan, M.M. (2009) Molecular programming of the corticosteroid stress axis during zebrafish development. **Comp Biochem Physiol A Mol Integr Physiol**, 153: (1): 49-54.
- Amores, A., Force, A., Yan, Y.L., et al. (1998) Zebrafish hox clusters and vertebrate genome evolution. **Science**, 282: (5394): 1711-1714.
- Arakane, F., King, S.R., Du, Y., et al. (1997) Phosphorylation of steroidogenic acute regulatory protein (StAR) modulates its steroidogenic activity. **J Biol Chem**, 272: (51): 32656-32662.
- Arlt, W. and Allolio, B. (2003) Adrenal insufficiency. **Lancet**, 361: (9372): 1881-1893.
- Auer, T.O. and Del Bene, F. (2014) CRISPR/Cas9 and TALEN-mediated knock-in approaches in zebrafish. **Methods**, 69: (2): 142-150.
- Bader, M. (2010) Tissue renin-angiotensin-aldosterone systems: Targets for pharmacological therapy. **Annu Rev Pharmacol Toxicol**, 50: 439-465.
- Bandiera, R., Vidal, V.P., Motamedi, F.J., et al. (2013) WT1 maintains adrenal-gonadal primordium identity and marks a population of AGP-like progenitors within the adrenal gland. **Dev Cell**, 27: (1): 5-18.
- Barrangou, R., Fremaux, C., Deveau, H., et al. (2007) CRISPR provides acquired resistance against viruses in prokaryotes. **Science**, 315: (5819): 1709-1712.
- Beato, M. and Klug, J. (2000) Steroid hormone receptors: an update. **Hum Reprod Update**, 6: (3): 225-236.
- Beckert, V. and Bernhardt, R. (1997) Specific aspects of electron transfer from adrenodoxin to cytochromes p450<sub>scc</sub> and p450<sub>11beta</sub>. **J Biol Chem**, 272: (8): 4883-4888.
- Bedell, V.M., Wang, Y., Campbell, J.M., et al. (2012) In vivo genome editing using a high-efficiency TALEN system. **Nature**, 491: (7422): 114-118.
- Bedell, V.M., Westcot, S.E. and Ekker, S.C. (2011) Lessons from morpholino-based screening in zebrafish. **Brief Funct Genomics**, 10: (4): 181-188.
- Belkina, N.V., Lisurek, M., Ivanov, A.S., et al. (2001) Modelling of three-dimensional structures of cytochromes P450 11B1 and 11B2. **J Inorg Biochem**, 87: (4): 197-207.
- Beratan, D.N., Betts, J.N. and Onuchic, J.N. (1992) Tunneling pathway and redox-state-dependent electronic couplings at nearly fixed distance in electron transfer proteins. **The Journal of Physical Chemistry**, 96: (7): 2852-2855.
- Bern, H.A. (1967) Hormones and endocrine glands of fishes. Studies of fish endocrinology reveal major physiologic and evolutionary problems. **Science**, 158: (3800): 455-462.
- Bibikova, M., Beumer, K., Trautman, J.K., et al. (2003) Enhancing gene targeting with designed zinc finger nucleases. **Science**, 300: (5620): 764.
- Blackburn, P.R., Campbell, J.M., Clark, K.J., et al. (2013) The CRISPR system--keeping zebrafish gene targeting fresh. **Zebrafish**, 10: (1): 116-118.
- Bloem, L.M., Storbeck, K.H., Schloms, L., et al. (2013) 11beta-hydroxyandrostenedione returns to the steroid arena: biosynthesis, metabolism and function. **Molecules**, 18: (11): 13228-13244.
- Boch, J., Scholze, H., Schornack, S., et al. (2009) Breaking the code of DNA binding specificity of TAL-type III effectors. **Science**, 326: (5959): 1509-1512.

- Bottner, B., Denner, K. and Bernhardt, R. (1998) Conferring aldosterone synthesis to human CYP11B1 by replacing key amino acid residues with CYP11B2-specific ones. **Eur J Biochem**, 252: (3): 458-466.
- Brandt, M.E. and Vickery, L.E. (1992) Expression and characterization of human mitochondrial ferredoxin reductase in *Escherichia coli*. **Arch Biochem Biophys**, 294: (2): 735-740.
- Brentano, S.T., Black, S.M., Lin, D., et al. (1992) cAMP post-transcriptionally diminishes the abundance of adrenodoxin reductase mRNA. **Proc Natl Acad Sci U S A**, 89: (9): 4099-4103.
- Bureik, M., Zollner, A., Schuster, N., et al. (2005) Phosphorylation of bovine adrenodoxin by protein kinase CK2 affects the interaction with its redox partner cytochrome P450<sub>sc</sub> (CYP11A1). **Biochemistry**, 44: (10): 3821-3830.
- Burova, T.V., Bernhardt, R. and Pfeil, W. (1995) Conformational stability of bovine holo and apo adrenodoxin--a scanning calorimetric study. **Protein Sci**, 4: (5): 909-916.
- Bury, N.R. and Sturm, A. (2007) Evolution of the corticosteroid receptor signalling pathway in fish. **Gen Comp Endocrinol**, 153: (1-3): 47-56.
- Cade, L., Reyon, D., Hwang, W.Y., et al. (2012) Highly efficient generation of heritable zebrafish gene mutations using homo- and heterodimeric TALENs. **Nucleic Acids Res**, 40: (16): 8001-8010.
- Cao, P.R. and Bernhardt, R. (1999) Modulation of aldosterone biosynthesis by adrenodoxin mutants with different electron transport efficiencies. **Eur J Biochem**, 265: (1): 152-159.
- Capecchi, M.R. (1989) Altering the genome by homologous recombination. **Science**, 244: (4910): 1288-1292.
- Cermak, T., Doyle, E.L., Christian, M., et al. (2011) Efficient design and assembly of custom TALEN and other TAL effector-based constructs for DNA targeting. **Nucleic Acids Res**, 39: (12): e82.
- Chai, C., Liu, Y.W. and Chan, W.K. (2003) Ff1b is required for the development of steroidogenic component of the zebrafish interrenal organ. **Dev Biol**, 260: (1): 226-244.
- Chandrasekar, G., Lauter, G. and Hauptmann, G. (2007) Distribution of corticotropin-releasing hormone in the developing zebrafish brain. **J Comp Neurol**, 505: (4): 337-351.
- Cho, S.W., Kim, S., Kim, Y., et al. (2014) Analysis of off-target effects of CRISPR/Cas-derived RNA-guided endonucleases and nickases. **Genome Research**, 24: (1): 132-141.
- Choulika, A., Perrin, A., Dujon, B., et al. (1995) Induction of homologous recombination in mammalian chromosomes by using the I-SceI system of *Saccharomyces cerevisiae*. **Mol Cell Biol**, 15: (4): 1968-1973.
- Christian, M., Cermak, T., Doyle, E.L., et al. (2010) Targeting DNA double-strand breaks with TAL effector nucleases. **Genetics**, 186: (2): 757-761.
- Clark, B.J., Soo, S.C., Caron, K.M., et al. (1995) Hormonal and developmental regulation of the steroidogenic acute regulatory protein. **Mol Endocrinol**, 9: (10): 1346-1355.
- Colombe, L., Fostier, A., Bury, N., et al. (2000) A mineralocorticoid-like receptor in the rainbow trout, *Oncorhynchus mykiss*: cloning and characterization of its steroid binding domain. **Steroids**, 65: (6): 319-328.
- Colombo, L., Dalla Valle, L., Fiore, C., et al. (2006) Aldosterone and the conquest of land. **J Endocrinol Invest**, 29: (4): 373-379.
- Cong, L., Zhou, R., Kuo, Y.-c., et al. (2012) Comprehensive interrogation of natural TALE DNA-binding modules and transcriptional repressor domains. **Nat Commun**, 3: 968.
- Dahlem, T.J., Hoshijima, K., Jurynek, M.J., et al. (2012) Simple methods for generating and detecting locus-specific mutations induced with TALENs in the zebrafish genome. **PLoS Genet**, 8: (8): e1002861.

- de Souza, F.S., Bumashny, V.F., Low, M.J., et al. (2005) Subfunctionalization of expression and peptide domains following the ancient duplication of the proopiomelanocortin gene in teleost fishes. **Mol Biol Evol**, 22: (12): 2417-2427.
- de Waal, P.P., Wang, D.S., Nijenhuis, W.A., et al. (2008) Functional characterization and expression analysis of the androgen receptor in zebrafish (*Danio rerio*) testis. **Reproduction**, 136: (2): 225-234.
- Dekker, M.J., Koper, J.W., van Aken, M.O., et al. (2008) Salivary cortisol is related to atherosclerosis of carotid arteries. **J Clin Endocrinol Metab**, 93: (10): 3741-3747.
- den Broeder, M.J., van der Linde, H., Brouwer, J.R., et al. (2009) Generation and characterization of FMR1 knockout zebrafish. **PLoS One**, 4: (11): e7910.
- Dereeper, A., Guignon, V., Blanc, G., et al. (2008) Phylogeny.fr: robust phylogenetic analysis for the non-specialist. **Nucleic Acids Res**, 36: (Web Server issue): W465-469.
- Dickmeis, T. (2009) Glucocorticoids and the circadian clock. **J Endocrinol**, 200: (1): 3-22.
- Diotel, N., Do Rego, J.L., Anglade, I., et al. (2011) The brain of teleost fish, a source, and a target of sexual steroids. **Front Neurosci**, 5: 137.
- Doyle, E.L., Booher, N.J., Standage, D.S., et al. (2012) TAL Effector-Nucleotide Targeter (TALE-NT) 2.0: tools for TAL effector design and target prediction. **Nucleic Acids Res**, 40: (W1): W117-W122.
- Eisen, J.S. and Smith, J.C. (2008) Controlling morpholino experiments: don't stop making antisense. **Development**, 135: (10): 1735-1743.
- Esvelt, K.M., Mali, P., Braff, J.L., et al. (2013) Orthogonal Cas9 proteins for RNA-guided gene regulation and editing. **Nat Meth**, 10: (11): 1116-1121.
- Ewen, K.M., Kleser, M. and Bernhardt, R. (2011) Adrenodoxin: the archetype of vertebrate-type [2Fe-2S] cluster ferredoxins. **Biochim Biophys Acta**, 1814: (1): 111-125.
- Ewen, K.M., Ringle, M. and Bernhardt, R. (2012) Adrenodoxin--a versatile ferredoxin. **IUBMB Life**, 64: (6): 506-512.
- Fan, J. and Papadopoulos, V. (2013) Evolutionary origin of the mitochondrial cholesterol transport machinery reveals a universal mechanism of steroid hormone biosynthesis in animals. **PLoS One**, 8: (10): e76701.
- Feldman, D., Krishnan, A.V., Swami, S., et al. (2014) The role of vitamin D in reducing cancer risk and progression. **Nat Rev Cancer**, 14: (5): 342-357.
- Force, A., Lynch, M., Pickett, F.B., et al. (1999) Preservation of duplicate genes by complementary, degenerative mutations. **Genetics**, 151: (4): 1531-1545.
- Fraser, R., Ingram, M.C., Anderson, N.H., et al. (1999) Cortisol effects on body mass, blood pressure, and cholesterol in the general population. **Hypertension**, 33: (6): 1364-1368.
- Freel, E.M., Ingram, M., Wallace, A.M., et al. (2008) Effect of variation in CYP11B1 and CYP11B2 on corticosteroid phenotype and hypothalamic-pituitary-adrenal axis activity in hypertensive and normotensive subjects. **Clin Endocrinol (Oxf)**, 68: (5): 700-706.
- Freeman, M.R., Dobritsa, A., Gaines, P., et al. (1999) The dare gene: steroid hormone production, olfactory behavior, and neural degeneration in *Drosophila*. **Development**, 126: (20): 4591-4602.
- Fu, Y., Foden, J.A., Khayter, C., et al. (2013) High-frequency off-target mutagenesis induced by CRISPR-Cas nucleases in human cells. **Nat Biotech**, 31: (9): 822-826.
- Fu, Y., Sander, J.D., Reyon, D., et al. (2014) Improving CRISPR-Cas nuclease specificity using truncated guide RNAs. **Nat Biotech**, 32: (3): 279-284.
- Fuller, P.J., Yao, Y., Yang, J., et al. (2012) Mechanisms of ligand specificity of the mineralocorticoid receptor. **J Endocrinol**, 213: (1): 15-24.

- Fuzzen, M.L., Bernier, N.J. and Van Der Kraak, G. (2011) Differential effects of 17beta-estradiol and 11-ketotestosterone on the endocrine stress response in zebrafish (*Danio rerio*). **Gen Comp Endocrinol**, 170: (2): 365-373.
- Gagnon, J.A., Valen, E., Thyme, S.B., et al. (2014) Efficient mutagenesis by Cas9 protein-mediated oligonucleotide insertion and large-scale assessment of single-guide RNAs. **PLoS One**, 9: (5): e98186.
- Gaj, T., Gersbach, C.A. and Barbas, C.F., 3rd (2013) ZFN, TALEN, and CRISPR/Cas-based methods for genome engineering. **Trends Biotechnol**, 31: (7): 397-405.
- Gilmour, K.M. (2005) Mineralocorticoid receptors and hormones: fishing for answers. **Endocrinology**, 146: (1): 44-46.
- Goldstone, J.V., McArthur, A.G., Kubota, A., et al. (2010) Identification and developmental expression of the full complement of Cytochrome P450 genes in Zebrafish. **BMC Genomics**, 11: 643.
- Gonzalez-Nunez, V., Gonzalez-Sarmiento, R. and Rodriguez, R.E. (2003a) Cloning and characterization of a full-length pronociceptin in zebrafish: evidence of the existence of two different nociceptin sequences in the same precursor. **Biochim Biophys Acta**, 1629: (1-3): 114-118.
- Gonzalez-Nunez, V., Gonzalez-Sarmiento, R. and Rodriguez, R.E. (2003b) Identification of two proopiomelanocortin genes in zebrafish (*Danio rerio*). **Brain Res Mol Brain Res**, 120: (1): 1-8.
- Gonzalez, F.J. (1988) The molecular biology of cytochrome P450s. **Pharmacol Rev**, 40: (4): 243-288.
- Grassi Milano, E., Basari, F. and Chimenti, C. (1997) Adrenocortical and adrenomedullary homologs in eight species of adult and developing teleosts: morphology, histology, and immunohistochemistry. **Gen Comp Endocrinol**, 108: (3): 483-496.
- Grinberg, A. and Bernhardt, R. (1998) Structural and functional consequences of substitutions at the Pro108-Arg14 hydrogen bond in bovine adrenodoxin. **Biochem Biophys Res Commun**, 249: (3): 933-937.
- Grinberg, A.V., Hannemann, F., Schiffler, B., et al. (2000) Adrenodoxin: structure, stability, and electron transfer properties. **Proteins**, 40: (4): 590-612.
- Grunwald, D.J. (2013) A revolution coming to a classic model organism. **Nat Methods**, 10: (4): 303, 305-306.
- Guo, D.F., Sun, Y.L., Hamet, P., et al. (2001) The angiotensin II type 1 receptor and receptor-associated proteins. **Cell Res**, 11: (3): 165-180.
- Guschin, D.Y., Waite, A.J., Katibah, G.E., et al. (2010) A rapid and general assay for monitoring endogenous gene modification. **Methods Mol Biol**, 649: 247-256.
- Hannemann, F., Rottmann, M., Schiffler, B., et al. (2001) The Loop Region Covering the Iron-Sulfur Cluster in Bovine Adrenodoxin Comprises a New Interaction Site for Redox Partners. **Journal of Biological Chemistry**, 276: (2): 1369-1375.
- Hanukoglu, I. (2006) Antioxidant protective mechanisms against reactive oxygen species (ROS) generated by mitochondrial P450 systems in steroidogenic cells. **Drug Metab Rev**, 38: (1-2): 171-196.
- Hasemann, C.A., Kurumbail, R.G., Boddupalli, S.S., et al. (1995) Structure and function of cytochromes P450: a comparative analysis of three crystal structures. **Structure**, 3: (1): 41-62.
- Hillegass, J.M., Villano, C.M., Cooper, K.R., et al. (2008) Glucocorticoids alter craniofacial development and increase expression and activity of matrix metalloproteinases in developing zebrafish (*Danio rerio*). **Toxicol Sci**, 102: (2): 413-424.
- Hiort, O., Holterhus, P.M., Werner, R., et al. (2005) Homozygous disruption of P450 side-chain cleavage (CYP11A1) is associated with prematurity, complete 46,XY sex reversal, and severe adrenal failure. **J Clin Endocrinol Metab**, 90: (1): 538-541.

- Howe, K., Clark, M.D., Torroja, C.F., et al. (2013) The zebrafish reference genome sequence and its relationship to the human genome. **Nature**.
- Hsu, H.-J., Hsiao, P., Kuo, M.-W., et al. (2002) Expression of zebrafish *cyp11a1* as a maternal transcript and in yolk syncytial layer. **Gene Expression Patterns**, 2: (3-4): 219-222.
- Hsu, H.J., Liang, M.R., Chen, C.T., et al. (2006) Pregnenolone stabilizes microtubules and promotes zebrafish embryonic cell movement. **Nature**, 439: (7075): 480-483.
- Hsu, H.J., Lin, G. and Chung, B.C. (2003) Parallel early development of zebrafish interrenal glands and pronephros: differential control by *wt1* and *ff1b*. **Development**, 130: (10): 2107-2116.
- Hsu, H.J., Lin, J.C. and Chung, B.C. (2009) Zebrafish *cyp11a1* and *hsd3b* genes: structure, expression and steroidogenic development during embryogenesis. **Mol Cell Endocrinol**, 312: (1-2): 31-34.
- Hsu, P.D., Lander, E.S. and Zhang, F. (2014) Development and applications of CRISPR-Cas9 for genome engineering. **Cell**, 157: (6): 1262-1278.
- Hsu, P.D., Scott, D.A., Weinstein, J.A., et al. (2013) DNA targeting specificity of RNA-guided Cas9 nucleases. **Nat Biotech**, 31: (9): 827-832.
- Hu, M.C., Hsu, H.J., Guo, I.C., et al. (2004) Function of *Cyp11a1* in animal models. **Mol Cell Endocrinol**, 215: (1-2): 95-100.
- Huang, P., Xiao, A., Zhou, M., et al. (2011) Heritable gene targeting in zebrafish using customized TALENs. **Nat Biotechnol**, 29: (8): 699-700.
- Hui, E., Yeung, M.C., Cheung, P.T., et al. (2014) The clinical significance of aldosterone synthase deficiency: report of a novel mutation in the *CYP11B2* gene. **BMC Endocr Disord**, 14: (1): 29.
- Hwang, W.Y., Fu, Y., Reyon, D., et al. (2013a) Heritable and precise zebrafish genome editing using a CRISPR-Cas system. **PLoS One**, 8: (7): e68708.
- Hwang, W.Y., Fu, Y., Reyon, D., et al. (2013b) Efficient genome editing in zebrafish using a CRISPR-Cas system. **Nat Biotechnol**, 31: (3): 227-229.
- Imamichi, Y., Mizutani, T., Ju, Y., et al. (2013) Transcriptional regulation of human ferredoxin 1 in ovarian granulosa cells. **Mol Cell Endocrinol**, 370: (1-2): 1-10.
- Imamichi, Y., Mizutani, T., Ju, Y., et al. (2014) Transcriptional regulation of human ferredoxin reductase through an intronic enhancer in steroidogenic cells. **Biochim Biophys Acta**, 1839: (1): 33-42.
- Jao, L.E., Wente, S.R. and Chen, W. (2013) Efficient multiplex biallelic zebrafish genome editing using a CRISPR nuclease system. **Proc Natl Acad Sci U S A**, 110: (34): 13904-13909.
- Jiang, W., Bikard, D., Cox, D., et al. (2013) RNA-guided editing of bacterial genomes using CRISPR-Cas systems. **Nat Biotechnol**, 31: (3): 233-239.
- Kandari, a.H., Katsumata, N., Alexander, S., et al. (2006) Homozygous mutation of P450 side-chain cleavage enzyme gene (*CYP11A1*) in 46, XY patient with adrenal insufficiency, complete sex reversal, and agenesis of corpus callosum. **J Clin Endocrinol Metab**, 91: (8): 2821-2826.
- Kari, G., Rodeck, U. and Dicker, A.P. (2007) Zebrafish: an emerging model system for human disease and drug discovery. **Clin Pharmacol Ther**, 82: (1): 70-80.
- Kassahn, K.S., Dang, V.T., Wilkins, S.J., et al. (2009) Evolution of gene function and regulatory control after whole-genome duplication: comparative analyses in vertebrates. **Genome Res**, 19: (8): 1404-1418.
- Katsumata, N., Ohtake, M., Hojo, T., et al. (2002) Compound heterozygous mutations in the cholesterol side-chain cleavage enzyme gene (*CYP11A*) cause congenital adrenal insufficiency in humans. **J Clin Endocrinol Metab**, 87: (8): 3808-3813.
- Kawamoto, T., Mitsuuchi, Y., Toda, K., et al. (1990) Cloning of cDNA and genomic DNA for human cytochrome P-45011 beta. **FEBS Lett**, 269: (2): 345-349.
- Kayes-Wandover, K.M., Schindler, R.E., Taylor, H.C., et al. (2001) Type 1 aldosterone synthase deficiency presenting in a middle-aged man. **J Clin Endocrinol Metab**, 86: (3): 1008-1012.

- Keegan, C.E. and Hammer, G.D. (2002) Recent insights into organogenesis of the adrenal cortex. **Trends Endocrinol Metab**, 13: (5): 200-208.
- Kim, C.J., Lin, L., Huang, N., et al. (2008) Severe combined adrenal and gonadal deficiency caused by novel mutations in the cholesterol side chain cleavage enzyme, P450scc. **J Clin Endocrinol Metab**, 93: (3): 696-702.
- Kimmel, C.B., Ballard, W.W., Kimmel, S.R., et al. (1995) Stages of embryonic development of the zebrafish. **Dev Dyn**, 203: (3): 253-310.
- Kimura, T. and Suzuki, K. (1965) Enzymatic reduction of non-heme iron protein (adrenodoxin) by reduced nicotinamide adenine dinucleotide phosphate. **Biochem Biophys Res Commun**, 20: (4): 373-379.
- Kimura, T. and Suzuki, K. (1967) Components of the electron transport system in adrenal steroid hydroxylase. Isolation and properties of non-heme iron protein (adrenodoxin). **J Biol Chem**, 242: (3): 485-491.
- Krasowski, M.D., Drees, D., Morris, C.S., et al. (2014) Cross-reactivity of steroid hormone immunoassays: clinical significance and two-dimensional molecular similarity prediction. **BMC Clin Pathol**, 14: 33.
- Kumai, Y., Nesan, D., Vijayan, M.M., et al. (2012) Cortisol regulates Na<sup>+</sup> uptake in zebrafish, *Danio rerio*, larvae via the glucocorticoid receptor. **Mol Cell Endocrinol**, 364: (1-2): 113-125.
- Kumar, N.N., Benjafield, A.V., Lin, R.C., et al. (2003) Haplotype analysis of aldosterone synthase gene (CYP11B2) polymorphisms shows association with essential hypertension. **J Hypertens**, 21: (7): 1331-1337.
- Kumar, R. and McEwan, I.J. (2012) Allosteric modulators of steroid hormone receptors: structural dynamics and gene regulation. **Endocr Rev**, 33: (2): 271-299.
- Kusakabe, M., Kobayashi, T., Todo, T., et al. (2002) Molecular cloning and expression during spermatogenesis of a cDNA encoding testicular 11beta-hydroxylase (P45011beta) in rainbow trout (*Oncorhynchus mykiss*). **Mol Reprod Dev**, 62: (4): 456-469.
- Labrie, F., Belanger, A., Luu-The, V., et al. (1998) DHEA and the intracrine formation of androgens and estrogens in peripheral target tissues: its role during aging. **Steroids**, 63: (5-6): 322-328.
- Labrie, F., Luu-The, V., Lin, S.X., et al. (2000) Role of 17 beta-hydroxysteroid dehydrogenases in sex steroid formation in peripheral intracrine tissues. **Trends Endocrinol Metab**, 11: (10): 421-427.
- Lala, D.S., Ikeda, Y., Luo, X., et al. (1995) A cell-specific nuclear receptor regulates the steroid hydroxylases. **Steroids**, 60: (1): 10-14.
- Lambeth, J.D. and Kriengsiri, S. (1985) Cytochrome P-450scc-adrenodoxin interactions. Ionic effects on binding, and regulation of cytochrome reduction by bound steroid substrates. **J Biol Chem**, 260: (15): 8810-8816.
- Langheinrich, U. (2003) Zebrafish: a new model on the pharmaceutical catwalk. **Bioessays**, 25: (9): 904-912.
- Laurent, P. and Perry, S. (1990) Effects of cortisol on gill chloride cell morphology and ionic uptake in the freshwater trout, *Salmo gairdneri*. **Cell and Tissue Research**, 259: (3): 429-442.
- Law, S.H. and Sargent, T.D. (2014) The serine-threonine protein kinase PAK4 is dispensable in zebrafish: identification of a morpholino-generated pseudophenotype. **PLoS One**, 9: (6): e100268.
- Lee, S.J. (2014) Dynamic regulation of the microtubule and actin cytoskeleton in zebrafish epiboly. **Biochem Biophys Res Commun**, 452: (1): 1-7.
- Li, T., Huang, S., Jiang, W.Z., et al. (2011) TAL nucleases (TALNs): hybrid proteins composed of TAL effectors and FokI DNA-cleavage domain. **Nucleic Acids Res**, 39: (1): 359-372.

- Liang, F., Han, M., Romanienko, P.J., et al. (1998) Homology-directed repair is a major double-strand break repair pathway in mammalian cells. **Proc Natl Acad Sci U S A**, 95: (9): 5172-5177.
- Lieschke, G.J. and Currie, P.D. (2007) Animal models of human disease: zebrafish swim into view. **Nat Rev Genet**, 8: (5): 353-367.
- Lin, C.H., Tsai, I.L., Su, C.H., et al. (2011) Reverse effect of mammalian hypocalcemic cortisol in fish: cortisol stimulates Ca<sup>2+</sup> uptake via glucocorticoid receptor-mediated vitamin D3 metabolism. **PLoS One**, 6: (8): e23689.
- Lin, D., Shi, Y.F. and Miller, W.L. (1990) Cloning and sequence of the human adrenodoxin reductase gene. **Proc Natl Acad Sci U S A**, 87: (21): 8516-8520.
- Liu, G., Zheng, X.X., Xu, Y.L., et al. (2014) Effect of aldosterone antagonists on blood pressure in patients with resistant hypertension: a meta-analysis. **J Hum Hypertens**.
- Liu, Y.W. (2007) Interrenal organogenesis in the zebrafish model. **Organogenesis**, 3: (1): 44-48.
- Logan, D.W., Burn, S.F. and Jackson, I.J. (2006) Regulation of pigmentation in zebrafish melanophores. **Pigment Cell Res**, 19: (3): 206-213.
- Lohr, H. and Hammerschmidt, M. (2011) Zebrafish in endocrine systems: recent advances and implications for human disease. **Annu Rev Physiol**, 73: 183-211.
- Losel, R. and Wehling, M. (2003) Nongenomic actions of steroid hormones. **Nat Rev Mol Cell Biol**, 4: (1): 46-56.
- Luo, X., Ikeda, Y., Lala, D.S., et al. (1995) A cell-specific nuclear receptor plays essential roles in adrenal and gonadal development. **Endocr Res**, 21: (1-2): 517-524.
- Luo, X., Ikeda, Y. and Parker, K.L. (1994) A cell-specific nuclear receptor is essential for adrenal and gonadal development and sexual differentiation. **Cell**, 77: (4): 481-490.
- Ma, A.C., Lee, H.B., Clark, K.J., et al. (2013) High efficiency In Vivo genome engineering with a simplified 15-RVD GoldyTALEN design. **PLoS One**, 8: (5): e65259.
- Maeder, M.L., Linder, S.J., Reyon, D., et al. (2013) Robust, synergistic regulation of human gene expression using TALE activators. **Nat Meth**, 10: (3): 243-245.
- Mahfouz, M.M., Li, L., Shamimuzzaman, M., et al. (2011) De novo-engineered transcription activator-like effector (TALE) hybrid nuclease with novel DNA binding specificity creates double-strand breaks. **Proc Natl Acad Sci U S A**, 108: (6): 2623-2628.
- Manna, P.R., Dyson, M.T. and Stocco, D.M. (2009) Regulation of the steroidogenic acute regulatory protein gene expression: present and future perspectives. **Mol Hum Reprod**, 15: (6): 321-333.
- Martinovic-Weigelt, D., Wang, R.L., Villeneuve, D.L., et al. (2011) Gene expression profiling of the androgen receptor antagonists flutamide and vinclozolin in zebrafish (*Danio rerio*) gonads. **Aquat Toxicol**, 101: (2): 447-458.
- McCormick, S.D., Regish, A., O'Dea, M.F., et al. (2008) Are we missing a mineralocorticoid in teleost fish? Effects of cortisol, deoxycorticosterone and aldosterone on osmoregulation, gill Na<sup>+</sup>,K<sup>+</sup> -ATPase activity and isoform mRNA levels in Atlantic salmon. **Gen Comp Endocrinol**, 157: (1): 35-40.
- McGonnell, I.M. and Fowkes, R.C. (2006) Fishing for gene function--endocrine modelling in the zebrafish. **J Endocrinol**, 189: (3): 425-439.
- Meimaridou, E., Kowalczyk, J., Guasti, L., et al. (2012) Mutations in NNT encoding nicotinamide nucleotide transhydrogenase cause familial glucocorticoid deficiency. **Nat Genet**, 44: (7): 740-742.
- Mellon, S.H., Bair, S.R. and Monis, H. (1995) P450c11B3 mRNA, transcribed from a third P450c11 gene, is expressed in a tissue-specific, developmentally, and hormonally regulated fashion in the rodent adrenal and encodes a protein with both 11-hydroxylase and 18-hydroxylase activities. **J Biol Chem**, 270: (4): 1643-1649.

- Mercer, A.C., Gaj, T., Fuller, R.P., et al. (2012) Chimeric TALE recombinases with programmable DNA sequence specificity. **Nucleic Acids Res**, 40: (21): 11163-11172.
- Meyer, J. (2008) Iron-sulfur protein folds, iron-sulfur chemistry, and evolution. **J Biol Inorg Chem**, 13: (2): 157-170.
- Miller, J.C., Tan, S., Qiao, G., et al. (2011) A TALE nuclease architecture for efficient genome editing. **Nat Biotechnol**, 29: (2): 143-148.
- Miller, W.L. (1998) Why Nobody Has P450scc (20,22 Desmolase) Deficiency. **Journal of Clinical Endocrinology and Metabolism**, 83: (4): 1399.
- Miller, W.L. (2005) Minireview: regulation of steroidogenesis by electron transfer. **Endocrinology**, 146: (6): 2544-2550.
- Miller, W.L. (2013) Steroid hormone synthesis in mitochondria. **Mol Cell Endocrinol**, 379: (1-2): 62-73.
- Miller, W.L. and Auchus, R.J. (2011) The molecular biology, biochemistry, and physiology of human steroidogenesis and its disorders. **Endocr Rev**, 32: (1): 81-151.
- Mommsen, T., Vijayan, M. and Moon, T. (1999) Cortisol in teleosts: dynamics, mechanisms of action, and metabolic regulation. **Reviews in Fish Biology and Fisheries**, 9: (3): 211-268.
- Moscou, M.J. and Bogdanove, A.J. (2009) A simple cipher governs DNA recognition by TAL effectors. **Science**, 326: (5959): 1501.
- Mullins, M. (1995) Genetic nomenclature guide. Zebrafish. **Trends Genet**, 31-32.
- Mussolino, C., Morbitzer, R., Lutge, F., et al. (2011) A novel TALE nuclease scaffold enables high genome editing activity in combination with low toxicity. **Nucleic Acids Res**, 39: (21): 9283-9293.
- Nasevicius, A. and Ekker, S.C. (2000) Effective targeted gene 'knockdown' in zebrafish. **Nat Genet**, 26: (2): 216-220.
- Nelson, D.H., Meakin, J.W., Dealy, J.B., Jr., et al. (1958) ACTH-producing tumor of the pituitary gland. **N Engl J Med**, 259: (4): 161-164.
- Nelson, D.R., Goldstone, J.V. and Stegeman, J.J. (2013) The cytochrome P450 genesis locus: the origin and evolution of animal cytochrome P450s. **Philos Trans R Soc Lond B Biol Sci**, 368: (1612): 20120474.
- Nesan, D., Kamkar, M., Burrows, J., et al. (2012) Glucocorticoid receptor signaling is essential for mesoderm formation and muscle development in zebrafish. **Endocrinology**.
- Nesan, D. and Vijayan, M.M. (2012) Embryo exposure to elevated cortisol level leads to cardiac performance dysfunction in zebrafish. **Mol Cell Endocrinol**, 363: (1-2): 85-91.
- Nesan, D. and Vijayan, M.M. (2013) The transcriptomics of glucocorticoid receptor signaling in developing zebrafish. **PLoS One**, 8: (11): e80726.
- Nichols, J.T., Pan, L., Moens, C.B., et al. (2013) *barx1* represses joints and promotes cartilage in the craniofacial skeleton. **Development**, 140: (13): 2765-2775.
- Ogishima, T., Mitani, F. and Ishimura, Y. (1989) Isolation of two distinct cytochromes P-45011 beta with aldosterone synthase activity from bovine adrenocortical mitochondria. **J Biochem**, 105: (4): 497-499.
- Omura, T. (2011) Recollection of the early years of the research on cytochrome P450. **Proc Jpn Acad Ser B Phys Biol Sci**, 87: (10): 617-640.
- Otto, D.M., Henderson, C.J., Carrie, D., et al. (2003) Identification of novel roles of the cytochrome p450 system in early embryogenesis: effects on vasculogenesis and retinoic Acid homeostasis. **Mol Cell Biol**, 23: (17): 6103-6116.
- Pandey, A.V. and Fluck, C.E. (2013) NADPH P450 oxidoreductase: Structure, function, and pathology of diseases. **Pharmacol Ther**, 138: (2): 229-254.

- Parajes, S., Chan, A.O., But, W.M., et al. (2012) Delayed diagnosis of adrenal insufficiency in a patient with severe penoscrotal hypospadias due to two novel P450 side-chain cleavage enzyme (CYP11A1) mutations (p.R360W; p.R405X). **Eur J Endocrinol**, 167: (6): 881-885.
- Parajes, S., Griffin, A., Taylor, A.E., et al. (2013) Redefining the initiation and maintenance of zebrafish interrenal steroidogenesis by characterizing the key enzyme Cyp11a2. **Endocrinology**.
- Parajes, S., Kamrath, C., Rose, I.T., et al. (2011) A novel entity of clinically isolated adrenal insufficiency caused by a partially inactivating mutation of the gene encoding for P450 side chain cleavage enzyme (CYP11A1). **J Clin Endocrinol Metab**, 96: (11): E1798-1806.
- Parajes, S., Loidi, L., Reisch, N., et al. (2010) Functional consequences of seven novel mutations in the CYP11B1 gene: four mutations associated with nonclassic and three mutations causing classic 11 $\beta$ -hydroxylase deficiency. **J Clin Endocrinol Metab**, 95: (2): 779-788.
- Pattanayak, V., Lin, S., Guilinger, J.P., et al. (2013a) High-throughput profiling of off-target DNA cleavage reveals RNA-programmed Cas9 nuclease specificity. **Nat Biotech**, 31: (9): 839-843.
- Pattanayak, V., Lin, S., Guilinger, J.P., et al. (2013b) High-throughput profiling of off-target DNA cleavage reveals RNA-programmed Cas9 nuclease specificity. **Nat Biotechnol**, 31: (9): 839-843.
- Peter, M., Partsch, C.J. and Sippell, W.G. (1995) Multiteroid analysis in children with terminal aldosterone biosynthesis defects. **J Clin Endocrinol Metab**, 80: (5): 1622-1627.
- Peterson, R.T., Link, B.A., Dowling, J.E., et al. (2000) Small molecule developmental screens reveal the logic and timing of vertebrate development. **Proc Natl Acad Sci U S A**, 97: (24): 12965-12969.
- Phillips, J.B. and Westerfield, M. (2014) Zebrafish models in translational research: tipping the scales toward advancements in human health. **Dis Model Mech**, 7: (7): 739-743.
- Picado-Leonard, J., Voutilainen, R., Kao, L.C., et al. (1988) Human adrenodoxin: cloning of three cDNAs and cycloheximide enhancement in JEG-3 cells. **J Biol Chem**, 263: (7): 3240-3244.
- Pikulkaew, S., Benato, F., Celeghein, A., et al. (2011) The knockdown of maternal glucocorticoid receptor mRNA alters embryo development in zebrafish. **Dev Dyn**, 240: (4): 874-889.
- Pippal, J.B., Cheung, C.M., Yao, Y.Z., et al. (2011) Characterization of the zebrafish (*Danio rerio*) mineralocorticoid receptor. **Mol Cell Endocrinol**, 332: (1-2): 58-66.
- Postlethwait, J.H., Yan, Y.L., Gates, M.A., et al. (1998) Vertebrate genome evolution and the zebrafish gene map. **Nat Genet**, 18: (4): 345-349.
- Prasad, R., Kowalczyk, J.C., Meimaridou, E., et al. (2014) Oxidative stress and adrenocortical insufficiency. **J Endocrinol**, 221: (3): R63-73.
- Privalov, P.L. (1979) Stability of proteins: small globular proteins. **Adv Protein Chem**, 33: 167-241.
- Prunet, P., Sturm, A. and Milla, S. (2006) Multiple corticosteroid receptors in fish: from old ideas to new concepts. **Gen Comp Endocrinol**, 147: (1): 17-23.
- Reed, G.H. and Wittwer, C.T. (2004) Sensitivity and specificity of single-nucleotide polymorphism scanning by high-resolution melting analysis. **Clin Chem**, 50: (10): 1748-1754.
- Reyon, D., Tsai, S.Q., Khayter, C., et al. (2012) FLASH assembly of TALENs for high-throughput genome editing. **Nat Biotechnol**, 30: (5): 460-465.
- Rosmond, R. (2005) Role of stress in the pathogenesis of the metabolic syndrome. **Psychoneuroendocrinology**, 30: (1): 1-10.
- Rubtsov, P., Karmanov, M., Sverdlova, P., et al. (2009) A novel homozygous mutation in CYP11A1 gene is associated with late-onset adrenal insufficiency and hypospadias in a 46,XY patient. **J Clin Endocrinol Metab**, 94: (3): 936-939.
- Sahakitrungruang, T., Tee, M.K., Blackett, P.R., et al. (2011) Partial defect in the cholesterol side-chain cleavage enzyme P450scc (CYP11A1) resembling nonclassic congenital lipid adrenal hyperplasia. **J Clin Endocrinol Metab**, 96: (3): 792-798.

- Salamov, A.A., Nishikawa, T. and Swindells, M.B. (1998) Assessing protein coding region integrity in cDNA sequencing projects. **Bioinformatics**, 14: (5): 384-390.
- Sampath-Kumar, R. (1994) Existence of adrenodoxin-like peptide in teleost fishes: Immunohistochemical evidence. **Journal of Experimental Zoology**, 270: (6): 557-561.
- Sander, J.D., Cade, L., Khayter, C., et al. (2011) Targeted gene disruption in somatic zebrafish cells using engineered TALENs. **Nat Biotechnol**, 29: (8): 697-698.
- Sander, J.D. and Joung, J.K. (2014) CRISPR-Cas systems for editing, regulating and targeting genomes. **Nat Biotechnol**, 32: (4): 347-355.
- Sander, J.D., Maeder, M.L., Reyon, D., et al. (2010) ZiFiT (Zinc Finger Targeter): an updated zinc finger engineering tool. **Nucleic Acids Res**, 38: (Web Server issue): W462-468.
- Sander, J.D., Zaback, P., Joung, J.K., et al. (2007) Zinc Finger Targeter (ZiFiT): an engineered zinc finger/target site design tool. **Nucleic Acids Res**, 35: (Web Server issue): W599-605.
- Sandor, T., Vinson, G.P., Jones, I.C., et al. (1966) Biogenesis of corticosteroids in the European eel *Anguilla anguilla* L. **J Endocrinol**, 34: (1): 105-115.
- Sato, H., Ashida, N., Suhara, K., et al. (1978) Properties of an adrenal cytochrome P-450 (P-45011beta) for the hydroxylations of corticosteroids. **Arch Biochem Biophys**, 190: (1): 307-314.
- Schartl, M. (2014) Beyond the zebrafish: diverse fish species for modeling human disease. **Dis Model Mech**, 7: (2): 181-192.
- Schiffler, B., Kiefer, M., Wilken, A., et al. (2001) The interaction of bovine adrenodoxin with CYP11A1 (cytochrome P450scc) and CYP11B1 (cytochrome P45011beta). Acceleration of reduction and substrate conversion by site-directed mutagenesis of adrenodoxin. **J Biol Chem**, 276: (39): 36225-36232.
- Schiffler, B., Zöllner, A. and Bernhardt, R. (2011) Kinetic and optical biosensor study of adrenodoxin mutant AdxS112W displaying an enhanced interaction towards the cholesterol side chain cleavage enzyme (CYP11A1). **European Biophysics Journal**, 40: (12): 1275-1282.
- Schmid-Burgk, J.L., Schmidt, T., Kaiser, V., et al. (2013) A ligation-independent cloning technique for high-throughput assembly of transcription activator-like effector genes. **Nat Biotechnol**, 31: (1): 76-81.
- Schoonheim, P.J., Chatzopoulou, A. and Schaaf, M.J. (2010) The zebrafish as an in vivo model system for glucocorticoid resistance. **Steroids**, 75: (12): 918-925.
- Schulte-Merker, S. and Stainier, D.Y. (2014) Out with the old, in with the new: reassessing morpholino knockdowns in light of genome editing technology. **Development**, 141: (16): 3103-3104.
- Scott, R.R. and Miller, W.L. (2008) Genetic and clinical features of p450 oxidoreductase deficiency. **Horm Res**, 69: (5): 266-275.
- Sheftel, A.D., Stehling, O., Pierik, A.J., et al. (2010) Humans possess two mitochondrial ferredoxins, Fdx1 and Fdx2, with distinct roles in steroidogenesis, heme, and Fe/S cluster biosynthesis. **Proc Natl Acad Sci U S A**, 107: (26): 11775-11780.
- Shen, B., Zhang, W., Zhang, J., et al. (2014) Efficient genome modification by CRISPR-Cas9 nickase with minimal off-target effects. **Nat Meth**, 11: (4): 399-402.
- Siegfried, K.R. and Nusslein-Volhard, C. (2008) Germ line control of female sex determination in zebrafish. **Dev Biol**, 324: (2): 277-287.
- Simpson, E.R. and Waterman, M.R. (1988) Regulation of the synthesis of steroidogenic enzymes in adrenal cortical cells by ACTH. **Annu Rev Physiol**, 50: 427-440.
- Sparkes, R.S., Klisak, I. and Miller, W.L. (1991) Regional mapping of genes encoding human steroidogenic enzymes: P450scc to 15q23-q24, adrenodoxin to 11q22; adrenodoxin reductase to 17q24-q25; and P450c17 to 10q24-q25. **DNA Cell Biol**, 10: (5): 359-365.
- Sreenivasan, R., Cai, M., Bartfai, R., et al. (2008) Transcriptomic analyses reveal novel genes with sexually dimorphic expression in the zebrafish gonad and brain. **PLoS One**, 3: (3): e1791.

- Stocco, D.M. (2001) StAR protein and the regulation of steroid hormone biosynthesis. **Annu Rev Physiol**, 63: 193-213.
- Streisinger, G., Walker, C., Dower, N., et al. (1981) Production of clones of homozygous diploid zebra fish (*Brachydanio rerio*). **Nature**, 291: (5813): 293-296.
- Streubel, J., Blucher, C., Landgraf, A., et al. (2012) TAL effector RVD specificities and efficiencies. **Nat Biotechnol**, 30: (7): 593-595.
- Strushkevich, N., MacKenzie, F., Cherkesova, T., et al. (2011) Structural basis for pregnenolone biosynthesis by the mitochondrial monooxygenase system. **Proc Natl Acad Sci U S A**, 108: (25): 10139-10143.
- Sturm, A., Bury, N., Dengreville, L., et al. (2005) 11-deoxycorticosterone is a potent agonist of the rainbow trout (*Oncorhynchus mykiss*) mineralocorticoid receptor. **Endocrinology**, 146: (1): 47-55.
- Suzuki, K. and Kimura, T. (1965) An Iron Protein as a Component of Steroid 11-Beta-Hydroxylase Complex. **Biochem Biophys Res Commun**, 19: 340-345.
- Swart, A.C., Schloms, L., Storbeck, K.H., et al. (2013) 11beta-hydroxyandrostenedione, the product of androstenedione metabolism in the adrenal, is metabolized in LNCaP cells by 5alpha-reductase yielding 11beta-hydroxy-5alpha-androstanedione. **J Steroid Biochem Mol Biol**, 138: 132-142.
- Tajima, T., Fujieda, K., Kouda, N., et al. (2001) Heterozygous mutation in the cholesterol side chain cleavage enzyme (p450scc) gene in a patient with 46,XY sex reversal and adrenal insufficiency. **J Clin Endocrinol Metab**, 86: (8): 3820-3825.
- Thiboutot, D., Jabara, S., McAllister, J.M., et al. (2003) Human skin is a steroidogenic tissue: steroidogenic enzymes and cofactors are expressed in epidermis, normal sebocytes, and an immortalized sebocyte cell line (SEB-1). **J Invest Dermatol**, 120: (6): 905-914.
- To, T.T., Hahner, S., Nica, G., et al. (2007) Pituitary-interrenal interaction in zebrafish interrenal organ development. **Mol Endocrinol**, 21: (2): 472-485.
- Tong, S.K., Hsu, H.J. and Chung, B.C. (2010) Zebrafish monosex population reveals female dominance in sex determination and earliest events of gonad differentiation. **Dev Biol**, 344: (2): 849-856.
- Uhlmann, H., Beckert, V., Schwarz, D., et al. (1992) Expression of bovine adrenodoxin in *E. coli* and site-directed mutagenesis of /2 Fe-2S/ cluster ligands. **Biochem Biophys Res Commun**, 188: (3): 1131-1138.
- Uhlmann, H. and Bernhardt, R. (1995) The Role of Threonine 54 in Adrenodoxin for the Properties of Its Iron-Sulfur Cluster and Its Electron Transfer Function. **Journal of Biological Chemistry**, 270: (50): 29959-29966.
- Uhlmann, H., Kraft, R. and Bernhardt, R. (1994) C-terminal region of adrenodoxin affects its structural integrity and determines differences in its electron transfer function to cytochrome P-450. **J Biol Chem**, 269: (36): 22557-22564.
- Urnov, F.D., Miller, J.C., Lee, Y.L., et al. (2005) Highly efficient endogenous human gene correction using designed zinc-finger nucleases. **Nature**, 435: (7042): 646-651.
- van Impel, A., Zhao, Z., Hermkens, D.M., et al. (2014) Divergence of zebrafish and mouse lymphatic cell fate specification pathways. **Development**, 141: (6): 1228-1238.
- Voutiainen, R., Picado-Leonard, J., Diblasio, A.M., et al. (1988) Hormonal and Developmental Regulation of Adrenodoxin Messenger Ribonucleic Acid in Steroidogenic Tissues. **The Journal of Clinical Endocrinology & Metabolism**, 66: (2): 383-388.
- Wagle, M., Mathur, P. and Guo, S. (2011) Corticotropin-releasing factor critical for zebrafish camouflage behavior is regulated by light and sensitive to ethanol. **J Neurosci**, 31: (1): 214-224.

- Wang, X.G. and Orban, L. (2007) Anti-Mullerian hormone and 11 beta-hydroxylase show reciprocal expression to that of aromatase in the transforming gonad of zebrafish males. **Dev Dyn**, 236: (5): 1329-1338.
- Weng, J.-H., Liang, M.-R., Chen, C.-H., et al. (2013) Pregnenolone activates CLIP-170 to promote microtubule growth and cell migration. **Nat Chem Biol**, 9: (10): 636-642.
- White, P.C., Curnow, K.M. and Pascoe, L. (1994) Disorders of steroid 11 beta-hydroxylase isozymes. **Endocr Rev**, 15: (4): 421-438.
- Whitworth, J.A., Williamson, P.M., Mangos, G., et al. (2005) Cardiovascular consequences of cortisol excess. **Vasc Health Risk Manag**, 1: (4): 291-299.
- Wilson, K.S., Matrone, G., Livingstone, D.E., et al. (2013) Physiological roles of glucocorticoids during early embryonic development of the zebrafish (*Danio rerio*). **J Physiol**, 591: (Pt 24): 6209-6220.
- Woods, I.G., Kelly, P.D., Chu, F., et al. (2000) A comparative map of the zebrafish genome. **Genome Res**, 10: (12): 1903-1914.
- Wyman, C. and Kanaar, R. (2006) DNA double-strand break repair: all's well that ends well. **Annu Rev Genet**, 40: 363-383.
- Xie, J., Wang, W.Q., Liu, T.X., et al. (2008) Spatio-temporal expression of chromogranin A during zebrafish embryogenesis. **J Endocrinol**, 198: (3): 451-458.
- Xu, C., Tabebordbar, M., Iovino, S., et al. (2013a) A zebrafish embryo culture system defines factors that promote vertebrate myogenesis across species. **Cell**, 155: (4): 909-921.
- Xu, X., Zeng, H., Xiao, D., et al. (2013b) Genome wide association study of obesity. **Zhong Nan Da Xue Xue Bao Yi Xue Ban**, 38: (1): 95-100.
- Yu, C., Zhang, Y., Yao, S., et al. (2014) A PCR based protocol for detecting indel mutations induced by TALENs and CRISPR/Cas9 in zebrafish. **PLoS One**, 9: (6): e98282.
- Zhang, G.X., Wang, B.J., Ouyang, J.Z., et al. (2010) Polymorphisms in CYP11B2 and CYP11B1 genes associated with primary hyperaldosteronism. **Hypertens Res**, 33: (5): 478-484.
- Zhao, Y., Yang, Z., Phelan, J.K., et al. (2006) Zebrafish *dax1* is required for development of the interrenal organ, the adrenal cortex equivalent. **Mol Endocrinol**, 20: (11): 2630-2640.
- Ziegler, G.A., Vornrhein, C., Hanukoglu, I., et al. (1999) The structure of adrenodoxin reductase of mitochondrial P450 systems: electron transfer for steroid biosynthesis. **J Mol Biol**, 289: (4): 981-990.
- Ziv, L., Muto, A., Schoonheim, P.J., et al. (2013) An affective disorder in zebrafish with mutation of the glucocorticoid receptor. **Mol Psychiatry**, 18: (6): 681-691.
- Zon, L.I. and Peterson, R.T. (2005) In vivo drug discovery in the zebrafish. **Nat Rev Drug Discov**, 4: (1): 35-44.
- Zu, Y., Tong, X., Wang, Z., et al. (2013) TALEN-mediated precise genome modification by homologous recombination in zebrafish. **Nat Methods**, 10: (4): 329-331.

## PUBLICATIONS

**Redefining the initiation and maintenance of zebrafish interrenal steroidogenesis by characterizing the key enzyme *cyp11a2***

Parajes S., Griffin A., Taylor A.E., Rose I.T., Miguel-Escalada I., Hadzhiev Y., Arlt W., Shackleton C., Müller F., Krone N.

Endocrinology (2013) 154, 2702 – 2711

**The duplicated mitochondrial ferredoxin *Fdx1b* regulates steroidogenesis in zebrafish**

Griffin A., Parajes S., Taylor A.E., Shackleton C., Müller F., Krone N. (*manuscript in preparation*)

## ORAL COMMUNICATIONS

**Genetic engineering using TALENS to study the redox regulation of steroidogenesis *in vivo***

Griffin A., Parajes S., Taylor AE., Müller F., and Krone N.

2014 European Society for Paediatric Endocrinology Conference (Dublin, Ireland)

**New insights into the regulation of steroidogenesis: P450 side-chain cleavage enzyme (*Cyp11a2*) and ferredoxin (*Fdx1b*) specifically regulate steroid hormone synthesis in zebrafish**

Griffin A., Parajes S., Taylor AE., Shackleton C., Müller F., and Krone N.

2013 European Zebrafish Meeting (Barcelona, Spain)

***In vivo* studies into mitochondrial redox regulation of steroidogenesis**

Griffin A., Parajes S., Taylor AE., Shackleton C., Müller F., and Krone N.

2012 Young Active Researchers in Endocrinology Meeting (Dresden, Germany)

## POSTER PRESENTATIONS

**The zebrafish ferredoxin orthologue *Fdx1b* is essential for the redox regulation of interrenal steroidogenesis in larvae and adult fish.**

Griffin A., Parajes S., Taylor AE., Shackleton C., Müller F., and Krone N.

2013 British Society for Endocrinology Annual Meeting (Harrogate, United Kingdom)

**New insights into the regulation of steroidogenesis: P450 side-chain cleavage enzyme (*Cyp11a2*) and ferredoxin (*Fdx1b*) specifically regulate interrenal steroid synthesis in zebrafish**

Griffin A., Parajes S., Taylor AE., Shackleton C., Müller F., and Krone N.

2013 ENDO: The Endocrine Society's Annual Meeting & Expo (San Fransco, United States of America.)

***In vivo* studies into mitochondrial redox regulation of steroidogenesis**

Griffin A., Parajes S., Taylor AE., Shackleton C., Müller F., and Krone N.

2013 Northern European Zebrafish Meeting (Manchester, United Kingdom)

